

# DISSERTATION

submitted to the  
Combined Faculties for the Natural Sciences and for Mathematics  
of the Ruperto-Carola University of Heidelberg, Germany  
for the degree of  
Doctor of Natural Sciences

presented by  
**Diplombiologin Sophia Deil**  
born in Jena

Date of oral examination: \_\_\_\_\_



New insights into PEXEL-mediated protein export in  
*Plasmodium falciparum*: The role of N-terminal acetylation

Referees: Prof. Dr. Michael Lanzer  
Prof. Dr. Christine Clayton



---

Ich erkläre hiermit, dass ich die vorliegende Doktorarbeit selbstständig unter Anleitung verfasst und keine anderen als die angegebenen Quellen und Hilfsmittel benutzt habe.

Des Weiteren erkläre ich hiermit, dass ich an keiner anderen Stelle ein Prüfungsverfahren beantragt bzw. die Dissertation in dieser oder anderer Form bereits anderweitig als Prüfungsarbeit verwendet oder einer anderen Fakultät als Dissertation vorgelegt habe.

Die vorliegende Arbeit wurde am Department für Infektiologie, Abteilung Parasitologie des Universitätsklinikums Heidelberg in der Zeit von November 2009 bis April 2014 (inklusive Elternzeit von Mitte März 2010 bis Ende April 2011) unter der Leitung von Prof. Dr. Michael Lanzer durchgeführt.

---

Ort, Datum

---

Sophia Deil



## Acknowledgements

I would like to thank Prof. Dr. Michael Lanzer for giving me the opportunity to join his laboratory and work on this interesting topic, which fascinated me throughout my thesis. He showed constant support despite my maternity leave and always had an open door in case of questions. Furthermore, I would like to thank Prof. Dr. Christine Clayton and Prof. Dr. Friedrich Frischknecht for their valuable contributions in my TAC meetings and Prof. Dr. Stephan Frings for his participation as the fourth examiner in my defence committee. I am also very grateful for the help of Dr. Cecilia Sanchez, who essentially contributed to the progress of my lab work and provided me with experimental data, helpful protocols and information.

Huge thanks goes to Annika Günther, who conducted her teacher's thesis with great enthusiasm and talent under my supervision and contributed eleven constructs to this study. Furthermore, I would like to thank Dr. Marcel Deponte for computing the 3-D protein model of our candidate transferase for active-site mutagenesis and my colleague and friend Mirko Singer for the generation of a knockout of this protein in the rodent parasite *Plasmodium berghei*. I also would like to thank the group of Dr. Christine Schaeffer-Reiss in Strasbourg for their mass spectrometric analysis of our mutant proteins. Moreover, I am very grateful to Mike Blackman, Dr. Alexander Maier, Mauro Azevedo, Markus Ganter, Nadine Hertrich, Dr. Theodora Saridaki and Dr. Bianca Derrer for providing me with the different plasmids and cells necessary for the experiments. Special thanks go to my colleague and friend Katharina Ehrhardt for her scientific as well as personal enrichment of my daily work and her help in proofreading this manuscript. Furthermore, I would like to acknowledge all members of the Lanzer group, who gave me a good and inspiring time throughout my thesis: Miriam Griesheimer, Elisa Kless, Marina Müller, Nicole Kilian, Carolin Geiger, Anurag Dave, Sebastiano Bellanca, Sonia Molliner, Martin Dittmer, Hani Kartini Agustar, Marvin Haag, Sirikamol Srismith, Carine Djuika, Marek Cyrklaff, Felix Müller, Eike Pfefferkorn, Alessia Valdarno and former members of the lab. Particular thanks go to Stefan Prior, who prepared massive amounts of parasites for mass spectrometry and partly assisted me during my pregnancy. I also would like to express my gratitude for the funding and to

## ACKNOWLEDGEMENTS

---

the supportive team of my graduate school HBIGS, namely Manuela Arlt, Claudia Roos, Martina Galvan, Dr. Rolf Lutz and especially Sandra Martini for her family support.

I deeply thank my family for their ongoing support in all matters of life, especially Katrin and Rudolf Völler as well as Rita and Ulrich Deil for taking great care of our daughter when work time was needed. I also thank my brother Thomas Völler and his wife Anne Krämer for proofreading parts of this manuscript and my friends for delighting my life so much outside the lab. Last but not least, I would like to express my greatest thanks to the most important people in my life:

My husband Christoph Deil for his continuous support and love, especially during this intense last part of my thesis.

My daughter Anna for the sunshine in her heart and the joy she brings to our life and my new-born son Lukas for allowing me to finish my lab work and write the thesis manuscript late into my pregnancy.

## Table of Contents

Acknowledgements .....	I
Table of Contents .....	III
Summary .....	VII
Zusammenfassung .....	VIII
List of Abbreviations .....	IX
List of Figures .....	XV
<b>1 INTRODUCTION .....</b>	<b>1</b>
1.1 Malaria .....	1
1.1.1 The malaria parasite <i>Plasmodium falciparum</i> .....	3
1.1.2 Clinical manifestation .....	7
1.1.3 Prevention and treatment .....	8
1.2 Modifications of the host erythrocyte .....	10
1.2.1 Maurer's clefts .....	11
1.2.2 Knobs .....	13
1.2.3 New permeation pathways .....	14
1.3 Protein transport in intraerythrocytic stages of <i>P. falciparum</i> .....	14
1.3.1 Intracellular trafficking .....	15
1.3.2 Protein export into the host cell .....	17
1.3.2.1 The PEXEL motif .....	19
1.3.2.2 Translocation into the host cell .....	21
1.3.2.3 Alternative export pathways .....	23
1.3.2.4 The STEVOR protein family .....	23
1.4 N <sup>α</sup> -terminal protein acetylation .....	25
1.5 Aim of the study .....	29
<b>2 MATERIALS AND METHODS .....</b>	<b>31</b>
2.1 Materials .....	31
2.1.1 Equipment .....	31
2.1.2 Disposables .....	33
2.1.3 Chemicals .....	34

## TABLE OF CONTENTS

---

2.1.4	Biological material .....	34
2.1.5	Buffers, media and solutions .....	42
2.2	Cell culture.....	46
2.2.1	Culture of <i>P. falciparum</i> .....	46
2.2.2	Freezing of parasites .....	46
2.2.3	Thawing of parasites .....	46
2.2.4	Determining parasitaemia.....	47
2.2.5	Parasite synchronization.....	47
2.2.6	Magnetic cell sorting (MACS column) .....	47
2.2.7	Limiting dilution assay* .....	48
2.2.8	Determination of drug IC <sub>50</sub> value* .....	49
2.3	Transfection of <i>P. falciparum</i> .....	51
2.3.1	Preparation .....	51
2.3.2	Electroporation of infected red blood cells.....	52
2.3.3	Electroporation of uninfected red blood cells* .....	52
2.3.4	Selection procedure .....	52
2.4	Microbiological methods.....	53
2.4.1	Preparation of chemocompetent <i>E. coli</i> * .....	53
2.4.2	Transformation and culture of <i>E. coli</i> * .....	53
2.4.3	Selection and storage.....	54
2.5	Molecularbiological methods .....	54
2.5.1	Nucleic acids .....	54
2.5.1.1	Electrophoresis of DNA and RNA.....	54
2.5.1.2	DNA extraction from agarose gels.....	55
2.5.1.3	Photometric determination of DNA/RNA concentration .....	55
2.5.1.4	Enzymatic digestion of DNA.....	55
2.5.1.5	Dephosphorylation of DNA with alkaline phosphatase .....	56
2.5.1.6	Ligation .....	56
2.5.1.7	Polymerase chain reaction (PCR) .....	56
2.5.1.8	Plasmid isolation from bacteria .....	58
2.5.1.9	Sequencing of DNA.....	59
2.5.1.10	Isolation of genomic DNA from <i>P. falciparum</i> *.....	59

2.5.1.11	Isolation of total RNA from <i>P. falciparum</i> .....	59
2.5.1.12	cDNA synthesis by reverse transcription .....	60
2.5.2	Proteins.....	60
2.5.2.1	Preparation of parasite protein extracts* .....	60
2.5.2.2	Differential lysis assay* .....	61
2.5.2.3	Western blot analysis .....	62
2.5.2.4	Protein expression and purification* .....	63
2.6	Confocal fluorescence microscopy* .....	64
2.7	Flow cytometry* .....	65
2.8	Mass spectrometry* .....	66
2.8.1	Sample preparation for loading buffer elutions .....	66
2.8.2	LC-MS/MS analysis .....	67
2.8.3	Protein identification .....	68
<b>3</b>	<b>RESULTS.....</b>	<b>69</b>
3.1	Mutagenesis of the PEXEL motif of STEVOR and KAHRP .....	69
3.1.1	Subcellular localization of STEVOR <sup>1-80</sup> mutants .....	71
3.1.2	Subcellular localization of KAHRP <sup>1-69</sup> mutants.....	80
3.1.3	Processing of particular STEVOR <sup>1-80</sup> mutants .....	83
3.2	Characterization of a putative N-acetyltransferase (PfNAT) .....	86
3.2.1	Identification of PfNAT.....	86
3.2.2	Colocalization with other ER proteins .....	89
3.2.3	Endogenous tagging of PfNAT.....	92
3.2.4	Mutagenesis of the putative catalytic domain of PfNAT .....	94
3.2.5	Knockout attempts on PfNAT.....	98
3.2.5.1	Via double crossover recombination (pCC/pHTK vector system).....	98
3.2.5.2	Via conditional excision (DiCre/loxP system) .....	102
3.2.6	Knockdown attempts on PfNAT using the DD system .....	105
3.2.6.1	Microscopic quantification of PfNAT <sup>GFPDD24</sup> regulation.....	107
3.2.6.2	Flow cytometric analysis of PfNAT <sup>GFPDD24</sup> regulation.....	110
3.2.6.3	Cotransfection with STEVOR <sup>mCherry</sup> .....	113
3.2.6.4	Pulse-chase analysis of protein export in PfNAT <sup>GFPDD24</sup> parasites ....	115

## TABLE OF CONTENTS

---

<b>4</b>	<b>DISCUSSION</b> .....	<b>117</b>
4.1	Mutagenesis of the PEXEL motif of STEVOR and KAHRP .....	117
4.2	Characterization of a putative N-acetyltransferase (PfNAT) .....	123
<b>5</b>	<b>OUTLOOK</b> .....	<b>135</b>
<b>6</b>	<b>REFERENCES</b> .....	<b>139</b>
<b>7</b>	<b>APPENDIX</b> .....	<b>163</b>

## Summary

The apicomplexan parasite *Plasmodium falciparum* is the causative agent of the most severe form of malaria with more than 600 000 death cases per year, mainly among young children and pregnant women. The development of the parasite within human erythrocytes is accompanied by extensive remodelling of the host cells. The establishment of nutrient acquisition pathways, the genesis of membranous structures within the red blood cell (RBC) cytosol and the formation of a cytoadherence complex on the surface of the host cell represent important examples of these modifications that contribute both to parasite survival and virulence. For this purpose *P. falciparum* exports hundreds of effector proteins into the RBC with the majority of them bearing a characteristic pentameric sequence termed *Plasmodium* export element (PEXEL), which is cleaved in the parasite after the third and N-terminally acetylated at the fourth amino acid position. To gain a better understanding of this important export signal, a mutagenesis screen on the PEXEL motif (<sup>48</sup>RLLAQ<sup>52</sup>) of a GFP-tagged model protein (STEVAR<sup>1-80</sup>) was conducted in this study. The localization of the mutant proteins to different compartments of the parasitized erythrocyte was determined by fluorescence microscopy. In addition, mass spectrometric analysis of representative mutants confirmed a correlation between processing of the export motif and protein trafficking. In summary, amino acid replacements within position 1<sup>1</sup> (R<sup>48</sup>) and 3 (L<sup>50</sup>), representing the most conserved amino acids, had detrimental effects on PEXEL cleavage and protein export. In contrast, positions 2 (L<sup>49</sup>) and 5 (Q<sup>52</sup>) proved to be more permissive towards mutations and mostly maintained the wild-type export phenotype. Special attention was paid to position 4 (A<sup>51</sup>), which is acetylated after cleavage and appeared more restricted than originally assumed. One interesting finding was the deficiency of non-acetylated mutant proteins to be exported into the host cell indicating N-terminal acetylation as a prerequisite for proper targeting of PEXEL proteins. Consequently, the second part of this study focussed on the characterization of a putative N-acetyltransferase (PfNAT) that might be responsible for this allegedly important post-translational modification. The localization of the candidate transferase to the parasite endoplasmic reticulum, the compartment of PEXEL processing, was confirmed by single crossover integration of a GFP tag into the endogenous locus. Despite the use of two different approaches, the attempted deletion of the gene for loss-of-function studies was unsuccessful. However, a conditional downregulation of protein levels by ~50% was achieved using a destabilization domain, which facilitated further investigations.

---

<sup>1</sup> The data for this position were almost all obtained in previous work by Dr. P. Henrich (2008) and are shown for the sake of completeness. Amino acid single letter codes see Abbreviations.

### Zusammenfassung

*Plasmodium falciparum* aus dem Stamm der Apicomplexa ist der Hauptverursacher von schwerwiegender Malaria, an der jährlich über 600 000 Menschen sterben, darunter vor allem Kleinkinder und schwangere Frauen. Während seiner asexuellen Entwicklung in menschlichen Erythrozyten modifiziert der Parasit seine Wirtszellen, was maßgeblich zu seinem Überleben als auch zu seiner Virulenz beiträgt. Der Aufbau von Nährstofftransportwegen, die Bildung eines membranösen Netzwerkes im Zytoplasma des roten Blutkörperchens sowie eines Zytoadferenzkomplexes an dessen Oberfläche stellen einige dieser Veränderungen dar. Zu diesem Zweck transportiert der Parasit hunderte von Effektorproteinen in den Erythrozyten, von denen die Mehrheit das sogenannte *Plasmodium* Export-Element (PEXEL) besitzt. Diese Sequenz besteht aus fünf aufeinanderfolgenden Aminosäuren, welche im Parasiten nach der 3. Position proteolytisch gespalten und daraufhin an der 4. Position N-terminal acetyliert werden. Um dieses wichtige Exportsignal besser zu verstehen, wurde in dieser Doktorarbeit das PEXEL-Motiv (<sup>48</sup>RLLAQ<sup>52</sup>) eines GFP-markierten Modellproteins (STE<sup>VOR</sup><sup>1-80</sup>) einer ausführlichen Mutagenese unterzogen, gefolgt von einer fluoreszenzmikroskopischen Analyse zur Lokalisation der mutierten Proteine in intra-erythrozytären Parasitenstadien. Massenspektrometrische Untersuchungen an ausgewählten Mutanten konnten außerdem einen Zusammenhang zwischen enzymatischer Prozessierung des PEXEL-Motivs und dem Proteinexport nachweisen. Zusammenfassend wurde festgestellt, dass der Austausch von stark konservierten Aminosäuren an Position 1<sup>2</sup> (R<sup>48</sup>) und 3 (L<sup>50</sup>) sich nachteilig auf den Proteintransport auswirkte. Dagegen wurden Mutationen an Position 2 (L<sup>49</sup>) und 5 (Q<sup>52</sup>) überwiegend toleriert ohne den Export zu beeinflussen. Spezielles Interesse galt der Aminosäure an Position 4 (A<sup>51</sup>), welche nach der proteolytischen Spaltung acetyliert wird. Interessanterweise wurden nicht-acetylierte Proteine nicht über die parasitophore Vakuole hinaus transportiert, was auf eine wichtige Rolle von N-terminaler Acetylierung im Exportprozess hinweist. Folglich konzentrierte sich der zweite Teil der Studie auf die Charakterisierung der mutmaßlich verantwortlichen N-Acetyltransferase (PfNAT). Das Enzym konnte mit Hilfe von genetischer Integration eines GFP-Markers im endoplasmatischen Retikulum des Parasiten nachgewiesen werden. Des Weiteren wurde die Deletion des Genes mit zwei verschiedenen Methoden ohne Erfolg versucht. Dennoch gelang es, die Proteinmenge von PfNAT mithilfe einer destabilisierenden Domäne um 50% zu reduzieren und für weitere funktionelle Studien zu nutzen.

---

<sup>2</sup> Diese Position wurde von Dr. P. Henrich (2008) mutiert und zum Zwecke der Vollständigkeit integriert. Aminosäuren siehe Abkürzungsverzeichnis.

---

## List of Abbreviations

3D	3 Dimensional
A	Adenine or Alanine
<i>A. terreus</i>	<i>Aspergillus terreus</i>
aa	Amino acids
acetyl-CoA	acetyl coenzyme A
AcT	Acetyl-CoA transporter
Ap	Apicoplast
APS	Ammonium persulphate
ARF	ADP ribosylation factors
ATP	Adenosine triphosphate
BB	<i>Babesia bovis</i>
B.C.	Before Christ
Bla	$\beta$ -Lactamase gene for ampicillin resistance
bp	Base pair
BS	Blasticidin S
BSA	Bovine serum albumin
C	Cytosine or Cysteine
CaCl <sub>2</sub>	Calcium chloride
CAD	Conditional aggregation domain
CDC	Centers for Disease Control and Prevention
cDNA	complementary DNA
CM	<i>Cryptosporidium muris</i>
COP	Coat protein complex
CRT	Chloroquine resistance transporter
CSA	Chondroitin sulphate A
CSP	Circumsporozoite protein
C-terminus	Carboxy-terminus
D	Aspartic acid
Da	Dalton
DBL	Duffy binding-like
dd	double distilled
DD	Destabilization domain
DHFR	Dihydrofolate reductase
DHFR-TS	dihydrofolate reductase-thymidylate synthase
DHPS	Dihydropteroate synthase
DIC	Differential interference contrast
DMSO	Dimethyl sulfoxide
DNA	Desoxyribonucleic acid
dNTP	Desoxyribonucleoside triphosphate
DTT	Dithiothreitol

## LIST OF ABBREVIATIONS

---

E	Glutamic acid
<i>E. coli</i>	<i>Escherichia coli</i>
EDTA	Ethylenediaminetetraacetate
EGTA	Ethyleneglycoltetraacetate
EMP	Erythrocyte membrane protein
ER	Endoplasmic reticulum
ERAD	ER-associated degradation pathway
ERD	ER retention defective
ET	<i>Eimeria tenella</i>
EtBr	Ethidium bromide
EXP	Exported protein
FKBP	FK506-binding protein
FRB	FKBP12-rapamycin binding protein
FV	Food vacuole
for	Forward
g	Gram
G	Glycine or Guanine
gDNA	genomic DNA
GDP	Gross domestic product
gene ID	gene identity
GFP	Green fluorescent protein
GNAT	GCN5-related N-acetyltransferase
h	hour or human
H	Histidine
H <sub>2</sub> O	Water
HDAC	Histone deacetylase
HEPES	N-(2-Hydroxyethyl)piperacin-N'-(2-ethylsulphonacid)
HR	Homology region
HSP	Heat shock protein
HU	Hemolytic unit
I	Isoleucine
ibid.	<i>ibidem</i> , source for reference in preceding section
ICAM	Intercellular adhesion molecule
IFA	Indirect fluorescence assay
IPTG	isopropyl $\beta$ -D-1-thiogalactopyranoside
iRBC	infected red blood cell
IRS	indoor residual spraying
ITNs	insecticide-treated bed nets
k	kilo
K	Lysine
KAHRP	Knob associated histidine rich protein
kb	Kilobase pairs

X

## LIST OF ABBREVIATIONS

---

KCl	Potassium chloride
kDa	Kilodalton
KH <sub>2</sub> PO <sub>4</sub>	Potassium dihydrogen phosphate
K <sub>2</sub> HPO <sub>4</sub>	Dipotassium hydrogen phosphate
KOH	Potassium hydroxide
kV	Kilovolt
l	Litre
L	Leucine
LB	Luria Bertani
LC-MS/MS	Liquid chromatography-mass spectrometry/mass spectrometry
LSA	liver-stage antigen
m	Milli
mm	millimetre
M	Molar
MACS	Magnetic activated cell sorter
MAHRP	Membrane associated histidine-rich protein
MC	Maurer's cleft
MDa	Megadalton
MESA	mature-parasite-infected erythrocyte surface antigen
MgSO <sub>4</sub>	Magnesium sulphate
min	Minute
ml	millilitre
MSP	Merozoite surface antigen
mRNA	Messenger RNA
msec	Milliseconds
n	Nano
N	Asparagine
NaCl	Sodium chloride
NaH <sub>2</sub> PO <sub>4</sub>	Sodium dihydrogen phosphate
NaOH	sodium hydroxide
NAT	N-acetyltransferase
NC	<i>Neospora caninum</i>
NH <sub>4</sub> Cl	Ammonium chloride
NPP	New permeation pathway
N-acetylation	Protein N <sup>α</sup> -terminal acetylation
N-terminus	Amino-terminus
ON	Over night
O <sub>2</sub>	Oxygen
°C	degree Celcius
OD	Optical density
P	Proline

## LIST OF ABBREVIATIONS

---

<i>P.</i>	<i>Plasmodium</i>
PAGE	Polyacrylamide gel electrophoresis
Pb	<i>Plasmodium berghei</i>
PB	Phosphate buffer
PBS	Phosphate buffered saline
PCR	Polymerase chain reaction
PDB	Protein Data Bank
PEXEL	Plasmodium export element
Pf	<i>Plasmodium falciparum</i>
PFA	Paraformaldehyde
pH	Potential hydrogenii
PHIST	<i>Plasmodium</i> helical interspersed sub-telomeric
PIPES	piperazine-N,N'-bis(2-ethanesulfonic acid)
PMSF	Phenylmethylsulphonyl fluoride
PMV	Plasmepsin V
PNEP	PEXEL-negative exported protein
POD	Peroxidase
PP1	Protein phosphatase
PPEP	PEXEL-positive exported protein
PPM	Parasite plasma membrane
PTEX	<i>Plasmodium</i> translocon of exported proteins
PV	Parasitophorous vacuole
PVDF	polyvinylidene difluoride
PVM	Parasitophorous vacuolar membrane
Q	Glutamine
R	Arginine
Rab	Ras-related proteins in brain
RBC	Red blood cell
rev	Reverse
REX	Ring exported protein
RIFIN	Repetitive interspersed family
RNA	Ribonucleic acid
RNAse	Ribonuclease
rpm	revolutions per minute
RPMI	Rosewell Park Memorial Institute
RT	Room temperature or Reverse transcriptase
S	Serine
<i>Saccharomyces cerevisiae</i>	<i>Saccharomyces cerevisiae</i>
Sap	Saponin
SAP	Shrimp alkaline phosphatase
SBP	Skeleton binding protein
SDS	Sodium dodecyl sulphate

---

sec	Second
Sec	Secretion
SEM	Standard error of the mean
SN	Supernatant
SRP	signal recognition particle
SP	Signal peptide
STEVOR	Subtelomeric variant open reading frame
T	Thymine or Threonine
T4	bacteriophage T4
TAE	Tris/acetic acid/EDTA
Taq	<i>Thermus aquaticus</i>
TCA	Trichloroacetic acid
TEMED	triethylmethylethyldiamine
TG	<i>Toxoplasma gondii</i>
TK	Thymidine kinase
TM	Transmembrane domain
TMPP	N-tris (2,4,6-trimethoxy-phenyl) phosphonium acetyl succinimide
TNF	Tumor necrosis factor
TP	Transit peptide or <i>Theileria parva</i>
Tris	tris (hydroxymethyl)-aminomethane
TVN	Tubovesicular network
U	Units
UTR	Untranslated region
UV	Ultra violet
V	Volt or Valine
v/v	volume to volume
VTS	Vacuolar targeting signal
W	Tryptophan
w/v	weight to volume
WHO	World Health Organization
x	times, any amino acid
Y	Tyrosine
$\alpha$	Anti-
$\mu$	Micro
$\mu$ F	Microfarad
5-FC	5-Fluorocytosine



## List of Figures

Figure 1. Classification of countries by stage of malaria elimination (WHO, 2012) .....	1
Figure 2. Life cycle of <i>Plasmodium falciparum</i> (Boddey & Cowman, 2013).....	4
Figure 3. The blood-stage cycle of malaria parasite development (Boddey & Cowman, 2013).....	5
Figure 4. Modifications of the erythrocyte (Bernhard-Nocht-Institute, 2009) .....	11
Figure 5. Adhesion of an infected RBC to an endothelial cell (Maier et al, 2009) .....	12
Figure 6. Knob structure and the cytoskeleton in <i>P. falciparum</i> -infected RBCs (Maier et al, 2009) .....	13
Figure 7. Intracellular secretory transport in <i>P. falciparum</i> (Tonkin et al, 2006a).....	17
Figure 8. PEXEL-mediated protein export (Boddey et al, 2010).....	20
Figure 9. Model of the <i>Plasmodium</i> translocon of exported proteins (Boddey & Cowman, 2013) .....	22
Figure 10. Full-length STEVOR and STEVOR <sup>1-80</sup> tagged to GFP (Przyborski et al, 2005) .....	24
Figure 11. Molecular functions of N-terminal acetylation (Starheim et al, 2012).....	27
Figure 12. Mutagenesis screen of the PEXEL motif of STEVOR <sup>1-80</sup> .....	70
Figure 13. Export phenotypes of wild-type and R <sup>48</sup> (P3) mutants of STEVOR <sup>1-80</sup> .....	72
Figure 14. Export phenotypes of L <sup>49</sup> (P2) and L <sup>50</sup> (P1) mutants of STEVOR <sup>1-80</sup> .....	74
Figure 15. Export phenotypes of A <sup>51</sup> (P1') mutants of STEVOR <sup>1-80</sup> .....	76
Figure 16. Western blot analysis of selected A <sup>51</sup> mutants after differential lysis.....	77
Figure 17. Export phenotypes of Q <sup>52</sup> (P2') mutants of STEVOR <sup>1-80</sup> .....	79
Figure 18. Export phenotypes of A <sup>57</sup> (P1') mutants of KAHRP <sup>1-69</sup> .....	82
Figure 19. PfNAT as a putative N-acetyltransferase .....	88
Figure 20. Localization of PfNAT and other marker proteins within the ER.....	90
Figure 21. Endogenous tagging of PfNAT with GFP via homologous recombination.....	93
Figure 22. Molecular model of NAT domain from 3PP9 and PfNAT (by Dr. M. Deponte) .....	95
Figure 23. Mutagenesis of the putative catalytic domain of PfNAT .....	97
Figure 24. Knockout strategy for <i>PfNAT</i> using the pCC/pHTK vector system and PCR analysis.....	100
Figure 25. Knockout strategy for <i>PfNAT</i> using the DiCre recombinase system and PCR analysis .....	103
Figure 26. Localization of PfNAT <sup>synth</sup> .....	105
Figure 27. Localization of PfNAT <sup>GFPDD24</sup> during intraerythrocytic parasite development .....	106
Figure 28. Microscopic quantification of ligand-based regulation of PfNAT <sup>GFPDD24</sup> .....	109
Figure 29. Flow cytometric analysis of ligand-based regulation of PFNAT <sup>GFPDD24</sup> .....	111
Figure 30. Effects of stabilizing ligand on parasite growth .....	113
Figure 31. Export of STEVOR <sup>mCherry</sup> in PfNAT <sup>GFPDD24</sup> parasites.....	114
Figure 32. Pulse-chase analysis of protein export in regulated PfNAT <sup>GFPDD24</sup> clonal line .....	116
Figure 33. pARL-STEVEOR <sup>1-80</sup> -GFP (original vector by T. Gilberger).....	163
Figure 34. pARL-PfNAT-3'-GFPHADD24 (HADD24 tag provided by M. Azevedo) .....	163
Figure 35. pCC and pHTK vector systems (provided by A. Maier & N. Hertrich),.....	163
Figure 36. pHH1-PfNAT_C-term-loxP (provided by M. Blackman) .....	164
Figure 37. Prestained Protein ladder      Figure 38. GeneRuler, 1kb+ DNA ladder .....	168



# 1 Introduction

## 1.1 Malaria

Malaria is a vector-borne disease that is caused by infection with the protozoan parasite *Plasmodium* (Phylum: Apicomplexa, Class: Sporozoa, Order: Coccidia, Suborder: Haemosporidiae, Family: Plasmodiidae) and transmitted by the infectious bite of a female *Anopheles* mosquito. From the 120 *Plasmodium* species that parasitize land vertebrates, only 5 species infect humans: *P. falciparum*, *P. vivax*, *P. ovale*, *P. malariae* and *P. knowlesi* (Boddey & Cowman, 2013; Carter & Mendis, 2002).

The parasites develop in liver hepatocytes and red blood cells of the human body and reproduce sexually in the midgut of the blood-feeding female *Anopheles* mosquito. There are 400 species of *Anopheles* mosquitoes worldwide, about 60 transmit malaria under natural conditions and 30 of these are of major importance especially the *Anopheles gambiae* and *A. funestus* complex (Tuteja, 2007). Infection with *P. falciparum* causes the most severe form of the disease representing most of the death cases and is the predominant malaria parasite in Africa (WHO, 2013). According to the World Health Organization (WHO) 3.4 billion people representing 48% of the world's population live in 104 endemic countries at constant risk of infection with *Plasmodium* parasites, including Africa, Southeast Asia, Oceania, the Indian Subcontinent, Central and South America (Figure 1). Around 207 million people suffered from malaria worldwide in 2012 with an estimated number of 627 000 malaria deaths, 77% of these in children under 5 years of age (WHO, 2013).

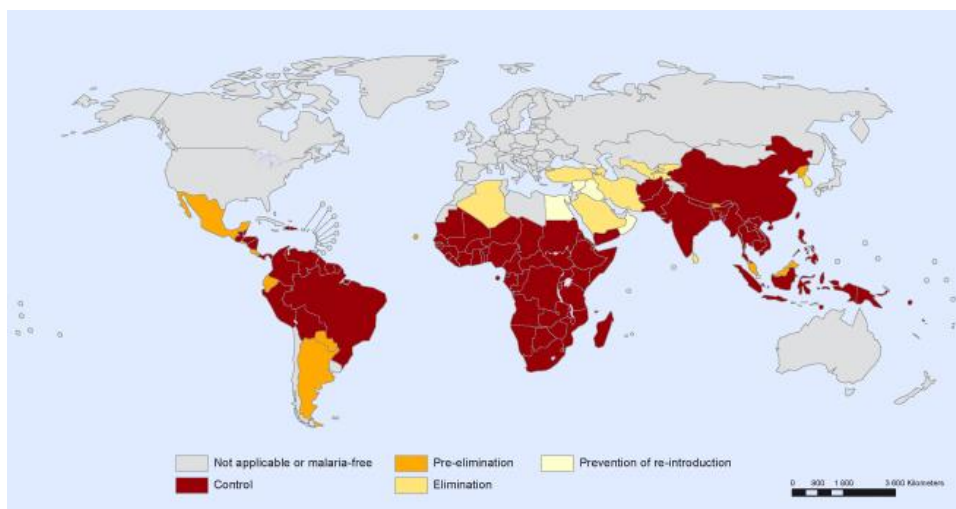


Figure 1. Classification of countries by stage of malaria elimination (WHO, 2012)

## INTRODUCTION

---

The majority of cases (80%) and deaths (90%) occurred in sub-Saharan Africa. Malaria is among the top ten causes of deaths in low-income countries, disproportionately affecting the poorest populations, and poses a major health problem and essential hindrance to economic development (Barat et al, 2004; WHO, 2011). One estimate of the impact of malaria on the national income in Africa put the economic burden at 0.6–1.0% of the gross domestic product (GDP) with many social and economic fields influenced such as population growth, investments, worker productivity, agriculture, tourism, premature mortality and medical costs (Chima et al, 2003; Sachs & Malaney, 2002; Tuteja, 2007; WHO, 1999). Fortunately, residents in endemic countries with regular transmission acquire partial immunity that potentially protects them from severe disease progression. However, non-immune individuals such as infants, children and pregnant women (in pregnancy-associated malaria) are at higher risk (Boddey & Cowman, 2013). Despite successful intervention strategies implemented during the last decades, resistances to previously effective treatments such as anti-malarial drugs or insecticides have spread, which render malaria-free countries endangered and pose a serious problem to the control and eradication of the disease (Alonso & Tanner, 2013; Mendis et al, 2009). Furthermore, more countries are increasingly affected as a consequence of expanding habitats of the vector mosquitoes (*Anopheles spec.*) due to climate change, forest clearings, increased precipitation, floods, slum development in big cities and mismanaged irrigation systems (Ramasamy & Surendran, 2012; Stich et al, 2000).

The disease was recorded in many civilized societies throughout history as early as 2700 years Before Christ (B.C.) (Cox, 2010). Among others Hippocrates left detailed descriptions in 400 B.C. and Chinese physicians used the healing properties of the quinghao plant, which contains the antimalarial artemisin, against fever and malaria as early as 2000 years ago (Cox, 2002; Dhingra et al, 2000; van Agtmael et al, 1999). The term ‘Malaria’ originates from the Italian ‘mal’aria’, which literally means ‘bad air’. This naming is based on the so-called miasmatic theory, which persisted throughout the 19<sup>th</sup> century and accused the gases rising from swamps and floodplains as being the causative agent of the feverish disease (Mehlhorn & Piekarski, 2002; Retief & Cilliers, 2006). In contradiction to this theory, the appearance of the protozoan parasite in a patient’s blood was first noticed in 1880 by the French army surgeon Charles Louis

Alphonse Laveran. Furthermore, Dr. Ronald Ross, a British officer in the Indian Medical Service, revealed in 1897 the transmission of avian malaria by mosquitos. This finding was complemented by the Italian scientists Giovanni Batista Grassi, Amico Bignami and Guiseppe Bastianelli who identified female *Anopheles* mosquitos as the vectors for human malaria and demonstrated the complete blood-mosquito cycles of *P. falciparum*, *P. vivax* and *P. malariae*. Finally, Henry Shortt and Cyril Garnham contributed the discovery in 1948 that malaria parasites develop in the liver before entering the blood stream (Cox, 2010).

### **1.1.1 The malaria parasite *Plasmodium falciparum***

*Plasmodium* belongs to the phylum Apicomplexa, a diverse group of unicellular protozoans, which are obligate, intracellular parasites with motile stages (Ravindran & Boothroyd, 2008). Apicomplexa are characterized by an apical complex that harbours the conoid, rhoptries, micronemes and dense granules for the invasion of host cells. Furthermore, this phylum is marked by a unique organelle termed the apicoplast that emerged from secondary endosymbiosis of a red alga with subsequent reduction in photosynthetic capabilities (Deponte et al, 2012). The remnant 4-membrane enclosed plastid of cyanobacterial origin retained a small circular genome (35 kilo base pairs, kb), whereas most genes became nuclear encoded and are involved in metabolic pathways such as biosynthesis of fatty acids, isoprenoids, haem and iron-sulphur clusters (Parsons et al, 2009). The absence of these prokaryote-like pathways in the human host render this organelle a potential drug target. The life cycle of *P. falciparum* is quite complex, with sexual reproduction in the invertebrate *Anopheles* vector and solely asexual replication cycles in the human host (Figure 2). During the blood meal of the mosquito, infective parasitic sporozoites are released from the arthropod salivary glands into the human host where they gradually leave the skin and enter the circulatory system to invade the liver. Remarkably, the parasites traverse several hepatocytes before final cell invasion, a process, which is not entirely understood, but seems to be a prerequisite for establishing a successful infection (Amino et al, 2008; Mota et al, 2001b; Mota & Rodriguez, 2001a). The sporozoites use surface proteins for invasion (e.g. circumsporozoite protein and thrombospondin-related adhesins), which specifically bind to heparin sulphate proteoglycans on hepatocytes in the region opposing the sinusoidal



glycolysis and proteolysis of haemoglobin (Miller et al, 2002). The detoxification of haem, a potentially harmful reactive by-product of haemoglobin digestion, is achieved through the formation of hemozoin crystals that are deposited in the food vacuole (Shio et al, 2010). During intracellular development parasite-induced modifications reduce the deformability of infected red blood cells (iRBCs) and lead to the sequestration of erythrocytes along the endothelium of blood vessels as well as intererythrocytic aggregation called rosetting. This cytoadherent phenotype is caused by the appearance of knob structures on the surface of iRBCs that facilitate the proper display of the major virulence determinant *P. falciparum* erythrocyte membrane protein 1 (PfEMP1) (Knuepfer et al, 2005b; Pasternak & Dzikowski, 2009; Rug et al, 2006; Wickert et al, 2003). This variant adhesion protein is intracellularly anchored to the cytoskeleton via binding to the knob-associated histidine-rich protein (KAHRP).

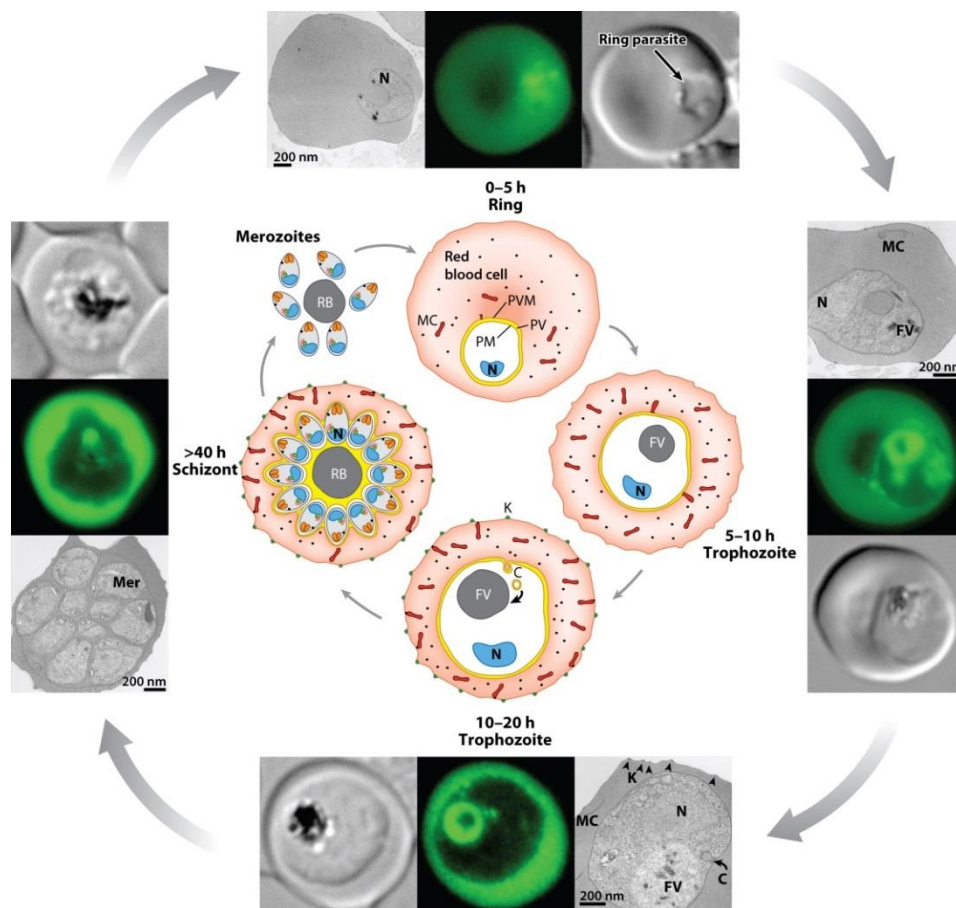


**Figure 3. The blood-stage cycle of malaria parasite development (Boddey & Cowman, 2013)**

Pictures: Electron micrograph; GFP fluorescence of a soluble exported protein (no name provided); Bright field. Abbreviations: C: cytostome; FV: food vacuole; K: knobs; MC: Maurer's cleft; N: nucleus; PM: parasite membrane; PV: parasitophorous vacuole; PVM: parasitophorous vacuolar membrane; RB: residual body.

## INTRODUCTION

---

The extracellular part of PfEMP1 consists of a cysteine-rich region and a variable number of duffy binding-like (DBL) domains, which interact with different host receptors on the vascular endothelium, such as chondroitin sulphate A (CSA), heparin sulphate, ICAM-1, thrombospondin, E-/P-Selectins, CD36 and more (Kyes et al, 2007; Scherf et al, 1998). PfEMP1 is encoded by the *var* multi-gene family, whose roughly 60 genes are mainly located in subtelomeric regions of chromosomes, a precondition in favour of recombinatorial events. Switching of *var* gene expression from one locus to the other in minor parasite subpopulations facilitates antigenic variance thereby circumventing specific humoral immune responses directed against the previous variant of PfEMP1 (Pasternak & Dzikowski, 2009). Furthermore, the cytoadherence induced by the parasite represents an effective immunoevasion technique by impairing circulation through the spleen and preventing subsequent destruction of the infected cells by splenic macrophages (Engwerda et al, 2005). However, sequestration of iRBCs can lead to occlusion of blood flow and infiltration of immune effector cells into affected areas such as the brain or placenta, which is linked to severe pathogenesis and death (Boddey & Cowman, 2013). The final schizont stage of intraerythrocytic development is characterized by multiple rounds of nuclear division and subsequent cytokinesis, which is completed by rupture of the host cell and the release of 8-24 merozoites into the blood stream (Tuteja, 2007). In the course of the infection a minor part of blood merozoites in iRBCs differentiates into gametocytes, which are ingested by a female *Anopheles* mosquito upon a blood meal (Mehlhorn, 2012). Several factors during this switch from the warm-blooded host to the arthropod mosquito such as a drop in temperature or the presence of xanthurenic acid trigger gametocyte activation. Subsequent gamete formation (micro- and macrogametes) and fertilization characterizes sexual reproduction in the midgut (Kuehn & Pradel, 2010). The resulting zygote becomes a motile ookinet that actively traverses the midgut endothelium before settling down between epithelium and basal lamina, where it develops into the oocyst. Many sporozoites are produced within the oocyst by asexual replication, are released into the haemolymph and invade the salivary glands for transmission into the next mammalian host. These motile salivary gland sporozoites are usually present in the mosquito glands from 10-18 days after the initial blood meal and remain infective for 1-2 months (Tuteja, 2007).

### 1.1.2 Clinical manifestation

There are different types of malaria that vary in their prepatence period, their severity of symptoms, their distribution and their mortality rate. Malaria tertiana (*P. vivax*, *P. ovale*) is characterized by sudden periodic fever lasting 3-4 hours, separated by 48 hours and is usually not lethal. These species also tend to form dormant hypnozoites in the liver, which can be reactivated years later. *P. vivax*, which preferentially infects reticulocytes by binding to Duffy blood group antigens, has the largest geographic distribution. However, the high frequency of the Duffy negativity trait among the majority of the African population reduced this parasites' occurrence in this area (Langhi & Bordin, 2006; WHO, 2013). The rarest type of malaria causing less than 10% of all infections is the quartan malaria (*P. malariae*). The feverish periods that are displayed every fourth day usually last 4-5 hours. Relapse of the disease is recorded as late as 30 years after infections by small long-lasting erythrocytic forms of the parasites (Tuteja, 2007). The most dangerous type of infection with a high mortality rate, Malaria tropica, is caused by *P. falciparum* and is responsible for more than half of the total malaria infections (Engwerda et al, 2005). Although the course of the disease can consist of periodic fevers (every 48 hours), it often displays unsynchronized egress with persistent fever at high temperatures. Infections with *P. falciparum* can display mild to severe symptoms resulting in minor clinical outcome or even death. Different factors influence the severity of the disease such as host immunity, genetic traits, age, pregnancy, access to medical treatment, social and geographic factors as well as parasite strain, infectivity, initial parasitic numbers, antigenic variance, drug resistance and others (Mackinnon & Read, 2004; Miller et al, 2002). Initial symptoms of malaria infections are rather unspecific including tiredness, diarrhoea, nausea, sweat periods, chills and dizziness. With the onset of disease, recurrent periods of a cold stage (sensation of cold, chills), a hot stage (fever, vomiting, headaches, and seizures) and a sweating stage (sweats, tiredness) are characteristic. The massive simultaneous release of merozoites into the blood stream coincides with a sharp incline in body temperature during the typical feverish periods. This reaction is caused by the activation of the immune system upon contact with erythrocytic cell debris, hemozoin and parasite antigens such as the merozoite surface protein (MSP-1) (Shio et al, 2010). Consequently, innate as well as adaptive immune responses are triggered such as release of pro-inflammatory cytokines

(e.g. tumor necrosis factor (TNF) by activated macrophages or T-cell activation and antibody production (Engwerda & Good, 2005; Ramasamy, 1998). However, the interplay between parasite and host immune system during infection is very complex and still subject to intense research (Chua et al, 2013; Malaguarnera & Musumeci, 2002; Scholzen et al, 2010; Yazdani et al, 2006). Characteristic signs of severe late-onset malaria are high parasitaemia, severe anaemia and neuronal complications. Furthermore, symptoms can include pulmonary oedema, kidney failure, tissue damage, black water fever, haemoglobinuria, enlarged spleen, liver damage and acidosis. Sequestration of infected erythrocytes with subsequent blockage of blood flow, oxygen deprivation and inflammation in the capillaries can induce multi-organ failure. If localized to the microvasculature of the brain, severe cerebral malaria is established. This leads to impaired vision, coordination and movement and usually is lethal after a short period of time (White et al, 2014). Pregnancy-associated malaria, which is caused by binding of conserved PfEMP1 motifs to pregnancy-specific host receptors (CSA), can lead to miscarriage, premature delivery, low birth weight and increased mortality in the newborn as well as severe anaemia or even death of the mother (Tuteja, 2007). Adult individuals living in endemic areas usually acquire semi-immunity after multiple infections, which protects them from the severe consequences of recurrent malaria (Ramasamy, 1998).

### **1.1.3 Prevention and treatment**

According to the World Malaria Report in 2013 the estimated malaria mortality rates fell worldwide between 2000 and 2012 by 42% in all age groups and by 48% in children under 5 years of age. This result was also representative for the WHO African Region (49% and 54%, respectively) (WHO, 2013). This reduction is attributed to several successful interventions including extensive vector control through the use of insecticide-treated bed nets (ITNs), indoor residual spraying (IRS) and larval control. Furthermore, increased surveillance and chemoprevention for the most susceptible populations, particularly children and pregnant women, as well as improved access to public health systems for rapid diagnosis and subsequent treatment with appropriate antimalarials reduced the number of clinical cases. However, despite these improvements there were still an estimated 627 000 malaria deaths worldwide in 2012

(uncertainty interval, 473 000–789 000) (WHO, 2013). This high number is a warning sign that the disease is still a major health problem with no general solution and requires future investigations on governmental, financial, public, medical and scientific levels to be combated.

Despite decades of research, no vaccine against malaria is currently available and the only candidate in phase 3 trials (RTS,S/AS01, targets *P. falciparum* circumsporozoite protein) proved less efficient than originally assumed (Goldstein & Shapiro, 1997; Salvador et al, 2012). In addition to the evaluation of new antigenic targets (such as e.g. parasite MSP-1, AMA-1), approaches for next-generation vaccines include whole-sporozoite vaccines, virosome/nanoparticle-based mimetope combination vaccines and the various facets of adjuvants and prime-boost concepts (Alonso & Tanner, 2013; Macrailld et al, 2011; Sutherland, 2007).

Serious problems for the treatment of malaria are the emerging parasite resistance mechanisms towards nearly all of the few effective anti-malarial drugs (Mendis et al, 2009; Turschner & Efferth, 2009). The most prominent drug for a long time was chloroquine (4-aminoquinoline), a chinine derivative that interferes with haemoglobin metabolism. It was in wide-spread use due to its low price, effectiveness and safety until the 1960s when resistant parasites emerged probably as a consequence of mutations in the *P. falciparum* chloroquine resistance transporter (PfCRT) (Bray et al, 2005; Sanchez et al, 2005). Further anti-malarial drugs include antifolates (e.g. pyrimethamine, proguanil), which were introduced in the 1940s and target the folate biosynthetic pathway of the parasite. However, resistances occurred rapidly, probably conferred by mutations in the genes encoding *P. falciparum* dihydrofolate reductase (PfDHFR) and dihydropteroate synthetase (PfDHPS) (Baird, 2005). Nevertheless, sulfadoxine-pyrimethamine is still successfully used as intermittent preventive treatment for pregnant women living in areas of high malaria transmission and monthly doses of amodiaquine-sulfadoxine-pyrimethamine given to children (3 months – 5 years old) represent a promising chemopreventive strategy to protect from severe malaria infections during the rainy season (White et al, 2014). Two other types of drugs are increasingly used: atovaquone (a mitochondrial inhibitor) and artemisin, a derivative from the Chinese herb quinghao that acts on haemoglobin metabolism. Especially artemisinin and its derivatives (e.g. artemether, artesunate) are the most potent compounds widely used in

combination therapy and by June 2008 all but four countries and territories with a high burden of the disease had adopted artemisinin-based combination therapy as the first-line treatment for malaria tropica (WHO, 2009). Unfortunately, parasite resistance to this drug has recently been detected in 4 countries of southeast Asia (Cambodia, Myanmar, Thailand and Viet Nam). However, artemisinin-based combination therapies remain highly effective in almost all settings, as long as the partner drug in the combination is locally effective (WHO, 2013). For this purpose, current efforts in the identification of new drugs, especially suited for combination therapy, must be intensified (Alonso & Tanner, 2013). Furthermore, research on non-toxic, long-lasting and affordable insecticides for indoor residual spraying that counteract the emerging resistances of mosquitos to pyrethroid insecticides needs to be expanded (Alonso & Tanner, 2013; Breman, 2009). The combat of malaria poses a big challenge to the international community and despite remarkable progress, the sustainment and expansion of political commitment, financial investments, health infrastructures, surveillance systems and pharmaceutical investigations should be devoted to the support of the people that suffer most from the disease (WHO, 2013).

### **1.2 Modifications of the host erythrocyte**

The replication of *Plasmodium* in red blood cells, which lack the capability of MHC-related antigen presentation, allows the parasite to hide from the immune system, an advantage that is further expanded by parasite-induced cytoadherence. Furthermore, the high amounts of haemoglobin in these cells represent a major nutritional source for amino acids. However, the residence in a terminally differentiated enucleated host cell that is small, prone to lysis, subject to permanent quality control and devoid of protein synthesis and transport systems is challenging (Elsworth et al, 2014). To circumvent these obstacles the parasites induce extensive modifications of the host cell for nutritional as well as immune evasive purposes including the establishment of export pathways to translocate multiple effector proteins into the erythrocyte cytoplasm (Boddey & Cowman, 2013). The insertion of transporters into host-derived membranes, the assembly of a tubovesicular network (TVN) and Maurer's clefts (MCs) as intermediate trafficking compartments in the RBC cytosol and especially the formation of surface knobs harbouring the major variant antigen PfEMP1 represent some examples

of these parasite-induced alterations outside its own boundaries (Figure 4) (Elsworth et al, 2014).

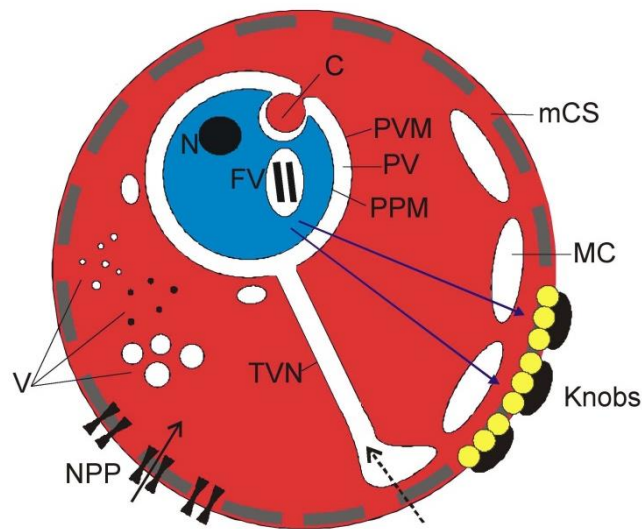


**Figure 4. Modifications of the erythrocyte (Bernhard-Nocht-Institute, 2009)**

Schematic drawing of asexual blood stages of *P. falciparum* modifying their host cell. The parasite (blue) resides in a parasitophorous vacuole (PV) formed by the PV membrane (PVM) separating it from the red blood cell (red). C: cytostomes. FV: food vacuole. mCS: modified cytoskeleton of the red blood cell. MC: flattened membranous structures called Maurer's clefts. N: nucleus. NPP: new permeation pathways in the red blood cell membrane. PPM: parasite plasma membrane. V: transport vesicles and protein aggregates.

### 1.2.1 Maurer's clefts

Maurer's clefts, first observed in 1902 by Georg Maurer as a dotted pattern within the cytoplasm of infected erythrocytes, are membranous structures of heterologous morphology and number that derive early after invasion from the PVM as mobile entities, which become tethered beneath the RBC membrane at ~20 hours post invasion (Lanzer et al, 2006; Maurer, 1902; McMillan et al, 2013; Sam-Yellowe, 2009). They usually consist of single disks or stacks of single-membrane-enclosed slits of ~30 nm height and at least 500 nm width surrounded by an electron-dense coat of round vesicle-like structures (Figure 5) (Frischknecht & Lanzer, 2008; Maier et al, 2009; Wickert & Krohne, 2007). In contrast to previous assumptions, there seems to be no fluid connection between the TVN and MCs and these compartments represent separate entities concerning transport of macromolecules (Frischknecht & Lanzer, 2008; Hanssen et al, 2008; Sam-Yellowe, 2009). The association with the RBC plasma membrane is facilitated by actin filaments that connect the clefts to the knobs as well as protein

## INTRODUCTION

---

interactions (e.g. MAHRP2) with the host membrane and cytoskeleton (Cyrklaff et al, 2011; Mbengue et al, 2012).

Functionally Maurer's clefts represent parasite-induced intermediate 'sorting' compartments for proteins *en route* to the erythrocyte membrane and it is assumed that the majority, if not all, exported proteins transiently passage through it (Mbengue et al, 2012; Tilley et al, 2008). Different mechanisms of protein trafficking to and from the clefts have been proposed including diffusion of membranous proteins during MC genesis, vesicular transport or transfer as chaperone-mediated soluble complexes (Hanssen et al, 2008; Kriek et al, 2003; Mbengue et al, 2012; Mundwiler-Pachlatko & Beck, 2013). An increasing number of proteins have been identified that reside in the Maurer's clefts, such as skeleton binding protein 1 (SBP1), membrane-associated histidine-rich protein 1 (MAHRP1) and ring-exported proteins 1 and 2 (REX1/2). Others are transiently associated with this organelle such as PfEMP1 and PfEMP3, knob-associated histidine-rich protein (KAHRP) and members of variant protein families such as the subtelomeric variable open reading frame family (STEVOR) (Sam-Yellowe, 2009). Most of these proteins are involved in MC architecture, cytoadherence, trafficking of PfEMP1 and knob formation (Dixon et al, 2011). Further studies revealed important roles of MC proteins by acting as chaperones (*P. falciparum* migration inhibitory factor, PfMIF) or enzymes (protein phosphatase 1, PP1) (Blisnick et al, 2006; Sam-Yellowe, 2009) and additional involvement in phospholipid biosynthesis, cell signalling and merozoite egress has been implicated (Lanzer et al, 2006).

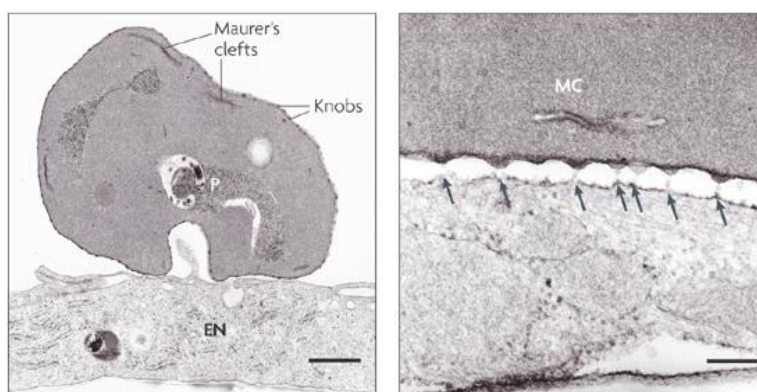


**Figure 5. Adhesion of an infected RBC to an endothelial cell (Maier et al, 2009)**

Electron micrograph of a knobby *P. falciparum*-infected RBC adhering to an endothelial cell. **Left:** Overview. **Right:** Detail of the interface between an infected red blood cell (top) and the endothelial cell (bottom). EN: endothelial cell. MC: Maurer's cleft. **arrows:** knobs. Scale bar 1  $\mu$ m (left), 100 nm (right).

### 1.2.2 Knobs

The development of *Plasmodium* within the erythrocyte is accompanied by the emergence of protrusions, so-called knobs, on the surface of the host cells from about 16 hours post-invasion (Figure 6) (Maier et al, 2009). These structures harbour the major virulence determinant protein, PfEMP1, which is displayed in an elevated manner facilitating binding to host tissue-specific receptors along the vascular endothelium for subsequent cytoadherence of iRBCs (Rug et al, 2006) (Horrocks et al, 2005). This parasite-induced adhesion process prevents splenic clearance and is associated with severe signs of malarial infections. The formation of knobs is a dynamic process with increasing knob density throughout parasite maturation from trophozoite to schizont stages (from 10–35 to 45–75 knobs/ $\mu\text{m}^2$ ) while their size varies inversely (from 160–110 to 70–100 nm in diameter) (Mbengue et al, 2012). The knobs consist of a complex of different proteins such as KAHRP, PfEMP3 and mature-parasite-infected erythrocyte surface antigen (MESA) that are connected to the sub-membrane cytoskeletal components spectrin, actin and ankyrin (Maier et al, 2009). These interactions probably result in increased rigidity and adhesiveness of the RBC membrane thereby contributing to parasite survival (Sanyal et al, 2012). KAHRP is an essential component of the knobs as knockout studies of this gene revealed a knob-less phenotype with a dramatic reduction in cytoadherence under flow conditions. Although the protein is dispensable for the delivery of PfEMP1 to the erythrocyte surface, their physical interaction seems important for the proper presentation of the adhesin (Crabb et al, 1997; Rug et al, 2006).

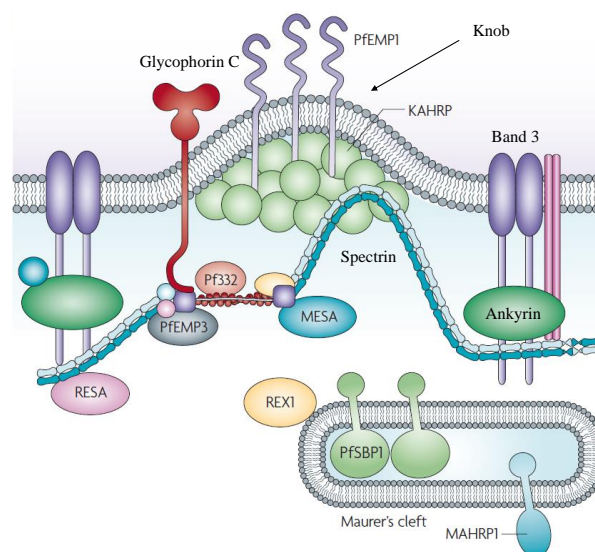


**Figure 6. Knob structure and the cytoskeleton in *P. falciparum*-infected RBCs (Maier et al, 2009)**

### **1.2.3 New permeation pathways**

Parasite development within the erythrocytes requires extensive nutrient acquisition as well as waste exchange. The major food source, haemoglobin, is not sufficient for parasite survival since it does not contain isoleucine and several other amino acids, such as glutamate, methionine, cysteine and proline are underrepresented (Mbengue et al, 2012). Since the erythrocyte is impaired in nutrient uptake, the parasite establishes new permeation pathways (NPP) to import essential molecules such as glucose, pantothenic acid and choline (Baumeister et al, 2006; Kirk & Saliba, 2007; Saliba & Kirk, 2001). The induced activity of specific transporters leads to increased permeability of the RBC membrane to low molecular weight solutes including amino acids, sugars, nucleosides, vitamins as well as organic and inorganic ions (Boddey & Cowman, 2013; Ginsburg & Stein, 2004). The origin of these pathways is still under debate and studies in favour of parasite-induced reactivation of host transporters or insertion of new transporters encoded by *Plasmodium* exist (Baumeister et al, 2010; Mbengue et al, 2012). The identification of two parasitic anion channels in the erythrocyte membrane (CLAG3.1/3.2) is consistent with the latter hypothesis (Nguitrageol et al, 2011). Interestingly, expression switching of these proteins was observed, which may assist in evading host immune responses (Boddey & Cowman, 2013). Furthermore the establishment of the TVN, a membranous system in the erythrocyte cytosol extending from the PVM to the RBC membrane, is suggested to facilitate nutrient transport (Haldar, 2005; Sherman, 2005; Tamez et al, 2008).

### **1.3 Protein transport in intraerythrocytic stages of *P. falciparum***

The establishment of a delicate protein transport system is a prerequisite for the survival in this terminally differentiated host cell. Therefore, *Plasmodium* parasites target a diversity of cellular compartments for protein trafficking. Apart from the common secretory system, these destinations include intracellular organelles such as rhoptries, micronemes, the digestive vacuole and the apicoplast as well as extracellular targets including the parasitophorous vacuolar membrane, the erythrocyte cytosol, Maurer's clefts and the RBC membrane (Deponte et al, 2012)..

### 1.3.1 Intracellular trafficking

Although the secretory pathways of malaria parasites share similarities with other eukaryotic systems, unique protein destinations indicate these specialized organelles as potential targets for intervention (Figure 7) (Tonkin et al, 2006a). The genome of *Plasmodium* harbours many homologues of core secretory proteins such as the Ras-related proteins in brain (Rabs), the ADP ribosylation factors (ARFs), the coat protein complex components (COP) and the secretion (Sec) apparatus, but there is still a lack of information on functionality of these components (ibid.). In general, most proteins enter the secretory pathway via an N-terminal signal peptide that guides translocation into the endoplasmic reticulum (ER). These signal peptides, usually 15-30 hydrophobic amino acids (aa) in length, are recognized by the signal recognition particle (SRP) upon emergence from the ribosome followed by subsequent binding of SRP to its ER receptor and co-translational insertion of the nascent protein into the ER lumen or membrane. In many cases, the signal peptide is cleaved by signal peptidase (Alberts, 2010). Alternatively to the classical signal sequence, many secreted parasite proteins contain recessed signal sequences in some distance from the amino (N)-terminus. The exact relevance of these non-canonical sequences is not entirely understood but may involve post-translational translocation or differential timing in export of certain proteins (Deponete et al, 2012). Furthermore, many proteins lack a typical signal peptide and instead use internal hydrophobic core regions or transmembrane domains for recruitment into the secretory pathway (Cooke et al, 2004). The ER resembles a simple perinuclear structure with two protruding ‘horns’ that extends upon parasite maturation (van Dooren et al, 2005). Entry of soluble as well as membranous proteins into the ER is accompanied by chaperone-mediated folding into the correct tertiary structure necessary for subsequent trafficking steps (Shonhai et al, 2007). Interestingly, *Plasmodium* has only a limited or absent capacity for N-glycosylation, a common post-translational modification within the ER. Although components of the ER-associated degradation pathway (ERAD) of terminally misfolded proteins are conserved among *Plasmodium* species, this process of proteasomal targeting is not well studied (Deponete et al, 2012). In accordance with other eukaryotic systems, the ER seems to be compartmentalized into regions with accumulation of the COPII coat complex for vesicle-budding and protein exit (transitional ER) (Lee et al, 2008). Retention of ER-resident proteins is achieved by

## INTRODUCTION

---

classical C-terminal signals such as the KDEL-sequence (alternatively SDEL) that is recognized by the Golgi-based receptor ER Retention Defective 2 (ERD2) (Elmendorf & Haldar, 1993; Kulzer et al, 2009; Kumar & Zheng, 1992; Tonkin et al, 2006b). Although the Golgi apparatus appears rudimentary in *Plasmodium* its existence and basic *cis-/trans*-structure was established using typical Golgi markers (Struck et al, 2005; Struck et al, 2008). The exact function of this organelle is still controversial and many trafficking routes seem to circumvent a traditional Golgi passage (Bannister et al, 2000; Mattei et al, 1999). The late secretory steps from the *trans*-Golgi are less understood despite the presence of homologues encoding clathrin coat components, multiple clathrin adaptors, soluble N-ethylmaleimide-sensitive-factor attachment receptors (SNAREs) and Rab proteins in the plasmodial genome (Deponte et al, 2012). Apart from the signal sequences guiding ER entry, additional motifs provide necessary information for subsequent targeting of proteins to their final destinations (Tonkin et al, 2006a).

A unique organelle of apicomplexa is the previously-mentioned apicoplast, which is of endosymbiotic origin and enclosed by 4 membranes (Parsons et al, 2009). Most apicoplast proteins are nuclear encoded and post-translationally translocated into this organelle using a plant-like transit peptide that becomes exposed after cleavage of the signal peptide in the ER (Tonkin et al, 2008). Malaria parasites possess one single mitochondrion that extends into a branched tubular network throughout intraerythrocytic development. Apart from three genes in the desoxyribonucleic acid (DNA) of the mitochondrion all of the mitochondrial proteins are nuclear encoded and have to be reimported after cytosolic translation. In general, most mitochondrial proteins contain an N-terminal mitochondrial presequence that is characterized by a net positive charge and is predicted to form an amphiphilic helix. This assumption is transferred to *Plasmodium* and *in silico* analysis predicts a significant number of proteins (over 300) that are potentially targeted to the mitochondrion (Bender et al, 2003; Deponte et al, 2012). However, there is little experimental data on the import machinery of this organelle.

Targeting of proteins (e.g. Plasmepsin proteases) to the food vacuole (FV), the lysosomal compartment involved in haemoglobin digestion, requires an N-terminal signal peptide along with a heterologous prodomain. Interestingly, the trafficking route of these proteases includes the release into the PV with subsequent re-uptake via endosomes (Tonkin et al, 2006a). From 38 hours after invasion, merozoites are formed

and apical organelles essential for new cell invasion, such as rhoptries, micronemes and dense granules are established. Proteins destined to traffic to these compartments enter the secretory pathway either through a classical signal sequence or an internal hydrophobic domain (Bannister et al, 2000). Although post-Golgi sorting through special vesicle-mediated transport of these proteins is indicated, no conserved motifs have been identified so far (Deponete et al, 2012).

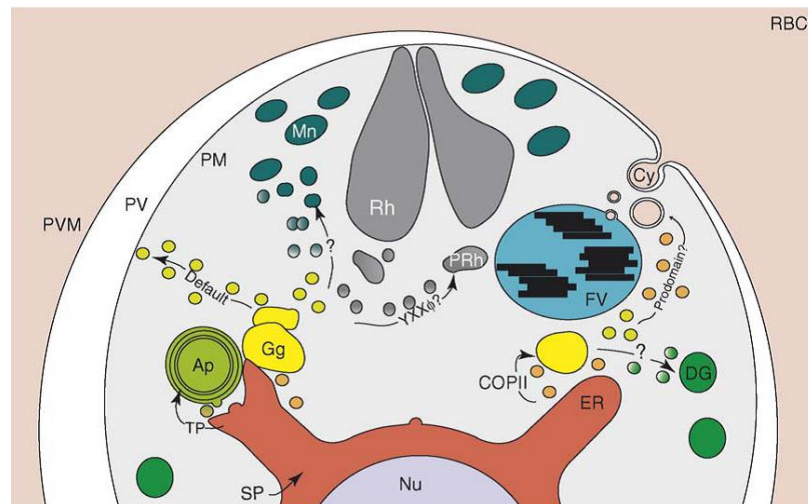


**Figure 7. Intracellular secretory transport in *P. falciparum* (Tonkin et al, 2006a)**

**Ap:** apicoplast. **Cy:** cytotomes. **DG:** dense granules. **ER:** endoplasmic reticulum. **FV:** food vacuole. **Gg:** Golgi apparatus. **Mn:** micronemes. **Nu:** nucleus. **PM:** (parasite) plasma membrane. **PRh:** pre-rhoptry compartments. **PV:** parasitophorous vacuole. **PVM:** parasitophorous vacuolar membrane. **Rh:** rhoptries. **SP:** signal peptide. **TP:** transit peptide. **YXX:** tyrosine-based sorting motif for rhoptry proteins in *Toxoplasma gondii*.

### 1.3.2 Protein export into the host cell

The remarkable ability of *Plasmodium* to remodel the erythrocyte according to its developmental needs is facilitated by expression of a large repertoire of specialized proteins that are trafficked through a complex export pathway into the host cell (Boddey & Cowman, 2013). The identification of a pentameric N-terminal sequence called *Plasmodium* export element (PEXEL, RxLxE/Q/D)<sup>3,4</sup> marked an important milestone in the characterization of the parasite's 'exportome' of more than 400 soluble and membrane PEXEL proteins (~8 % of protein coding genome) that are translocated beyond the PVM (Boddey et al, 2013; de Koning-Ward et al, 2009; Hiller et al, 2004; Marti et al, 2004). Among these proteins are the main knob-forming protein KAHRP, variant proteins of the

<sup>3</sup> The export motif is also named Vacuolar Targeting Signal (VTS) or Host Cell Targeting Signal (HCT).

<sup>4</sup> Amino acid codes see Abbreviations, x is any non-charged amino acid.

## INTRODUCTION

---

repetitive interspersed family (RIFIN), *Plasmodium* helical interspersed sub-telomeric (PHIST) and STEVOR families, putative serine/threonine kinases, heat shock proteins as well as other virulence determinants particularly involved in cytoadhesion and host cell modification (Boddey et al, 2013; Sijwali & Rosenthal, 2010). Although an increasing number of PEXEL-negative proteins (PNEPS) are identified, the PEXEL motif still characterizes the majority of exported proteins known today. Interestingly, non-falciparum *Plasmodium* species have a 5-10 fold smaller predicted PEXEL exportome with an increased number of PNEPS assumed to mark protein export in these organisms (Haase & de Koning-Ward, 2010; Heiber et al, 2013; Pasini et al, 2013). The explanation for this gene expansion and radiation is probably the functional dedication of many PEXEL proteins to support PfEMP1-mediated cytoadhesion, a process that is unique to *P. falciparum* (and *P. reichenowi*) (Boddey & Cowman, 2013). From the proportion of conserved PEXEL proteins between human and rodent malaria parasites half were shown to be essential in the rodent *P. berghei* model system (19 out of 33 orthologous genes) indicating substantial involvement in parasite survival (Matz et al, 2013; van Ooij et al, 2008). While the export motif is conserved among *Plasmodium* species it is apparently absent in this particular form in other Apicomplexans, apart from *Toxoplasma gondii* (Hsiao et al, 2013; Sargeant et al, 2006). A similar recessed motif (RxRL) was identified in effector proteins of oomycete plant pathogens (Whisson et al, 2007). However, in contrast to previous studies, recent evidence excludes a functional connection between these two export machineries (Bhattacharjee et al, 2006; Boddey & Cowman, 2013; Ellis & Dodds, 2011). The presence of PEXEL-exported proteins seems not restricted to asexual blood stage parasites. A functional role in gametocytogenesis has been implicated based on the overrepresentation of this group, such as members of the PHIST family, in the proteome of young gametocytes (Silvestrini et al, 2010). Furthermore, some PEXEL proteins are found in sporozoites including the liver-stage antigen-3 (LSA-3) and the major immunodominant circumsporozoite protein (CSP) and there is increasing evidence that host cell remodelling processes during liver-stage development are driven by the same export machinery as in the blood stages (Ingmundson et al, 2014; Ingmundson et al, 2012; Matthews et al, 2013; Singh et al, 2007).

### 1.3.2.1 The PEXEL motif

For successful export of proteins into the host cell cytoplasm two motifs are needed: a signal sequence for entry into the secretory pathway of the ER and the PEXEL motif for further translocation across the PVM (Goldberg & Cowman, 2010). The core export motif consists of five amino acids with the consensus sequence RxLx(x)E/Q/D and is located 20-30 amino acids C-terminal from the signal sequence (Hiller et al, 2004; Marti et al, 2004). After co- or posttranslational insertion into the ER the PEXEL motif is recognized by the ER-resident protease Plasmepsin V and cleaved after the conserved leucine residue (substrate residue P1)<sup>5</sup> (Figure 8) (Boddey et al, 2010; Crabb et al, 2010; Klemba & Goldberg, 2005; Russo et al, 2010). Plasmepsin V is one of ten aspartic proteases in *P. falciparum* and functionally distinct from the other members, which are mainly involved in haemoglobin degradation in the parasitic food vacuole or indicated in host spectrin degradation (Klemba & Goldberg, 2005). The enzyme is conserved in *Plasmodium* species, but absent in higher eukaryotes. It has a C-terminal transmembrane region with the protease domain presumably protruding into the lumen (Boddey et al, 2010). It was shown that cleavage occurred in the ER due to its sensitivity to Brefeldin A, an inhibitor of anterograde protein transport from ER to Golgi, which led to the accumulation of processed PEXEL proteins in this compartment (Chang et al, 2008; Osborne et al, 2010). Furthermore, Plasmepsin V seems dominant and exclusive over signal peptidase in cleavage activity, which highlights its important ‘gatekeeper’ role in freeing PEXEL cargo from the ER (Boddey et al, 2010; Russo et al, 2010). A spatial and temporal connection of the enzyme with downstream components of the export machinery such as chaperones or receptors was previously implicated as an important prerequisite for proper targeting of the PEXEL proteins to the PV and beyond (ibid.). In accordance with structural active-site predictions (Guruprasad et al, 2011), several mutagenic studies revealed the importance of the P3 arginine and P1 leucine of the PEXEL motif in mediating proper processing by the protease, with cleavage and export deficiency in various proteins bearing alanine replacements (Boddey et al, 2010; Boddey et al, 2009; Hiller et al, 2004; Marti et al, 2004; Tarr et al, 2013). In contrast, the P2’ conserved residue (E/Q/D) is dispensable for proteolysis but seems important for

---

<sup>5</sup> By convention, amino acid residues in a substrate undergoing cleavage are designated P1, P2, P3 etc. in the N-terminal direction from the cleaved bond (P1-P1’). Likewise, the residues in C-terminal direction are designated P1’, P2’, P3’ (Schechter & Berger, 1967).

## INTRODUCTION

downstream trafficking steps (Boddey et al, 2010; Tarr et al, 2013). A recent study using *in vitro* cleavage assays rejected previous assumptions that lysine could replace arginine at P3 and consequently excluded PfEMP1 proteins from the PEXEL repertoire. The authors could also show that proteins with 'relaxed' PEXEL motifs (RxLxxE/Q/D) were successfully cleaved, which resulted in a redefined exportome of 463 proteins (Boddey et al, 2013).

After cleavage, the new N-terminus (xE/Q/D) is subsequently N<sup>α</sup>-terminal acetylated (N-acetylated) by an unknown N-acetyltransferase (Chang et al, 2008; Osborne et al, 2010). The processed proteins are further trafficked to the parasitophorous vacuole where they are translocated into the RBC via a recently identified translocon (de Koning-Ward et al, 2009; Riglar et al, 2013). The functional relevance of the acetylated N-terminus in guiding protein export from the ER to the PV as well as the nature of the secretory machinery involved is not well understood and some studies are controversial (Boddey et al, 2009; Tarr et al, 2013). Different models are suggested including receptor- or chaperone-mediated vesicular escort to specialized export-competent zones at the parasite surface in close proximity to the translocation complex. Alternatively, exported proteins may enter the default secretion pathway with subsequent recognition by chaperones or the translocon complex in the PV (Boddey & Cowman, 2013; Crabb et al, 2010; Elsworth et al, 2014).

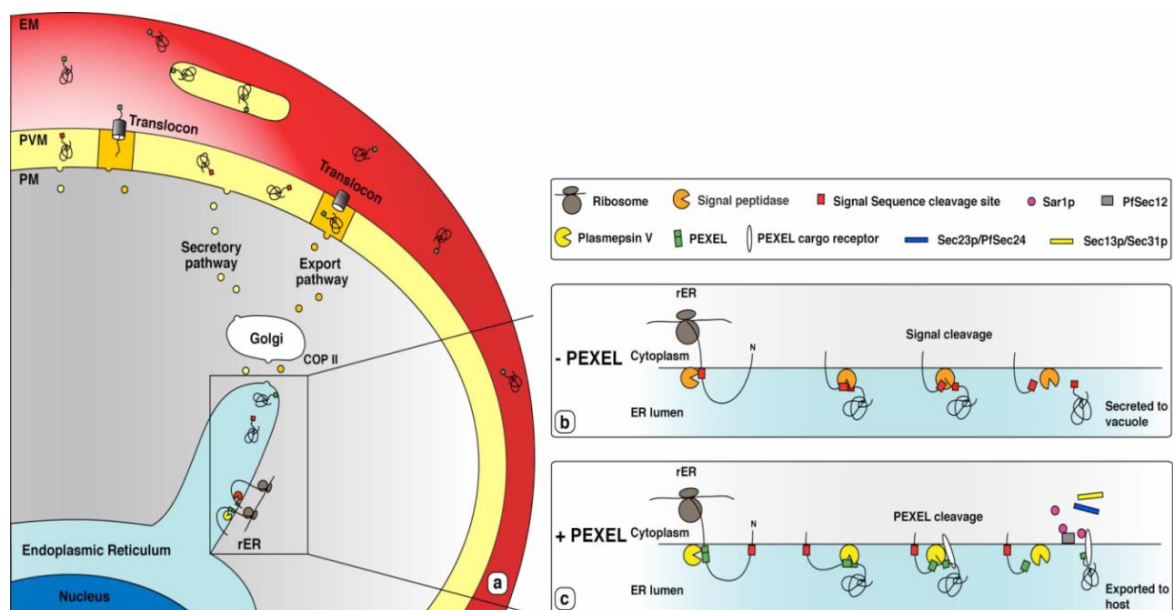


**Figure 8. PEXEL-mediated protein export (Boddey et al, 2010)**

### 1.3.2.2 Translocation into the host cell

For the successful translocation into the host erythrocyte protein unfolding and energy in form of adenosine triphosphate (ATP) are required and the recent identification of the putative *Plasmodium* translocon of exported proteins (PTEX) in the PVM confirmed these indications of a membrane-pore containing protein complex (Ansorge et al, 1996; de Koning-Ward et al, 2009; Gehde et al, 2008). The components of the PTEX are conserved among *Plasmodium* species but are absent from other apicomplexan parasites (Ingmundson et al, 2014). In addition to blood stages, expression of the complex was detected in gametocytes, sporozoites and late liver stages indicating a putative functional activity of the translocation machinery during these stages of infection (Matthews et al, 2013; Vaughan et al, 2012).

The translocon is a >1.2 megadalton (MDa) complex that consists of five components found on the vacuolar side of the PVM (Figure 9) (Bullen et al, 2012). Three of these proteins, exported protein 2 (EXP2), heat shock protein 101 (HSP101) and PTEX150, are essential core components, whereas two, thioredoxin 2 (Trx2) and PTEX88, are non-essential accessory components since their genes can be deleted in *P. berghei* (Matthews et al, 2013; Matz et al, 2013). The pore is most likely assembled through oligomerization of EXP2. HSP101, an AAA+ ATPase, forms a hexameric ring with a central port. Like other members of the HSP101/clpB family it probably functions as a chaperone in unfolding of the proteins prior to translocation (de Koning-Ward et al, 2009). The novel protein PTEX150 binds strongly to HSP101 and EXP2 and might fulfil a structural role. The role of Trx2 has not been experimentally determined yet but it may help to redox-regulate the complex or hydrolyse disulphide bonds during unfolding of cargo proteins (Elsworth et al, 2014). PTEX88 has no homologues outside of the *Plasmodium* genus and despite lacking information on its function in PTEX *ptex88*<sup>-</sup> deletion parasites show a severe growth defect of ~50% compared to wild-type parasites (Matz et al, 2013).

PTEX components are secreted into the nascent PV as early as 10 minutes after invasion, where they rapidly assemble in distinct foci along the PVM (Bullen et al, 2012; Riglar et al, 2013). The export of the ring-infected erythrocyte surface antigen (RESA) from the merozoites into the erythrocyte within minutes after invasion impressively represents this rapid timing of events (Riglar et al, 2013). The translocon preferentially binds exported over non-exported proteins and colocalizes with artificially trapped reporter

## INTRODUCTION

proteins (de Koning-Ward et al, 2009; Riglar et al, 2013). Interestingly, soluble PEXEL proteins and PNEPs are trapped in the PV when unfolding is inhibited by specific dihydrofolate reductase domains, whereas similarly blocked TM-containing PNEPs are trapped at the parasite plasma membrane (PPM) (Elsworth et al, 2014; Gruring et al, 2012; Heiber et al, 2013). This observation indicates that either a second translocon in the PPM is promoting transfer of TM proteins or PTEX may commonly facilitate export of all these proteins by spanning both the PPM and the PVM (Elsworth et al, 2014). After translocation through the pore in an unfolded manner PEXEL proteins are refolded in the erythrocyte cytoplasm by host as well as parasite-derived chaperones such as HSP70-x/HSP40-like family members (Boddey & Cowman, 2013).

Several different modes are identified for the subsequent trafficking steps depending on the proteins as well as their final destinations (RBC cytosol, cytoskeleton, MCs, RBC surface, knobs, TVN etc.) and there seems to be considerable diversity (Elsworth et al, 2014). While some soluble proteins move through bulk flow, integral (and probably many soluble) proteins are either chaperoned or transported in vesicles, sometimes the solubility profiles even change as shown for PfEMP1 (Haase & de Koning-Ward, 2010; Tilley et al, 2008). Most of the exported proteins transiently or permanently associate with the parasite-induced Maurer's clefts, which represent intermediate sorting compartments that are indispensable for proper assembly of the cytoadherence complex (Dixon et al, 2011; Mundwiler-Pachlatko & Beck, 2013).

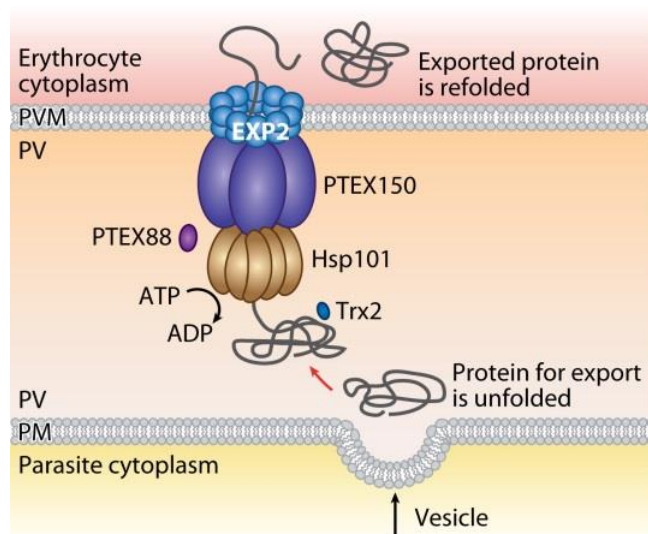


**Figure 9. Model of the *Plasmodium* translocon of exported proteins (Boddey & Cowman, 2013)**

### 1.3.2.3 Alternative export pathways

There is a growing number of PEXEL-negative proteins (PNEPS) identified and although only a few are characterized so far, they likely comprise a much larger repertoire than originally assumed. This seems especially relevant for non-*falciparum* *Plasmodium* species that contain fewer PEXEL proteins (Heiber et al, 2013; Pasini et al, 2013). Most of the known PNEPS localize to Maurer's clefts, such as MAHRP1 and 2, SBP1 or REX1 and 2 and recently PfEMP1 was added to this group (Boddey et al, 2013; Mundwiler-Pachlatko & Beck, 2013). The dissection of PNEP export signals is challenging, since they lack a common conserved motif. Several studies revealed that hydrophobic regions or transmembrane domains as well as certain other sequences within the N-terminal half of the proteins are required for proper entry into the ER and subsequent trafficking into the host cell (Dixon et al, 2008; Gruring et al, 2012; Haase et al, 2009; Pachlatko et al, 2010; Saridaki et al, 2009). PNEPS cannot be cleaved by Plasmepsin V and are not N-acetylated (Boddey & Cowman, 2013). Interestingly, unfolding of these proteins seems to be equally important suggesting a similar mode of translocation across the PVM as observed in PEXEL proteins (Heiber et al, 2013). This hypothesis of a convergence of PEXEL and non-PEXEL protein export at some point is further supported by a recent study that showed how the processed N-terminus of a PEXEL protein functionally replaced the unprocessed N-terminus of a PNEP in promoting the export of a reporter protein (Gruring et al, 2012). However, so far no direct interaction between PNEPs and the PTEX translocon could be confirmed (Boddey & Cowman, 2013).

### 1.3.2.4 The STEVOR protein family

The protein used in this study (gene ID: PF3D7\_0631900, PlasmoDB) belongs to the PEXEL-positive variant subtelomeric variant open reading frame (STEVOR) protein family (Aurrecochea et al, 2009). This group contains 30-40 members of transmembrane domain proteins that are localized to the Maurer's clefts and erythrocyte membrane (Cheng et al, 1998). As a putative function of these proteins the modification of the erythrocytic deformability has been suggested to support vascular sequestration. Furthermore, antigenic variation is implicated to contribute to immune evasion of the parasite (Blythe et al, 2004; Lavazec et al, 2007; Sanyal et al, 2012). According to the

## INTRODUCTION

name the corresponding genes are located in proximity to other variant families such as *var* or *rif* genes within the terminal 50 kb of *Plasmodium* chromosome telomers, a precondition that commonly facilitates duplication and recombination events (Cheng et al, 1998; Mok et al, 2008; Przyborski et al, 2005). Only a subset of *stevor* genes is transcribed in the parasite population at a time, with occasional switching of expression to a different locus (Sanyal et al, 2012). *Stevor* and *rif* genes are related with each other and share a common gene structure consisting of 2 exons that encode a signal peptide in the first exon followed by a PEXEL motif and up to two transmembrane domains in the second exon (Przyborski et al, 2005). A highly polymorphic region within the outer loop between the two transmembrane domains is assumed to confer antigenic variation in these proteins (Sanyal et al, 2012). The expression of STEVOR proteins peaks at 22 to 28 hours post invasion and protein expression was detected in trophozoite, schizont, gametocyte and sporozoite stages as well as in the apical complex of merozoites (Sanyal et al, 2012). The *P. falciparum* 3D7 strain possesses 31 *stevor* genes plus 10 pseudo genes (PlasmoDB, version11.0). The variant used in this study, PF3D7\_0631900 (1023 bp), has been investigated before and encodes a ~34 kilodalton (kDa) protein of 303 amino acids with 2 transmembrane domains that primarily localizes to Maurer's clefts in its full-length version (Figure 10A) (Henrich, 2008; Przyborski et al, 2005).

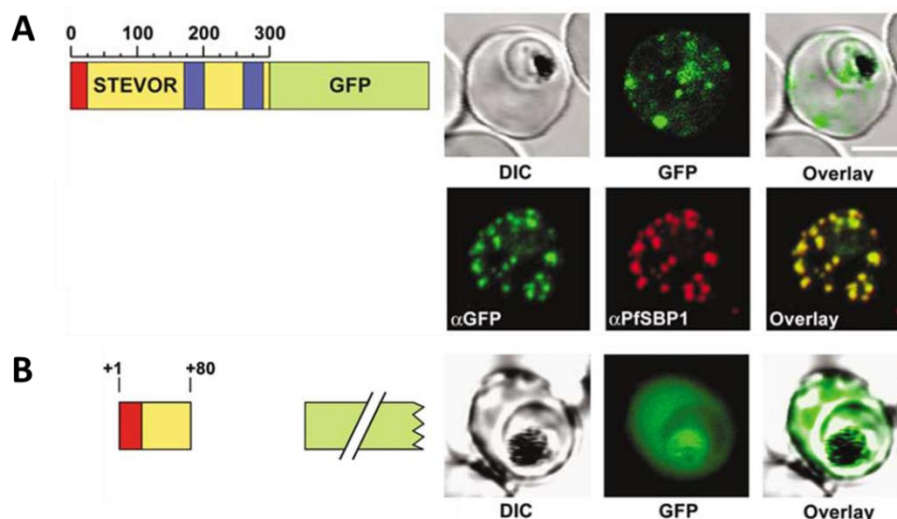


**Figure 10. Full-length STEVOR and STEVOR<sup>1-80</sup> tagged to GFP (Przyborski et al, 2005)**

Left: schematic drawing of the protein with ER signal sequence (red), transmembrane domains (blue) and GFP tag (green). The PEXEL motif is from aa 48-52. Right: Fluorescence images of iRBCs with *P. falciparum* transfectants expressing the (A) full-length and (B) shortened version of STEVOR tagged to GFP. Left, differential interference contrast (DIC); middle, GFP fluorescence; right, overlay. Middle panel of (A) shows IFA using  $\alpha$ -GFP antibodies against STEVOR<sup>GFP</sup> or  $\alpha$ -PfSBP1 antibodies against the Maurer's clefts marker PfSBP1. Modified from Przyborski et al (2005).

In this study a shortened version comprising the first 80 amino acids including the signal peptide, the PEXEL motif (<sup>48</sup>RLLAQ<sup>52</sup>) and enough linker region to separate it from an otherwise interfering green fluorescent protein (GFP) tag was used, as previously published (Knuepfer et al, 2005a; Przyborski et al, 2005). This 9.8 kDa protein (STEVOR<sup>1-80</sup>) is soluble and gets exported via the PEXEL-mediated pathway into the RBC cytosol (Figure 10B).

#### **1.4 N<sup>α</sup>-terminal protein acetylation**

N-terminal acetylation is a very common protein modification in eukaryotes with 50-70% of yeast and 70-90% of human proteins being co-translationally N-acetylated by around 6 classes of N-acetyltransferase complexes (NatA-NatF) with different substrate specificities (Van Damme et al, 2011a). Also ~75% of the plant kingdom proteomes show this chemical modification, which is characterized by the transfer of an acetyl group from acetyl-Coenzyme A (acetyl-CoA) to the  $\alpha$ -amino group of the first amino acid residue of a protein (Figure 11A) (Starheim et al, 2012). The acetylation removes the positive charge of the terminal amino group, thus changing the chemical properties of the protein N-terminus (ibid.). Despite the observed abundance, the exact biological role has remained enigmatic (Hollebeke et al, 2012). However, gene inactivation of NAT complex components in human cell lines was detrimental with oncogenesis and cell division defects thereby pointing to the importance of this mechanism (Bienvenut et al, 2012). Functional relevance in protein stability, localization and interaction has been determined for an increasing amount of cases such as proteasomal targeting by increased ubiquitination or induction of protein interactions such as the components of the neddylation complex (Figure 11B) (Hwang et al, 2010; Shemorry et al, 2013; Starheim et al, 2012). In the context of protein export interesting examples include acetylation-dependent membrane targeting of small GTPases and increased membrane affinity of acetylated alpha-synuclein (Dikiy & Eliezer, 2014; Scott et al, 2011). Remarkably, co-translational N-acetylation following initiator methionine removal seems to inhibit ER-translocation of cytosolic proteins (Forte et al, 2011). In contrast, post-translational acetylation occurs less frequent and is not well understood. Some published examples include certain plant chloroplast proteins (Bienvenut et al, 2012; Zybailov et al, 2008), regulatory peptides and hormones including the  $\alpha$ -melanocyte-stimulating hormone and

## INTRODUCTION

---

b-endorphin in mammals (Polevoda & Sherman, 2000) as well as acetylation of actin (Van Damme et al, 2011b). The connection between acetylation and cellular metabolism through its substrate, acetyl-CoA, is intriguing. It was shown that different acetyl-CoA levels influenced cellular proliferation by regulating acetylation-dependent apoptosis-regulatory proteins similar to the observed regulation of histone lysine acetylation and subsequent gene activation (Starheim et al, 2012). The involvement of NATs in cancer is controversial with studies pointing towards oncogenic as well as tumour suppressor function (ibid.). It is still unknown, if N-terminal acetylation is irreversible, as previously assumed, or reversible by yet undiscovered deacetylases like in the case of histones (HDACS).

Different NATs of diverse subunit composition facilitate the acetylation of their specific substrates, and especially higher eukaryotes show an increase in complexity through gene duplications and different splice variants (Hollebeke et al, 2012). Most of the enzymes are found in association with ribosomes and facilitate co-translational catalysis, but some of them also exist in a non-ribosomal state, especially in higher eukaryotes, where they act on different targets or independent of the complex as single subunits (Starheim et al, 2012). The major NAT representing the largest class of substrates with a strong evolutionary sequence conservation from lower to higher eukaryotes is the NatA complex, which is composed of the catalytic subunit Naa10p (Ard1p) and the auxiliary subunit Naa15p (Nat1p) (Arnesen et al, 2009). NatA acetylates S-, A-, T-, G-, V- and C-N termini after the initiator methionine is removed by aminopeptidases (Arnesen et al, 2009). The other NATs (NatB-NatF) acetylate the initiator methionine dependent on the following second amino acid residue. The NatB complex acetylates substrates with M-D-, M-E-, M-N- and M-Q-N termini and is important for acetylation of actin and tropomyosin. NatC prefers M-L-, M-F-, M-I- and M-W. NatD has only two substrates, the histones H2A and H4, and recognizes a longer stretch in the substrate than the other NATs. NatE, although partly composed of the same subunits as NatA, acetylates a specific set of N termini with methionines followed by hydrophobic residues and has been implicated in sister chromatid cohesion and chromosome resolution. Recently, NatF was identified in higher eukaryotes only. It also acetylates M-L-, M-F-, M-I- and M-W- and M-K-N termini (Starheim et al, 2012). The biological roles of these NATs are still subject to intense research. In the context of post-translational N-terminal

acetylation, it is worth mentioning that most of the (few) studies on yeast and plant acetylomes identified substrate specificity for NatA, meaning an overrepresentation of S-, A-, V- and T- N-termini predicted post-cleavage (Bienvenut et al, 2012; Helsens et al, 2011).

In *Plasmodium* information on acetylation in general is still lacking and rather limited to lysine acetylation of histones and actin (Chung et al, 2009; Goyal et al, 2012; Miao et al, 2013; Schmitz et al, 2005). The process of post-translational N-acetylation as described for PEXEL proteins after cleavage in the ER is highly interesting and the identification of the NAT that is responsible for this modification would mean considerable progress. Previous publications suggested some candidates, but so far without providing any further evidence (Boddey & Cowman, 2013; Chang et al, 2008; Osborne et al, 2010).

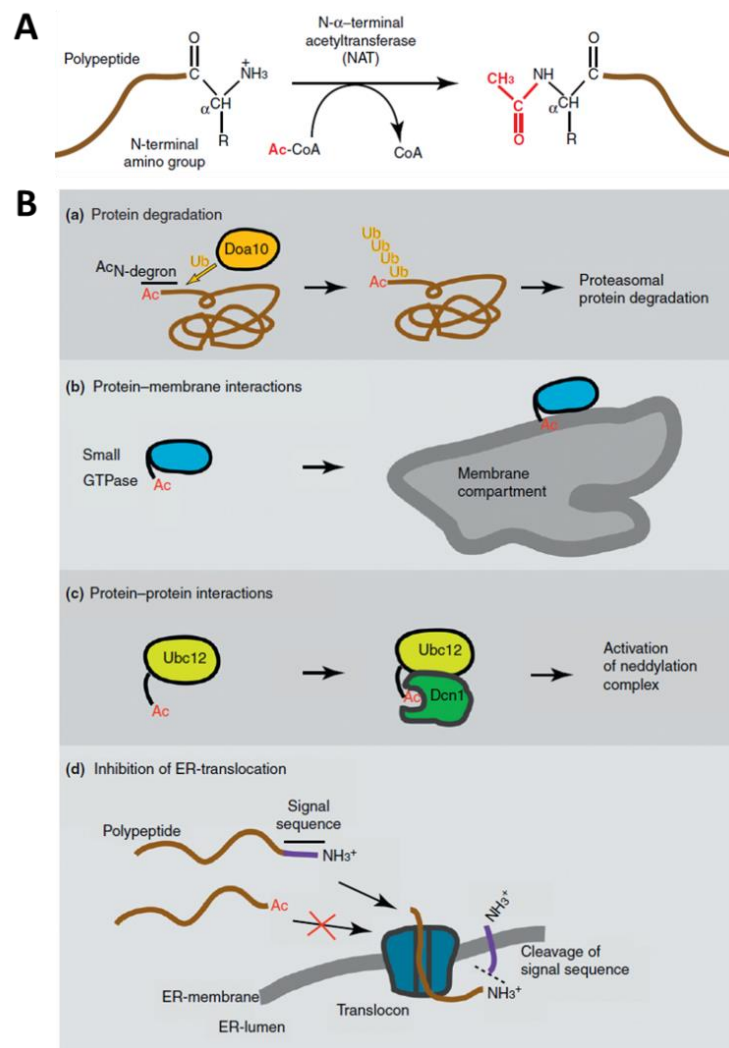


**Figure 11. Molecular functions of N-terminal acetylation (Starheim et al, 2012)**

(A) Chemical process of N-terminal acetylation catalysed by a NAT enzyme. (B) Examples of functional studies on the effects of this modification. Modified from Starheim et al (2012)



## 1.5 Aim of the study

The invasion of human erythrocytes by *P. falciparum* is accompanied by extensive parasite-induced modifications of the host cell, which contribute to parasite survival, cytoadhesion and host immune system evasion. The establishment of a protein export system to translocate hundreds of effector proteins into the terminally differentiated erythrocyte is a necessary prerequisite for this remodelling process. The majority of exported proteins are characterized by the PEXEL motif that is enzymatically processed in the parasite and proved to be essential for proper targeting beyond the parasitophorous vacuole (Hiller et al, 2004; Marti et al, 2004). It is of considerable interest to understand this bottleneck in the export mechanism as an attractive target for therapeutic interventions.

The aim of the first part of this study was to dissect the function of each position of the PEXEL motif by conducting a mutagenesis screen on the model protein STEVOR<sup>1-80</sup> (Przyborski et al, 2005). In detail, the capability of certain amino acids to functionally replace the wild-type counterparts in guiding proper processing and export of the mutant proteins was assessed. In continuation of previous work by P. Henrich (2008) positions 2 to 4 of the pentameric export motif were subjected to various amino acid replacements followed by transfection of *P. falciparum* parasites. The export phenotypes of the mutant GFP-tagged STEVOR<sup>1-80</sup> proteins were analysed by confocal fluorescence microscopy. Furthermore, some representative mutants were chosen for mass spectrometry analysis to determine their processing state with respect to cleavage and acetylation of the export motif. The repetition of certain replacements in a second PEXEL protein, KAHRP, should give information about the reproducibility of previous results.

The second part of this study focussed on the process of N-terminal acetylation after cleavage of the PEXEL motif in the endoplasmic reticulum (Chang et al, 2008). Of particular interest was the identification of a putative N-acetyltransferase that could be responsible for this common modification among exported proteins. The expression and localization of the candidate enzyme in *P. falciparum* parasites was determined with fluorescent reporter tags, also in the endogenous genomic background. Furthermore, the functional role was investigated by attempted deletion of the respective gene as well as conditional downregulation of the enzyme on protein level. A better understanding of PEXEL-mediated protein export can hopefully be achieved through this study.



## 2 Materials and Methods

Most of the methods mentioned in this chapter follow standard laboratory procedures for *P. falciparum* experiments and were already described in my diploma thesis (Risch, 2009). For the sake of completeness, these parts are copied here, whereas newly introduced methods are marked with an asterisk\*.

### 2.1 Materials

#### 2.1.1 Equipment

Analytical scales	Sartorius, Göttingen
Autoclave	Tuttnauer Systec 2540, Wettenberg
Camera, DC 120 Zoom digital	Kodak, New York
Centrifuges	
J2-MC	Beckman, Krefeld
RC5BPlus	Sorvall, Langenselbold
Megafuge 2.0R	Heraeus Instruments, Hanau
Megafuge 1.0R	Heraeus Instruments, Hanau
L-60 Ultracentrifuge	Beckman, Krefeld
Biofuge fresco	Heraeus Instruments, Hanau
Microcentrifuge MC13	Amicon Bioseparatia/ Millipore
CCD Camera	Princeton Instruments, USA
Computer-software	
Adobe Photoshop® 5.0	Adobe Systems Inc, USA
Bioedit	<a href="http://www.mbio.ncsu.edu/BioEdit/bioedit">http://www.mbio.ncsu.edu/BioEdit/bioedit</a>
CellQuest Pro	Becton Dickinson
ClustalW	<a href="http://www.ebi.ac.uk/Tools/clustalw/">http://www.ebi.ac.uk/Tools/clustalw/</a>
EndNote X6	ISI Research Soft, CA, USA
Expasy Proteomics server	<a href="http://www.expasy.ch/tools/pi_tool.html">http://www.expasy.ch/tools/pi_tool.html</a>
FIJI image analysis	<a href="http://fiji.sc/Fiji">http://fiji.sc/Fiji</a>
InterProScan4	<a href="http://www.ebi.ac.uk/Tools/pfa/iprscan/">http://www.ebi.ac.uk/Tools/pfa/iprscan/</a>
Kodak Digital Science 1D	Kodak, New York, USA
MS Powerpoint 2010	Microsoft Corporation, CA USA

## MATERIALS AND METHODS

---

MS Word 2010	Microsoft Corporation, CA USA
MS Excel 2010	Microsoft Corporation, CA USA
Mozilla Firefox	Microsoft Communications Corp., USA
Protein Data Bank	<a href="http://www.rcsb.org/pdb/home/home.do">http://www.rcsb.org/pdb/home/home.do</a>
pDRAW32 software	AcaClone software
PlasmoDB	<a href="http://plasmodb.org/plasmo/">http://plasmodb.org/plasmo/</a>
PSIPRED	<a href="http://bioinf.cs.ucl.ac.uk/psipred/">http://bioinf.cs.ucl.ac.uk/psipred/</a>
Serial Cloner 2.6	<a href="http://serialbasics.free.fr/Serial_Cloner.html">http://serialbasics.free.fr/Serial_Cloner.html</a>
SigmaPlot 11.0; 12.0	Systat Software Inc.
SMART	<a href="http://smart.embl-heidelberg.de/">http://smart.embl-heidelberg.de/</a>
Swiss-Model Server	<a href="http://swissmodel.expasy.org/">http://swissmodel.expasy.org/</a>
Zeiss Image Examiner	Zeiss, Jena
DNA electrophoresis apparatus	Biorad, München
Electroporator Gene Pulser® II	Biorad, München
Film developer	Hyperprocessor Amersham Biosciences, Freiburg
Film exposition cassettes	Sigma, Taufkirchen
Freezer -80°C, UF85-300S	Heraeus GmbH, Hanau
Freezers -20°C	Liebherr, Biberach
Fridges	Liebherr, Biberach
Gas burner gasprofi 1 micro	WLD-TEC
Heat block, Digi-block JR	Laboratory devices INC, USA
Icemachine AF 30	Scotsman, Milano, Italy
Incubator ( <i>P. falciparum</i> )	Heraeus Instruments
Incubator shaker Innova 4000/4300	New Brunswick Scientific Co. Inc.
Liquid nitrogen tank	Air Liquide, Ludwigshafen
MACS system	Miltenyi Biotec, Bergisch Gladbach
Magnetic stirrer	Heidolph, Schwabach
Microscopes:	
Confocal laser scanning microscope LSM 510	Zeiss, Jena
Light optical microscope Axiolab	Zeiss, Jena
Microwave oven	AEG, Nürnberg

---

GeneAmp PCR system 9700	AppliedBiosystems, CA USA
pH-meter pH 537	WTW, Weilheim
Pipetman Gilson P10; P20; P200; P1000	Abimed, Langenfeld
Pipetus- akku	Hirschmann Labortechnik, Eberstadt
pipetus® standard	Hirschmann Labortechnik, Eberstadt
Power supply: Power Pac 300	Biorad, München
Protein electrophoresis systems	Biorad, München
Printer hp LaserJet 1300	Hewlett Packard, Heidelberg
Quartz cuvettes	Hellma, Müllheim
Rotors: SS-34; GS-3	DuPont Instruments, Bad Homburg
	Beckman instruments, Palo Alto, CA, USA
Semidry Blot System	Genmall Biotechnology Co.,Ltd
Spectrophotometer UVIKON 923	Kontron Instruments,
Sterile work bench Herasafe	Heraeus Instruments, Hanau
Stop watch	Roth, Karlsruhe
UV-lamp Typ N-6 L	Benda Laborgeräte und Ultravioletstrahler
UV-Transilluminator	Gibco BRL, Karlsruhe
Vortex Genie 2	Roth, Karlsruhe
Water bath Julabo 7A	Julabo, Seelbach

### 2.1.2 Disposables

Aluminium foil	Roth, Karlsruhe
Cell culture plates	Greiner Bio-One, Kremsmünster
Centrifugation tubes, Polypropylen-12/75	Greiner Bio-one, Kremsmünster
Centrifugation tubes,	Greiner Bio-one, Kremsmünster
Polystyren-6, 0/38 mm	
Clingfilm Saran	Dow Chemical Company, Schwalbach
Coverslides	Roth, Karlsruhe
Cryovials	Nalgene®, Wiesbaden
Cuvettes	Sarstedt, Nümbrecht
Electroporation cuvettes	Biorad, München
Eppendorf tubes	Sarstedt, Nümbrecht

## MATERIALS AND METHODS

---

Falcon tubes (15 ml; 50 ml)	Corning incorporation, Bodenheim
Film BioMax MR	Kodak, New York, USA
Gloves	Hartmann, Heidenheim
Immersion oil	Zeiss, Jena 25
Kimwipes lite 200	Kimberly Clark
MACS-columns CS	Miltenyi Biotec, Bergisch Gladbach
Object slides	Marienfeld, Lauda-Königshofen
Parafilm	American International CanTM, USA
Plastic pipettes (1 ml; 2 ml; 5 ml; 10 ml; 25 ml)	Corning incorporation, Bodenheim
Pipette tips	Corning incorporation, Bodenheim
PVDF membrane	Biorad, München
Sterile filters (0,2 µm)	Millipore GmbH, Ashburn
Sterile filtration devices	Corning incorporation, Bodenheim
Thermo well PCR tubes	Corning incorporation, Bodenheim
WhatmanTM 3MM paper	Firma Whatman Paper Company
96-well plates, black, clear	Greiner Bio-One, Kremsmünster

### 2.1.3 Chemicals

The chemicals used in this study are from the firms Roth, Merck, Sigma, Serva, Thermo and Applichem and were ordered directly or through the Heidelberg Medical faculty.

### 2.1.4 Biological material

#### Enzymes and DNA/ Protein markers

1 kb Plus DNA-ladder	Fermentas, St.Leon-Rot
Page Ruler, prestained protein ladder+	Fermentas, St. Leon-Rot
Restriction enzymes	New England BioLabs, Schwalbach
DNA-polymerase EuroTaq	BioCat, Heidelberg
DNA-polymerase Phusion	Finnzymes, Finland
SAP	Promega, Mannheim
T4-DNA-Ligase	Invitrogen, Karlsruhe 26

**Kits**

High Pure Plasmid Isolation Kit	Roche, Mannheim
Gel Extraction/PCR purification Kit	Qiagen, Hilden
MaxiPrep Kit	Qiagen, Hilden
DNeasy Blood&Tissue Kit	Qiagen, Hilden
BM Chemiluminescence Blotting Substrate (POD)	Roche, Mannheim
SuperScript II RT Kit	Invitrogen, Karlsruhe
HisPur™ Cobalt Spin Columns	ThermoFisher Scientific, Ulm
Rapid DNA ligation Kit	Fermentas, St. Leon-Roth

**Antibodies**

mouse $\alpha$ -GFP monoclonal	Roche, Mannheim
rabbit $\alpha$ -mouse IgG POD	Dianova, Hamburg

**Parasite strains**

For this study, the 3D7 strain of *P. falciparum* parasites was used for transfection and genetic recombination techniques (Ponnudurai et al, 1981; Walliker et al, 1987). For the studies on DiCre-mediated excision a special 3D7 strain named 1G5 was kindly provided by M. Blackman. This strain is characterized by constitutive expression of the DiCre recombinase from the SERA 5 locus (Collins et al, 2013).

***Escherichia coli* (*E. coli*) strains**

Since the genome of *P. falciparum* and hence the transfection vector is very rich in AT-sequences, passage through bacteria can be difficult and unstable (Baca & Hol, 2000). The use of the special *E. coli* strain XL1-Blue improves transformation stability (Chahaun, 2002). Protein expression for purification purposes was carried out in BL21-CodonPlus-RIL bacteria (Stratagene, California), which harbour extra copies for tRNA genes (arginine $U$ -, leucine $W$ -and isoleucine $Y$ -tRNA) for optimal expression of heterologous proteins of organisms with A/T-rich genetic sequences (Flick et al, 2004). These bacterial cells were kindly provided by Dr. B. Derrer.

### **Vectors**

The pARL1a+-vector was originally provided by T. W. Gilberger (Wrenger & Muller, 2004) and is the standard episomal vector used in our laboratory for the transfection of *P. falciparum*. This vector harbours the 5' UTR of *PfCRT*, which was removed in this study for single crossover recombination experiments. Furthermore, the plasmid encodes GFP, the ampicillin resistance marker and human DHFR (hDHFR) that confers resistance of the parasites to the positive selection marker WR99210 (Hastings & Sibley, 2002). Alternatively, the positive selection marker cassette was exchanged with the blasticidin S deaminase gene from *Aspergillus terreus*, which confers resistance to blasticidin S (Mamoun et al, 1999). For double-knockout studies in the parasites, the pCC and pHTK vectors were used, which have the previously mentioned positive selection marker cassettes as well as negative selection marker genes that drive sensitivity to 5-fluorocytosine (5-FC) and ganciclovir, respectively (Duraisingh et al, 2002; Maier et al, 2006). These plasmids were kindly provided by A. Maier (pCC) and N. Hertrich (pHTK). For the conditional gene excision strategy using the loxP/DiCre system, the pHH1-SERA5del3-preDiCre vector was kindly provided by M. Blackman (Collins et al, 2013). It harbours two loxP sites in the CAM and PbDT UTRs, a multiple cloning site to introduce homology regions of interest (by replacing the SERA 5 gene fragment) and the hDHFR positive selection marker cassette. The vectors for the destabilization domain (DD) system were kindly provided by M. Azevedo (DD24 tag) as well as M. Ganther (DD29 tag) (de Azevedo et al, 2012). For conditional downregulation of the putative transferase (PfNAT), the DD24 domain (including an HA tag) was cloned into the previously generated pARL-PfNAT-GFP recombination vector. For protein expression the pET28a+ expression vector was used (Novagen), which was kindly provided by Dr. B. Derrer. Vector maps see Appendix.

### **Oligonucleotides + Polynucleotides**

Primers were obtained from Thermo Scientific (Ulm). Sequencing was carried out by GATC (Konstanz). Synthetic sequences of the putative transferase (PfNAT) were generated by GeneArt® at Life technologies (Darmstadt).

General primers

pARL-80 fwd	5' CTATAATATCCGTTAATAATAAATACACGCAG 3'
pARL +70 rev	5' CATAACATTTTTACAGTTATA 3'
GFP +80 rev	5' CAGAAAATTTGTGCCCATTAAC 3'
M13 fwd	5' GTAAAACGACGGCCAG 3'
M13 rev	5' CAGGAAACAGCTATGAC 3'
HA tag +26 rev	5' GCATAGTCAGGAACATCGTAAGGGTA 3'
3xHA_KpnI for	5' TGTGGTACCTACCCGTACGACGTCCCGG 3'
CAD AvrII for	5' TGATAGCCTAGGGGAGTGCAGGTGGAAACC 3'
pTEX150 -61 for	5' CACAGGAAACAGCTATGAC 3'

STEVOR<sup>1-80</sup> and KAHRP<sup>1-69</sup> mutagenesis

stev80AvrIIrev	5' TGATAGCCTAGGTTTCTTTATTGCGTCTTCGTTC 3'
stevXhoI for	5' TGTTAGCTCGAGATGAAGATGTATAACCTTAAAATGTT ATTG 3'
stevL49D for	5' CGATAAAATCAAGAGATTTAGCACAAACCC 3'
stevL49D rev	5' GGGTTTGTGCTAAATCTCTTGATTTTATCG 3'
stevL49E for	5' CGATAAAATCAAGAGAATTAGCACAAACCC 3'
stevL49E rev	5' GGGTTTGTGCTAATTCTCTTGATTTTATCG 3'
stevL49H for	5' CGATAAAATCAAGACATTTAGCACAAACCC 3'
stevL49H rev	5' GGGTTTGTGCTAAATGTCTTGATTTTATCG 3'
stevL49M for	5' CGATAAAATCAAGAATGTTAGCACAAACCC 3'
stevL49M rev	5' GGGTTTGTGCTAACATTCTTGATTTTATCG 3'
stevL49Q for	5' CGATAAAATCAAGACAATTAGCACAAACCC 3'
stevL49Q rev	5' GGGTTTGTGCTAATTGTCTTGATTTTATCG 3'
stevL49R for	5' CGATAAAATCAAGAAGATTAGCACAAACCC 3'
stevL49R rev	5' GGGTTTGTGCTAATCTTCTTGATTTTATCG 3'
stevL49W for	5' CGATAAAATCAAGATGGTTAGCACAAACCC 3'
stevL49W rev	5' GGGTTTGTGCTAACCATCTTGATTTTATCG 3'
stevL49Y for	5' CGATAAAATCAAGATATTTAGCACAAACCC 3'
stevL49Y rev	5' GGGTTTGTGCTAAATATCTTGATTTTATCG 3'
stevL50D for	5' CGATAAAATCAAGACTCGATGCACAAACCC 3'
stevL50D rev	5' GGGTTTGTGCATCGAGTCTTGATTTTATCG 3'
stevL50E for	5' CGATAAAATCAAGACTCGAAGCACAAACCC 3'
stevL50E rev	5' GGGTTTGTGCTTCGAGTCTTGATTTTATCG 3'
stevL50H for	5' CGATAAAATCAAGACTCCATGCACAAACCC 3'
stevL50H rev	5' GGGTTTGTGCATGGAGTCTTGATTTTATCG 3'
stevL50M for	5' CGATAAAATCAAGACTCATGGCACAAACCC 3'

## MATERIALS AND METHODS

---

stevL50M rev	5' GGGTTTGTGCCATGAGTCTTGATTTTATCG 3'
stevL50Q for	5' CGATAAAATCAAGACTCCAAGCACAAACCC 3'
stevL50Q rev	5' GGGTTTGTGCTTGGAGTCTTGATTTTATCG 3'
stevL50R for	5' CGATAAAATCAAGACTCAGAGCACAAACCC 3'
stevL50R rev	5' GGGTTTGTGCTCTGAGTCTTGATTTTATCG 3'
stevL50W for	5' CGATAAAATCAAGACTCTGGGCACAAACCC 3'
stevL50W rev	5' GGGTTTGTGCCAGAGTCTTGATTTTATCG 3'
stevL50Y for	5' CGATAAAATCAAGACTCTATGCACAAACCC 3'
stevL50Y rev	5' GGGTTTGTGCATAGAGTCTTGATTTTATCG 3'
stevA51D for	5' ATCAAGACTCTTAGATCAAACCCAAATCC 3'
stevA51D rev	5' GGATTTGGGTTTGATCTAAGAGTCTTGAT 3'
stevA51E for	5' ATCAAGACTCTTAGAACAAACCCAAATCC 3'
stevA51E rev	5' GGATTTGGGTTTGTCTAAGAGTCTTGAT 3'
stevA51H for	5' ATCAAGACTCTTACATCAAACCCAAATCC 3'
stevA51H rev	5' GGATTTGGGTTTGATGTAAGAGTCTTGAT 3'
stevA51M for	5' ATCAAGACTCTTAATGCAAACCCAAATCC 3'
stevA51Mrev	5' GGATTTGGGTTTGCATTAAGAGTCTTGAT 3'
stevA51Q for	5' ATCAAGACTCTTACAACAAACCCAAATCC 3'
stevA51Q rev	5' GGATTTGGGTTTGTGTAAGAGTCTTGAT 3'
stevA51R for	5' ATCAAGACTCTTAAGACAAACCCAAATCC 3'
stevA51R rev	5' GGATTTGGGTTTGTCTTAAGAGTCTTGAT 3'
stevA51T for	5' ATCAAGACTCTTAACACAAACCCAAATCC 3'
stevA51T rev	5' GGATTTGGGTTTGTGTTAAGAGTCTTGAT 3'
stevA51W for	5' ATCAAGACTCTTATGGCAAACCCAAATCC 3'
stevA51W rev	5' GGATTTGGGTTTGGCATAAGAGTCTTGAT 3'
stevA51Y for	5' ATCAAGACTCTTATATCAAACCCAAATCC 3'
stevA51Y rev	5' GGATTTGGGTTTGATATAAGAGTCTTGAT 3'
stevQ52D for	5' ATCAAGACTCTTAGCAGATACCCAAATCC 3'
stevQ52D rev	5' GGATTTGGGTATCTGCTAAGAGTCTTGAT 3'
stevQ52E for	5' ATCAAGACTCTTAGCAGAAACCCAAATCC 3'
stevQ52E rev	5' GGATTTGGGTTTCTGCTAAGAGTCTTGAT 3'
stevQ52H for	5' ATCAAGACTCTTAGCACATACCCAAATCC 3'
stevQ52H rev	5' GGATTTGGGTATGTGCTAAGAGTCTTGAT 3'
stevQ52K for	5' ATCAAGACTCTTAGCAAAGACCCAAATCC 3'
stevQ52Krev	5' GGATTTGGGTCTTTGCTAAGAGTCTTGAT 3'
stevQ52M for	5' ATCAAGACTCTTAGCAATGACCCAAATCC 3'
stevQ52Mrev	5' GGATTTGGGTGATTGCTAAGAGTCTTGAT 3'
stevQ52N for	5' ATCAAGACTCTTAGCAAATACCCAAATCC 3'
stevQ52N rev	5' GGATTTGGGTATTTGCTAAGAGTCTTGAT 3'



## MATERIALS AND METHODS

---

PF14\_0350\_aa530\_XhoI rev 5' TGTTAGCTCGAGAAAATCATCTTTATTAAGTATTTTTGAC 3'  
PF14\_0350\_bp1111\_NotI for 5' TTGGCGGCCGCGAAAGATACATCATCTACACAGAATGTG 3'  
PF14\_0350\_bp1111\_XhoI for 5'TGTTAGCTCGAGGAAAGATACATCATCTACACAGAATGTG  
PF14\_0350\_bp1303 rev 5' CTATACCTACACATCCTAC 3'  
PF14\_0350\_bp1304 for 5' TACCGTTTAAAGGTGACAATAC 3'  
PF14\_0350\_bp357 rev 5' TTCCAAATCTGGGCAATCTTTTC 3'  
PF14\_0350\_bp358 for 5' AATTTATATAAGAGTTACATTAAC 3'  
PF14\_0350\_locus 5' for 5' GTTATTATTTATTCGTGATCTAAACAAATAG 3'  
PF14\_0350\_locus 5' rev 5' ATTGATGATACTGTGTAAATAATGATTAC 3'  
FLAG (-) AvrII+KpnI 5' CCTACTTGTCATCGTCGTCCTTGTAATCC 3'  
FLAG (-) AvrII+KpnI w/o stop 5' CTTGTCATCGTCGTCCTTGTAATCC 3'  
FLAG (+) AvrII+KpnI 5' CTAGGGATTACAAGGACGACGATGACAAGTAGGGTAC 3'  
FLAG (+) AvrII+KpnI w/o stop 5' CTAGGGATTACAAGGACGACGATGACAAGGGTAC 3'

### Colocalization with other ER proteins

mCherry BamHI for 5' CGCGGATCCATGGTGAGCAAGGGCGAG 3'  
mcherry KpnI XmaI rev (no stop) 5' CGCCCGGGTACCTTTCTTGACAGCTCGTCCATG 3'  
PF10\_0360 XhoI for 5' TGTTAGCTCGAGATGTTCAATCGTTTATTTG 3'  
PF10\_0360 AvrII rev 5' TGATAGCCTAGGAAATTCTTTTCCAATATATTTTCG 3'  
Plasm.V\_Xho I for 5' TGTTAGCTCGAGATGAATAATTATTTTTTAAGGAAAG 3'  
Plasm. V\_Avr II rev 5' TGATAGCCTAGGTGTTGATTCTGTATGGGAG 3'

### Active-site mutagenesis

PF14\_0350\_GtoA1381\_for 5' GAATGAGAATTGCTAGCCGATTATTAAC 3'  
PF14\_0350\_GtoA1381\_rev 5' GTTAATAATCGGCTAGCAATTCTCATTC 3'  
PF14\_0350\_GtoA1500\_for 5' GTTAAGCAAAATGCTTTTAATTTATCTC 3'  
PF14\_0350\_GtoA1500\_rev 5' GAGATAAATTTAAAGCATTTTGCTTAAC 3'  
PF14\_0350\_YtoA1480\_for 5' CTGATAGCTTAGCTTTCGTTAAGC 3'  
PF14\_0350\_YtoA1480\_rev 5' GCTTAACGAAAGCTAAGCTATCAG 3'  
PF14\_0350\_RtoM1365\_for 5' GTAAAAAAGATAAATATGAGAATGAGAATTG 3'  
PF14\_0350\_RtoM1365\_rev 5' CAATTCTCATTCTCATATTATCTTTTTTTAC 3'  
PF14\_0350\_TandN1460\_for 5' GAATTTAAAGTTTTTGTAAACAATTTACTTACTGATAGC 3'  
PF14\_0350\_TandN1460\_rev 5' GCTATCAGTAAGTAAATTGTAAACAAAACTTTTAATTC 3'

### Knockout of PfNAT via pCC and pHTK system

PF14\_Flank 5' SacII for 5' TGACCGCGGGAAGATTTTTCAATTGTTGATGGATG 3'  
PF14\_Flank 5'SpeI rev 5' TGTTAGACTAGTGCTTAAATATATTCATCCTTCCCTTCTC 3'  
PF14\_Flank 3' NcoI for 5' TGTTAGCCATGGCTTTGCTTCTACAGAAATACAGAGC 3'

PF14_Flank 3' AvrII rev	5' TAGTCCTAGGGATATACATGAAGAAACACACCCTC 3'
PF14_InGene 5' SacII for	5' TGACCGCGGGATTAATATATTTAAGCAGAAAGAGAATAC 3'
PF14_InGene 5' SpeI rev	5' TGATGACTAGTCATCCTTCCACGTTAATGTAACTC 3'
PF14_InGene 3' NcoI for	5' TGATACCATGGCTCAAATTGTTAGGAGAGGTCTAATG 3'
PF14_InGene 3' AvrII rev	5' TAGTCCTAGGTCAATCCAAGATATTATTTGTATAGCTC 3'
pcc4_BSDcass_for	5' GCATAAGCCTTTGTCTCAAG 3'
pcc4_BSDcass_rev	5' CTTAGCCCTCCCACACAT 3'
pcc4_CDcass_for	5' GGTAAACACAGTAGTATCTG 3'
pcc4_CDcass_rev	5' CTACTCCGATAGAATCATCAG 3'
pHTK MCS 5' for	5' CTATATACTATGGAATACTAAATATATATCCAATGG 3'
pHTK MCS 5' rev	5' CTCAGAGATTGCATGCAAGC 3'
pHTK MCS 3' for	5' CTAATCATGTAAATCTTAAATTTTTTC 3'
pHTK MCS 3' rev	5' GTGTGAAATACCGCACAGATG 3'
pHTK_hDHFRcass_for	5' CATGGTTCGCTAAACTGCATC 3'
pHTK_hDHFRcass_rev	5' CCTTTCTCCTCCTGGACATC 3'
pHTK_TKcass_for	5' CTATTTACATGCATGTGCATGC 3'
pHTK_TKcass_rev	5' CAATACGGTGCGGTATCTGC 3'

#### Knockout of PfNAT via loxP/DiCre system

PF14_0350full_synth_XhoI for	5' TGTTAGCTCGAGATGAACATCTTCAAGCAAAAAG 3'
PF14_0350full_synth_AvrII rev	5' TGATAGCCTAGGATCCAAGATATTGTTGGTGTAG 3'
PF14_C-term_chim_SpeI for	5' CTAGACTAGTAGGAAAATTTCCGGAAGCG 3'
PF14_C-term_chim_loxP_HindIII rev	5' CCCAAGCTTTAATAACTTCGTATAATGTATGCTATACG AAGTTATTTTATTTTTTTTTTCGTTAGAAC 3'
PF14_C-term_synth_no Hind_for	5' TTGTTGTTCAACATCTCCGAAATC 3'
PF14_C-term_synth + 41 rev	5' CAT GAA GTG TCT GTT GGA G 3'
PF14_C-term_synth_XhoI rev	5' GGTACCCTCGAGATCCAAGATGTTG 3'
PF14_5'UTR_chim_SpeI for	5' TGATGACTAGTGAAGATTTTTCAATTGTTGATGGATG 3'
PF14_5'UTR_chim_HindIII rev	5'CCCAAGCTTTTAATTTATATTTTTTTATTTTTTATTTAATAC 3'
PF14_1st intron_HindIII rev	5' CAAGCTTTATTATAATATATATATGTTTTCCATAAG 3'
PF14_0350_fullsynth+120 rev	5' GTCTCTTTCTTCCAATTGTCTG 3'
PF14_0350_fullsynth+167 rev	5' TCAATGAGTTGAAGTGGTCG 3'
DiCre_Cre60 for	5' CCAGCAGCCTCACCATGGCC 3'
DiCre_Cre60 rev	5' CTGCCTCGCCCTTCTGACTCC 3'
CAM5' _BamHI for	5' CGCGGATCCTGATATATTTCTATTAGG 3'
CAM5' _SpeI rev	5' TGATGACTAGTAACCATTTTGTAAAAAAAATTTAAAATA 3'
PbDT3'UTR_AvrII for	5' TAGTCCTAGGGTCGAGGGATATGGCAGC 3'
PbDT3'UTR_NotI rev	5' TTGGCGGCCGCTACCCTG 3'

## MATERIALS AND METHODS

---

### Knockdown of PfNAT via DD system

DD24_KpnI for	5' CGGGGTACCATGGGAGTGCAGGTGGAAACC 3'
DD24_BspEI rev	5' TGTTAGTCCGGATTATTCCAGTTCTAGAAGCTCCACATC 3'
DD +22 rev	5' GGTTTCCACCTGCACTCC 3'
pCRK4-DD24 rev	5' TTGGGGAAGGTGCGCCCG 3'
PF14_0350_MluI rev	5' CGGCACGCGTATCCAAGATATTATTTGTATAGC 3'
PF14_0350_XhoI rev	5' TGTTAGCTCGAGATCCAAGATATTATTTGTATAGC 3'

### **2.1.5 Buffers, media and solutions**

Albumax II	5% (w/v) Albumax II in RPMI 25 mM HEPES L-Glutamine (Gibco), filter sterilize
ampicillin stock, 1000x	100 mg/ml in ddH <sub>2</sub> O
AP21998 stock, 1000x	1 mM in absolute ethanol
aprotinin stock, 200x	10 mg/ml in ddH <sub>2</sub> O
APS	10% (w/v) APS in ddH <sub>2</sub> O
Bacteria lysis buffer	50 mM Tris pH 8 2 mM EDTA 100 µg/ml lysozyme 0.1% TritonX-100
Cell culture media	
Non-transfectants	10% human serum 0.2 µg/ml Gentamycin 0.2 mM Hypoxanthine in RPMI 25 mM HEPES L-Glutamine (Gibco)
Transfectants	5% human serum 5% Albumax II 0.2 µg/ml Gentamycin 0.2 mM Hypoxanthine in RPMI 25 mM HEPES L-Glutamine
Coomassie Destaining Solution	20% methanol 7,5% acetic acid

---

Coomassie Staining Solution	5% methanol 10% acetic acid 0.05% Coomassie Brilliant Blue R-250
Cytomix	120 mM KCl 0.15 mM CaCl <sub>2</sub> 10 mM K <sub>2</sub> HPO <sub>4</sub> / KH <sub>2</sub> PO <sub>4</sub> , pH: 7.6 25 mM HEPES/2 mM EGTA pH 7.6 5 mM MgCl <sub>2</sub> in ddH <sub>2</sub> O adjust to pH 7.6 with KOH filter sterilize
DNA loading buffer	60% glycerol 60mM EDTA 0.25% Bromphenol Blue
Freezing Solution	6.2 M glycerol 0.14 M Na-lactate 0.5 mM KCL add ddH <sub>2</sub> O, adjust to pH 7.2 with 0.5 M NAHCO <sub>3</sub> , pH 9, filter sterilize
Gelatin Solution	0.5% (w/v) gelatin in HEPES-buffered RPMI 1640 filter sterilize
IC <sub>50</sub> lysis buffer	20mM Tris base (2.423g) in 1L adjust pH to 7.4 with concentrated HCl 5mM EDTA (10ml 0.5M EDTA) 0.008% w/v saponin (80mg saponin) 0.08% w/v Triton X-100 (0.8ml) mix, vacuum filter, store at RT for assay analysis: mix 10ml of lysis buffer with 1.2 µl SYBR green (10,000x final)
LB agar	10 g tryptone 5g yeast extract 5g NaCl

## MATERIALS AND METHODS

---

	15g agar
	ad 1l ddH <sub>2</sub> O
leupeptin stock, 250x	5 mg/ml in ddH <sub>2</sub> O
MACS buffer	1x PBS
	2 mM EDTA
	0.5% BSA
PBST	1xPBS
	0.1% Tween 20
PHEM buffer 0.4 M	240mM PIPES
	100mM HEPES
	8mM MgCl <sub>2</sub>
	40mM EGTA
	pH to 6.9
PIPES Buffer 0.5 M	151 g/l PIPES dissolve in 1M NaOH
PMSF stock, 100x	100 mM in isopropanol
Protease inhibitor mix (1x)	0.01 mg/ml Pepstatin A
	0.05 mg/ml aprotinin
	0.02 mg/ml leupeptin
	1 mM PMSF (add before use!)
Ringer solution	122.5 mM NaCl
	5.4 mM KCl
	1.2 mM CaCl <sub>2</sub>
	0.8 mM MgCl <sub>2</sub>
	11 mM D-Glucose
	10 mM HEPES
	1 mM NaH <sub>2</sub> PO <sub>4</sub> in ddH <sub>2</sub> O
	adjust pH: 7.4
RNA running buffer (20x)	41.86 g MOPS
	6.8 g NaOAc
	3.8 g EDTA
	ad 500 ml ddH <sub>2</sub> O
SDS loading buffer, 6x	0.35 M TrisCl (pH 6.8)

	36% glycerol
	10.28% SDS
	5% $\beta$ -mercaptoethanol
	0.012% bromophenol blue
SDS-PAGE running buffer	25 mM Tris
	250 mM glycine
	0.1% SDS
SDS-PAGE transfer buffer	5 mM Tris
	4 mM glycine
	0.03% SDS
Sorbitol Solution	5% (w/v) D-sorbitol in ddH <sub>2</sub> O
	filter sterilize
Super Broth	35 g tryptone
	30 g yeast extract
	5 g NaCl
	ad 1l ddH <sub>2</sub> O
SOB medium	20 g tryptone
	5 g yeast extract
	0.5 g NaCl
	5 g MgSO <sub>4</sub> x 7 H <sub>2</sub> O
	ad 1l ddH <sub>2</sub> O, autoclave
SOC medium:	SOB + 20 mM D-Glucose, sterile, freeze
1xTAE	4 mM Tris-acetate
	1 mM EDTA (pH 8.0)
TB buffer	10 mM PIPES buffer
	15 mM CaCl <sub>2</sub>
	250 mM KCL
	dissolve in H <sub>2</sub> O, adjust pH with KOH to 6.7,
	add 55 mM MnCl <sub>2</sub> , filter-sterilize
Thawing solution I	12% NaCl autoclave
Thawing solution II	1.6% NaCl autoclave

## MATERIALS AND METHODS

---

Thawing solution III	0.9% NaCl / 0.2% glucose filter sterilize
WR99210	20 $\mu$ M in RPMI 25 mM HEPES L-Glutamine
WR99210 stock	10 mM in 20% DMSO (v/v)

## 2.2 Cell culture

### 2.2.1 Culture of *P. falciparum*

Intraerythrocytic stages of *P. falciparum* parasites were grown continuously *in vitro* as described previously (Trager & Jensen, 1976, 2005). All experiments were carried out with the 3D7 strain (Ponnudurai et al, 1981; Walliker et al, 1987). Culture conditions consisted of an atmosphere of 3% CO<sub>2</sub>, 5% O<sub>2</sub>, 92% N<sub>2</sub> and 95% humidity at 37°C. Parasites were grown in 10 cm or 25 cm diameter petri dishes containing a final volume of 14 ml or 35 ml, respectively, of HEPES-buffered RPMI 1640 medium supplemented with 5-10% heat-inactivated A human serum, optionally 5% albumax II, 200  $\mu$ M hypoxanthine, 0.2  $\mu$ g/ml gentamycin as well as 3-4% group A erythrocytes. Parasitaemia was determined by Giemsa-stained blood smears and kept at 1-5%. Every 1-3 days the medium was exchanged and as soon as parasitaemia reached 5-10%, the parasite culture was split in order to avoid toxification of the media by parasitic metabolites.

### 2.2.2 Freezing of parasites

Successful freezing of *P. falciparum* requires ring stage parasites, which survive the freezing and thawing procedure best. The cells were resuspended in a volume of 14 ml of cell culture media and centrifuged (1900 rpm for 2 min, RT). The supernatant was discarded and 1/3 of the pellet volume of freezing solution was slowly added to the pellet (pellet in 14 ml culture plate ~0.5 ml). After 5 min incubation at RT, another 4/3 of pellet volume was added. The mix was distributed into cryovials, incubated for 5 min at RT and frozen. After short-term storage in a -80°C freezer long term storage was maintained in liquid nitrogen tanks.

### 2.2.3 Thawing of parasites

Frozen parasites in cryovials were removed from liquid nitrogen tanks and warmed up to 37°C. 200  $\mu$ l of thawing solution I (12% NaCl) was added drop wise followed by

transfer to a 15 ml falcon tube. 9 ml of thawing solution II (1.6% NaCl) was added dropwise with frequent shaking. The solution was centrifuged (1900 rpm for 2min, RT) and the supernatant removed. Finally, 7 ml of thawing solution III (0.6% NaCl, 0.9% glucose) was pipetted drop wise. After further centrifugation the pellet was resuspended in cell culture media and transferred to a prepared cell culture dish (14 ml) containing 0.5 ml of blood. From two days after onwards, media was exchanged daily and a selection marker (WR99210, 5 nM) was added optionally.

#### **2.2.4 Determining parasitaemia**

In order to determine parasitaemia and developmental stages, thin blood smears of around 50 µl of concentrated culture were air-dried on microscope slides, fixed in 100% methanol for 30sec, dried and stained in Giemsa solution for 10-20 min (Fleischer, 2004). Afterwards, the slides were washed with water and examined on a light microscope under oil immersion using a 100x objective. Parasitaemia, defined as the percentage of parasite-infected red blood cells, was determined by counting infected and uninfected cells and calculated with the following formula:

$(\text{number of infected erythrocytes} / \text{total number of erythrocytes}) \times 100 = \% \text{ parasitaemia}$

#### **2.2.5 Parasite synchronization**

For the purpose of synchronizing parasite cultures, different techniques can be applied according to further experimental applications. One of the most common techniques is sorbitol lysis (Lambros & Vanderberg, 1979), which osmotically destroys the tubovesicular network of late stage trophozoites, an induced transport system, which is absent in ring stages. Cell culture media was removed from a mixed stage plate and 10 ml of prewarmed, sterile 5% sorbitol was added. After resuspension and transfer to a 15 ml falcon tube, the parasites were incubated for 10 min at 37°C, centrifuged (1900 rpm for 2 min, RT) and after an optional washing step in RPMI medium transferred to a new petri dish containing the appropriate amount of new RPMI medium as well as 3-4% haematocrit.

#### **2.2.6 Magnetic cell sorting (MACS column)**

The enrichment of late stage parasites (trophozoites and schizonts) for consecutive experiments can be achieved by magnetic cell sorting (Ribaut et al, 2008; Uhlemann,

2000), which is based on the paramagnetic properties of the hemozoin crystal in the parasite food vacuole, a product of parasitic haem metabolism. Hemozoin-containing parasites are retained in the metal wool of the column as long as magnetic force is applied, whereas red blood cells (with ring stage parasites) are washed away. After equilibration of the column with MACS buffer the parasite culture was applied gradually onto the magnet-surrounded column and liquid outflow was reduced by the stopcock to maximal 1 drop per second. MACS buffer was added until the outflow was clear and finally the retained cells were eluted by the removal of the column from the magnet apparatus and application of 12-15 ml of MACS buffer at full outflow speed. The eluate was collected in a falcon tube and centrifuged (1900 rpm for 2 min, RT) before used in further experiments.

### **2.2.7 Limiting dilution assay\***

Clonal parasite populations are retrieved by limiting dilution of a culture in 96-well plates with an initial inoculum of 0.25 - 0.5 parasites/well. Individual clones in single wells can be detected by visual, microscopic or enzymatic detection methods after 2-5 weeks and can be used for further studies (Butterworth et al, 2011; Rosario, 1981). For the assay the parasitaemia of the starting *P. falciparum* culture in 10 ml of medium with 2% haematocrit of total RBCs (200  $\mu$ l, infected and uninfected) was carefully determined as a prerequisite for successful dilution of the parasites (clonal populations are impossible if more than one parasite occupies one well or all wells are positive). The total number of parasites in this starting culture was calculated from the parasitaemia, the haematocrit and the information that 1 ml of a suspension at 50% haematocrit usually harbours roughly  $5 \times 10^9$  RBCs (Bunn, 2011). A calculation example for 10 ml starting culture with 2% haematocrit and 3% parasitaemia is given (RBC = iRBC = parasite):

1.  $2\% \text{ haematocrit} \times 10 \text{ ml} = 50\% \text{ haematocrit} \times Y \text{ ml}$   
 $Y = 2\% \times 10 \text{ ml} / 50\% = 0.4 \text{ ml (at 50\%)}$
2.  $5 \times 10^9 \text{ RBCs} / 1 \text{ ml} = Y \text{ RBCs} / 0.4 \text{ ml}$   
 $Y = 2 \times 10^9 \text{ RBCs (in 10 ml of 2\% haematocrit or 0.4 ml of 50\%)}$
3.  $2 \times 10^9 \text{ iRBCs} / 100\% = Y \text{ iRBCs} / 3\%$   
 $Y = 6 \times 10^7 \text{ iRBCs in 10 ml} = 6 \times 10^6 \text{ iRBCs (=parasites) in 1ml}$

With this information in mind a serial dilution was conducted from  $5 \times 10^6$  parasites per ml to  $5 \times 10^1$  parasites per ml using 1:10 dilutions in a final volume of 10 ml. The samples were repeatedly inverted to ensure proper mixing. In the previous example the initial dilution sample ( $5 \times 10^6$  parasites / ml) is calculated as following:

4.  $10 \text{ ml} \times 5 \times 10^6 / 6 \times 10^6 = Y = 8.33 \text{ ml}$  of iRBCs from starting culture + 1.67 ml of medium

From the second last dilution (50 parasites per ml) two final dilutions of 5 parasites per ml and 2.5 parasites per ml were prepared in a final volume of 15 ml medium (1.5 ml and 0.75 ml of pre-dilution) plus 300  $\mu$ l uninfected fresh RBCs (2% haematocrit). 100  $\mu$ l of these suspensions were aliquoted into 96-well plates and incubated under the appropriate culture conditions. To control for the presence of parasites 5 ml of the final dilutions were transferred to small culture plates. For visual detection of positive wells it was important to use 96-well plates with conical (V-shaped) bottoms. Medium without selection marker was exchanged every second to fourth day until parasite appearance or for 2-5 weeks. The haematocrit was increased by 1% each week. The control plates usually were the first to become positive after 2 weeks followed by increasing numbers of positive wells in the 96-well plates after 2-3 weeks. A dark colour of the blood as well as a cloudy medium was indicative of parasitized wells and confirmed by microscopic analysis. Subsequently, the content of parasitized wells was transferred to small culture plates to increase parasite numbers for freeze-downs and further investigations. If more than 75% of the wells became positive, the experiment was repeated to ensure clonal populations.

### **2.2.8 Determination of drug IC<sub>50</sub> value\***

In order to use the appropriate concentrations of negative selections markers (5-fluorouracil and ganciclovir) for genetic recombination methods the 50% inhibitory concentration was determined in *P. falciparum* 3D7 intraerythrocytic cultures using a standard SYBR green I-based fluorescence assay (Johnson et al, 2007; Smilkstein et al, 2004). Parasite cultures at mixed stages of 0.5% parasitaemia with 3% haematocrit were prepared (~6 ml/ 96-well plate) for the assay and 50  $\mu$ l used per well. Furthermore, drug solutions were prepared at 6 times the highest concentration aimed for the assay. A range of drug concentrations was chosen based on literature (or tested in preceding IC<sub>50</sub>

## MATERIALS AND METHODS

measurements) to cover parasite viability from 0-100% with sufficient amount of data points in the curve to determine the IC<sub>50</sub> concentration. The pipetting scheme included appropriate dilution steps of the drugs (e.g. 1:2, 1:3) from the top row down as well as uninfected RBCs (0% growth) and untreated iRBCs (= 100% growth) as controls. Outer rows were omitted due to extensive evaporation. Each concentration was tested in duplicates and the assays were repeated 2-3 times. The plate scheme looked like this:

X	X	X	Drug1	Drug1	Drug2	Drug2	Drug3	Drug3	Drug4	Drug4	X
X	RBC	iRBC	Highest concentrations				→				X
X	RBC	iRBC	↓								X
X	RBC	iRBC									X
X	RBC	iRBC		Dilutions							X
X	RBC	iRBC									X
X	RBC	iRBC	↓								X
X	X	X	X	X	X	X	X	X	X	X	X

50 µl of complete medium was pipetted in each well plus 25 µl of the drug solution in the wells of the top row (in case of 1:3 dilution steps). This mix was resuspended well and 25 µl were transferred to the row below and so on. After diluting the last row, the final 25 µl were discarded. 50 µl of prepared parasites (see above) were added to each well to have a total volume of 100 µl with 1.5% final haematocrit. The plate was returned to the incubator for 72 h, and then frozen at -80°C for at least 2 h or until further use. On the day of measurement, the plates were thawed for at least 1 h and 100 µl of lysis buffer plus SYBR green I (1.2 µl SYBR green/ 10ml lysis buffer) was added per well while avoiding exposure to bright light. The plate was shaken briefly to mix the suspension and incubated in the dark for 1 h at RT. Afterwards, fluorescence was measured in the FLUOstar OPTIMA microtiter plate fluorescence reader (BMG Labtech) using the provided manufacturer's software at 520 nm of emission after excitation at 485 nm and specific program settings (gain 1380, 10 flashes/well, top optic). Afterwards, the mean fluorescence signal was calculated for the controls (RBCs, iRBCs) as well as the duplicates for each drug concentration. The value of uninfected RBCs was deducted as background from all iRBC measurements; the value for untreated iRBCs was set as 100% growth. The growth inhibition by the different drug concentrations was plotted in SigmaPlot (Version 11.0 or 12.0) and the IC<sub>50</sub> and IC<sub>90</sub> values were deducted from the fitted curves (Hill function, three parameters).

## **2.3 Transfection of *P. falciparum***

The transfection of *P. falciparum* followed two standard protocols, which include the introduction of plasmid DNA by electroporation of a 1-2% ring stage parasite culture or of uninfected erythrocytes prior to parasite invasion (Chahaun, 2002; Hasenkamp et al, 2013; Wu et al, 1995). Both methods have proven useful with the advantage of the latter one to be gentler to the parasites because they are not exposed to the trauma of electroporation.

### **2.3.1 Preparation**

#### **Parasites**

Parasites were synchronized with sorbitol a few days before transfection in order to guarantee a parasitaemia of 2-3% of late schizont or 1-2% early ring stages at the day of transfection depending on the protocols used. Prior to transfection the parasite culture was resuspended, centrifuged (1900 rpm for 2 min, RT) and the supernatant was removed. In case the parasitaemia was too high, a dilution in blood yielded the appropriate ratio.

#### **Transfection vectors**

After isolation of the transfection plasmids by a Plasmid Maxi Kit, the concentration and quality was estimated by spectrophotometry and agarose gel electrophoresis, respectively. A volume equal to 100-120 µg of DNA was used for transfection. After addition of ddH<sub>2</sub>O to a final volume of 180 µl, 20 µl of 3 M sodium acetate (pH 5.2) and 2.5 vol of ice-cold absolute ethanol were used for precipitation of the plasmid DNA. Short vortexing and incubation at -20°C for 1 h resulted in the visible condensation of DNA. After centrifugation (13 000 rpm for 30 min, 4°C), the pellet was desalted with 500 µl of 70% ethanol. Finally, after further centrifugation (13 000 rpm for 15 min, 4°C), the pellet was air-dried and resuspended in 30 µl of sterile TE-buffer and stored at -20°C ON. Prior to transfection, the DNA was supplemented with 370 µl of sterile cytomix.

### **2.3.2 Electroporation of infected red blood cells**

A fresh culture dish with 14 ml medium and 0.4 ml of fresh erythrocytes was prepared in advance shortly before the transfection procedure. 200  $\mu$ l of 1-2% ring stage-infected erythrocytes were combined with 400  $\mu$ l of DNA/cytomix, immediately transferred to an electroporation cuvette (2 mm) and electroporated in the gene pulser (Biorad) with 0.31 kV and 0.950  $\mu$ F at the highest capacity setting. Quickly afterwards the sample was pipetted into the prepared culture plate and incubated immediately in the appropriate atmosphere.

### **2.3.3 Electroporation of uninfected red blood cells\***

1 ml of fresh uninfected RBCs was mixed with 6 ml of cytomix, centrifuged (1900 rpm for 2 min, RT) and the supernatant was removed. This washing step was repeated once more, before 400  $\mu$ l of packed cell pellet was mixed with 400  $\mu$ l of prepared DNA/cytomix and transferred to two pre-chilled electroporation cuvettes (2 mm). These cuvettes were cooled on ice for 5 min, then electroporated in the gene pulser (Biorad) with a voltage of 0.31 kV and a capacitance of 950  $\mu$ F at high capacity setting. The time constant should be between 8-12 msec. The samples were returned on ice for 5 min, then transferred to 15 ml falcon tubes by rinsing the cuvette with 2x2 ml of complete medium. After centrifugation (1900 rpm for 2 min, RT) the supernatant was discarded and the pellet of DNA loaded RBCs was resuspended in a 14 ml culture dish including 14 ml of medium and 100  $\mu$ l of 2-3% (or less) schizont-infected RBCs for a final parasitaemia of around 0.5%. The culture was returned to the incubator and medium was exchanged daily. The transfection procedure was repeated with these parasites and new DNA 48 hours later to increase the chance to invade loaded RBCs. Subsequently, parasites were split to 2-3% and subjected to drug selection.

### **2.3.4 Selection procedure**

48 hours after transfection, the medium was exchanged and the positive selection markers WR99210 or Blasticidin S were added to a final concentration of 5 nM and 9 mM, respectively (Hastings & Sibley, 2002; Mamoun et al, 1999). Starting from the third day of transfection medium (14 ml) and selection marker were exchanged daily for one week, during which the parasites disappeared from the blood smears. This was

followed by splitting the culture in half using fresh erythrocytes in the second week and a three weeks period of providing fresh medium and marker twice a week until the parasites appeared again in the blood smear. 200  $\mu$ l of fresh erythrocytes were added every second week. The selection period usually lasted 21-30 days.

## **2.4 Microbiological methods**

### **2.4.1 Preparation of chemocompetent *E.coli*\***

For preparation of chemocompetent XL-1 Blue *E. coli* cells, 10 ml of Luria Broth medium was inoculated with a single bacterial colony and incubated at 37°C under shaking conditions (220 rpm) overnight. The next day, 250 ml of SOB medium was inoculated with this preculture to a final OD<sub>600</sub> of 0.1/ml and shaken again for ~2 h at 37°C until 0.6 OD/ml. At that point the flask was cooled on ice for 10 min, followed by centrifugation (6000 rpm for 25 min, 4°C). All consecutive steps are carried out on ice with pre-chilled solutions. The pellet was resuspended in 80 ml of ice-cold TB buffer and incubated on ice for 10 min. After centrifugation (6000 rpm for 10 min, 4°C) and removal of the supernatant the pellet was resuspended in 20 ml of TB buffer. 1.4 ml of DMSO was carefully added to this suspension under agitation followed by 10 min of incubation on ice. Finally, the competent cells were aliquoted into 1.5 ml Eppendorf tubes (100  $\mu$ l each) that were pre-chilled using dry-ice plus ethanol. The bacteria were stored at -80 °C until further use.

### **2.4.2 Transformation and culture of *E. coli*\***

Plasmid DNA was introduced into chemocompetent XL-1 Blue *E. coli* bacteria by heat shock (Chan et al, 2013). For this purpose, 50  $\mu$ l of frozen bacterial cells were thawed on ice and mixed with 1-10  $\mu$ l of DNA. After incubation on ice for 15-30 min the cells were incubated in the 42°C water bath for 45 sec followed by 2 min cooling on ice. Then the transformed bacteria were supplemented with 1 ml of prewarmed SOC medium and incubated for 1h at 37°C under shaking conditions (220 rpm). Finally, the bacterial suspension was pelleted or directly plated (100  $\mu$ l) onto selective LB agar plates and incubated overnight at 37°C.

### **2.4.3 Selection and storage**

Positive clones were grown on selective LB agar plates containing the appropriate antibiotic (ampicillin: 100 µg/ml, kanamycin: 50 µg/ml) and further investigated using colony PCRs. The plasmids were either stored at -20°C after isolation (High Pure Plasmid Isolation kit) or as transformed colonies on LB agar plates at 4°C. Furthermore, glycerol stocks of transformed bacteria (25% glycerol) were produced and stored at -80°C. For further use, a small pipette tip was quickly scratched over the surface of the frozen stocks and used for inoculation.

## **2.5 Molecularbiological methods**

### **2.5.1 Nucleic acids**

#### **2.5.1.1 Electrophoresis of DNA and RNA**

DNA and RNA can be separated according to fragment size using agarose gel electrophoresis. For DNA electrophoresis, 1.0%-1.5% agarose gels were prepared by weighing in the agarose, dilution in 1xTAE buffer, boiling until dissolution and cooling. Ethidium bromide was added to the dissolved agarose to a final concentration of 1 µg/ml short before pouring. It intercalates with DNA allowing visualization by ultra violet (UV) irradiation. After polymerization, the gels were loaded with appropriate amounts of DNA sample diluted in DNA loading buffer (1:5, v/v) and separated together with a convenient DNA size standard. Electrophoresis was conducted at a constant voltage in 1xTAE (30 ml gels maximum 90 V, 150 ml gels maximum 140 V). The gels were photographed using the Electrophoresis Documentation and Analysis System 120 (Kodak).

For the control of isolated RNA, 0.28 g LE-agarose, 2 ml of 20x RNA running buffer and 30 ml of ddH<sub>2</sub>O were heated, supplemented with 0.5 µl ethidium bromide and 7.9 ml formaldehyde and poured into a ribonuclease (RNase) free gel chamber. RNA loading buffer was added to the samples (1:1) and electrophoresis was performed at 60 mV for 45-60 min.

### 2.5.1.2 DNA extraction from agarose gels

DNA ranging from 70 bp to 10 kb was extracted using the QIAquick gel extraction kit protocol (Qiagen), which uses binding of DNA to a silica membrane in high salt conditions, whereas contaminants pass through. Briefly, the DNA fragment was excised under a weak UV lamp, weighed and 3 volumes of QG buffer were added to 1 volume of gel (mg = ml). The mix was incubated at 50°C for 10 min, supplemented with 1 volume of isopropanol, applied to the provided column and centrifuged (13 000 rpm for 1 min, RT). After the absorption of DNA in high salt-content conditions and a washing step, elution was performed with low-salt buffer (10 mM Tris-Cl, pH 8.5). DNA concentration and quality were analysed using a spectrophotometer and agarose gel electrophoresis, respectively.

### 2.5.1.3 Photometric determination of DNA/RNA concentration

DNA concentration was measured by spectrophotometry using the UVIKON 923 photometer (Kontron instruments). The absorbance (OD) at 260 nm was analysed for DNA and RNA, where an OD<sub>260</sub> of 1 equals 50 µg/ml dsDNA and 40 µg/ml ssRNA. Dilutions were included using the following formula:

$$\text{OD}_{260} \times 50 \text{ (dsDNA)} \times \text{dilution factor} / 1000 = X \text{ } \mu\text{g}/\mu\text{l}$$

$$\text{OD}_{260} \times 40 \text{ (ssRNA)} \times \text{dilution factor} / 1000 = X \text{ } \mu\text{g}/\mu\text{l}$$

### 2.5.1.4 Enzymatic digestion of DNA

Restriction endonucleases were used to digest insert and vector DNA for subsequent cloning as well as to control the appropriate fragment sizes of plasmid inserts, e.g. prior to sequencing. Buffers were chosen according to the manufacturer's recommendations. Restriction temperature ranged from RT to 37°C and duration from 1 h to ON. Depending on the respective purpose, different reaction mixes were prepared as follows:

	<b>control digest of mini/maxi prep (15 µl)</b>	<b>restriction digest of vector DNA (20 µl)</b>	<b>restriction digest of insert DNA (20 µl)</b>
DNA	1-5 µl (1.5 µg)	~5 µl (10 µg)	12 µl
Enzyme 1	0.4 µl	0.8 µl	0.8 µl
Enzyme 2	0.4 µl	0.8 µl	0.8 µl

## MATERIALS AND METHODS

---

Buffer 10x	1,5 µl	2 µl	2 µl
BSA 10x	1.5 µl	2 µl	2 µl
ddH <sub>2</sub> O	ad 15 µl	ad 20 µl	ad 20 µl
incubation time	1.5 h	min.2 h	min.2 h
temperature	37°C	37°C	37°C

### 2.5.1.5 Dephosphorylation of DNA with alkaline phosphatase

Shrimp alkaline phosphatase (SAP) from *Pandalus borealis* catalyses the dephosphorylation of 5' phosphates from DNA in order to prevent religation of plasmid vectors (Sambrook, 2001). Appropriate ligation is only possible with the insert, which still has intact phosphate groups. SAP is completely and irreversibly inactivated by heat. After restriction digest, 2 µl of SAP buffer 10x and 1 µl of SAP enzyme (Promega) were added to 20 µl of vector digest mix (DNA conc. ~10 µg), incubated for 30 min at 37°C and heat-inactivated for 15 min at 65°C. The sample was subsequently gel extracted.

### 2.5.1.6 Ligation

T4 DNA ligase was used for ligation, which is isolated from bacteriophage T4 and catalyses the formation of a phosphodiester bond between juxtaposed 5'-phosphate and 3'-hydroxyl termini in duplex DNA or RNA with blunt or cohesive ends. The restricted fragments were purified by gel extraction or direct purification protocols. The molar ratio of vector to insert was kept at about 1:3. In 10 µl final volume, 2 µl of Ligase buffer (10x) and 1 µl of T4 Ligase (Invitrogen) were added to the vector:insert mix, followed by 1.5 h incubation at RT or ON at 15°C.

### 2.5.1.7 Polymerase chain reaction (PCR)

Polymerase chain reaction (Mullis et al, 1986; Saiki et al, 1985) was used for amplification of genes, targeted mutagenesis and colony screening of bacteria. Different PCR methods were applied.

### Colony PCR

The following PCR reaction mix was prepared on ice and 1 colony per tube was picked with a pipette tip and added.

<b>25 µl reaction mix</b>		<b>PCR program</b>		
Primer for (50 µM)	0.25 µl	94 °C	7'	
Primer rev (50 µM)	0.25 µl	94 °C	45"	} 30x
MgCl <sub>2</sub> (50 mM)	1.25 µl	50 °C	45"	
dNTPs (2 mM)	2.5 µl	68 °C	1'10"	
Euro Taq buffer 10x	2.5 µl	68 °C	10'	
ddH <sub>2</sub> O	18 µl	4 °C	pause	
Euro Taq polymerase	0.25 µl			

### Megaprimer synthesis PCR (site-directed mutagenesis I)

For site-directed mutagenesis (Barik, 1997, 2002; Ling & Robinson, 1997) two PCR reactions were prepared, each containing one external primer annealing close to each end of the gene of interest as well as one internal primer that introduced the desired mutation, e.g. alanine replacements. The products of the 2 PCRs were two megaprimers that overlapped in the area of mutation and were used as templates in the subsequent overlap extension PCR (see below).

<b>50 µl reaction mix</b>		<b>PCR program</b>		
Primer for (50 µM)	0.5 µl	98 °C	1'	
Primer rev (50 µM)	0.5 µl	98 °C	30"	} 25x
MgCl <sub>2</sub> (50 mM)	0.2 µl	61 °C	30"	
DNA template	1 µl	72 °C	25"	
dNTPs (2 mM)	5 µl	72 °C	10'	
Phusion buffer HF 5x	10 µl	4 °C	pause	
Phusion polymerase	0.5 µl			
ddH <sub>2</sub> O	32.5 µl			

### Overlap extension PCR (site-directed mutagenesis II)

The megaprimers were extracted and subjected to a second PCR called overlap extension PCR (Ho et al, 1989). Additionally, this PCR also contained external primers for further amplification but, importantly, was lacking the template DNA.

<b>50 µl reaction mix</b>		<b>PCR program</b>		
Primer for (25 µM)	1 µl	98 °C	1'	
Primer rev (25 µM)	1 µl	98 °C	30"	} 20x
(MgCl <sub>2</sub> (50 mM)	0.2 µl	60 °C	1'30"	
Megaprimer X	1.5 µl	72 °C	20"	
Megaprimer Y	1.5 µl	95 °C	30"	} 20x
dNTPs (2 mM)	5 µl	50 °C	50"	
Phusion buffer HF 5x	10 µl	72 °C	30"	
Phusion polymerase	0.5 µl	72 °C	10'	
ddH <sub>2</sub> O	29.5 µl	4 °C	pause	

### PCR on genomic DNA of *P. falciparum*\*

For cloning as well as to control for genetic recombination, gDNA was extracted from *P. falciparum* parasites using the DNeasy Blood&Tissue (Qiagen) kit as described in section 2.5.1.10. The elution volume was usually 2x 100 µl, of which 0.5 µl-2 µl were used for PCR amplification, depending on the concentration of the gDNA. The reaction mix was identical to the one for colony PCR and the program consisted of the following:

94 °C	2-4'	} 35x
92 °C	30"	
54 °C	35"	
62 °C	1'10"	
62 °C	10'	
4 °C	pause	

### 2.5.1.8 Plasmid isolation from bacteria

Small scale (mini) plasmid isolation from bacteria was achieved using High Pure Plasmid Isolation kit (Roche), which is based on alkaline lysis and specific adsorption of released DNA onto glass fibre columns. According to the standard protocol, an overnight bacteria culture was centrifuged (3800 rpm for 7 min, RT) and the pellet was treated with suspension and lysis buffer and incubated for 5 min, RT. After addition of chilled DNA binding buffer and incubation for 5 min on ice, the suspension was centrifuged (13 000 rpm for 10 min, 4°C). The supernatant was pipetted onto the column and centrifuged (13 000 rpm for 1 min, RT). After two washing steps the DNA was eluted with 30 µl of elution buffer and stored at -20°C.

Large-scale (maxi) plasmid isolation was performed using the Plasmid Maxi Kit (Qiagen) according to the manufacturer's protocol. Briefly, 400 ml bacteria suspension containing the appropriate amount of antibiotic was grown overnight. The cells were harvested by centrifugation (5000 rpm for 15 min, 4°C) and sequentially mixed and incubated with resuspension, lysis and neutralization buffers. Precipitation of genomic DNA, proteins and cell debris was carried out on ice. The supernatant containing the plasmid DNA was separated from debris by centrifugation (13 000 rpm for 30 min, 4°C) and loaded onto an equilibrated tip. After several washing steps, DNA was eluted, precipitated with isopropanol and centrifuged (11 000 rpm for 30 min, 4°C). The DNA pellet was air-dried and resuspended in 10 mM Tris-HCl buffer, pH 8.5.

### **2.5.1.9 Sequencing of DNA**

After mini or maxi isolations and control digests, plasmids were sent to GATC (Konstanz) for sequencing at a recommended concentration of 30-100 ng/ $\mu$ l in a total volume of 30  $\mu$ l. Appropriate primers were sent in 10 pmol/ $\mu$ l. The sequencing order was purchased online and the sequencing results were downloaded in .abi format and analysed using BioEdit (Hall, 1999) and ClustalW (Larkin et al, 2007).

### **2.5.1.10 Isolation of genomic DNA from *P. falciparum*\***

For maximum yield of genomic DNA (gDNA) from *P. falciparum* intraerythrocytic cultures it is recommended to use 1-2 big (35 ml) culture plates with parasites of trophozoite to schizont stage at a parasitaemia of 5%. Parasitized cultures were centrifuged (1900 rpm for 2 min, RT) and the pellets resuspended in 10 ml of 1x PBS/0.1% saponin. After inversion and incubation on ice for 3-5 min the lysate was centrifuged (4000 rpm for 10 min, 4°C or RT) and the pellet washed with 1 ml of 1x PBS. The supernatant was discarded and the parasite pellet was either frozen or directly used for gDNA extraction using the DNeasy Blood & Tissue Kit (Quiagen). Briefly, parasites were treated with lysis buffer and proteinase K followed by addition of 100% ethanol to adjust buffer conditions. Separation of DNA from contaminants is achieved through specific binding to silica-based membranes in the presence of high concentrations of chaotropic salt. After centrifugation (8000 rpm for 1 min, RT) and two washing steps the clean DNA is eluted in elution buffer or water and stored at -20°C.

### **2.5.1.11 Isolation of total RNA from *P. falciparum***

In order to prepare messenger RNA (mRNA) for complementary DNA (cDNA) synthesis, total parasite RNA was extracted with TRIzol® reagent (Invitrogen) following the manufacturer's protocol. Parasites were used that were repeatedly subjected to gelatine flotation in order to ensure a knob-forming phenotype. After the removal of medium from 6 big plates with 5-7% parasitaemia, the erythrocytes were resuspended in 1xPBS, transferred into 50 ml falcon tubes and centrifuged (2000 rpm for 2 min, 4°C, from 800 rpm downwards without break). After an additional washing step in PBS, the parasites were lysed in PBS/0.2% freshly prepared prewarmed saponin (ratio 1:1, e.g. 25 ml each) and centrifuged (3800 rpm for 8 min, 4°C, with break). After removal of the

supernatant, 5 x the parasite pellet volume of prewarmed TRIzol was added. The mix was shortly vortexed and stored at -80°C ON in a 50 ml Falcon tube.

One day after, the RNA pellet was heated to 30°C for 5 min. All subsequent steps were carried out under sterile conditions using sterile material in order to prevent RNase contamination. 0.2 ml chloroform was added per 0.75 ml of TRIzol and samples were vigorously shaken for 15 sec and incubated at 30°C for 10 min. Following centrifugation (12 000 x g for 10 min, 2-8°C), the suspension separates into a lower red phenol-chloroform phase, an interphase and an upper aqueous phase, which contains the RNA. This upper phase was transferred carefully into a clean tube and RNA was precipitated using 0.5 ml of isopropanol per 0.75 ml of TRIzol initially used. The samples were incubated at 30°C for 10 min and centrifuged (12 000x g for 10 min, 4°C). The gel-like RNA pellet was washed once with 75% ethanol, vortexed shortly and centrifuged (7500x g for 5 min, 4°C). The RNA pellet was air-dried briefly and dissolved in the appropriate volume of RNase free water (50 – 300 µl) followed by heating up to 55°C for 10 min. RNA quality was analysed on an RNA gel and quantified by spectrophotometry, before being processed further in cDNA synthesis.

### **2.5.1.12 cDNA synthesis by reverse transcription**

For reverse transcription the SuperScript First-Strand Synthesis System for RT-PCR (Invitrogen) was used. The protocol followed strictly manufacturer's recommendations and was carried out with 5 µg total RNA. Briefly, first strand cDNA synthesis was primed with oligo(dT) primers, which specifically hybridized to polyA tails of mRNA. Reverse transcriptase (RT) bound these primers and synthesized first-strand cDNA transcripts. RNase H removes RNA from the cDNA:RNA hybrids. After synthesis the target cDNA was directly amplified in a conventional PCR using gene specific primers to yield the DNA of interest.

## **2.5.2 Proteins**

### **2.5.2.1 Preparation of parasite protein extracts\***

Total proteins were extracted from *P. falciparum* transfectant parasites and used for antibody detection of different GFP-tagged fusion proteins in western blots. Briefly, parasites were purified using the magnetic column and pelleted by centrifugation (1900

rpm for 2 min, RT). The pellet was washed once with 1xPBS and then resuspended in 10x the pellet volume of lysis buffer containing 1xPBS, 0.07% saponin and protease inhibitors (leupeptin, aprotinin, PMSF, pepstatin A). Alternatively, membrane proteins were extracted by simple lysis with 10x the pellet volume of H<sub>2</sub>O (plus protease inhibitors). After incubation at 37°C for 1-3 min, the sample was centrifuged (13 000 rpm for 1 min, 4°C) and separated into supernatant and pellet. The supernatant was supplied with an equal volume of SDS loading buffer, while the pellet was washed once in cold 1xPBS plus protease inhibitors. The supernatant of the washing step was discarded and the volume of the pellet sample was adjusted with PBS and loading buffer to the same as the supernatant. Samples were stored at -20° until further use.

#### **2.5.2.2 Differential lysis assay\***

This method is used to roughly define the localization and orientation of proteins in the different cellular compartments such as the RBC cytoplasm, the parasitophorous vacuole (PV) and the parasite cytoplasm. Mainly, distinction can be achieved by the accessibility of different compounds to these compartments and the proteins residing within (Blumenthal & Habig, 1984; Saridaki et al, 2009; Spielmann et al, 2006). Treatment of infected erythrocytes with tetanolysin specifically destroys the erythrocyte plasma membrane due to its cholesterol content, whereas the PVM is unaffected. Additional lysis with saponin further breaks the MC and PVM membranes but leaves the parasite plasma membrane (PPM) intact. Infected erythrocytes of 5% parasitaemia, rich in trophozoites, were isolated using the MACS column and washed in 1xPBS. In parallel, a 1:200 dilution of tetanolysin (stock: 1 mg/ml, 500 U/ml) was activated with 10 mM dithiothreitol (DTT) for 15 min at RT. The pellet was resuspended in a suitable volume of buffer (80-400 µl, dependant on pellet size) containing 1xPBS, activated tetanolysin (4 µl/ 100 µl buffer) as well as protease inhibitors (leupeptin, aprotinin, PMSF). This suspension was incubated on ice for 10 min, then at 37°C for 3 min. After centrifugation (13 000 rpm for 1 min, 4°C) the supernatant was removed and supplemented with equal amounts of SDS loading buffer (= Tet, SN). The pellet was washed once with 1xPBS followed by addition of lysis buffer (same volume as before) containing 1xPBS, 0.07% saponin and protease inhibitors. After incubation at 37°C for 1 min, the sample was centrifuged (13 000 rpm for 1 min, 4°C) and the supernatant supplemented with equal

## MATERIALS AND METHODS

---

amounts of SDS loading buffer (= Tet+Sap, SN). The pellet, corresponding to the parasite fraction, was washed once with cold 1xPBS and centrifuged as before. After removal of the supernatant, the volume of the pellet sample was adjusted to the supernatant samples with PBS and protein loading buffer for rough comparison of protein amounts (= Tet+Sap, P). Samples were stored at -20 °C.

### 2.5.2.3 Western blot analysis

Western blot analysis followed the differential lysis assay and consisted of SDS polyacrylamide gel electrophoresis (PAGE) (Laemmli, 1970), semi-dry transfer, antibody labelling (Burnette, 1981) and chemoluminescence detection (Thorpe & Kricka, 1986).

### SDS-PAGE

10% SDS gels were prepared as following and polymerized for 1 h - ON:

10%	separating gel	stacking gel
H <sub>2</sub> O	4 ml	3.4 ml
Acrylamide/bis 29:1	3.3 ml	0.83 ml
Tris lower pH 8.8	2.5 ml	-
Tris upper pH 6.8	-	0.63 ml
SDS 10%	100 µl	50 µl
APS 10%	100 µl	50 µl
TEMED	5 µl	6 µl

Pellet samples were optionally subjected to sonication or pipetted repeatedly and denatured at 75°C for 3 min prior to loading. The gels ran in 1x SDS running buffer at 200 V and 60 mA until the loading buffer front reached the end of the gel.

### Semi-dry transfer and antibody labelling

During semi-dry transfer the proteins were transferred from the SDS-gel onto a polyvinylidene difluoride (PVDF) membrane, which was subsequently subjected to antibody labelling. Briefly, the gel was placed onto a methanol/SDS transfer buffer-equilibrated PVDF membrane, which was further surrounded by 3 layers of wetted Whatman papers. The transfer was conducted at 15 V and 230 mA for 1 h. Subsequently,

the membrane was blocked in 5% skim milk/PBS for 1 h at RT or ON at 4°C. After blocking, the primary antibody (dilution in 1% BSA/PBS) was applied for 1 h at RT, followed by 3 washing steps in PBST (PBS, 0.1% Tween 20). Blocking in 5% skim milk/PBS for 30 min at RT was followed by incubation with the secondary antibody (dilution in 1% BSA/PBS) for 30 min at RT, 3 washes in PBST and, finally, the addition of chemoluminescence chemicals. The membranes were immediately wrapped into ceran foil and detection was achieved by x-ray film exposure and development.

#### **2.5.2.4 Protein expression and purification\***

For the purpose of establishing an *in vitro* acetylation assay as well as generating antibodies against the putative transferase, that was central to this study (PfNAT), two fragments of the protein comprising amino acids 146-527 (excluding N-terminal transmembrane domains and C-terminal putative ER retention signals, full length: 544 aa) and 380-527 were cloned into the pET28a+ expression vector and subsequently purified from transformed *E. coli* RIL cells using His-tag based affinity purification columns (HisPur Cobalt spin columns, Thermo Scientific). Native purification conditions were initially used to retrieve functional protein for the enzymatic assay. However, due to deposition in bacterial inclusion bodies the yield of soluble protein was very low and contaminated with additional proteins. Therefore, subsequent extractions for antibody production were carried out under denaturing conditions (Gopal & Kumar, 2013).

#### **Optimization of protein expression**

In a first step, the best expression conditions for the protein fragments in *E. coli* RIL and RIPL cells were tested using different temperatures, growth periods and concentrations of the inducer isopropyl  $\beta$ -D-1-thiogalactopyranoside (IPTG). Soluble proteins were separated from insoluble material and both fractions were compared using SDS-PAGE (15% gel) followed by staining with Coomassie-Blue.

Briefly, an overnight culture of transformed RIL bacteria was grown in the presence of the selective antibiotics chloramphenicol (34  $\mu$ g/ml) and kanamycin (50  $\mu$ g/ml) and diluted on the next day in LB medium to an OD<sub>600</sub> of 0.2 OD/ml. After 30 min of incubation at 37°C (OD<sub>600</sub> ~0.5/ml), selective antibiotics and IPTG (0.1 mM, 0.4 mM, 1

## MATERIALS AND METHODS

---

mM) were added and the cultures were grown at different temperatures (18°C, 30°C, 37°C) for various durations (2 h, 4 h, 6 h, ON). The suspension was then centrifuged (4000 rpm for 5 min, RT) and the pellet was washed once with H<sub>2</sub>O. Cells were lysed with lysis buffer containing lysozyme (100 µg/ml) and Triton X-100 (0.1%), treated with protease inhibitors (aprotinin, leupeptin, PMSF), sonicated and centrifuged (13 000 rpm, for 5 min, 4°C). Supernatant and pellet were separated, adjusted for the same volume and equally supplemented with protein loading buffer for SDS-PAGE.

### **Protein purification**

Small-scale and large-scale protein purification under native and denaturing conditions was conducted using the HisPur Cobalt spin columns (Thermo Scientific). Small aliquots were taken at several steps for SDS-PAGE to control for the presence of the proteins of interest. An overnight starter culture of transformed RIL bacteria was set up at 37°C in LB medium plus chloramphenicol and kanamycin as selective antibiotics. On the next day, the culture was diluted in a larger volume (100-800 ml) and incubated at 37°C under shaking conditions to 0.5 OD<sub>600</sub>/ml for induction with 0.1 mM IPTG (plus addition of antibiotics). After 2-4 h the suspension was pelleted (4000 rpm for 10 min, RT) and the pellet was washed with H<sub>2</sub>O and weighed. 1 ml of lysis buffer (column equilibration buffer plus lysozyme, TritonX-100 and protease inhibitors) was added per 0.1 mg of pellet weight. After 15 min rotation on a wheel (RT or 4°C, depending on protocol), the samples were sonicated and centrifuged (13 000 rpm for 15 min, 4°C). The supernatant was retrieved for purification under native or denaturing conditions on the HisPur™ Cobalt Spin Column (Thermo Scientific) according to the manufacturer's protocol. Alterations were made in the imidazole concentrations of washing (10 mM, 50 mM) and elution (100 mM – 500 mM) buffers and number of washing steps to increase the purity of the eluate. The fractionated samples were stored at -80°C.

### **2.6 Confocal fluorescence microscopy\***

The localization of endogenous GFP/mCherry-tagged proteins within the parasites and RBCs of mutant transfectant lines was analysed by confocal laser scanning microscopy. Infected erythrocytes were enriched using the MACS column and washed twice in pre-warmed Ringer solution, before being added to a perfusion chamber containing Ringer

solution. Optionally, parasite DNA was stained with Hoechst 33342 (15 nM) that was added to the Ringer solution. After settling onto the cover slips, the parasites were mounted onto the LSM 510 laser-scanning microscope (Zeiss, Jena) and viewed with a 63x or 100x magnification objective (Plan-Apochromat 63x/100x, 1.4 Oil; C-Apochromat 63x/100x, 1.2 H<sub>2</sub>O immersion) in bright field (DIC), wide-field fluorescence (HBO-lamp) and confocal fluorescence. GFP fusion proteins were excited using a 488 nm Argon ion laser and emission was detected through a 505-550 nm band pass filter. For excitation of the Hoechst 33342 dye the UV-Laser was used (364 nm) and emission was detected with a 385-470 nm band pass filter. Fluorescence of mCherry-tagged fusion proteins was excited using a 543 nm Helium-Neon laser and emission was detected through a 560 nm low pass filter. Images were collected using the LSM Imaging software (Zeiss, Jena) and further processed using FIJI (Schindelin et al, 2012). In the subsequent 'Results' section, nuclear staining with Hoechst is always represented by the blue channel, GFP fluorescence is depicted in the green channel, mCherry in the red channel, DIC imaging is in the bright field channel and a fourth image represents the overlay of the former channels. For quantitative image analysis, settings were optimized to prevent extensive bleaching and saturation of pixels in the brightest intensities. Raw images were used for quantification purposes, while qualitative images were carefully processed concerning brightness, contrast, signal amplification and background reduction using the FIJI image analysis software.

## 2.7 Flow cytometry\*

The quantification of fluorescence in live *P. falciparum* parasites expressing a regulable GFP-tagged version of the candidate protein in this study (PfNAT) was achieved through flow cytometric analysis using a FACScalibur (Becton Dickinson) as previously described (Staalsoe et al, 1999). Briefly, iRBCs of a 5 ml culture plate were magnet-purified on the MACS column with minimum exposure to light, pelleted (1900 rpm for 2 min, RT), washed twice in Ringer solution, resuspended in 100 µl of Ringer solution and incubated in the 37°C water bath. For direct FACS analysis, 40 µl of this suspension was added to 400 µl of 1xPBS and transferred into suitable vials. In parallel, DNA staining with EtBr (1 µg/ ml) was carried out in 60 µl 1xPBS plus 40 µl parasite suspension at 37°C for 10 min. After incubation, the 100 µl of sample were added to 300 µl of 1xPBS

and transferred to suitable vials. Fluorescence was collected in the GFP channel (FL1-H) of the FACScalibur, whereas EtBr staining was collected in the respective channel (FL2-H). 50 000 cells were counted per measurements and plotted in histograms using the CellQuest Pro analysis software 6.0.4 (Becton Dickinson). A region of interest excluding background fluorescence was determined (M2) and information such as the geometric mean and gated events was collected for this selected area. The remaining 20  $\mu$ l of parasite samples were centrifuged and smeared on a glass slide for Giemsa-staining and microscopic observation of developmental stage and parasitaemia.

### **2.8 Mass spectrometry\***

*P. falciparum* parasites expressing different GFP-tagged mutant STEVOR<sup>1-80</sup> and KAHRP<sup>1-69</sup> proteins were analysed for N-terminal cleavage and acetylation of the PEXEL motif. This part was conducted in collaboration with the group of Dr. Christine Schaeffer-Reiss at the Laboratoire de Spectrométrie de Masse BioOrganique in Strasbourg. The methods are provided in their final reports and copied for the sake of completeness. Prior to mass spectrometric analysis, sample preparation included large-scale purification of mutant transgenic parasites using the MACS column, saponin lysis of these iRBCs and affinity-purification of the GFP-tagged fusion proteins from pellet and saponin fractions using anti-GFP antibody-coupled agarose beads (carried out by Dr. C. Sanchez and S. Prior).

#### **2.8.1 Sample preparation for loading buffer elutions**

##### **Gel electrophoresis**

Samples were loaded on a 15% SDS polyacrylamide gel for electrophoresis. After migration the gels were stained using colloidal blue during 4 days. All the major bands were then excised from the gel and put into a costar 96 well plate. Destaining, reduction, alkylation and dehydration were then performed using an automated system (MassPREP, Waters, Manchester, UK). The gel slices were washed twice with 50  $\mu$ L of 25 mM ammonium hydrogen carbonate ( $\text{NH}_4\text{HCO}_3$ ) and 50  $\mu$ L of acetonitrile. The cysteine residues were reduced by 50  $\mu$ l of 5 mM TBP at 57°C and alkylated by 50  $\mu$ l of 55 mM iodoacetamide. Finally a dehydration step with acetonitrile was performed.

**In-gel labelling reaction**

The N-termini of the proteins are then labelled using N-tris (2,4,6-trimethoxy-phenyl) phosphonium acetyl succinimide (TMPP), which, apart from improving the ionization and fragmentation pattern of a sample, can only bind to unmodified N-termini (Bland et al, 2014). 100 µg of TMPP in 80/20 water/acetonitrile (2 µL) are added to each gel bands before adding 50 µL of the reaction buffer, which consisted of 50 mM Tris-HCl pH = 8.20. The reaction is done over 1 hour under agitation and then 2 µL of 50 % hydroxylamine were added to quench the reaction (30 min with agitation). The gel slices are then transferred to a new plate and 4 cycles of washing and dehydration are performed using the Massprep automated system.

**Digestion**

The proteins were then cleaved in gel with 62.5 ng of modified porcine trypsin (Promega, Madison, WI, USA) in 50 µL of 25 mM hydrogen carbonate at 37°C overnight. The tryptic peptides were then extracted twice using 30µL of a CH<sub>3</sub>CN/H<sub>2</sub>O 60/40 + 1% HCOOH solution for the first extraction and 10µL 100% CH<sub>3</sub>CN for the second one. The extracts corresponding to the same bands were pooled and then the volumes were reduced by speed vacuuming to eliminate acetonitrile and concentrate the peptides. The samples were then ready to be analysed by LC-MS/MS.

**2.8.2 LC-MS/MS analysis**

Samples were analysed using an ultra-performance liquid chromatography system (NanoAcquity, Waters, Milford MA, USA) coupled to a high resolution nanoElectrospray-Quadrupole-Time of Flight type mass spectrometer (Maxis, Bruker Daltonics, Bremen, Germany). The samples were trapped on a 20 x 0.18 mm, 5 µm Symmetry C18 precolumn (Waters), and the peptides were separated on a ACQUITY UPLC® BEH130 C18 column (Waters), 75 µm x 250 mm, 1.7 µm particle size. The solvent system consisted of 0.1% formic acid in water (solvent A) and 0.1% formic acid in acetonitrile (solvent B). Trapping was performed during 1 min at 15 µL/min with 99% of solvent A and 1% of solvent B. Elution was performed at a flow rate of 450 nL/min, using 6-43.5% gradient (solvent B) over 35 min at 45°C followed by 90% (solvent B) over 1 min before the reconditioning of the column at 99% of solvent A over 6 min.

The Maxis equipped with a nanosprayer was operated in the positive ion mode. Mass calibration of the TOF was achieved prior to analysis from  $m/z$  50 to 2200 using Tunemix (Agilent technologies, Waldbronn, Germany). Online correction of this calibration was performed using two Tunemix ions ( $m/z$  299.2945 and 922.0098) as recalibration masses. The capillary voltage was set to 4500 V and the end plate offset to -500 V. For tandem MS experiment, the system was operated with automatic switching between MS and MS/MS modes. The MS scan is performed over an  $m/z$  range of [50;2200] at 0.2 seconds/scan. The MS/MS time is regulated by the intensity of the selected peak on the MS spectrum; it ranges from 0.1 to 1.4 seconds/scan over the same  $m/z$  range. The five most abundant peptides, preferably doubly and triply charged ions, were selected on each MS spectrum for further isolation and Collision Induced Dissociation (CID) using an optimized collision energy depending on the charge state and the  $m/z$  of the ion. The selected peptides are then excluded for 0.8 seconds. The complete system was fully controlled by Compass Hystar (Bruker).

### **2.8.3 Protein identification**

MS data collected during analysis were processed, converted to .mgf files using Compass Data Analysis 4 (Bruker). The mgf peak list files were then submitted to Mascot search engine (Matrix Sciences, London, UK) version 2.3.01 on a local server. Searches were performed against a composite target-decoy database generated using internally developed tools (<http://msda.u-strasbg.fr>) and containing the NCBI protein sequences of *P. falciparum*, the sequences of the chimerical STEVOR proteins and common contaminants (trypsin and human keratins). Searches were performed with a tolerance of 5 ppm for precursor ions and 0.02 Da for fragment ions allowing a maximum of two miss cleavages site for semitrypsin or semiAspN. Carbamidomethylation of cysteine residues, oxidation of methionine residues, acetylation of peptide N-terminal residues, and TMPP labelling of peptide N-terminal residues were searched as variable modifications. All spectra that yielded N-terminus identification were manually reinspected.

### 3 Results

#### 3.1 Mutagenesis of the PEXEL motif of STEVOR and KAHRP

The human erythrocyte is extensively modified upon invasion by *P. falciparum*, which is facilitated by the export of various parasitic effector proteins into the host cell. The majority of these proteins contain the PEXEL motif that mediates trafficking beyond the parasitophorous vacuole (Hiller et al, 2004; Marti et al, 2004). The processing of the PEXEL motif in the ER was shown to be essential for successful export of the respective proteins (Boddey et al, 2009). Although cleavage of this pentameric amino acid motif after the conserved leucine by the aspartic acid protease Plasmeprin V as well as consecutive acetylation of the newly formed N-terminus was experimentally verified, the details of the entire process are still unknown. However, these steps represent a major bottleneck in the export of these virulence-relevant proteins, which renders them as promising drug targets (Haase & de Koning-Ward, 2010; Russo et al, 2010).

So far, mutagenic studies on the PEXEL motif were mainly restricted to deletions of the whole motif as well as alanine exchanges of the conserved amino acids of different proteins (Boddey et al, 2010; Boddey et al, 2009; Hiller et al, 2004; Marti et al, 2004). Although these initial studies provided valuable information on the importance of this motif in guiding proper export, a more detailed analysis would dissect the motif into its relevant characteristics.

In order to assess the variability of amino acids among all five PEXEL positions in relation to the export phenotype this study included an extensive mutagenesis analysis of the PEXEL motif of a GFP-tagged soluble exported protein of the STEVOR family. Several amino acids with different chemical properties were chosen for the exchange to test the importance of size, charge or polarity within the given sequence context (Figure 12). Furthermore, mass spectrometry was conducted on chosen mutants to investigate the importance of PEXEL cleavage and acetylation in correlation with the export phenotype. In order to confirm their relevance some amino acid exchanges were repeated in a second GFP-tagged PEXEL protein, namely KAHRP.

The first position (R<sup>48</sup>) of the PEXEL motif (apart from R<sup>48</sup>K) was already investigated by our former PhD student P. Henrich in his thesis (Henrich, 2008). For complementary reasons the results of this mutagenesis will be included and shortly discussed. In

## RESULTS

continuation of this project, the present study concentrated on the second to fifth PEXEL position (L<sup>49</sup>-Q<sup>52</sup>). A. Günther contributed 11 of the STEVOR<sup>1-80</sup> mutants under my supervision in the course of her teacher's thesis.

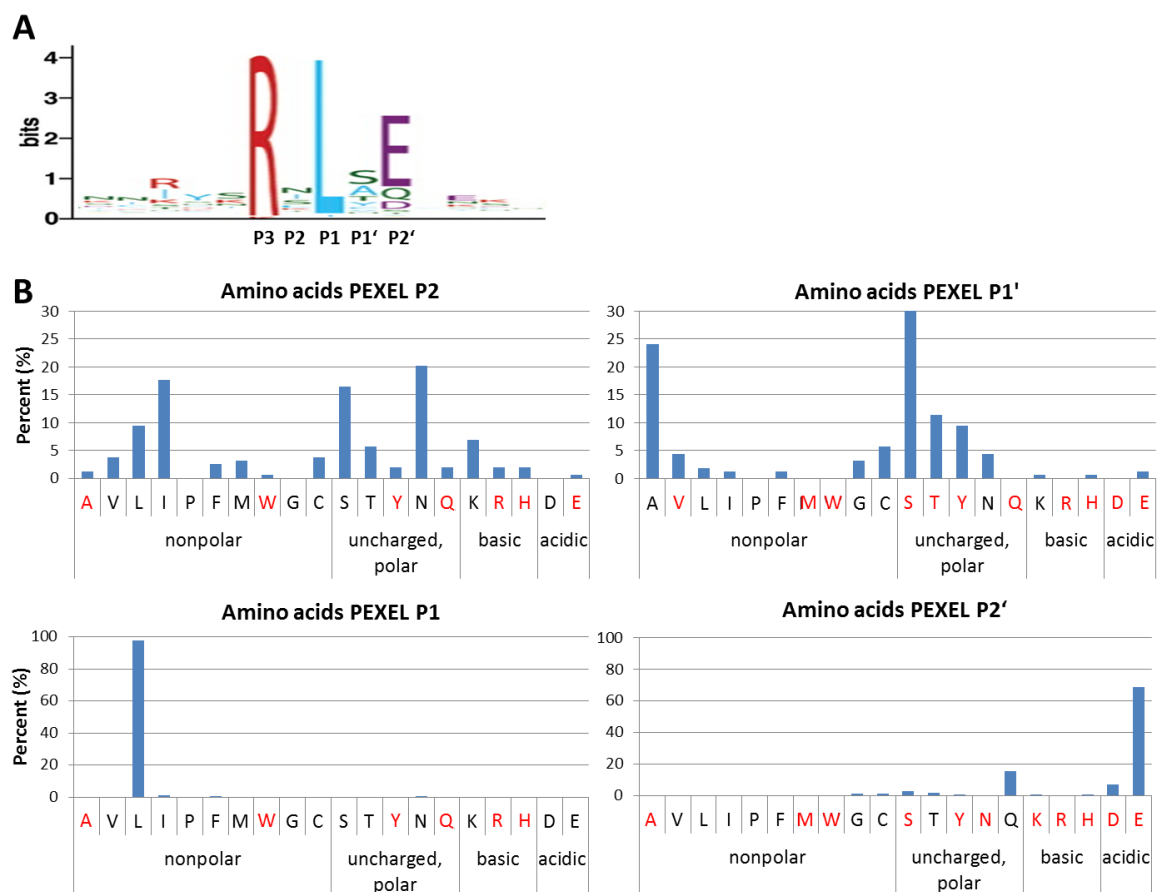


**Figure 12. Mutagenesis screen of the PEXEL motif of STEVOR<sup>1-80</sup>**

(A) Sequence logo representing the conservation of the PEXEL motif in 158 predicted *P. falciparum* proteins excluding the multiple gene families of *var*, *rif* and *stevor*. The height of each letter is proportional to the frequency of amino acids in each position. The total letter height indicates the amount of information (bits) contained in the amino acids at that position. Amino acid color coding: red, basic; purple, acidic; blue, hydrophobic; green, polar amino acids. Adaptation from Marti et al (2004). Substrate cleavage site residues are designated P3-P2-P1-P1'-P2' with hydrolysis between P1 and P1'. Nomenclature adopted from Guruprasad et al (2011). (B) Histograms of relative occurrence of each amino acid in positions P2-P2' of the PEXEL motifs of 158 predicted proteins by Marti et al (2004). Amino acids chosen for replacement of L<sup>49</sup> (P2), L<sup>50</sup> (P1), A<sup>51</sup> (P1') and Q<sup>52</sup> (P2') in STEVOR<sup>1-80</sup> shown in red. Classification adopted from Alberts (2010).

### 3.1.1 Subcellular localization of STEVOR<sup>1-80</sup> mutants

The following mutagenesis analysis was conducted on a member of the PfSTEVOR protein family (gene ID: PF3D7\_0631900, PlasmoDB), a transmembrane protein that localizes to the Maurer's clefts in its full-length version. It was previously shown that a short soluble version of this protein comprising the first 80 amino acids including the signal peptide and PEXEL motif (aa 48-52) is translocated into the RBC cytosol thereby rendering it a suitable model protein to investigate PEXEL-mediated protein export (Przyborski et al, 2005).

In this study the gene encoding the first 80 amino acids of STEVOR followed by GFP (STEVOR<sup>1-80</sup>) was cloned into the pARL1a+ vector under the *PfCRT* promoter for episomal transfection into the *P. falciparum* 3D7 strain. Single amino acid mutations were introduced into the PEXEL motif by megaprimer synthesis and subsequent overlap extension PCR followed by standard cloning procedures, sequencing and transfection. The parasites were positively selected for plasmid uptake with WR99210 within a period of 3-6 weeks and analysed under the confocal laser scanning microscope. The localization of the fluorescent proteins was determined for all stages of intraerythrocytic development. In addition, trophozoite-stage parasites were purified with a magnetic column to gain a better overview of the export phenotype. Representative images of at least 25 parasitized RBCs with young to mature trophozoites recorded on two or more different dates are shown for every mutant. The wild-type version of STEVOR<sup>1-80</sup>, representing proper PEXEL-mediated protein export, was characterized by an evenly distributed fluorescence within the RBC cytosol after successful translocation beyond the PVM. Furthermore, a stage-dependent proportion of the chimeric proteins was present in the ER of early trophozoites as well as residual fluorescence of lysis-resistant GFP in the food vacuoles of late-stage parasites as a consequence of haemoglobin digestion (Figure 13A). The amino acid exchanges within the first position of the PEXEL motif of STEVOR<sup>1-80</sup> uniformly resulted in intraparasitic retention of the mutant proteins (Figure 13B). This phenotype was described previously for R<sup>48</sup>A and was attributed to a defect in cleavage by Plasmepsin V within the parasite ER, which renders the mutant proteins incapable to exit this compartment (Boddey et al, 2009).

## RESULTS

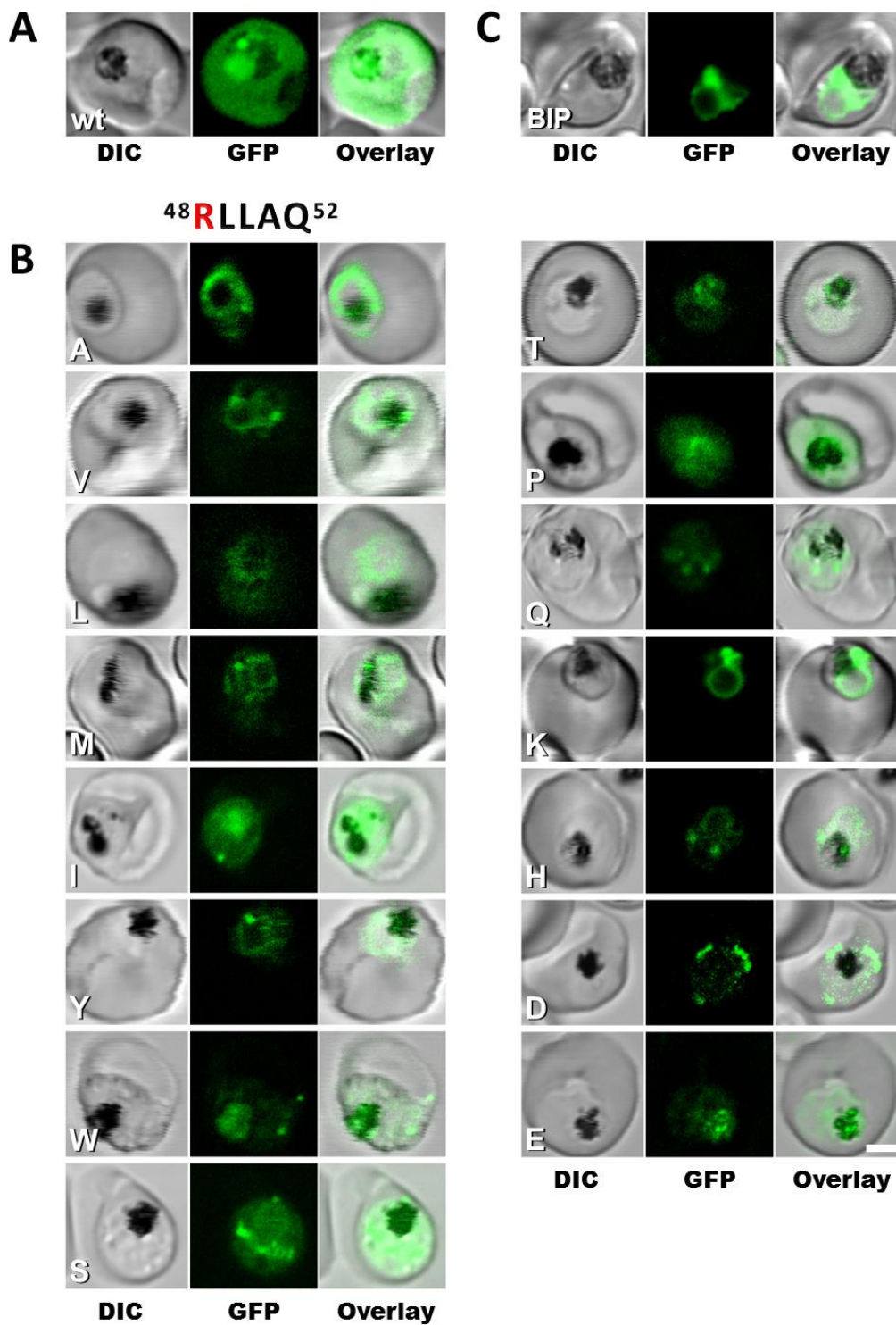


**Figure 13. Export phenotypes of wild-type and R<sup>48</sup> (P3) mutants of STEVOR<sup>1-80</sup>**

Confocal images of live *P. falciparum*-infected erythrocytes. Transfectant parasites at trophozoite stage expressing different chimeric GFP-tagged fusion proteins of wild-type and mutated STEVOR<sup>1-80</sup>. (A) Wild-type STEVOR<sup>1-80</sup> was exported into the RBC, with residual fluorescence in the food vacuole as well as ER. (B) All parasites with mutations in R<sup>48</sup> (P3) showed an intraparasitic retention. These data (apart from R<sup>48</sup>K) were generated by Dr. P. Henrich (Henrich, 2008). (C) Localization of BIP<sup>GFP</sup> as a known soluble marker protein of the ER. Left images, differential interference contrast (DIC); middle images, GFP fluorescence; right images, overlay of both channels. Scale bar: 2  $\mu$ m.

In contrast to previous assumptions, that lysine can replace arginine at P3 (Boddey et al, 2009), R<sup>48</sup>K was not exported but instead also localized to a perinuclear compartment indicative of the ER, which was confirmed by comparison with parasites that expressed GFP-tagged BIP, an established soluble marker protein of this organelle (Figure 13C) (Kumar & Zheng, 1992). This result is in agreement with data acquired through *in vitro* cleavage assays using recombinant Plasmepsin V and synthetic PEXEL peptides, which characterize the lysine mutant (R<sub>P3</sub>→K) as a non-cleavable peptide (Boddey et al, 2013). As recently shown, the residues that line the active site binding pocket of Plasmepsin V in the S3 subsite specifically complement the corresponding side-chains of arginine at P3, an interaction that is crucial for hydrolysis of the motif (Guruprasad et al, 2011).

In summary, the conservation of this amino acid in almost all putatively exported PEXEL proteins (Figure 12A) as well as the results of P. Henrichs mutagenesis screen at this position points to a functional restriction that is limited to arginine and most likely relevant for cleavage by Plasmepsin V.

In contrast, the amino acid exchanges within the second PEXEL position (L<sup>49</sup>) did not interfere with export of the chimeric proteins into the RBC cytosol (Figure 14A). All mutants showed a fluorescence pattern comparable to the STEVOR<sup>1-80</sup> wild-type phenotype. This microscopic observation was further confirmed by quantitative analysis of relative fluorescence in the infected RBC cytosol of representative images using the FIJI software (Figure 14B). For this purpose, raw fluorescence intensities of the whole parasitized cells as well as the parasites only were measured in unmodified suitable images with subsequent background reduction (n=14 cells on average). From this the relative fluorescence in the parasites as well as the host cell cytosol were calculated and the latter presented in histograms for all mutants generated in this screen. The proportion of wild-type GFP-tagged STEVOR<sup>1-80</sup> that is exported into the host cell cytosol is around 56%, taking into account the intra-ER as well as residual food-vacuolar pool of fluorescent protein in the parasite. The data obtained for L<sup>49</sup> are in a similar range (L<sup>49</sup>H, E, Y slightly reduced), which supports the general conclusion based on sequence conservation data that this position is rather permissive towards different amino acid structures. On the contrary, mutagenesis of the third PEXEL position of STEVOR<sup>1-80</sup> (L<sup>50</sup>) had a drastic effect on export of the mutant chimeric GFP proteins.

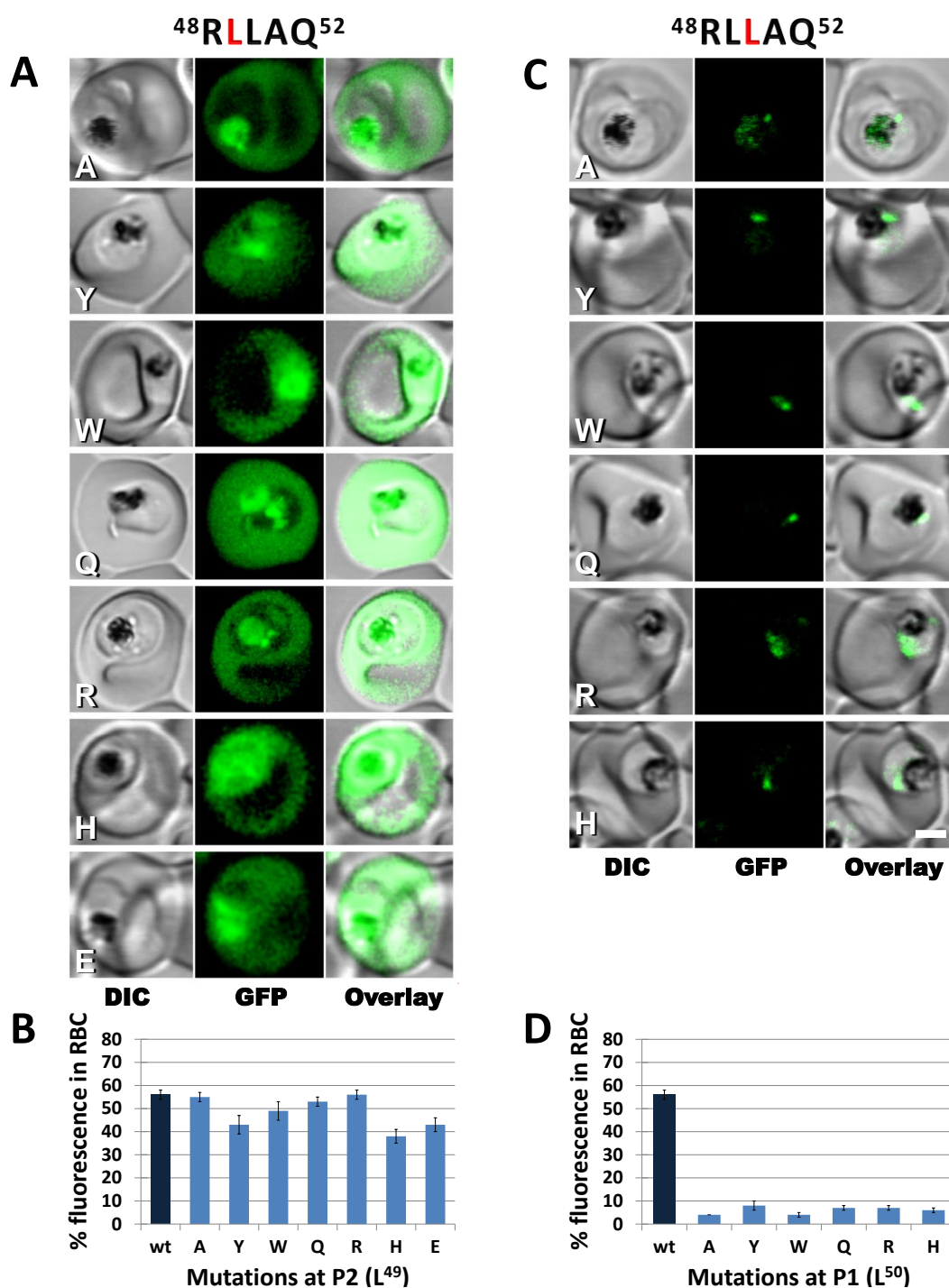


**Figure 14. Export phenotypes of L<sup>49</sup> (P2) and L<sup>50</sup> (P1) mutants of STEVOR<sup>1-80</sup>**  
 Confocal images and quantification of *P. falciparum* parasites at trophozoite stage expressing chimeric GFP-tagged fusion proteins of wild-type and mutated STEVOR<sup>1-80</sup>. (A) Amino acid exchanges at position L<sup>49</sup> (P2) do not interfere with a normal export into the RBC cytoplasm. Left images, differential interference contrast (DIC); middle images, GFP fluorescence; right images, overlay of both channels. Scale bar: 2  $\mu$ m. (B) Relative fluorescence in iRBC cytosol demonstrating amount of exported STEVOR<sup>1-80</sup> protein in different P2 mutants. Error bars are standard error of the mean (SEM). wt, wild type. (C) L<sup>50</sup> (P1) mutants are unable to be exported but instead localize to a bright spot in the parasite. Image order like in (A). (D) Relative fluorescence in iRBC cytosol demonstrating amount of exported STEVOR<sup>1-80</sup> protein in different P1 mutants. Error bars are standard error of the mean (SEM). wt, wild type.

In all cases the fluorescence was confined to a very particular bright spot within the parasite, most likely representing a subdomain of the ER (Figure 14C). As described previously, the ER of *Plasmodium* contains several sub-compartments that are involved in export (Lee et al, 2008; Struck et al, 2008). Image analysis revealed a concomitant reduction in host cytosolic fluorescence from ~56% of the wild-type to an average of 6% in the mutants (Figure 14D). Since the P1 mutant L→A in other PEXEL proteins was previously identified to be localized to the ER due to a defect in cleavage by Plasmepsin V, the data obtained here are consistent with the implicated functional importance of this amino acid at this position (Boddey et al, 2009).

The amino acid exchanges of the fourth PEXEL position (A<sup>51</sup>) resulted in two different export phenotypes (Figure 15). The majority of mutant STEVOR<sup>1-80</sup> proteins surrounded the parasite as a bright fluorescent ring indicative of an accumulation within the parasitophorous vacuole. Translocation into the RBC cytosol was reduced in those mutants from 56% to 12% on average (Figure 15B). Frequently, parasite-induced cytostomes for haemoglobin uptake were detectable as fluorescently labelled extensions of the PV into the cytosol. Interestingly, a few transfectant lines were able to partially (A<sup>51</sup>V) or completely (A<sup>51</sup>S, A<sup>51</sup>T) export the mutant GFP chimeric proteins into the host cell with a final localization identical to the wild-type STEVOR<sup>1-80</sup>. Since the sequence conservation of amino acids at this position is quite weak in all putative PEXEL proteins (apart from exclusion of charged amino acids), the findings of two different export phenotypes was quite surprising and the majority of mutant chimeric proteins being retained in the PV was unexpected, especially in comparison to the above described L<sup>49</sup> mutants, where the export was not altered. After proteolytic cleavage in the ER, the remaining N-terminus is acetylated as proven by mass spectrometry in independent studies (Boddey et al, 2009; Chang et al, 2008; Osborne et al, 2010). Although post-translational acetylation after protein cleavage is a rather special process, N-terminal protein acetylation in general occurs very frequently in eukaryotic organisms (Starheim et al, 2012). However, its importance with regard to PEXEL-mediated protein export is uncertain so far (Boddey & Cowman, 2013).

The data of the mutagenesis screen presented in this study here demonstrate that position P1' (A<sup>51</sup>) is not as flexible in amino acid structure as previously assumed and the process of acetylation at this position might indeed influence the final localization of mutant

## RESULTS

proteins. This hypothesis was investigated in more detail by mass spectrometric analysis as described in chapter 3.1.3.

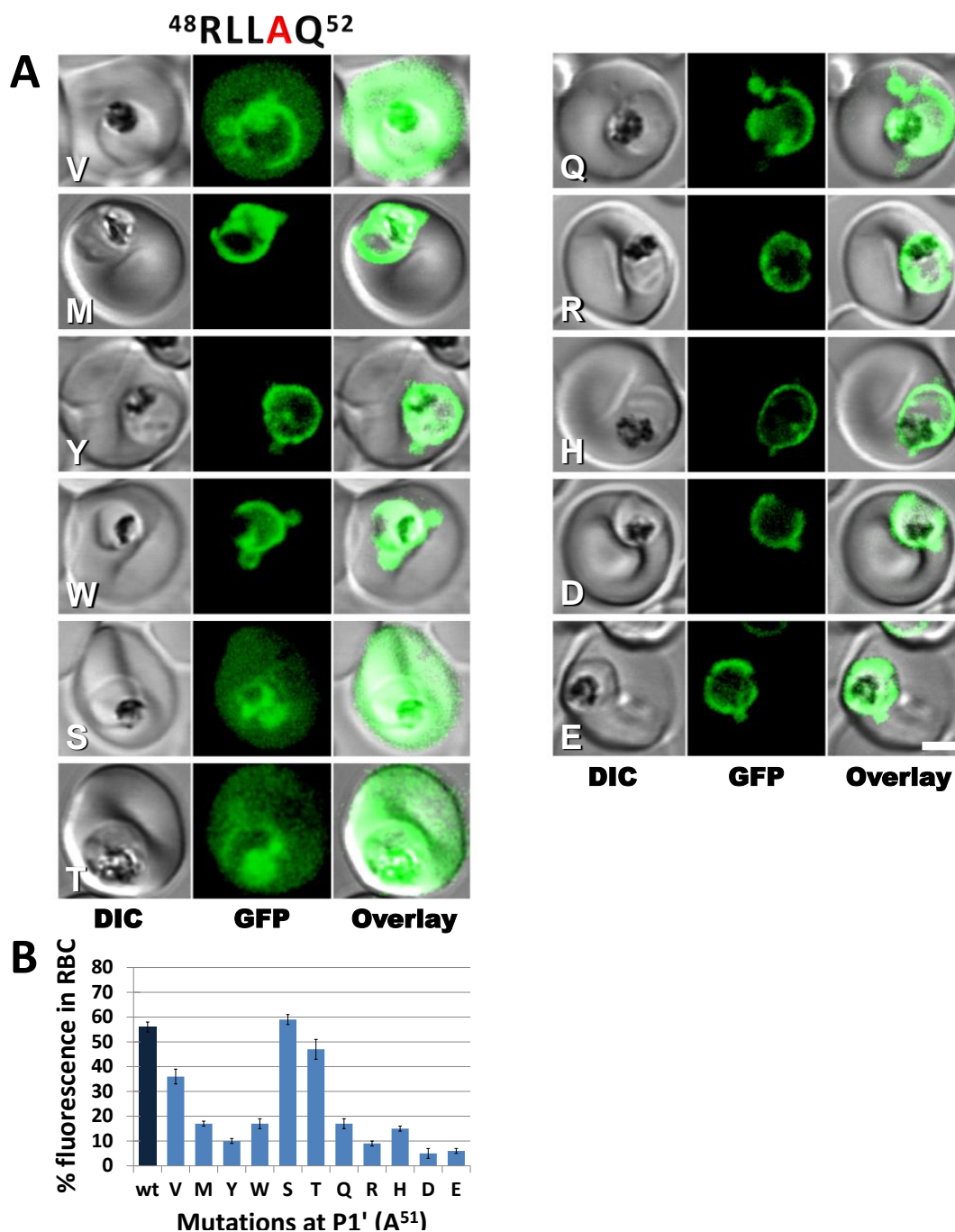


**Figure 15. Export phenotypes of A<sup>51</sup> (P1') mutants of STEVOR<sup>1-80</sup>**

(A) Confocal images of live *P. falciparum*-infected erythrocytes with transfectant parasites at trophozoite stage expressing different chimeric GFP-tagged fusion proteins of mutated STEVOR<sup>1-80</sup>. 4 constructs were contributed by A. Günther under supervision (Günther, 2012). Mutations within position A<sup>51</sup> (P1') show two different phenotypes; A<sup>51</sup>S, T and partially V are exported into the RBC cytoplasm, whereas all other mutants are retained in the PV. Left images, differential interference contrast (DIC); middle images, GFP fluorescence; right images, overlay of both channels. Scale bar: 2  $\mu$ m. (B) Relative fluorescence in RBC cytosol demonstrating amount of exported STEVOR<sup>1-80</sup> protein in different P1' mutants as determined by quantitative image analysis using FIJI. Error bars are SEM. wt, wild type.

In order to confirm the microscopic observations, some of the A<sup>51</sup> mutants were subjected to differential lysis with tetanolysin and saponin followed by western blot analysis using  $\alpha$ -GFP antibodies (Figure 16). Treatment of iRBCs with the bacterial toxin tetanolysin permeabilizes the erythrocyte membrane without affecting the PVM due to differences in membrane cholesterol content (Blumenthal & Habig, 1984). In a next step, the addition of saponin to tetanolysin-treated parasite pellets disrupts the PVM and releases the proteinaceous content of the vacuole, whereas the parasite plasma membrane stays intact (Ansorge et al, 1996; Ansorge et al, 1997; Siddiqui et al, 1979). As can be seen in Figure 16, the export of wild-type STEVOR<sup>1-80</sup> as well as A<sup>51</sup>S into the host cell was confirmed by detection of the proteins in the tetanolysin supernatant representing the erythrocytic cytosol fraction. Depending on the overall developmental stage of the parasite culture (young trophozoites to schizonts) a reasonable proportion of exported STEVOR<sup>1-80</sup> is endocytosed upon haemoglobin digestion and degraded in the food vacuole as indicated by the prominent band of 27 kDa in the saponin pellet fractions corresponding to lysis-resistant GFP.

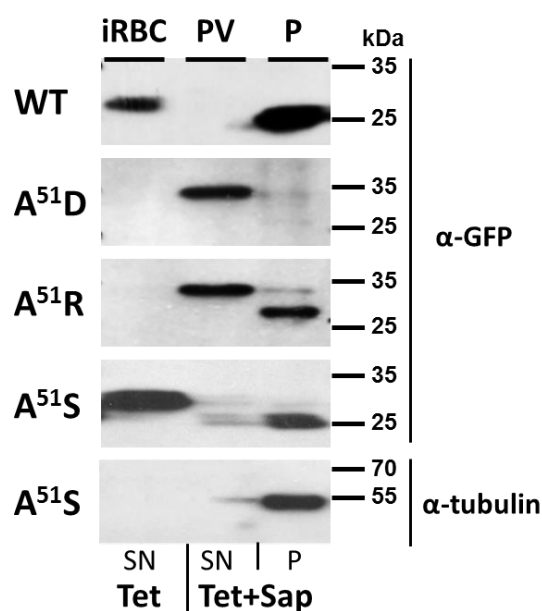


**Figure 16. Western blot analysis of selected A<sup>51</sup> mutants after differential lysis**

The localization of selected STEVOR<sup>1-80</sup> proteins with mutations at position A<sup>51</sup> was investigated by differential lysis of iRBCs using tetanolysin and saponin. After purification iRBCs were lysed with tetanolysin and divided into cytosolic supernatant (iRBC) and pellet. The PVM was further permeabilized by saponin treatment of the pellet to release the content of the vacuole (PV). The remaining pellet corresponds to the parasite fraction (P). All samples were probed with antibodies against  $\alpha$ -GFP and subsequently against tubulin (~50 kDa, to control for intact parasites as exemplified for A<sup>51</sup>S). The upper main bands correspond to processed STEVOR<sup>1-80</sup> (~31 kDa), whereas the lower main band represents GFP alone (~27 kDa). kDa, kilodalton; P, parasite (top)/ pellet (bottom); Sap, saponin; SN, supernatant; Tet, tetanolysin.

## RESULTS

---

In accordance with the microscopic observations, A<sup>51</sup>R and D accumulated in the supernatant of saponin-treated tetanolysin pellets, which is representative of the parasitophorous vacuolar compartment that both fluorescent proteins were confined to. Detection of tubulin in intact parasites was used as a control to exclude excessive lysis that would prevent proper sample fractionation. All STEVOR<sup>1-80</sup> proteins showed a size rather corresponding to the processed form of the PEXEL motif (~31kDa) in contrast to the unprocessed version (~ 37 kDa). However, as previously mentioned, alternative cleavage within the signal sequence can occur and the determination of N-terminal processing by mass spectrometry is inevitable (Boddey et al, 2009).

In the next step, the last position of the pentameric PEXEL motif was examined to address the question if the sequence conservation of E/Q/D (Q<sup>52</sup> in STEVOR) was a limiting determinant for the successful translocation of the proteins into the RBC cytosol. Interestingly, most of the mutant STEVOR<sup>1-80</sup> proteins were able to guide normal export into the host cell comparable to the wild type (Figure 17A). The only obvious deviation from this phenotype was detected in the two mutant strains where Q<sup>52</sup> was exchanged with positively charged amino acids (Q<sup>52</sup>K, Q<sup>52</sup>R). Here, the fluorescence was mainly limited to the PV and export beyond the PVM was reduced from 56% to 15% (Figure 17B). In the Q<sup>52</sup>D mutant, some parasites showed full export of the GFP chimera; however, a significant number of parasites exhibited only a partial export phenotype with a visible amount of protein retained in the PV. Since aspartic acid (D) is one of the conserved residues at this position (E/Q/D) this finding was unexpected but it indicates the importance of taking the individual sequence context into consideration.

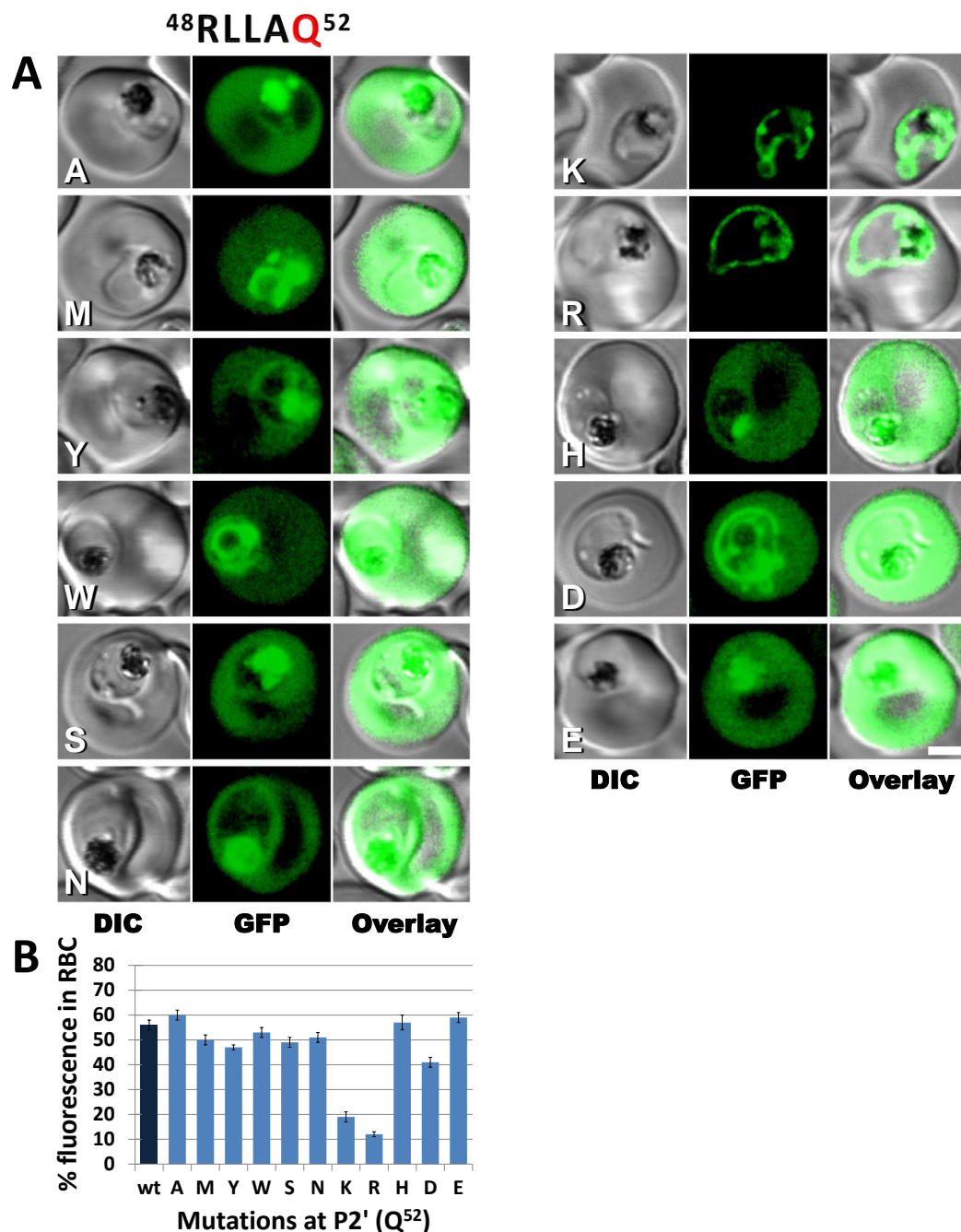


**Figure 17. Export phenotypes of Q<sup>52</sup> (P2') mutants of STEVOR<sup>1-80</sup>**

(A) Confocal images of live *P. falciparum*-infected erythrocytes with transfected parasites at trophozoite stage expressing different chimeric GFP-tagged fusion proteins of mutated STEVOR<sup>1-80</sup>. 7 constructs were contributed by A. Günther under supervision (Günther, 2012). The majority of Q<sup>52</sup> (P2') mutants show the wild-type phenotype of proper PEXEL-mediated protein export, only positively charged amino acid replacements (Q<sup>52</sup>K, R) block traversal of the PVM, which results in a vacuolar retention. Left images, differential interference contrast (DIC); middle images, GFP fluorescence; right images, overlay of both channels. Scale bar: 2  $\mu$ m. (B) Relative fluorescence in RBCs demonstrating amount of exported STEVOR<sup>1-80</sup> protein in different P2' mutants as determined by quantitative image analysis using FIJI. Error bars are standard error of the mean (SEM). wt, wild type.

### 3.1.2 Subcellular localization of KAHRP<sup>1-69</sup> mutants

Up to this point the mutagenesis screen on the export motif was conducted on STEVOR<sup>1-80</sup> and revealed a more complex dimension of variability and conservation than originally assumed, especially in the fourth (A<sup>51</sup>) and fifth (Q<sup>52</sup>) PEXEL position. While A<sup>51</sup> was shown to be more restricted than the sequence conservation data implicate, mutations in Q<sup>52</sup> did not interfere with successful export of the respective proteins apart from positively charged replacements (Q<sup>52</sup>K, Q<sup>52</sup>R) despite the theoretical sequence restriction (E/Q/D).

In the course of this study special attention was paid to A<sup>51</sup>, which is acetylated after cleavage, a process that might influence consecutive trafficking steps. Although STEVOR<sup>1-80</sup> proved to be a good model protein for PEXEL-mediated export, selected mutations at this position were repeated in a second PEXEL protein, KAHRP, to confirm the data obtained before and prove their relevance. It was previously established that the first 69 amino acids of KAHRP, which contain a signal peptide as well as the PEXEL motif (aa 54-58), are sufficient to direct a chimeric GFP fusion protein to the cytoplasm of *P. falciparum*-infected erythrocytes (Marti et al, 2004).

Therefore, the gene encoding the first 69 amino acids of KAHRP (gene ID: PF3D7\_0202000, PlasmoDB) followed by the coding sequence for GFP (further denoted as KAHRP<sup>1-69</sup>) was cloned into the pARL1a+ vector under the *PfCRT* promoter for episomal transfection into the *P. falciparum* 3D7 strain. The following single amino acid replacements at position A<sup>57</sup> were introduced by megaprimer PCR and standard cloning procedures: V, S, T, R, D. All constructs were sequenced and control digested prior to transfection. After transfection intraerythrocytic parasite stages were positively selected for plasmid uptake by WR99210 for the period of 3-6 weeks. The transfectant lines were analysed by confocal fluorescence microscopy and representative images of at least 25 infected RBCs with young to mature trophozoites recorded on minimal 2 different dates are shown (Figure 18A, B). Furthermore, suitable representative images of each mutation (n=14 cells on average) were subjected to quantitative image analysis using FIJI to determine the relative amount of exported GFP-tagged protein in the RBC cytosol (Figure 18C).

The distribution of the wild-type KAHRP<sup>1-69</sup> was identical to STEVOR<sup>1-80</sup> with a clear translocation of the GFP-tagged protein into the RBC cytoplasm, bright fluorescence of

---

lysis-resistant GFP in the food vacuole of mature parasite stages and some residual intraparasitic fluorescence indicative of ER localization (Figure 18A).

The transfectant parasites expressing KAHRP<sup>1-69</sup> with the mutations A<sup>57</sup>V, R and D showed a bright ring of fluorescence surrounding the parasite and a reduction in export to the host cell cytosol from ~62% to ~7% on average (Figure 18B, C). These data indicate that the soluble GFP chimeric proteins are secreted into the PV but are unable to cross the PVM. This phenotype is identical to the STEVOR<sup>1-80</sup> A<sup>51</sup>R and D mutants thus confirming the previously acquired results. The replacement with valine at this position showed partial export ability in the STEVOR<sup>1-80</sup> background, however this was absent in the KAHRP<sup>1-69</sup> mutant with a clear defect in translocation. This difference might be attributed to the surrounding sequence context of these two proteins, which probably influences the outcome of the mutagenesis as reported previously in other studies (Boddey et al, 2009).

Interestingly, the A<sup>57</sup>S mutant and the majority of A<sup>57</sup>T expressing parasites showed a normal export phenotype comparable to the wild type and identical to the respective STEVOR<sup>1-80</sup> mutants. This finding provides additional proof that serine and threonine can replace alanine successfully at this position with regard to a possible functional role in processing or protein interactions. A minor proportion of the A<sup>57</sup>T expressing parasites also displayed retention in the PV, so the mutation might not be able to adequately replace the wild-type alanine in all parasites. This infrequent observation of different export phenotypes in one transfection has previously been reported (Boddey et al, 2009; Heiber et al, 2013).

## RESULTS

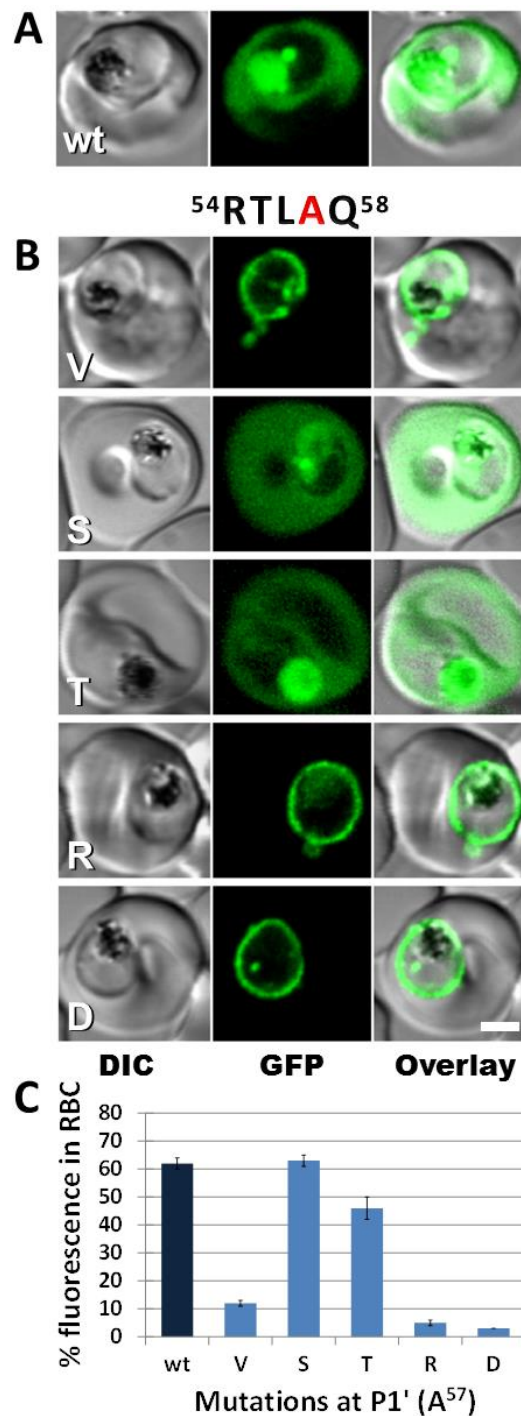


**Figure 18. Export phenotypes of A<sup>57</sup> (P1') mutants of KAHRP<sup>1-69</sup>**  
 Confocal images of live *P. falciparum*-infected erythrocytes and quantification of fluorescence in RBC cytosol. Transfectant parasites at trophozoite stage expressing different GFP-tagged fusion proteins of KAHRP<sup>1-69</sup> are shown. (A) The wild-type PEXEL motif of KAHRP<sup>1-69</sup> was able to guide export of the reporter into the RBC cytoplasm. A stage-dependent proportion can be found in the ER as well as the food vacuole. (B) Mutations at position A<sup>57</sup> (P1') resulted in different phenotypes; A<sup>57</sup>S and T showed a fluorescence distribution comparable to the wild-type with successful traversal of the PVM, whereas the other mutant proteins (A<sup>57</sup>V, R and D) were confined to the PV. Left images, differential interference contrast (DIC); middle images, GFP fluorescence; right images, overlay of both channels. Scale bar: 2 μm. (C) Quantification of exported KAHRP<sup>1-69</sup> chimaeras determined by relative fluorescence in RBC cytoplasm. Error bars are SEM.

### 3.1.3 Processing of particular STEVOR<sup>1-80</sup> mutants

In addition to the localization of the different mutants, the next part of the study aimed at finding a correlation between the export of PEXEL proteins and processing of this motif. In particular, the cleavage and acetylation state of chosen STEVOR<sup>1-80</sup> mutants was of interest in order to understand the observed implications of certain amino acid exchanges. Therefore, mass spectrometry was conducted, which represents a suitable tool to identify cleavage sites and protein modifications. This work was done in collaboration with Dr. C. Schaeffer-Reiss at the mass spectrometry platform in Strasbourg. In order to distinguish free N-termini from acetylated ones, N-tris (2,4,6-trimethoxy-phenyl) phosphonium acetyl succinimide (TMPP) was used as a label. Apart from improving the ionization and fragmentation pattern of a sample, this labelling reagent can only bind to unmodified N-termini (Bland et al, 2014). In case of N-terminal acetylation, TMPP cannot access the peptide thus providing indirect proof of this protein modification.

The aim was to analyse mutant STEVOR<sup>1-80</sup> proteins of each PEXEL position that represent certain export phenotypes concerning retention or translocation of the chimeric proteins. The protein samples were collected from saponin-lysed iRBCs after magnetic purification and divided into supernatant and pellet fractions (this work was mainly done by S. Prior). After immunoaffinity chromatography with  $\alpha$ -GFP agarose (this work was done by Dr. C. Sanchez), the proteins were separated on SDS-Gels, excised and labelled with TMPP after reduction and alkylation. Digestion with trypsin was carried out in the gel slices, the tryptic peptides were extracted, pooled and analysed by LC-MS/MS to determine the mass and amino acid sequence of N-terminal peptides.

As can be seen in Table 1 the wild-type STEVOR<sup>1-80</sup> was processed as expected with cleavage at P1 (L<sup>50</sup>) and N-terminal acetylation at P1' (A<sup>51</sup>). The R<sup>48</sup>A mutant was not cleaved and consequently not acetylated most likely due to a disturbed interaction with the active site of Plasmepsin V that seems specifically suited to harbour arginine at this position (Guruprasad et al, 2011). In contrast, L<sup>49</sup>A was normally processed with respect to cleavage and acetylation, which is further supported by a normal export phenotype into the RBC cytoplasm. In line with R<sup>48</sup>A, L<sup>50</sup>A was also identified neither cleaved nor N-terminally acetylated. The fact that all mutants at both positions were unable to exit the ER clearly demonstrates the importance of the cleavage event for the first steps of

## RESULTS

PEXEL-mediated trafficking. Furthermore, these results confirm published data on the processing of other PEXEL proteins such as GBP130 (Boddey et al, 2009). A more diverse processing pattern was determined for different A<sup>51</sup> mutants (A<sup>51</sup>R, S, D) allowing interesting assumptions to be made. While A<sup>51</sup>S was normally processed, acetylated and exported to the host cell cytosol, A<sup>51</sup>R and A<sup>51</sup>D were cleaved but their N-termini were not acetylated. Both mutant GFP-tagged proteins accumulated in the PV and were unable to traverse the PVM. For the first time, these data indicated a possible relevance of acetylation in guiding proper translocation of a PEXEL protein beyond the PVM.

Position	Sequence	Cleaved at P1	Acetylated at P1'	Export into RBC
wt	<sup>48</sup> RLLA <sup>52</sup> Q	Yes	Yes	Yes
<sup>48</sup> R	<sup>48</sup> ALLA <sup>52</sup> Q	No	No	No, parasite
<sup>49</sup> L	<sup>48</sup> RALA <sup>52</sup> Q	Yes	Yes	Yes
<sup>50</sup> L	<sup>48</sup> RLAA <sup>52</sup> Q	No	No	No, parasite
<sup>51</sup> A	<sup>48</sup> RLLS <sup>52</sup> Q	Yes	Yes	Yes
<sup>51</sup> A	<sup>48</sup> RLLD <sup>52</sup> Q	Yes	No	No, PV
<sup>51</sup> A	<sup>48</sup> RLLR <sup>52</sup> Q	Yes	No	No, PV
<sup>52</sup> Q	<sup>48</sup> RLLA <sup>52</sup> A	Yes	Yes	Yes
<sup>52</sup> Q	<sup>48</sup> RLLAN <sup>52</sup>	Yes	Yes	Yes
<sup>52</sup> Q	<sup>48</sup> RLLAR <sup>52</sup>	Yes	Yes	No, PV

**Table 1. Mass spectrometry conducted on different PEXEL mutants of STEVOR<sup>1-80</sup>**

Mass spectrometric analysis of mutant STEVOR<sup>1-80</sup> proteins to determine the processing state of the PEXEL motif in comparison to their export phenotype. Proteins were extracted from saponin supernatants and pellets of *P. falciparum* transfectant lines followed by affinity purification. This was performed by S. Prior and Dr. C. Sanchez. Samples were separated by SDS gel electrophoresis, TMPP-labelled and subjected to tryptic digest followed by LC-MS/MS analysis. This part was conducted in collaboration with the group of Dr. C. Schaeffer-Reiss at the Laboratoire de Spectrométrie de Masse BioOrganique in Strasbourg. Cleavage of the PEXEL motif after P1 (L<sup>50</sup>) and consecutive N-terminal acetylation of P1' (A<sup>51</sup>) was determined for the wild-type STEVOR<sup>1-80</sup> protein as well as for L<sup>49</sup>A, A<sup>51</sup>S, Q<sup>52</sup>A, N and R mutants. Apart from Q<sup>52</sup>R, these proteins were also normally exported as assessed by fluorescence microscopy (chapter 3.1.1). The absence of PEXEL cleavage occurred in the R<sup>48</sup>A and L<sup>50</sup>A mutant proteins, which were retained within the parasite. A<sup>51</sup>R and D were cleaved but not acetylated and furthermore not exported beyond the PVM.

The mutant proteins of the last PEXEL position (Q<sup>52</sup>) also showed a different processing pattern in accordance to their cellular localization. Q<sup>52</sup>A and Q<sup>52</sup>N were normally processed and exported into the host cell, whereas Q<sup>52</sup>R was identified as being cleaved and acetylated but was clearly retained in the parasitophorous vacuole as described above. This result indicates that acetylation might be a necessary prerequisite but not entirely sufficient for protein export. Other factors such as protein interactions, membrane targeting or chaperone guiding might be involved in the correct trafficking process and these might be influenced by mutagenesis at this position.

Several attempts were made by our collaborators to analyse KAHRP<sup>1-69</sup> wild type, A<sup>57</sup>S and A<sup>57</sup>R by mass spectrometry but, due to unsuitable protease cleavage sites in the protein sequence, this was unfortunately without any success.

### 3.2 Characterization of a putative N-acetyltransferase (PfNAT)

The previous experiments revealed that the A<sup>51</sup> mutant proteins that were limited to the PV (A<sup>51</sup>D, R) were in fact cleaved but not N-terminally acetylated. This finding led to the assumption that acetylation or related interactions during this process might be an important prerequisite for the proper targeting of PEXEL proteins beyond the PVM. Although the majority of eukaryotic proteins are co-translationally acetylated at the N-terminus (e.g. 70-90% in human cell lines) and involvement of this modification in protein degradation, interactions and localization has been implicated, the exact biological function remains elusive (Starheim et al, 2012). This lack of knowledge is even more prominent for post-translational N- $\alpha$ -acetylation after proteolytic cleavage events as observed in the PEXEL motif (Helsens et al, 2011; Wang et al, 2010). Published examples include among others the discovery of processed chloroplast proteins in *Arabidopsis thaliana*. Interestingly, the new N-termini of these proteins after cleavage in the plastid were predominantly occupied by alanine, serine, valine or threonine, which are also preferential substrates of the NatA transferases (Bienvenut et al, 2012). This observation is in accordance with the ability of A<sup>51</sup>S, T and V to replace the wild-type alanine in the STEVOR<sup>1-80</sup> background as presented in chapter 3.1.1. As a consequence, the second part of this study concentrated on the identification of a putative N-acetyltransferase that could be responsible for this apparently important post-translational protein modification.

#### 3.2.1 Identification of PfNAT

The bioinformatic search in PlasmoDB (Version 11.0) for a putative N-acetyltransferase (NAT) in *P. falciparum* revealed 10 candidates with a suitable transferase domain (Table 2). Since recent studies identified Plasmepsin V as an ER-resident protein and most likely cleavage takes place in this compartment, it was suggested that the consecutive acetylation process is localized to the ER (Chang et al, 2008) or maybe other compartments along the export pathway such as the Golgi complex or even the PV. As a consequence the putative N-acetyltransferase was expected to possess sequences, which allow the protein to enter the secretory pathway (signal peptide or transmembrane domain). This limitation was only fulfilled by one of the ten candidate NATs. Therefore, this protein (gene ID in PlasmoDB: PF3D7\_1437000, previous ID: PF14\_0350) was

chosen for the study and will henceforth be termed *P. falciparum* N-acetyltransferase (PfNAT). It has a length of 544 aa, no signal peptide but two N-terminal transmembrane domains separated by a small loop region, and a C-terminal putative N-acetyltransferase domain that is highly conserved among different *Plasmodium* species (Figure 19A, B). A secondary structure prediction of the carboxy (C)-terminus (aa 380-525) using the prediction program PSIPRED (Buchan et al, 2013) revealed a sequence of  $\alpha$ -helices and  $\beta$ -sheets that is characteristic of the GCN5-related N-acetyltransferase (GNAT) domain profile with a structurally conserved topology of  $\beta 1-\alpha 1-\alpha 2-\beta 2-\beta 3-\beta 4-\alpha 3-\beta 5-\alpha 4-\beta 6$  that forms a three-dimensional V-fold (Figure 19C, D) (Vetting et al, 2005). In contrast to the so-called HAT core ( $\beta 2-\beta 3-\beta 4-\alpha 3-\beta 5-\alpha 4$ ) the N-( $\beta 1-\alpha 1$ ) and C-terminal ( $\beta 6$ ) parts are usually less conserved. Proteins of this huge family catalyse the transfer of an acetyl group from the CoA donor to a primary amine of the acceptor and are involved in various cellular processes of prokaryotes and eukaryotes such as N-terminal protein acetylation (NATs), histone acetylation (HATs), neurohormone production (SNATs), antibiotic resistance (AAC) and others (Dyda et al, 2000; Gautschi et al, 2003; Vetting et al, 2005).

Gene ID	UniProt ID	Protein Length	# Exons	# TM Domains	SignalP Scores	Description
PF3D7_0109500	-	155	2	0	0	N-acetyltransferase, putative
PF3D7_0629000	C6KTC5	291	1	0	0	conserved protein, unknown function
PF3D7_0805400	C0H4R5	225	6	0	0	acetyltransferase, putative
PF3D7_0823300	Q8IB67	1465	4	0	0	histone acetyltransferase GCN5 (GCN5)
PF3D7_0924900	C0H559	184	9	0	0	conserved protein, unknown function
PF3D7_1003300	Q8IK04	152	1	0	0	N-acetyltransferase, putative
PF3D7_1144800	Q8IHR9	658	1	0	0	conserved Plasmodium protein, unknown function
PF3D7_1244100	Q8I4Y9	1296	5	0	0	N-alpha-acetyltransferase 15, NatA auxiliary subunit, putative
PF3D7_1323300	Q8IE83	352	1	0	0	acetyltransferase, GNAT family, putative
<b>PF3D7_1437000</b>	<b>Q8IL96</b>	<b>544</b>	<b>3</b>	<b>2</b>	<b>0</b>	<b>N-acetyltransferase, putative</b>

**Table 2. Database search of putative N-acetyltransferases in *P. falciparum* 3D7**

Search on PlasmoDB for N-acetyltransferases in *Plasmodium* retrieved 10 ortholog groups with 10 representative genes in *P. falciparum* strain 3D7 (last access: 1/4/14). Additional information concerning protein length, number of exons and transmembrane domains, probability to contain signal peptides as well as the putative function is provided. The candidate gene chosen for this study is marked in bold red.



In order to assess the localization of PfNAT inside the parasite, the full-length coding sequence was cloned without the stop codon into the pARL1a+-GFP vector under the *PfCRT* promoter and episomally transfected into the *P. falciparum* 3D7 strain. After 6 weeks of positive selection using WR99210 the transfectant parasites were analysed in all stages under the confocal fluorescence microscope and images of at least 30 infected RBCs of young to mature trophozoite stages were taken at different occasions. As can be seen in Figure 20A, the GFP-tagged transmembrane protein localizes to an intraparasitic perinuclear compartment reminiscent of the ER, which is characterized by a perinuclear ring that extends upon maturation of the parasite.

### 3.2.2 Colocalization with other ER proteins

To investigate whether PfNAT actually occupies the same subcellular compartment as Plasmepsin V (PfPMV, gene ID in PlasmoDB: PF3D7\_1323500), the protease that cleaves the PEXEL motif beforehand, transfectant parasites were established that co-expressed PfPMV<sup>GFP</sup> and PfNAT<sup>mCherry</sup>. To do so, the gene encoding full-length Plasmepsin V (590 aa) was cloned from 3D7 gDNA into the pARL1a+-GFP vector and transfected episomally into *P. falciparum* 3D7 parasites. Transfectant selection and microscopic analysis was carried out as described above. Indeed, both fluorescent proteins were localized to the same perinuclear compartment (Figure 20B). As a control, that this result was not caused by an unspecific co-expression of the two fluorescent tags, single transfectants of PfPMV<sup>GFP</sup> and PfNAT<sup>mCherry</sup> were analysed with the same result (Figure 20A). Furthermore, a putative acetyl-CoA transporter was identified by bioinformatics research in the course of this study that potentially delivers the acetyl-CoA necessary for the acetylation process into the ER. The protein sequence of the chosen gene (gene ID: PF3D7\_1036800), henceforth termed *P. falciparum* acetyl-CoA transporter (PfAcT) shows some homology to the mammalian transporter AT-1 (33% sequence identity to human AT-1, 96% coverage, e-value  $8e^{-84}$ ), which was previously described as an ER-resident transporter that regulates the acetylation state of several ER-based proteins (Jonas et al, 2010). PfAcT is the only protein in *P. falciparum* (according to PlasmoDB, Version 11.0) having this putative function and existing homologues in other *Plasmodium* species.

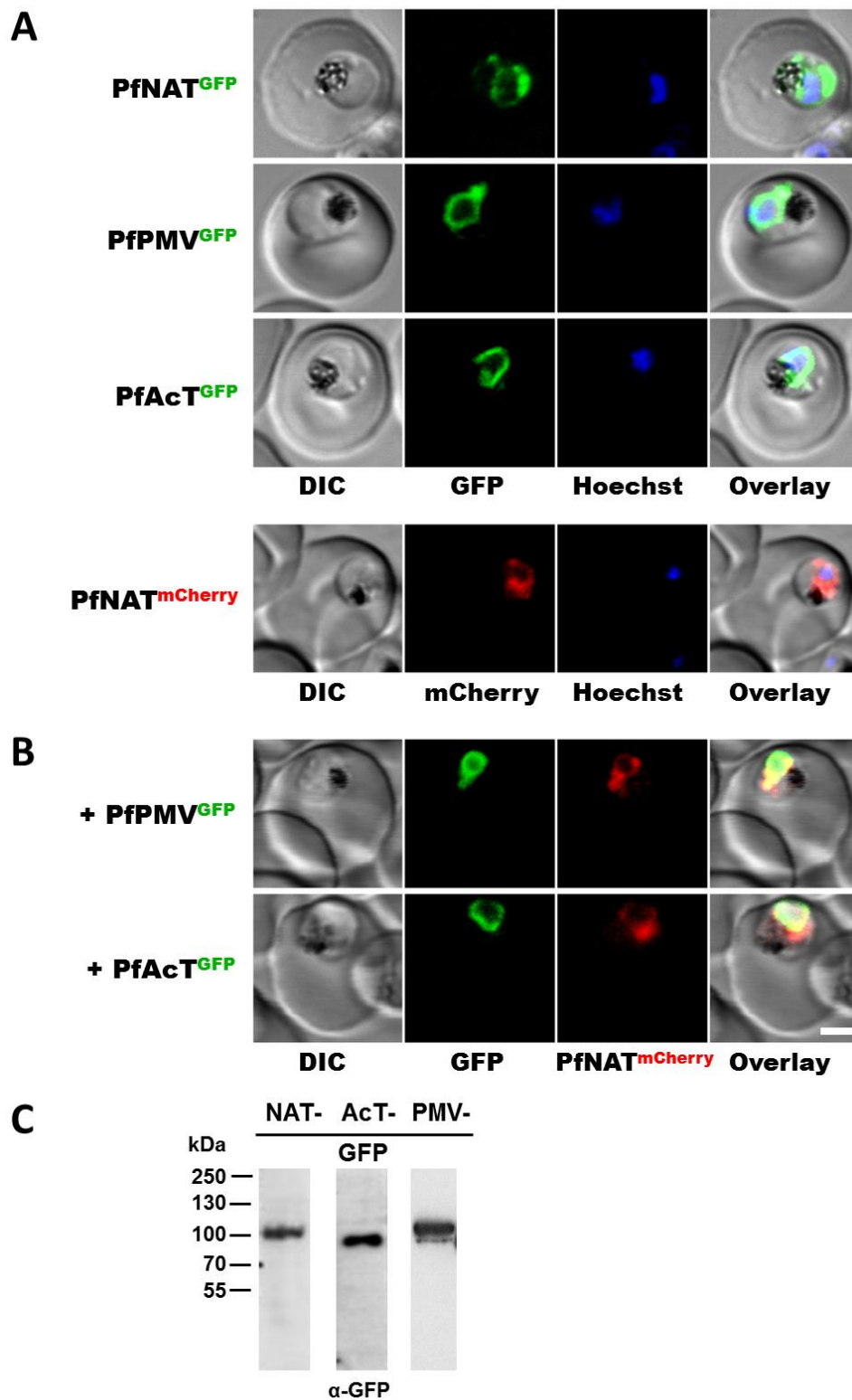


**Figure 20. Localization of PfNAT and other marker proteins within the ER**

Confocal images of live *P. falciparum*-infected erythrocytes. Transfectant parasites at trophozoite stage expressing different fluorescent fusion proteins from episomal plasmids are shown. (A) Localization of the putative transferase PfNAT (tagged to GFP or mCherry). GFP-fusion proteins of Plasmepsin V (PfPMV) as well as a putative acetyl-CoA transporter (PfAcT) occupy the same perinuclear compartment that is indicative of the ER.

(Figure 20 continued) **(B)** Cotransfection of PfNAT<sup>mCherry</sup> with the latter two proteins confirms this assumption although different subcompartments of the ER might be targeted as indicated by a slightly different localization within one parasite. Left images, differential interference contrast (DIC); middle left images, GFP or mCherry fluorescence; middle right images, nuclear staining with Hoechst (A) or mCherry fluorescence (B); right images, overlay of all channels. Scale bar: 2  $\mu$ m. **(C)** Western blot analysis of parasites expressing PfNAT<sup>GFP</sup> (~ 91 kDa), PfAcT<sup>GFP</sup> (~ 97 kDa) and PfPMV<sup>GFP</sup> (~ 96 kDa). Transfectants were isolated from RBCs by saponin lysis and mixed with loading buffer. Detection with  $\alpha$ -GFP antibodies confirmed the predicted sizes although slight deviations occurred due to protein sequence-specific migration characteristics.

Therefore the gene encoding the full-length protein (590 aa) including 10 putative transmembrane domains was amplified from cDNA of the 3D7 strain and cloned into the pARL1a+-GFP transfection vector. Transfection of the 3D7 strain and selection by WR99210 was followed by confocal fluorescence analysis as described above. Furthermore, the construct was used for a cotransfection with PfNAT<sup>mCherry</sup> similar to PfPMV<sup>GFP</sup>. Indeed, both single and double transfectants showed a clear ER-restricted localization of PfAcT<sup>GFP</sup> in the parasite comparable to PfNAT and PfPMV (Figure 20A, B). Interestingly, although all three proteins were generally limited to the ER, the microscopic data of the cotransfectants implicated certain differences in distribution within this compartment by means of an imperfect colocalization of PfNAT<sup>mCherry</sup> with the others. This indication of a functional subdivision of the ER in *P. falciparum* was previously reported (Struck et al, 2008). The proper size of the fusion constructs was confirmed by western blot analysis of parasite lysates and detection with  $\alpha$ -GFP antibodies (Figure 20C). Slight deviations from the expected masses probably resulted from sequence-specific characteristics such as hydrophobicity, charge distribution or various transmembrane domains (Rath et al, 2009; Shi et al, 2012).

### 3.2.3 Endogenous tagging of PfNAT

Up to this point the localization of PfNAT in the ER has been determined using transfectants, which episomally overexpressed the GFP-tagged protein. In order to demonstrate the endogenous expression and ER targeting of this protein, a single crossover strategy was applied to introduce a C-terminal GFP tag under the gene-specific promoter by homologous recombination. For this purpose a gene fragment containing 1.1 kb of the 3' end of the *PfNAT* gene including an intron was amplified from 3D7 gDNA as a homology region and cloned without a stop codon into the pARL1a+-GFP vector that was devoid of the previously used *PfCRT* promoter (Figure 21A). *P. falciparum* 3D7 parasites were transfected and positively selected with WR99210 as described above and, upon reappearance of the parasites, cycled for 3-4 weeks without the selection marker followed by 1 week in presence of WR99210. When the replication rate of the parasites was stabilized gDNA was extracted and subjected to PCR in order to confirm recombination events. Suitable primer pairs were chosen to control for quality of the gDNA, presence of episomal plasmid as well as recombination of the plasmid into the locus of *PfNAT*. Since the first cycle did not result in any single crossover recombination, the transfectant parasites were either cycled for a second round off the selection drug or the cycles without drug pressure were prolonged to 4-10 weeks. After the second cycle a minor proportion of parasites had successfully recombined along the homology region and inserted the plasmid into the *PfNAT* locus as confirmed by sequencing of the recombination PCR band (Figure 21B). After a limiting dilution of this mixed population over the period of 3 weeks using a starting parasitaemia of 0.25 and 0.5 parasites per well in 96-well plates, a clonal population deriving from only one fluorescent clone out of 30 microscopically analysed potential clones could be obtained and verified by PCR. While the episomal, promoter-free construct was non-fluorescent, the parasite line expressing GFP-tagged PfNAT under the endogenous promoter exhibited a significant fluorescence in the ER as described for the episomally overexpressed version (Figure 21C). Furthermore, the correct size of the fusion protein was confirmed by western blot analysis (Figure 21D). This finding provides proof that the gene is indeed expressed and the corresponding PfNAT protein is synthesized in detectable quantities and localized to the expected subcellular compartment, namely the ER.

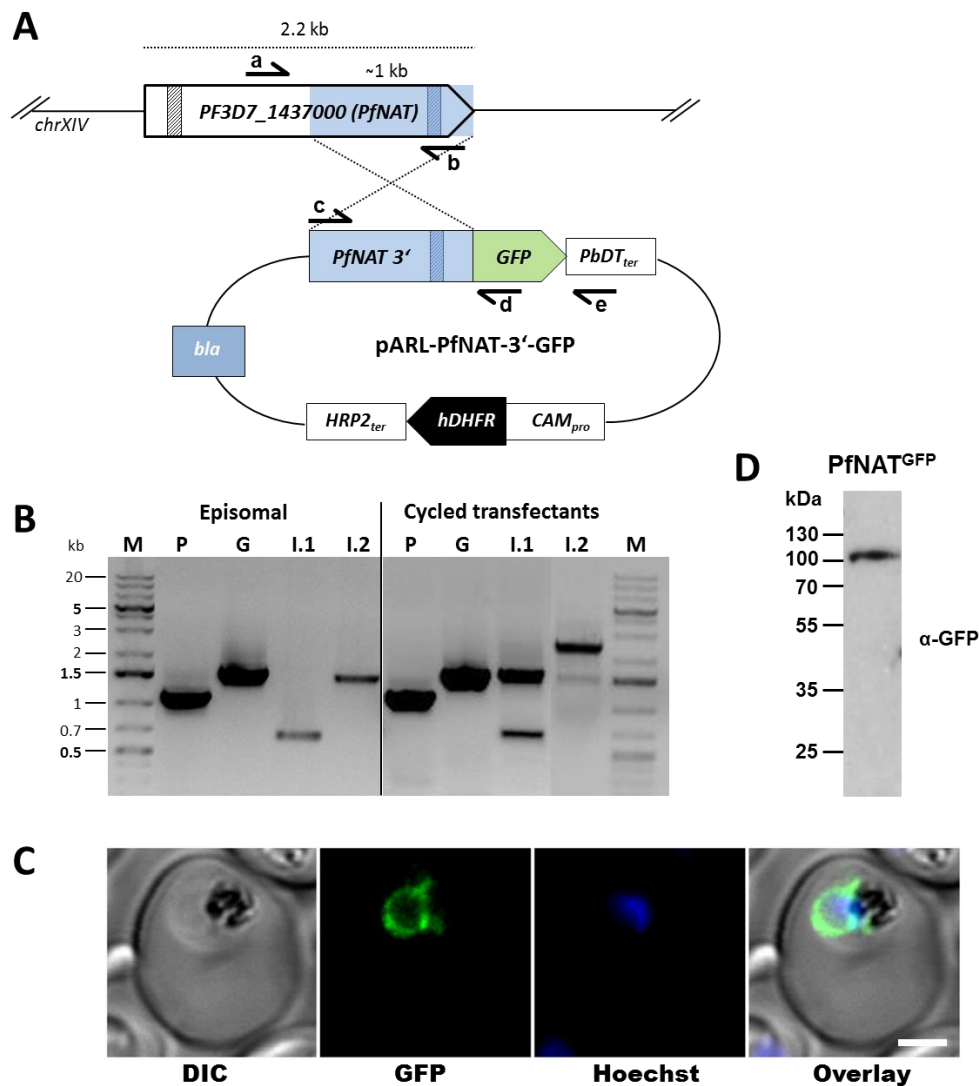


**Figure 21. Endogenous tagging of PfNAT with GFP via homologous recombination**

Establishment of clonal parasites that express PfNAT<sup>GFP</sup> under the endogenous promoter after homologous recombination. (A) Design of the integration plasmid pARL-PfNAT-3'-GFP. The gene fragment encoding the C-terminal part of PfNAT was cloned without a stop codon as a region homologous to PfNAT (blue, ~1 kb) for single crossover recombination. The sequences encoding GFP and the *PbDHFR-TS* 3'UTR as a terminator region were inserted downstream. The positive selection marker cassette (black box) is shown as well as the primers (black arrows) used for PCR analysis (a-e). *bla*, ampicillin resistance gene; *CAM<sub>pro</sub>* promoter of the *CAM* gene; *chrXIV*, chromosome 14; *HRP2<sub>ter</sub>* and *PbDT<sub>ter</sub>*, terminator regions of the *HRP2* and *PbDHFR-TS* genes; hatched boxes, introns. (B) Representative PCR analysis of genomic DNA from cycled transfectants to determine recombination events. Clonal parasites (clone F9) after limiting dilution showed the same band pattern. As a control transfectants prior to drug cycling are shown that express the plasmid in an episomal manner. Primers were chosen to detect the plasmid (P, c+d, 1.1 kb), genomic DNA (G, a+b, 1.6 kb) as well as integration of the plasmid after recombination (I.1, a+d, 1.7 kb and I.2, a+e, 2.3 kb). Unspecific bands appear in I.1 (0.6 kb) and I.2 (1.5 kb) of the control as well as integrants. M, DNA size ladder. (C) Confocal images of live *P. falciparum*-infected RBCs at the trophozoite stage show an intraparasitic localization of PfNAT<sup>GFP</sup> to the ER. Left images, differential interference contrast (DIC); middle left images, GFP fluorescence; middle right images, nuclear staining with Hoechst; right images, overlay of all channels. Scale bar: 2  $\mu$ m. (D) Western blot analysis of parasite lysates derived from PfNAT<sup>GFP</sup> expressing clones after saponin treatment. The predicted size of PfNAT<sup>GFP</sup> (~91 kDa) was approximated as confirmed by  $\alpha$ -GFP antibody detection.

## RESULTS

---

In summary, this part of the study included the identification of a putative N-acetyl transferase in *P. falciparum* (PfNAT) that might be involved in the acetylation of PEXEL proteins after their proteolytic cleavage. The localization of this protein in the ER together with the ER-resident protease Plasmepsin V (PfPMV) as well as a newly identified putative acetyl-CoA transporter (PfAcT) using GFP or mCherry fusion proteins indicate a local accumulation of factors involved in PEXEL processing within this compartment. The detectable expression of *PfNAT* under its endogenous promoter as well as the final targeting site of the protein was confirmed by introducing a GFP-tag into the locus via single crossover recombination.

### 3.2.4 Mutagenesis of the putative catalytic domain of PfNAT

In the next step the putative function of PfNAT was addressed by active-site mutagenesis. The analysis of dominant-negative phenotypes can be a valuable tool to address enzyme function, especially if the protein of interest is essential. In the context of PEXEL processing, this method was previously described for Plasmepsin V, where an episomal overexpression of a catalytically dead active-site mutant of PfPMV clearly competed with the endogenous enzyme for substrate binding and revealed a mixed population of cleaved and uncleaved HRPII protein (Russo et al, 2010).

Since the above-mentioned results implicate acetylation as a prerequisite necessary for proper export of PEXEL proteins the following mutagenesis experiment tested the hypothesis that the episomal expression of a catalytically impaired PfNAT could have a dominant-negative effect on the normal export phenotype of STEVOR<sup>1-80</sup>.

This part of the study was done in collaboration with Dr. M. Deponete who kindly established a three-dimensional model of the C-terminus of PfNAT based on the proper alignments with a structurally resolved putative streptothricin acetyltransferase domain from *Bacillus anthracis* (Protein Data Bank, PDB ID: 3PP9, unpublished) as well as a putative GNAT from *Staphylococcus aureus* (PDB ID: 3D8P, unpublished) (Figure 22A, B) (Berman et al, 2000). Based on this model and manual alignment of other GNATs, suitable amino acids were identified that might play an important role in catalysis or binding of acetyl-CoA to the active site. Consequently, mutations included PfNAT Y<sup>493</sup>A, R<sup>456</sup>M, T<sup>484</sup>V and N<sup>488</sup>L, with Y<sup>493</sup>A as a single mutant and RTN as a triple mutant.

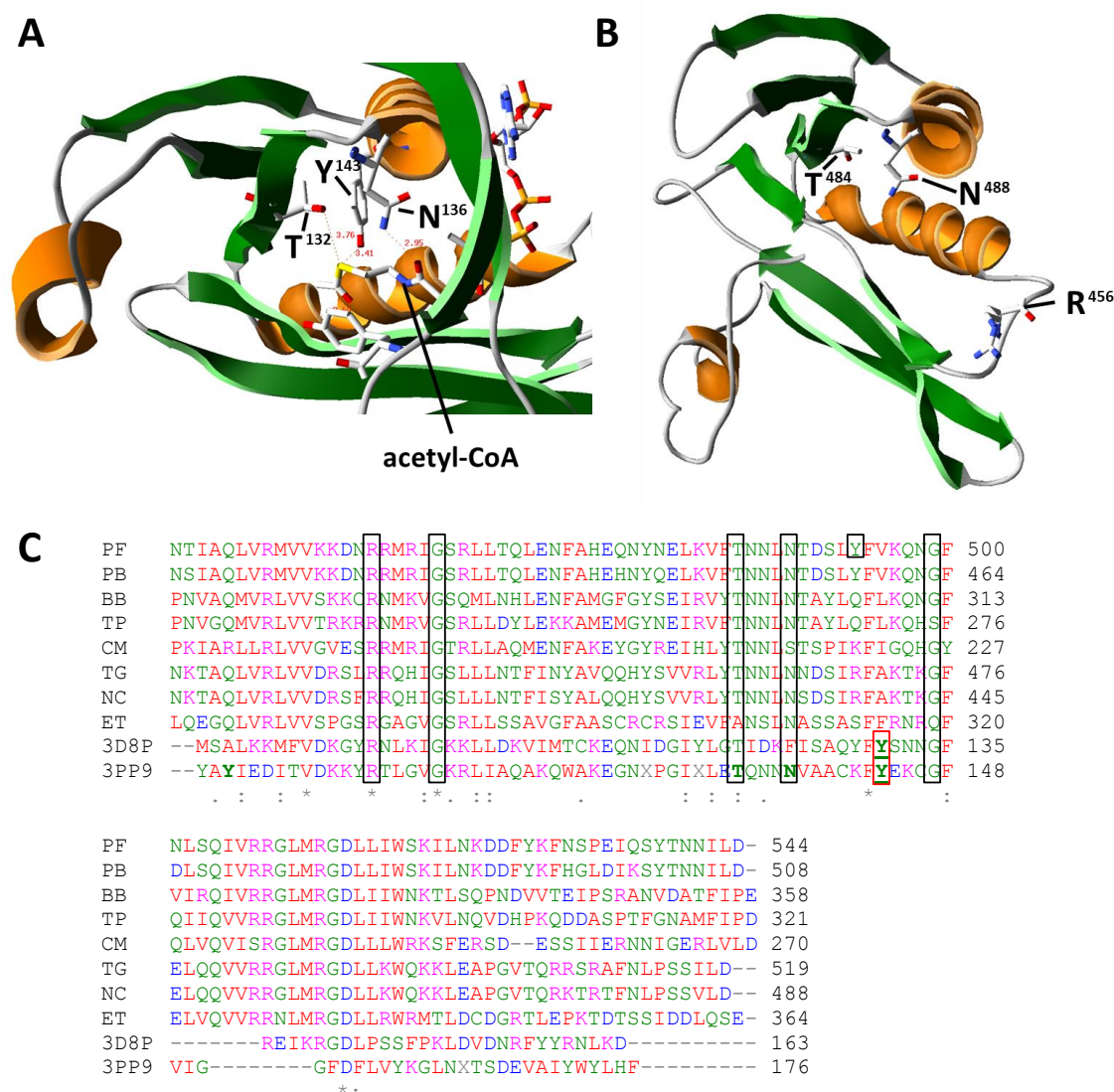


**Figure 22. Molecular model of NAT domain from 3PP9 and PfNAT (by Dr. M. Deponte)**

Establishment of a model of the PfNAT C-terminus by Dr. M. Deponte to identify amino acids that are important for catalysis or binding of acetyl-CoA. The model is based on crystal structure-derived sequence alignments with a putative streptothricin acetyltransferase from *Bacillus anthracis* (PDB ID: 3PP9) as well as an acetyltransferase of the GNAT family from *Staphylococcus aureus* (PDB ID: 3D8P). (A) 3D model of 3PP9 chain A zoomed to catalytic site in complex with acetyl-CoA. Three potentially relevant amino acids are shown with their molecular distance to acetyl-CoA: Y<sup>143</sup> (3.41 Å); T<sup>132</sup> (3.76 Å) and N<sup>136</sup> (2.95 Å). Not shown: R<sup>104</sup> potentially binds acetyl-CoA, but not inside the active center (3.45 Å). (B) A stable 3D model of the PfNAT C-terminus (aa 393-522) including the putative transferase domain was created in automated mode on the SWISS-MODEL Server (Biasini et al, 2014) based on a suitable sequence alignment (force field energy: -6,53MJ/mol) with 3D8P. Y<sup>130</sup> from 3D8P cannot be clearly aligned, however in PfNAT the tyrosine two amino acids upstream (Y<sup>493</sup>) was chosen for mutagenesis. Furthermore, R<sup>456</sup>, T<sup>484</sup> and N<sup>488</sup> were identified as candidates with a putative function in catalysis or binding of acetyl-CoA. (C) Alignment of C-termini of putative orthologous NATs in Apicomplexa as well as the previously mentioned bacterial transferases 3D8P and 3PP9 (resolved crystal structures). Detailed gene IDs are listed in the Appendix. The amino acids chosen for replacement mutagenesis are framed in black boxes. The active site tyrosine is framed in red without a counterpart in *Plasmodium*. Due to their sequence conservation G<sup>461</sup> and G<sup>499</sup> of PfNAT are assumed to be of structural relevance. PF, *Plasmodium falciparum*; PB, *Plasmodium berghei*; BB, *Babesia bovis*; TP, *Theileria parva*; CM, *Cryptosporidium muris*; TG, *Toxoplasma gondii*; NC, *Neospora caninum*; ET, *Eimeria tenella*. Amino acid colours and consensus symbols see description of Figure 19.

## RESULTS

---

The amino acid exchanges were chosen with the aim to conserve structural features while abolishing functional characteristics of the respective side chains with the prospect of rendering the expressed protein catalytically dead. In addition, two glycines with overall noticeable sequence conservation in aligned GNAT domains were targeted assuming a structural relevance, with G<sup>499</sup>A as a single mutant and G<sup>461</sup>A/G<sup>499</sup>A as a double mutant (Figure 22C). The mutations were introduced into the full-length coding sequence of *PfNAT* using megaprimers followed by overlap extension PCR and subsequently cloned into the pARL1a+-mCherry vector under the *PfCRT* promoter. 3D7 parasites were co-transfected with constructs encoding wild-type or mutated PfNAT<sup>mCherry</sup> and STEVOR<sup>1-80</sup> and positively selected using WR99210 and blasticidin S (BS). As a control to confirm the same localization of both fluorescent tags, if fused to the same gene, parasites were co-transfected with plasmids encoding PfNAT<sup>GFP</sup> as well as PfNAT<sup>mCherry</sup>. After drug selection the parasite lines were analysed by confocal fluorescence microscopy as described above. As can be seen in Figure 23A the signals of PfNAT<sup>mCherry</sup> and PfNAT<sup>GFP</sup> colocalize within the same parasite. In contrast, STEVOR<sup>1-80</sup> shows the expected translocation into the RBC cytosol if co-expressed with the wild-type PfNAT<sup>mCherry</sup>, while the transferase is again retained in the ER compartment (Figure 23B).

Despite different mutations in the putative catalytic domain or conserved sequence motifs of PfNAT co-expression with STEVOR<sup>1-80</sup> did not alter the export phenotype of the PEXEL protein and no dominant-negative effect could be observed (Figure 23C).

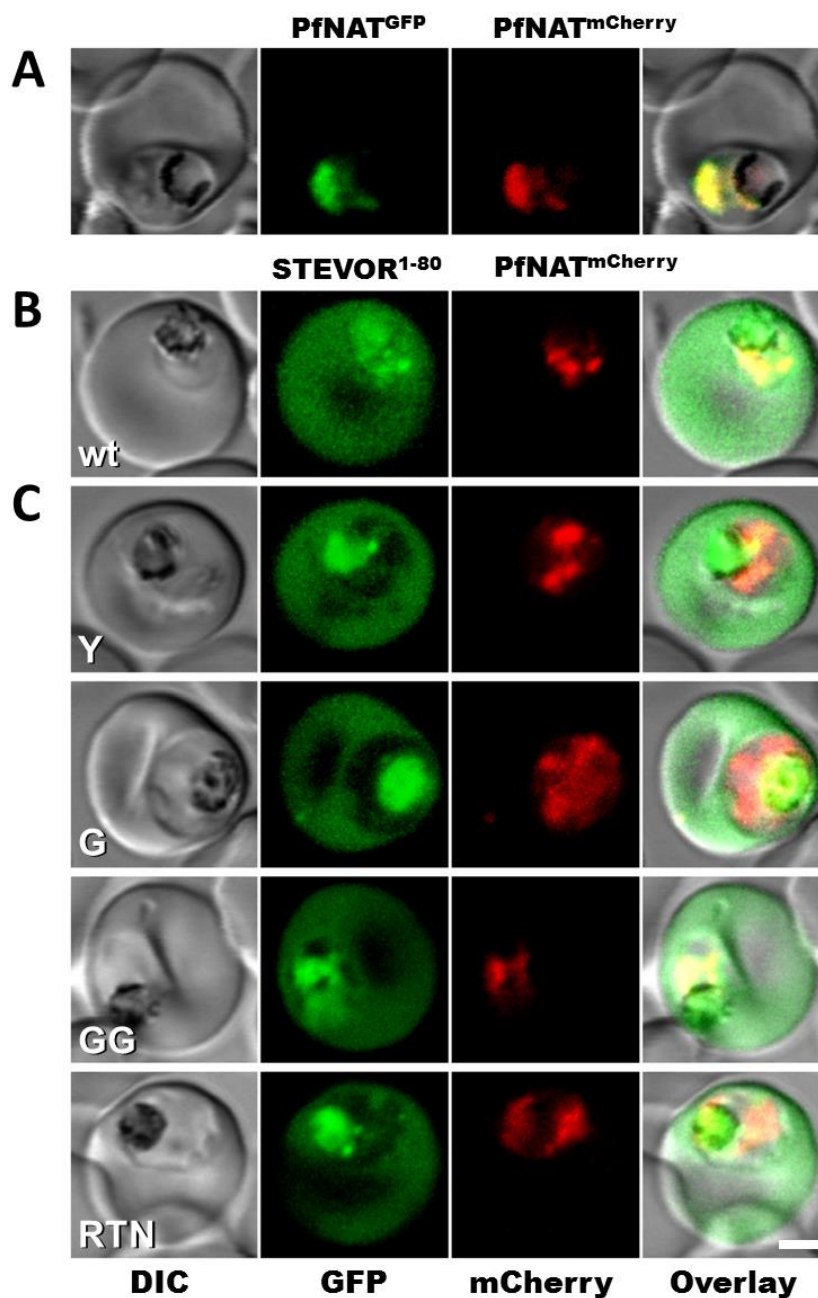


**Figure 23. Mutagenesis of the putative catalytic domain of PfNAT**

Confocal images of live *P. falciparum*-infected erythrocytes. Transfectant parasites at trophozoite stage expressing different fluorescent fusion proteins from episomal plasmids are shown. (A) Cotransfection of PfNAT<sup>mCherry</sup> and PfNAT<sup>GFP</sup> shows a spatial overlap of both fusion proteins occupying the same compartment. (B) Cotransfection of wild-type PfNAT<sup>mCherry</sup> with STEVOR<sup>1-80</sup> shows the residence of the putative transferase in the ER as well as the export of the soluble PEXEL protein into the RBC cytoplasm. (C) All transfectants bearing mutations in the putative catalytic domain (Y, RTN) or other conserved sequences (G, GG) of PfNAT<sup>mCherry</sup> exhibit the normal export phenotype of co-expressed STEVOR<sup>1-80</sup> with no dominant-negative effect. wt, PfNAT wild type; Y, mutation of PfNAT Y<sup>493</sup>A; G, G<sup>499</sup>A; GG, G<sup>461</sup>A/G<sup>499</sup>A; RTN, R<sup>456</sup>M, T<sup>484</sup>V and N<sup>488</sup>L. Left images, differential interference contrast (DIC); middle left images, GFP fluorescence; middle right images, mCherry fluorescence; right images, overlay of all channels. Scale bar: 2  $\mu$ m.

### 3.2.5 Knockout attempts on PfNAT

In the past gene disruptions in *P. falciparum* were mainly achieved by single crossover homologous recombination, more recent methods include the selection of double crossover integrants using a combination of positive and negative selection markers (Limenitakis & Soldati-Favre, 2011; Maier et al, 2006). Furthermore, the use of site-specific recombinases such as the DiCre/loxP system for conditional gene deletion has recently been adapted to *P. falciparum* (Collins et al, 2013).

Both methods were used in an attempt to delete the *PfNAT* gene in order to investigate its putative role in PEXEL-mediated protein export.

#### 3.2.5.1 Via double crossover recombination (pCC/pHTK vector system)

Double crossover recombination is achieved by the replacement of the targeted gene via two flanking homologous segments with the cassette expressing the positive selection marker gene. In *P. falciparum* this event is greatly enhanced by negative selection against the plasmid backbone using plasmid encoded thymidine kinase (TK, pHTK vector) of the *Herpes simplex* virus or the bifunctional cytosine deaminase/uracil phosphoribosyl transferase (CDUP, pCC vector) from *Saccharomyces cerevisiae*. These proteins convert normally innocuous ganciclovir and 5-FC, respectively, into toxic metabolites that inhibit the *de novo* pyrimidine biosynthesis pathway and nucleic acid synthesis directly (Duraisingh et al, 2002; Maier et al, 2006; Ménard, 2013). Only parasites that remove the plasmid backbone with the negative selection marker cassettes by double crossover recombination survive the treatment with the compounds. Both vector systems were employed for the following experiments. Furthermore, pCC1 and pCC4 vectors harbouring the human *DHFR* gene (selection with WR99210) or *blasticidin S deaminase* gene from *A. terreus* (selection with BS) as positive selection markers were used.

Two different sets of *PfNAT* homology regions flanking the positive selection cassettes were cloned into the pHTK, pCC1 and pCC4 vectors comprising either 0.5 kb of 5' and 3' terminal gene fragments or 1 kb of flanking 5' and 3' untranslated regions (UTR) (Figure 24A). *P. falciparum* 3D7 parasites were transfected with these constructs and positively selected on WR99210 or BS. Unfortunately, no parasites transfected with plasmids containing the *PfNAT* flanking UTRs ever reappeared despite repeated

transfections. This might indicate either plasmid instability or a regulatory effect of these sequences on the positive selection cassettes as putative promotor/terminator regions. Consequently, the expression of hDHFR and BSD might be disturbed leading to sensitivity towards the compounds. Upon reappearance, the transfectants were either immediately exposed to different concentrations of the negative selection markers (4  $\mu$ M, 10  $\mu$ M, 20  $\mu$ M ganciclovir; 0.23  $\mu$ M, 0.46  $\mu$ M, 1  $\mu$ M, 6 $\mu$ M 5-FC) or cycled off the positive selection marker for at least 3 weeks followed by reapplication to increase single crossover parasite populations prior to negative selection pressure. The concentrations tested for ganciclovir and 5-FC were based on personal communication with experienced collaborators, IC<sub>50</sub> measurements obtained with the transfectants and observations in the parasite cultures concerning death and recovery rates. The recommendations included a dosage that would kill most of the parasites (~IC<sub>90</sub>) but prevent toxic ‘bystander’ effects on integrants as repeatedly reported (Maier et al, 2006). The parasite population that successfully undergoes double crossover recombination should reappear 5-17 days after drug-induced clearance (A. Maier, *personal communication*). In this study, a dosage of 0.23  $\mu$ M and 0.46  $\mu$ M 5-FC was insufficient to significantly reduce the parasite population, although these concentrations were recommended by our collaborators. Differences in culture conditions or parasite strains might explain these results. In contrast, 1  $\mu$ M and 6  $\mu$ M of 5-FC proved to be suitable concentrations with reproducible recovery periods of 6-21 days, depending on construct and cycle. Similarly, 4  $\mu$ M of ganciclovir had nearly no effect on parasite growth, whereas 10  $\mu$ M and 20  $\mu$ M were sufficient to clear the parasites from the culture for 15-21 days. Following negative selection and parasite recovery, gDNA was extracted from the cultures and subjected to PCR analysis. Primers were carefully chosen to control for sufficient quality of the gDNA, presence of episomal plasmid as well as 5’ or 3’ recombination of the plasmid into the locus of *PfNAT*. Furthermore, the same primers were used in different combinations to ensure their functionality and negative control templates such as parental gDNA of untransfected 3D7 parasites as well as the pure plasmid DNA were included (Figure 24B). The length of the PCR fragments representative of recombination was in the same range as the gDNA control in order to ensure that negative results could not be attributed to PCR-related amplification problems. If the quality of the control bands (plasmid, gDNA) was unsatisfactory, the

## RESULTS

PCR was repeated under different conditions until a clear result was obtained. In summary, no parasite population with double crossover recombination was obtained with any construct despite the use of variable drug concentrations and cycling conditions (Table 3). This result was in accordance with a prior set of investigations using the pCC vector system carried out by my colleague Dr. C. Sanchez.

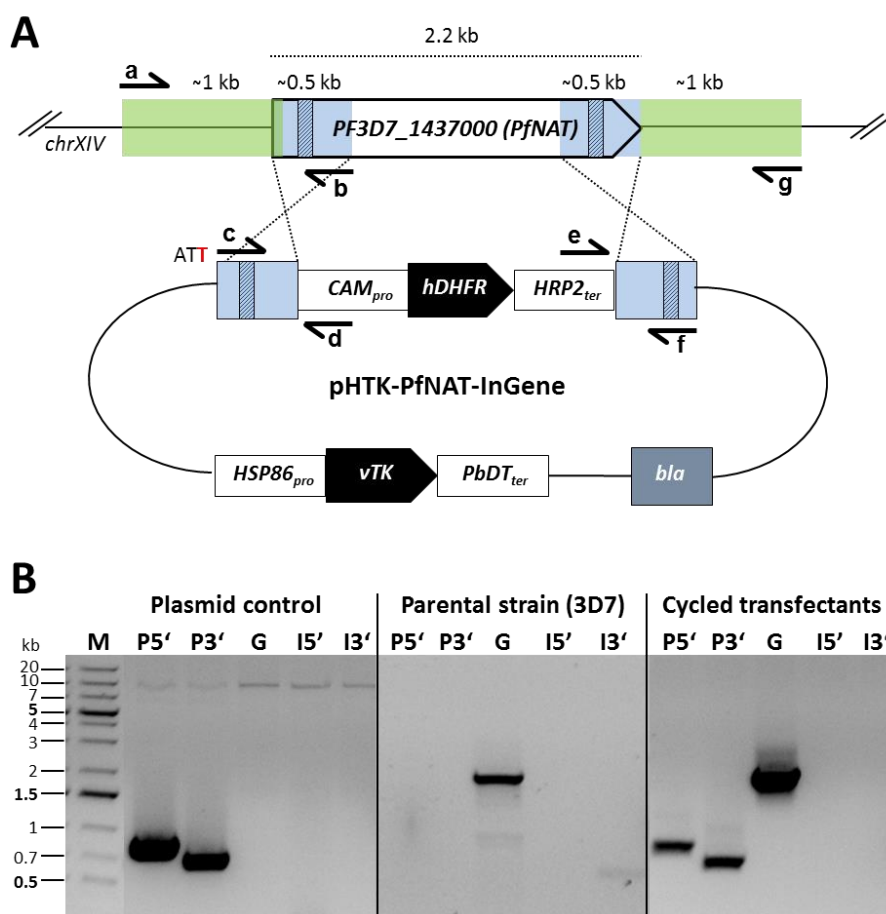


**Figure 24. Knockout strategy for *PfNAT* using the pCC/pHTK vector system and PCR analysis**  
 Disruption of the PF3D7\_1437000 (*PfNAT*) gene in *P. falciparum* by double crossover recombination using the pHTK/pCC1/4 vector system with positive (WR, BS) and negative (5-FC, ganciclovir) selection. (A) Design of the knockout plasmids as exemplified for pHTK-PfNAT-InGene. Two sets of regions homologous to *PfNAT* were chosen to flank the positive selection marker cassette; either 0.5 kb of terminal gene fragments (blue) or 1 kb of adjacent UTRs (green). The start codon of the 5' gene fragment was mutated to ATT to prevent successful transcription in case of single crossover events. Selection marker cassettes (black boxes) for positive selection encoded either hDHFR (pHTK/pCC1 vectors) or BS (pCC4 vector) and for negative selection either vTK (pHTK vector) or CDUP (pCC vectors). Primers used for PCR analysis are shown as black arrows (a-g). *bla*, ampicillin resistance gene; *CAM<sub>pro</sub>* and *HSP86<sub>pro</sub>*, promoters of the *CAM* and *HSP86* genes; *chrXIV*, chromosome 14; *HRP2<sub>ter</sub>* and *PbDT<sub>ter</sub>*, terminator regions of the *HRP2* and *PbDHFR-TS* genes; hatched boxes, introns. (B) Representative PCR analysis of genomic DNA from cycled transfectants to determine recombination events. Control DNA from the parental strain 3D7 and the initial plasmids was included. Primers were chosen to detect the plasmidal 5' (P5', c+d, 0.7 kb) and 3' homologous regions (P3', e+f, 0.6 kb), genomic DNA (G, a+b, 1.8 kb) as well as integration of the plasmid after recombination along the 5' (I5', a+d, 2.0 kb) as well as 3' (I3', e+g, 1.8 kb) fragments. M, DNA size ladder.

Since the accessibility of the *PfNAT* locus to genetic manipulation could be verified in aforementioned experiments (see chapter 3.2.3) and both vector systems (pCC, pHTK) have proven useful for gene knockouts in previous studies (Duraisingh et al, 2002; Maier et al, 2008) the inability to gain double crossover integrant parasites indicates a possible essentiality of the gene although it is not a definite proof. A gene knockout screen by Maier et al (2008) estimated that one fourth of the investigated PEXEL proteins are essential for intraerythrocytic parasite growth. Assuming a putative role of PfNAT in propagating correct export of PEXEL proteins the disruption of this gene could have drastic effects on parasite viability even under laboratory conditions.

construct	positive selection drug (+conc.)	cycle no.	duration OFF 1 <sup>st</sup> drug (days)	reappearance after 1 <sup>st</sup> drug exposure (days)	negative selection drug (+conc.)	reappearance after 2 <sup>nd</sup> drug exposure (days)
<b>pCC1-PfNAT-InGene</b>	WR (5nM)	0	-	-	5-FC (1 µM)	9
		0	-	-	5-FC (6 µM)	21
		1	31	7	5-FC (1 µM)	7
		1	31	7	5-FC (6 µM)	7
		2	27	0	5-FC (1 µM)	7
		2	27	0	5-FC (6 µM)	7
<b>pCC4-PfNAT-InGene</b>	BS (9 mM)	0	-	-	5-FC (0.23 µM)	0
		0	-	-	5-FC (0.46 µM)	0
		1	31	11	5-FC (6 µM)	14
		1	37	12	5-FC (6 µM)	9
<b>pCC4-PfNAT-InGene</b> (2 <sup>nd</sup> transfection)	BS (9 mM)	0	-	-	5-FC (1 µM)	6
		0	-	-	5-FC (6 µM)	9
		1	31	7	5-FC (1 µM)	14
		1	31	7	5-FC (6 µM)	-
		2	27	0	5-FC (1 µM)	16
		2	27	0	5-FC (6 µM)	16
<b>pHTK-PfNAT-InGene</b>	WR (5nM)	0	-	-	ganciclovir (4 µM)	0
		1	31	13	ganciclovir (10 µM)	21
		1	31	13	ganciclovir (20 µM)	15
		2	27	7	ganciclovir (10 µM)	10
		2	27	7	ganciclovir (20 µM)	16

**Table 3. Cycling of transfectants to acquire knockout of *PfNAT* via double crossover recombination**

Summary of different attempts to gain knockout parasites using the pHTK/pCC vector system. Only parasites with in-gene homologous regions emerged from the drug selection after transfection. Parasites were either directly (cycle no. 0) subjected to negative selection (5-FC or ganciclovir) or cultured in absence of the positive selection drug (WR, BS) for at least three weeks prior to reapplication of the first drug and subsequent negative selection drug (cycle no. 1). In order to reinforce loss of episomes, parasites were cycled for a second round off the positive selection drug (cycle no. 2). The reappearance periods after drug application varied from immediate (0 days) and medium (7-21 days) to no recovery at all (-). After negative selection, genomic DNA was collected from the parasites and analysed by PCR.

### 3.2.5.2 Via conditional excision (DiCre/loxP system)

As an alternative approach to dissect the function of the candidate N-acetyltransferase a conditional gene knockout based on the DiCre/loxP recombinase system was attempted (Andenmatten et al, 2013; Jullien et al, 2003). The DiCre recombinase recognizes 34 bp short loxP sites that flank a sequence of interest and mediates site-specific excision or inversion of the intervening part depending on the relative orientation of the loxP motifs. The regulation of recombinase activity is achieved by its expression in two separate, enzymatically inactive polypeptides, each fused to the FK506-binding protein 12 (FKBP12) or FKBP12-rapamycin binding protein (FRB). The addition of rapamycin induces heterodimerization of the two components, which restores recombinase activity. The system has successfully been employed in *Toxoplasma gondii* but only recently been adapted to *P. falciparum* with a good excision efficiency (close to 100%) within the time span of a single intraerythrocytic growth cycle (Andenmatten et al, 2013; Collins et al, 2013). For this part of the study, the gene fragment encoding the C-terminal part of PfNAT including the putative acetyltransferase domain was chosen to be flanked by loxP sites ('floxed') with the aim to gain enzymatically inactive enzyme upon successful conditional excision. This sequence of *PfNAT* (~890 bp of 3' end w/o stop codon) was synthesized (by GENEART) including intron removal and codon optimization in order to ensure that single homologous recombination occurs in front of the 5' flanking loxP site and not within the sequence fragment encoding the NAT domain (Figure 25A). This artificial sequence was cloned with a separating loxP site downstream to a gene fragment (~1 kb) of *PfNAT* that served as homology region. The resulting insert was exchanged with the SERA5 fragment of the pHH1-SERA5del3-preDiCre vector (kindly provided by M. Blackman), which has previously been used for this system (Collins et al, 2013). Although the newly introduced loxP site was inserted into a coding region of the *PfNAT* gene, it was intentionally placed within a putatively unstructured part of the translated protein to cause minimum interference with protein function. The vector backbone already contained two loxP sites in the terminator region (PbDT 3'UTR) and the hDHFR cassette promoter region (CAM 5'UTR). Although the final construct had 3 instead of 2 loxP sites in the same orientation the excision by the recombinase was supposed to include the complete 'floxed' part (M. Blackman, *personal communication*). The plasmid was transfected into the 3D7-based 1G5-DiCre clonal strain (kindly provided by

M. Blackman) that constitutively expresses the two inactive recombinase subunits after integration into the *SERA5* locus (Collins et al, 2013). The parasites were positively selected using WR99210 and subjected to different cycling periods off the drug ranging from 3.5-7 weeks after which drug pressure was reapplied. Furthermore, parasites were cycled a second and third time (3 weeks no drug) to ensure loss of episomes. In order to check for recombination events gDNA was extracted and subjected to PCR with the aforementioned considerations (see chapter 3.2.5.1). In addition primers were used to detect the DiCre cassette in the parasites (Figure 25B).

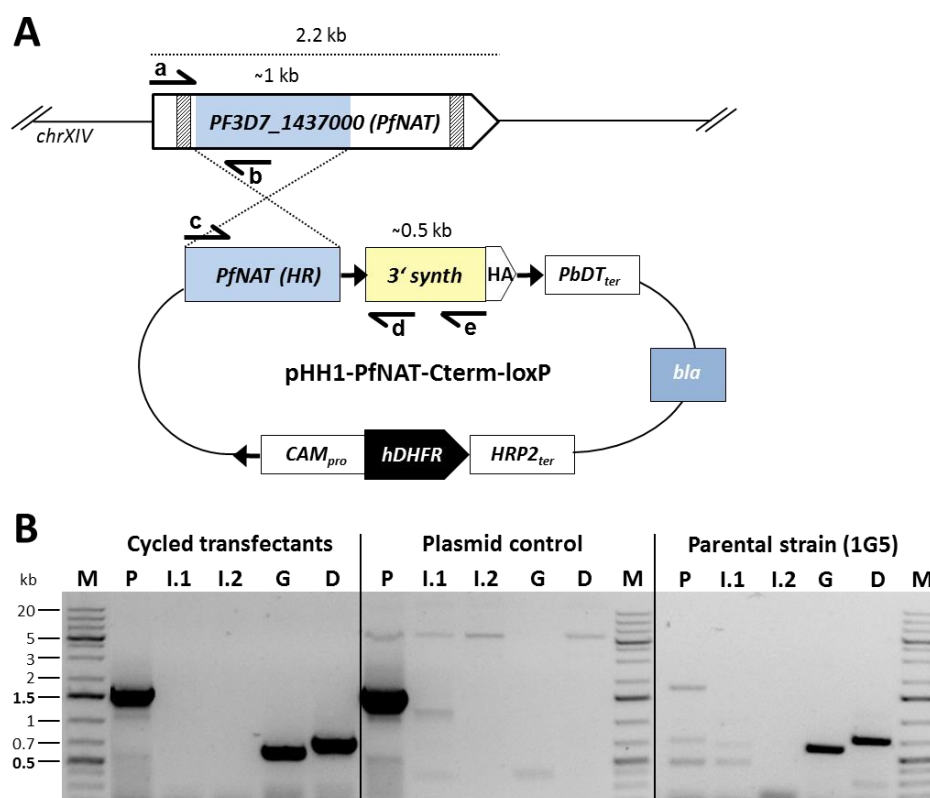


**Figure 25. Knockout strategy for *PfNAT* using the DiCre recombinase system and PCR analysis**  
 Conditional partial excision of the PF3D7\_1437000 (*PfNAT*) gene in *P. falciparum* after single crossover recombination using the DiCre/loxP recombinase system and rapamycin was attempted. (A) Design of the knockout plasmid as exemplified for pHH1-PfNAT-Cterm-loxP. In this construct, the gene fragment encoding the C-terminal part of the transferase including the NAT domain was codon-optimized (3' synth) and flanked by loxP sites (black arrows) for excision. A region homologous to *PfNAT* (~1 kb, HR) was cloned 5' to this sequence, a triple HA tag as well as the *PbDHFR-TS* 3'UTR as a terminator region are inserted downstream. The positive selection marker cassette (black box) is shown as well as the primers used for PCR analysis (a-e). The expression cassette for the DiCre recombinase subunits is stably inserted into the genome of the parental 1G5 strain (Collins et al, 2013). *bla*, ampicillin resistance gene; *CAM<sub>pro</sub>* promoter of the *CAM* gene; *HRP2<sub>ter</sub>* and *PbDT<sub>ter</sub>*, terminator regions of the *HRP2* and *PbDHFR-TS* genes; hatched boxes, introns. (B) Representative PCR analysis of genomic DNA from cycled transfectants to determine recombination events. Control templates from the parental strain 1G5 and the initial plasmid were included. Primers were chosen to detect the plasmid (P, c+e, 1.5 kb), genomic DNA (G, a+b, 0.6 kb) as well as integration of the plasmid after recombination (I.1, a+e, 1.8 kb and I.2, a+d, 1.4 kb). In addition the presence of the DiCre cassette within the parental 1G5 strain was confirmed by specific primers (D, 0.7 kb).

## RESULTS

Despite different cycling conditions and PCR-confirmed presence of episomal plasmid within the transfectants no single crossover integration into the locus of *PfNAT* could be detected in any of the cultures (Table 4). One possible explanation could be that the translated loxP, though very short (11 aa), interferes with protein structure or motifs in a negative manner thereby reducing PfNAT function. In order to circumvent this problem, a second set of vectors was constructed that contained larger resynthesized sequence parts of *PfNAT* with loxP sites in the first intron (PfNAT-1<sup>st</sup>Intr) or even 50 bp into the 5' UTR (PfNAT-fullsynth). Furthermore, the redundant third loxP site was removed from these vectors ( $\emptyset$ loxP). Although the successful expression and correct localization of codon-optimized full-length PfNAT<sup>synth</sup> could be confirmed in the context of episomal expression of a GFP-tagged fusion protein (Figure 26), no single crossover recombination occurred so far with these transfectants (ongoing experiments).

construct	positive selection drug (+conc.)	cycle no.	duration OFF 1 <sup>st</sup> drug (days)	reappearance after 1 <sup>st</sup> drug exposure (days)
pHH1-PfNAT-Cterm-loxP	WR (5nM)	1	26	0
		1	33	8
		1	48	16
		2	26	0
		3	25	0
		3	41	0
pHH1-PfNAT-1 <sup>st</sup> Intr-PbDT $\emptyset$ loxP	WR (5nM)	1	26	3
		2	26	0
pHH1-PfNAT-1 <sup>st</sup> Intr-CAM $\emptyset$ loxP	WR (5nM)	1	26	3
		2	26	4
pHH1-PfNAT-fullsynth-PbDT $\emptyset$ loxP	WR (5nM)	1	23	3
		2	26	0
pHH1-PfNAT-fullsynth-CAM $\emptyset$ loxP	WR (5nM)	1	21	3
		2	26	4

**Table 4. Cycling of transfectants to acquire knockout of *PfNAT* via DiCre-mediated excision**

Summary of different attempts to gain knockout parasites using the DiCre/loxP recombinase system. Parasites of the 1G5 strain (kindly provided by M. Blackman) were transfected with single crossover integration constructs containing loxP-flanked codon-optimized sequences of *PfNAT*. Transfectants were cultured in absence of the positive selection drug (WR, BS) for at least three weeks prior to reapplication. The cycles were repeated to reinforce loss of episomes and accumulate potential integrants. After recovery of the parasites (0-16 days), genomic DNA was collected and analysed by PCR.

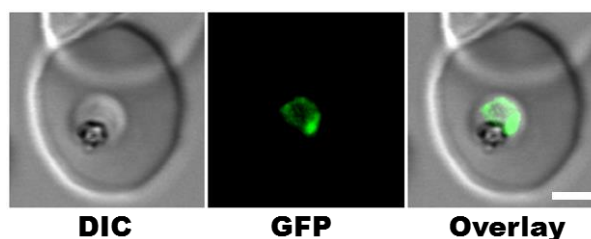


**Figure 26. Localization of PfNAT<sup>synth</sup>**

Confocal images of live *P. falciparum*-infected erythrocytes. Transfectant parasites at trophozoite stage expressing codon-optimized full-length PfNAT<sup>synth</sup> from episomal plasmids are shown. In accordance with previous constructs the putative transferase localizes to a perinuclear compartment that is indicative of the ER. Left image, differential interference contrast (DIC); middle image, GFP fluorescence; right image, overlay of all channels. Scale bar: 2  $\mu$ m.

### 3.2.6 Knockdown attempts on PfNAT using the DD system

The inducible regulation of proteins can provide valuable insights into their function during cell development, especially if a knockout of the respective gene is unavailable. In recent years, the destabilization domain (DD) system was successfully used for this purpose in different cell systems and some studies have confirmed its applicability in the malaria parasite *P. falciparum* (Armstrong & Goldberg, 2007; Banaszynski et al, 2006; Chu et al, 2008; de Azevedo et al, 2012). The method is based on the fusion of the DD tag, which consists of a mutant form of the human FK506-binding protein 12 (FKBP), to a protein of interest. Upon expression, the fusion protein is unstable and targeted to proteasomal degradation unless stabilized by the small synthetic cell-permeable ligand Shield-1 (commercial name: D/D-solubilizer, Clontech) that binds to the DD tag. This drastic change in protein quantity by removal or addition of the ligand therefore enables the functional analysis of the protein of interest.

In order to explore the role of PfNAT despite the occurring inability to knock out the gene, a functional knock down on protein level was attempted using the DD system. For this purpose the 330 bp gene encoding a variant DD domain, DD24 (kindly provided by M. de Azevedo), was cloned C-terminally with an additional HA tag into the pARL-PfNAT-3'-GFP vector previously used for single crossover recombination (see chapter 3.2.3) and transfected into *P. falciparum* 3D7 parasites. After positive selection with WR99210 the transfectants were constantly grown in the presence of the stabilizing ligand (200 nM D/D solubilizer, Clontech) and cycled 3-4 weeks off WR99210 followed by 1 week under drug pressure. After a few days of recovery gDNA was isolated and analysed by PCR. Suitable primer pairs were chosen to control for quality of the gDNA,

## RESULTS

presence of episomal plasmid as well as recombination of the plasmid into the locus of *PfNAT*. Furthermore, negative control templates were used including parental gDNA of untransfected 3D7 parasites as well as the pure plasmid DNA. Indeed, single crossover homologous recombination into the endogenous locus appeared after the first cycle and clonal populations were obtained by limiting dilution (Figure 27A).

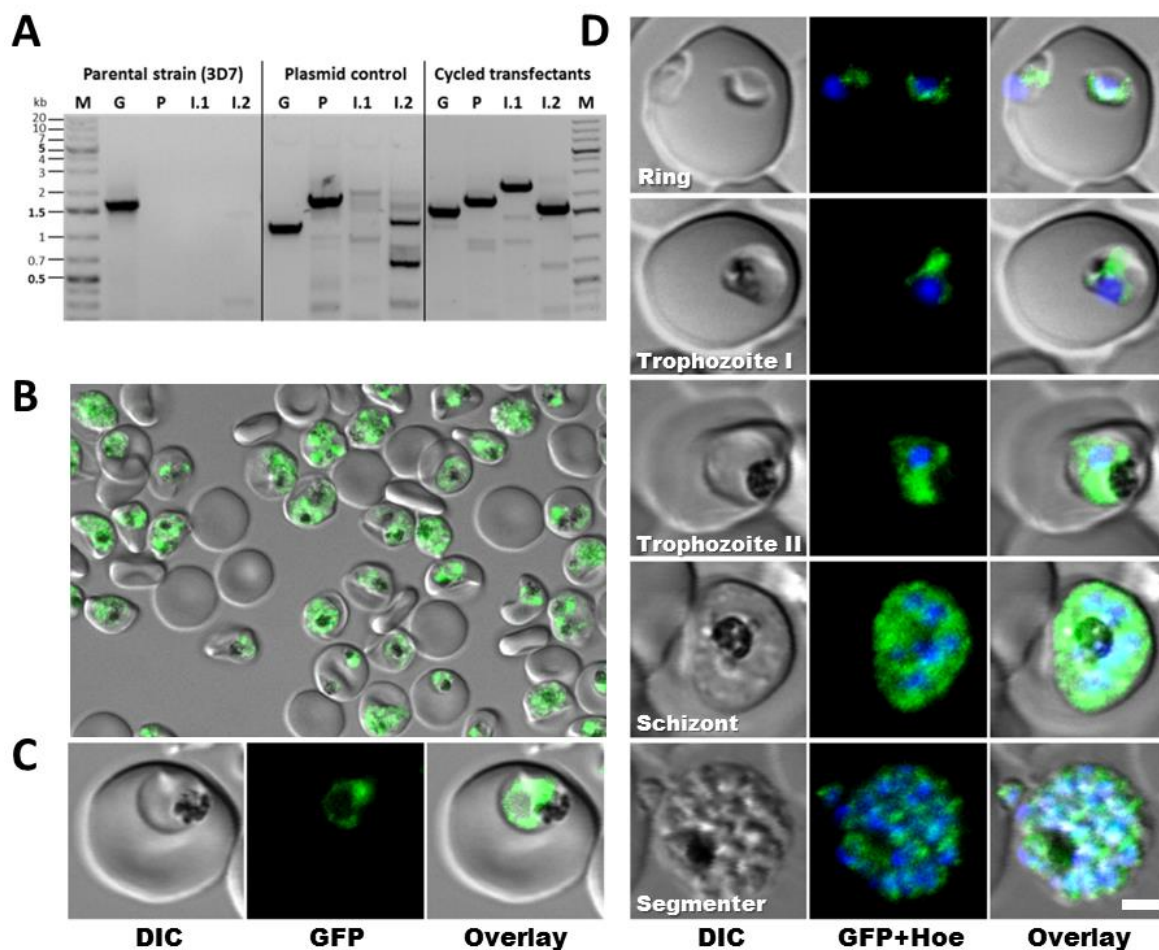


**Figure 27. Localization of PfNAT<sup>GFPDD24</sup> during intraerythrocytic parasite development**

Establishment of clonal parasites that express PfNAT<sup>GFPDD24</sup> under the endogenous promoter after homologous recombination (A) Representative PCR analysis of genomic DNA from cycled transfectants (clone D8) to determine recombination events. Control templates from the parental strain 3D7 and the initial plasmid were included. Primers were chosen to detect genomic DNA (G, 1.7 kb), the plasmid (P, 1.9 kb), as well as integration of the plasmid after recombination (I.1, 2.5 kb and I.2, 1.7 kb). Unspecific bands repeatedly appeared in the plasmid control and to a minor extent in the integrants. (B) Confocal overview image of purified live *P. falciparum*-infected RBCs shows fluorescence of PfNAT<sup>GFPDD24</sup> in every parasite. Overlay of GFP fluorescence and DIC image. (C) Confocal image of a single parasite at the trophozoite stage shows the ER localization of PfNAT<sup>GFPDD24</sup> as previously observed for episomal as well as single crossover PfNAT<sup>GFP</sup>. (D) Microscopic observation of PfNAT<sup>GFPDD24</sup> fluorescence throughout the intraerythrocytic cycle. Protein expression is present in ring stages and continues through trophozoite (I: early, II: mature) and schizont development until the formation of daughter merozoites. Left images, differential interference contrast (DIC); middle images, GFP fluorescence and nuclear staining with Hoechst (D); right images, overlay of all channels. Scale bar: 2  $\mu$ m.

The microscopic analysis of one clonal line (clone D8) revealed the same intraparasitic perinuclear localisation of PfNAT<sup>GFPDD24</sup> as in the previous experiments thereby confirming the proper expression and targeting of the DD-tagged fusion protein to the ER (Figure 27B, C). Due to the clonal character all parasites were fluorescent, which greatly improved the detection. As can be seen in Figure 27D, the protein is already expressed in ring stages early during intraerythrocytic development and fluorescence continues until the formation of daughter merozoites. After schizont rupture the released merozoites also still show a weak fluorescent pattern indicating a fragmentation of the ER and distribution of parental or synthesis of new protein.

### 3.2.6.1 Microscopic quantification of PfNAT<sup>GFPDD24</sup> regulation

Having established a clonal line of parasites expressing PfNAT<sup>GFPDD24</sup> the next step assessed the regulation of the protein by the DD system using microscopic analysis on single cell level. As previously published, the effects of removal/addition of the ligand on protein de-/stabilization are quite rapid with measurable differences observed already 6 hours later, though peaks are reached around 20 hours later (Armstrong & Goldberg, 2007).

For this part of the study a comparison at 24 hours after ligand removal was considered a good time point to ensure significant differences in protein levels. This can be clearly seen in Figure 28A by the uniform reduction in fluorescence intensity of PfNAT<sup>GFPDD24</sup> in parasites cultured without the ligand for this time period. In addition, a western blot analysis of parasite lysates at this time point confirmed a reduced amount of fusion protein in the sample without ligand compared to the treated ones, whereas the loading control using antibodies directed against human Band III protein revealed equal amounts of sample (Figure 28B). This finding supports the assumption that a reduction in fluorescence intensity can be attributed to a decrease in the amount of fluorescent protein.

For the single cell quantification PfNAT<sup>GFPDD24</sup> parasites were split into one sample with maintained ligand exposure (200nM D/D solubilizer, Clontech) and one without ligand in the medium. In order to exclude any unspecific results related to the ligand itself the same procedure was repeated for the PfNAT<sup>GFP</sup> clonal parasites. After 24 hours all samples were purified on the MACS column and analysed under the confocal

## RESULTS

---

microscope using the same settings for each (Figure 28C). Special attention was given to optimize pinhole and gain settings in order to prevent saturation of the maximum fluorescence intensity signals. The focal plains were carefully chosen based on the brightest representation in the histograms and every four images a new overview field was taken to reduce fluorescence decrease due to photobleaching. For quantification, the mean pixel intensities in the fluorescence channel of 20 RBCs infected with trophozoite-stage parasites were measured in unprocessed images using the FIJI program. In each picture the mean pixel intensities of uninfected RBC were determined and deducted from the respective iRBC values. Finally, the decrease in fluorescence intensity was plotted as percentage compared to PfNAT<sup>GFP</sup> +ligand (Figure 28D). The ligand itself did not exhibit any significant effects on the fluorescence intensity of PfNAT<sup>GFP</sup> apart from a slight decrease in untreated parasites (9%). However, the addition of the HADD24 tag to this protein resulted in a striking reduction in fluorescence intensity in the range of 30%. This phenomenon has previously been documented to a minor extent for soluble DD24 tagged reporter proteins (GFP and luciferase) and might be caused by imperfect stabilization of the fusion protein in the presence of the ligand or increased degradation due to the DD tag itself (de Azevedo et al, 2012). The removal of the ligand for 24 hours resulted in a further reduction in fluorescence by about 50% compared to the treated parasites (to 35% of treated PfNAT<sup>GFP</sup> strain). In addition PfNAT<sup>GFPDD24</sup> parasites that were continuously grown without the stabilizing ligand were investigated and a similar result was obtained (to 38% of treated PfNAT<sup>GFP</sup> strain). It is worth mentioning that these parasites did not show any obvious defect in growth, which might be due to an insufficient downregulation of PfNAT or target effects that are characterized by other determinants such as cytoadhesion for example.

Taken together, these data represent a first indication that the DD system is potentially useful to target an ER-resident transmembrane protein for proteasomal degradation.

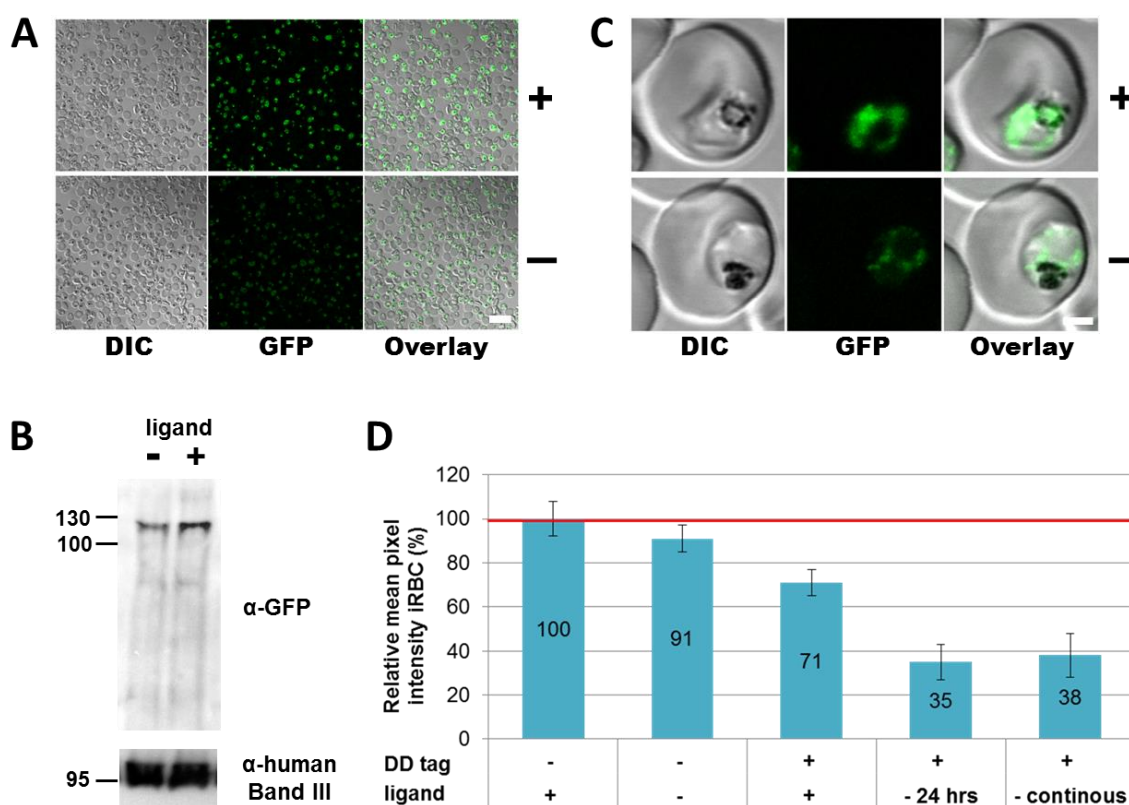


**Figure 28. Microscopic quantification of ligand-based regulation of PfNAT<sup>GFPDD24</sup>**

Analysis of downregulation of PfNAT<sup>GFPDD24</sup> on protein level upon ligand removal. (A) Confocal overview image of clonal parasite line that was continuously cultured with ligand (+, 200 nM D/D solubilizer) or for 24 hours in absence of ligand (-). For comparative reasons image acquisition was strictly under the same conditions and settings. The reduction in fluorescence is clearly visible. Left images, differential interference contrast (DIC); middle images, GFP fluorescence; right images, overlay of all channels. Scale bar: 20  $\mu$ m. (B) Western blot analysis of parasites depicted in (A). Membrane fractions of equal samples (treated, non-treated) were obtained by hypotonic lysis, the pellets were resuspended in equal amounts of loading buffer and subjected to SDS-PAGE and Western blot detection using  $\alpha$ -GFP antibodies. The expected size of PfNAT<sup>GFPDD24</sup> is 107 kDa, however PfNAT<sup>GFP</sup> also runs slightly higher. As a loading control, the membranes were probed with  $\alpha$ -human Band III antibodies. (C) Confocal images of single PfNAT<sup>GFPDD24</sup> expressing parasites that were continuously cultured with ligand (+, 200 nM D/D solubilizer) or for 24 hours in absence of ligand (-). Image settings were optimized to prevent saturation and strictly kept unchanged for all data acquisitions. These kinds of images were the basis for the single cell microscopic quantification as summarized in (D). Left images, differential interference contrast (DIC); middle images, GFP fluorescence; right images, overlay of all channels. Scale bar: 2  $\mu$ m. (D) Histogram representing the relative difference in fluorescence intensities of PfNAT<sup>GFP</sup> (-DD tag) and PfNAT<sup>GFPDD24</sup> (+ DD tag) expressing single parasites treated with or without ligand. The bars represent relative mean pixel intensities of 20 imaged parasitized RBCs with a background deduction of uninfected RBCs. PfNAT<sup>GFP</sup> parasites under ligand exposure were set to 100% as a reference point. Error bars represent the relative standard error of the mean (rSEM). A ~50% reduction in fluorescence of PfNAT<sup>GFPDD24</sup> upon ligand removal is clearly visible.

### 3.2.6.2 Flow cytometric analysis of PfNAT<sup>GFPDD24</sup> regulation

To further characterize the regulation potential of the DD system the sensitivity of single cell microscopy was complemented by the statistical advantages of fluorescence-based flow cytometry, which facilitates the acquisition of data from thousands of cells. A time course was conducted over 48 hours with PfNAT<sup>GFPDD24</sup> parasites that were tightly synchronized prior to ligand removal. Cultures of ring-stage parasites of a high parasitaemia (~5%) were divided into ligand-treated (200 nM D/D-solubilizer) and untreated samples. Every 12 hours a small volume was removed, medium was exchanged and fresh drug added to the treated culture. The samples were either directly used for FACS analysis or washed and incubated for 10 min at 37°C with ethidium bromide (EtBr, 1 µg/ml final) to determine developmental stages. Fluorescence signals of PfNAT<sup>GFPDD24</sup> samples plus and minus ligand was collected in the GFP channel (FL1-H) of the FACScalibur, whereas EtBr staining was collected in the respective channel (FL2-H). 50 000 cells were counted per measurements and plotted as an overlay of treated (green line) and untreated (grey line) samples (Figure 29A). A region of interest excluding background fluorescence was determined (M2) and information such as the geometric mean and gated events was collected for this selected area. The comparison of the geometric means of the two samples at one time point was regarded as representing the shift in mean GFP fluorescence intensity and therefore as the determinant for downregulation of PfNAT<sup>GFPDD24</sup> upon ligand removal. The plots in Figure 29A are representative examples from one of two independent time-course experiments. The histograms in Figure 29C and D depict the geometric mean (in %) of untreated parasites compared to ligand-treated parasites (= 100% reference) at 12 hour-intervals for GFP and EtBr summarized for both time-courses. At the 24-hour and 36-hour time points a clear difference in the GFP fluorescence can be observed in the treated culture with a larger proportion of parasites in M2 exhibiting around 30% brighter fluorescence intensity (shift in geometric mean). The staining with EtBr reveals that these parasites are in the trophozoite to schizont stages where the fluorescence signal is strongest, whereas the low signal during other time-points is not properly resolvable. An important aspect of this experiment was to assess if the untreated parasites have an immediate growth defect or developmental delay, since the effect of ligand-removal on protein quantity was reported to occur as early as 6 hours (Armstrong & Goldberg, 2007).

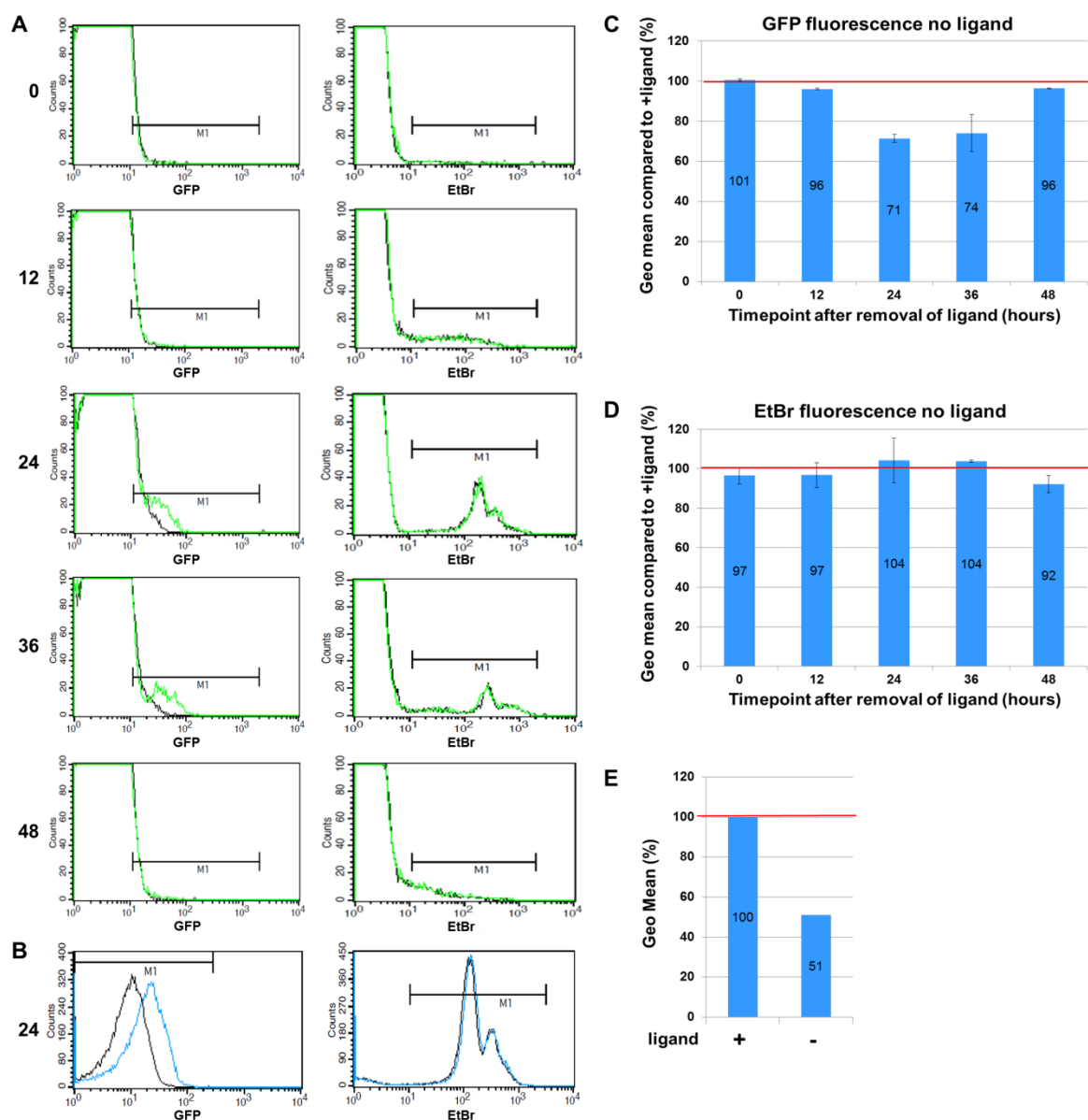


**Figure 29. Flow cytometric analysis of ligand-based regulation of PfNAT<sup>GFPDD24</sup>**

Investigation of reduction in PfNAT<sup>GFPDD24</sup> fluorescence intensity upon ligand removal during a 48-hour time course. Synchronous parasites were divided into ligand-treated (200nM) and untreated cultures at time point 0. Every 12 hours samples were removed and directly analysed with the flow cytometer or stained with EtBr for stage determination. 50 000 cells were counted per measurement. **(A)** Fluorescence curves depicting intensities of GFP fluorescence (left) and EtBr fluorescence (right) of ligand-treated (green line) and untreated (black line) parasites at indicated time points. A difference in GFP fluorescence is obvious at 24- and 36-hour time points, where the parasites reach trophozoite and schizont stages. **(B)** Purification of a 24-hour sample to 90% parasitaemia reveals a distinct difference in GFP fluorescence of treated (blue line) versus untreated (black line) parasites, whereas the developmental stages are comparable (EtBr curves). **(C)** Histogram representing the relative difference of GFP fluorescence in terms of geometric mean at each time point of untreated samples compared to ligand-treated ones. A reduction of 30% is indicated at the 24- and 36-hour time points. **(D)** Histogram representing the relative difference of EtBr fluorescence in terms of geometric mean at each time point of untreated samples compared to ligand-treated ones. No significant differences are observed. **(C)** and **(D)** summarize data of two independent time course experiments. Error bars represent the standard error of mean (SEM). **(E)** Histogram representing a 50% reduction in GFP fluorescence intensity (based on shift in geometric mean) of the untreated sample of **(B)**, which was purified after 24 hours.

## RESULTS

---

As shown in Figure 29D, there was no obvious shift in geometric mean of EtBr fluorescence intensity corresponding to a visual overlap of untreated and treated samples during 48 hours. This result was also obtained with the parental strain 3D7 (data not shown). This indicates that neither the removal of the ligand in PfNAT<sup>GFPDD24</sup> parasites nor the ligand itself (at 200 nM concentration) has any negative effects on growth within one cycle. To further characterize the extent of downregulation of PfNAT<sup>GFPDD24</sup> the flow cytometric analysis was repeated with parasites that were purified 24 hours after ligand removal to more than 90% parasitaemia (Figure 29B). The peaks of GFP fluorescence are much more defined than in the previous time course and clearly show a shift towards higher fluorescence intensity in treated samples as represented in the histogram by a 50% higher geometric mean (Figure 29E). This result is not due to a difference in developmental stage of the two samples as shown by the clear overlay of the EtBr graphs, which indicate a mixed population of trophozoites and schizonts in both cultures. Taken together, these findings provide the proof of principle that the DD system can be successfully applied to a transmembrane protein of *P. falciparum* with a downregulation of around 50%.

The effect of the ligand on the viability of parental 3D7 as well as PfNAT<sup>GFPDD24</sup> clonal parasites was investigated over a period of 4 days to determine any possible unspecific growth reduction or a specific developmental delay due to downregulation of the transferase in PfNAT<sup>GFPDD24</sup> parasites (Figure 30). Initial cultures of 0.5% parasitaemia were supplied with fresh medium ( $\pm$  200 nM ligand) every day and diluted if they reached 4%. Parasitaemias of each culture were determined 2-3 times a day on Giemsa-stained thin blood smears (min. 1000 cells/slide) and the determination was repeated in an independent experiment with similar results. As shown in Figure 30A, the growth of PfNAT<sup>GFPDD24</sup> parasites was comparable between treated and untreated cultures. Although the parasites showed a slight developmental delay under ligand treatment (after 48 and 72 hours) they reached the parasitaemia of the untreated culture and no clear separation of the curves could be observed. This finding suggests that the downregulation of PfNAT<sup>GFPDD24</sup> by approximately 50% in absence of the ligand does not entail any significant growth defects. Furthermore, 3D7 parasites showed the same multiplication rate independent of ligand addition thereby excluding any unspecific effects of the compound at this concentration (Figure 30B). However, it needs to be

mentioned that previous studies indeed report a slight delay in development of parasites treated with ligand at a higher concentration (500nM) with 11% and 25% lower parasitaemia than the untreated controls after the first and second reinvasion cycle, respectively (de Azevedo et al, 2012). At higher concentrations the difference is even more prominent and toxic effects increase, which is the reason why this study used only 200 nM of D/D-solubilizer.

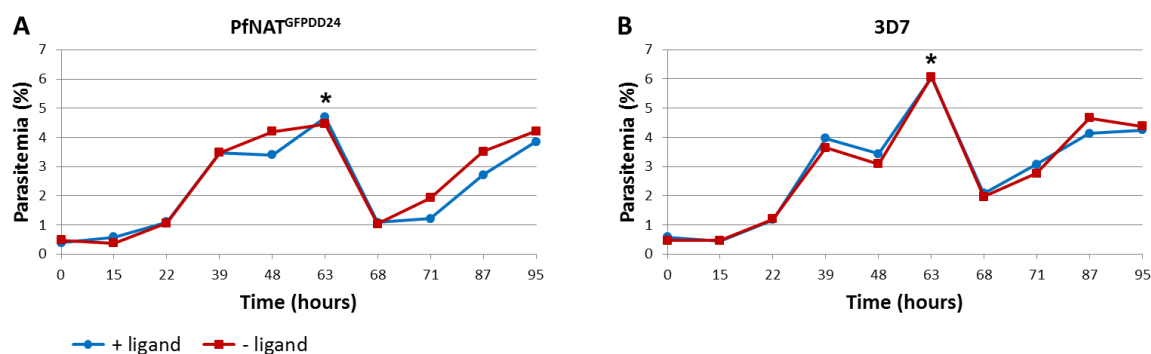


**Figure 30. Effects of stabilizing ligand on parasite growth**

Growth curves of PfNAT<sup>GFPDD24</sup> clonal parasites as well as parental 3D7 parasites to determine possible effects of the ligand on parasite viability. Parasites of ~0.5% parasitaemia were cultured in presence or absence of D/D solubilizer (200nM) over the period of 4 days. Medium was exchanged daily and parasitaemia was monitored regularly by counting of Giemsa-stained thin blood smears (~1000 cells/slide). After 63 hours, the culture was diluted to one fifth (asterisk) to prevent overgrowth. Data of one determination are shown as representative examples, with comparable results in a second independent experiment, both carried out by S. Prior. (A) Clonal PfNAT<sup>GFPDD24</sup> parasites did not exhibit an obvious difference in growth between ligand-treated and untreated cultures. Slight deviations in the curves after 48 hours and between 71-95 hours are very likely within the range of natural developmental variations. (B) Untransfected 3D7 parental parasites did not show any influence of the ligand on parasite development within the observed time frame.

### 3.2.6.3 Cotransfection with STEVOR<sup>mCherry</sup>

Previous studies using fluorescence-based data reported a 75% reduction of soluble luciferase<sup>GFPDD24</sup> in ligand-free samples of stably transfected parasites compared to treated controls (ligand concentration: 500 nM) (de Azevedo et al, 2012). It is still unclear to what extent the DD system is applicable for regulation of transmembrane proteins with co-translational insertion in the ER that might facilitate escape from proteasome degradation in the absence of the ligand. To my knowledge, only falcipain-2 has been tagged with a destabilization domain in *P. falciparum* and there is no quantitative information given on the extent of downregulation of this transmembrane protein (Armstrong & Goldberg, 2007). Having established that the amount of putative acetyltransferase central to this study (PfNAT) can be reduced by half using the DD system the question of its functional relevance was addressed. Although 50% are not

## RESULTS

sufficient for a conditional knock down of the protein it was worth to explore if an intermediate negative effect on protein export could be observed upon destabilization of PfNAT<sup>GFPDD24</sup>. For this purpose an episomal construct encoding STEVOR<sup>1-80</sup> tagged to mCherry (STEVOR<sup>mCherry</sup>) was generated and transfected into PfNAT<sup>GFPDD24</sup> clonal parasites. After positive selection using blasticidin S the parasites were divided into ligand-treated (200 nM) and untreated samples and the export phenotype of STEVOR<sup>mCherry</sup> was examined several days later under the confocal microscope. Despite an obvious reduction in GFP fluorescence intensity corresponding to reduced levels of PfNAT<sup>GFPDD24</sup> in untreated parasites, no difference in export of STEVOR<sup>mCherry</sup> could be observed (e.g. partial retention in the ER or PV) and the protein was properly translocated into the RBC cytosol (Figure 31). In order to assess in detail, whether the amount of exported PEXEL protein was different in both cultures, a quantification of STEVOR<sup>mCherry</sup> in the different compartments would have been interesting. However, this approach was unsuitable due to the episomal character of the constructs that leads to uneven protein expression due to plasmid concatomers. Although this particular experiment could not confirm any functional link between the downregulation of PfNAT and export of a PEXEL protein, the manipulation of the transferase by the DD system allows future investigations to target a wider range of possible effects (see chapter 4.2 for details).

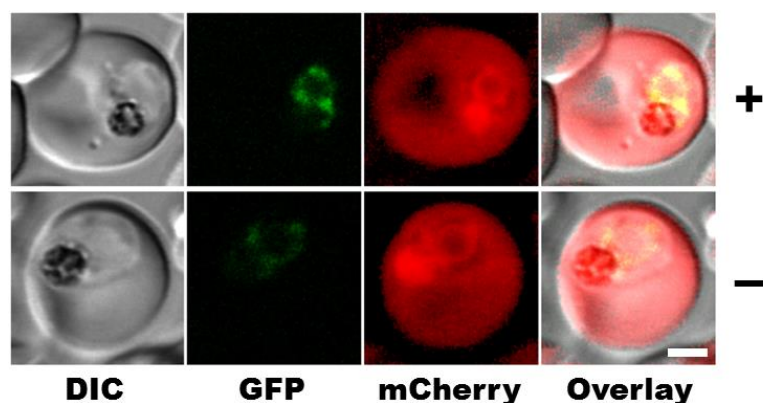


**Figure 31. Export of STEVOR<sup>mCherry</sup> in PfNAT<sup>GFPDD24</sup> parasites**

Confocal images of live *P. falciparum*-infected erythrocytes. Transfectant parasites at trophozoite stage expressing endogenously tagged PfNAT<sup>GFPDD24</sup> as well as episomally encoded STEVOR<sup>mCherry</sup>. The parasites were continuously cultured in presence (+) or absence (-) of ligand (200 nM D/D solubilizer). The export of STEVOR<sup>mCherry</sup> appears identical in both samples. Left images, differential interference contrast (DIC); middle left images, GFP fluorescence; middle right images, mCherry fluorescence; right images, overlay of all channels. Scale bar: 2  $\mu$ m.

### 3.2.6.4 Pulse-chase analysis of protein export in PfNAT<sup>GFPDD24</sup> parasites

Pulse-chase analysis using incorporation of low-energy radioisotopes such as [<sup>35</sup>S]methionine into the proteome is often used to follow the process of protein trafficking (Alberts, 2008; Ansorge et al, 1996; Bullen et al, 2012). In order to assess the impact of downregulation of the putative transferase on protein export into iRBCs, a pulse-chase experiment was conducted by Dr. C. Sanchez using the clonal parasite line established in this study (PfNAT<sup>GFPDD24</sup>) as well as control parental 3D7 *P. falciparum* parasites. It was assumed that reduced levels of PfNAT might alter the overall acetylation state of PEXEL proteins leading to impaired export of these into the host cell. For complementary reasons the results of this investigation will be presented here despite my pregnancy-associated forced absence due to the prohibited handling of radioisotopes. In order to assure sufficient reduction of PfNAT prior to the metabolic labelling of newly synthesized proteins with [<sup>35</sup>S]methionine ('pulse'), parasites were cultured in absence of the stabilizing ligand (D/D solubilizer, 200 nM) for 24 hours. For comparison a second sample was continuously supplied with the compound. Furthermore, a potential unspecific effect of the ligand on protein export was assessed by preparing parental 3D7 parasites in parallel. Prior to the pulse, synchronized parasites of young trophozoite stage were purified under sterile conditions using the magnetic MACS column, washed and then labelled with [<sup>35</sup>S]methionine in methionine-free medium for 1 hour at 37°C. After subsequent washing steps, the infected erythrocytes were returned to the incubator in complete medium supplemented with non-labelled methionine ('chase') and samples were taken at various time points (0, 1, 3, 5 hours). The cytosolic content of the iRBCs was released by mild hypotonic lysis and separated from the parasite pellets. Proteins were precipitated using trichloroacetic acid (TCA), immobilized on filter papers and washed with TCA and ethanol followed by liquid scintillation counting. The percentages of radiolabelled protein in the supernatants, corresponding to the fraction that was exported from the parasites into RBCs, are depicted in Figure 32. In summary, PfNAT<sup>GFPDD24</sup> parasites showed a higher accumulation of radiolabelled proteins in this fraction when the putative transferase was stabilized by continuous ligand treatment compared to untreated samples (Figure 32A). This difference was most prominent at the 1-hour time point with a marked increase in ligand-treated samples (21% vs. 9% in untreated). It was previously shown with a

## RESULTS

conditional protein aggregation system that a period of 1-2 hours is sufficient for trafficking of a PEXEL protein from the parasite to the PV and beyond (Saridaki et al, 2008). Consequently, this increase most likely represents the pool of radiolabelled proteins that got exported and lower levels in the untreated samples indicate an impairment of this process in the background of reduced levels of PfNAT. The slight decrease in radiolabel observed over time might be caused by decay of labelled proteins (functional 20S proteasome subunits were identified in erythrocytes) or, more likely, by concomitant re-uptake of RBC cytosolic content into parasites upon haemoglobin digestion (Neelam et al, 2011). In contrast to the difference observed in PfNAT<sup>GFPDD24</sup> parasites, both curves of the control parental 3D7 parasites showed the same pattern excluding any unspecific effects of the ligand on protein export (Figure 32B).

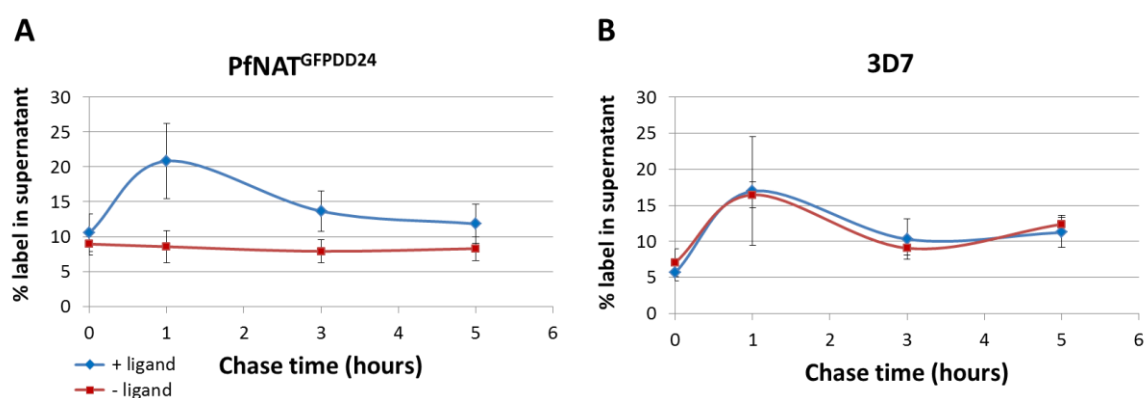


**Figure 32. Pulse-chase analysis of protein export in regulated PfNAT<sup>GFPDD24</sup> clonal line**  
Data kindly provided by Dr. C. Sanchez. Analysis of [<sup>35</sup>S]methionine-labelled proteins exported from *P. falciparum* parasites in dependence of ligand-based downregulation of PfNAT<sup>GFPDD24</sup>. Parasites were cultured in absence of the ligand (D/D solubilizer, 200 nM) for 24 hours or, alternatively, in continuous supply. The labelling period with [<sup>35</sup>S]methionine ('pulse') was 1 hour followed by incubation in complete culture medium ('chase') and sample removal at 0, 1, 3 and 5 hours after removal of the external radioisotope. Protein samples were subjected to mild hypotonic lysis and divided into parasite and supernatant fraction. Incorporation of radioactive label was measured by liquid scintillation counting and is shown here for the supernatant corresponding to the content of the RBC cytosol. (A) PfNAT<sup>GFPDD24</sup> clonal parasites cultured with (+) or without (-) ligand. A difference between both samples can be observed suggesting reduced protein export under destabilizing conditions of PfNAT. (B) Parental 3D7 parasites were used as a control to exclude unspecific effects of the ligand itself on protein export. Error bars are SEM.

---

## 4 Discussion

### 4.1 Mutagenesis of the PEXEL motif of STEVOR and KAHRP

During its intraerythrocytic development, *P. falciparum* establishes a complex trafficking system to export proteins involved in nutrient acquisition, cytoadherence and immunoevasion into the red blood cell (Elsworth et al, 2014). These parasite-induced alterations largely contribute to the pathogenesis of the disease and have initiated intense research to uncover common principles that might be suitable targets for pharmacological interventions. The discovery of the pentameric PEXEL motif (RxLxE/Q/D) allowed the prediction of several hundreds of putatively exported parasite proteins (Hiller et al, 2004; Horrocks & Muhia, 2005; Marti et al, 2004). Cleavage of this export motif by Plasmepsin V inside the endoplasmic reticulum (ER), acetylation of the newly formed N-terminus as well as the identification of a putative ATP-powered translocon in the parasitophorous vacuolar membrane (PVM) for entry of PEXEL proteins into the host cell represent important findings to further understand this complex process (Bullen et al, 2012; Chang et al, 2008; de Koning-Ward et al, 2009; Riglar et al, 2013; Russo et al, 2010). However, the exact role of the PEXEL motif within each step of the export pathway, its sequence limitations and the relevance of acetylation after processing has not been entirely elucidated (Boddey & Cowman, 2013). The aim of this study was to identify amino acids within the PEXEL motif that might be functionally important in guiding proper export of these proteins into the host cell. While previous studies focussed on various deletions or alanine exchanges of the conserved amino acids at positions P3<sup>6</sup> (R), P1 (L) and P2' (E/Q/D), essential information concerning the potential variability of amino acids at each position in relation to the export phenotype and processing of the motif is still missing (Boddey et al, 2010; Boddey et al, 2009; Hiller et al, 2004; Marti et al, 2004).

In order to expand the available data set, an extensive mutagenesis screen was conducted over the PEXEL motif (<sup>48</sup>RLLAQ<sup>52</sup>) of a member of the STEVOR protein family. The amino acid of each position (apart from R<sup>48</sup>, which was extensively studied by Dr. P. Henrich (2008)) was exchanged by site-directed mutagenesis with amino acids of

---

<sup>6</sup> By convention, amino acid residues in a substrate undergoing cleavage are designated P1, P2, P3 etc. in the N-terminal direction from the cleaved bond (P1-P1'). Likewise, the residues in C-terminal direction are designated P1', P2', P3' (Schechter & Berger, 1967).

## DISCUSSION

---

variable biochemical properties to assess the influence of size, charge or hydrophobicity. For simplification, a short GFP-tagged version of STEVOR that comprises the PEXEL motif and an adequate linker region (STEVOR<sup>1-80</sup>), was used. While the full-length STEVOR protein is usually inserted via transmembrane domains into parasite-derived Maurer's clefts that are tethered to the host cell plasma membrane, STEVOR<sup>1-80</sup> translocates as a soluble protein into the red blood cell cytoplasm as previously described (Przyborski et al, 2005). After successful transfection of *P. falciparum* parasites with various constructs the export phenotypes of the chimeric GFP-tagged proteins were analysed by confocal laser scanning microscopy. In an attempt to find a correlation between processing of the PEXEL motif and protein export some representative mutants were furthermore chosen for mass spectrometric analysis to determine their N-terminal cleavage and acetylation state.

The mutagenesis of the P3 position (R<sup>48</sup>) resulted in complete retention of all mutant proteins within the parasite ER (data from P. Henrich (2008) apart from R<sup>48</sup>K). This result is in agreement with former studies on KAHRP and GBP130 and was attributed to a defect in cleavage by Plasmepsin V (Boddey et al, 2010; Boddey et al, 2009). Mass spectrometric analysis on R<sup>48</sup>A indeed identified uncleaved protein N-termini. Interestingly, lysine was repeatedly proposed to functionally substitute for arginine at this position (Boddey et al, 2009; Hiller et al, 2004; Marti et al, 2004), an assumption that is in contradiction to the results of this screen as well as recently published data (Boddey et al, 2013). A detailed structural model of Plasmepsin V, which is based on available crystal structures of three other *Plasmodium* Plasmepsins (II-IV), revealed a specific precondition of the active site to accommodate arginine at the P3 position (Guruprasad et al, 2011). In contrast to this observed sequence restriction, the P2 position of the PEXEL motif (L<sup>49</sup>) appeared very tolerant towards amino acid exchanges with a wild-type export phenotype in all mutants. Furthermore, L<sup>49</sup>A was normally processed with cleavage after P1 (L<sup>50</sup>) and acetylation of the new N-terminus at P1' (A<sup>51</sup>) as shown by mass spectrometry. Since all mutant proteins showed the same localization it is appealing to extrapolate the mass spectrometric result to all L<sup>49</sup> mutants. However, detailed LC-MS/MS analysis of a broader selection of mutants should generally be considered to validate this assumption.

Mutation of the conserved P1 position (L<sup>50</sup>) was characterized by intraparasitic protein retention localized to a bright spot within the ER, which could represent a special

subcompartment (Lee et al, 2008). Similar to R<sup>48</sup>A, L<sup>50</sup>A was neither cleaved nor acetylated, which substantiates the importance of this position in PEXEL processing. In addition, this study could not confirm alternative cleavage within the putative signal sequences of these mutants by signal peptidase. This alternative processing was proposed by Boddey et al (2009) based on observations of minor subpopulations of KAHRP and GBP130 proteins with P3→A and P1→A mutations that entered the default secretory pathway into the PV. The results of our study indicate that Plasmepsin V is dominant over signal peptidase in temporal or spatial terms and that the release of PEXEL proteins from the ER in native conditions depends on this enzyme.

An important outcome of this screen was the sequence restriction at position P1' (A<sup>51</sup>), the residue to be N-acetylated after cleavage. Nearly all mutant chimeric proteins were retained in the PV with a clear defect in translocation to the erythrocyte cytoplasm. The only replacements capable of displaying the wild-type phenotype were serine (A<sup>51</sup>S), threonine (A<sup>51</sup>T) and partially valine (A<sup>51</sup>V). Although alignments of putative PEXEL proteins suggest a certain degree of diversity at P1' an over-representation of these amino acids is obvious (Figure 12). Importantly, this bias is probably caused by preferential acetylation of these residues by N-acetyltransferases (Bienvenut et al, 2012), a post-translational modification that is characteristic of PEXEL processing (Chang et al, 2008). Mass spectrometric analysis revealed normal processing of exported STEVOR<sup>1-80</sup> and A<sup>51</sup>S proteins, whereas PV-retained A<sup>51</sup>D and R mutants were cleaved but not acetylated. At that time, this was the very first indication of a functional relevance of acetylation for export of PEXEL proteins and prompted further investigations into this direction (see chapter 4.2). In support of this finding, a recent publication confirmed this result for mutation of P1' to aspartic acid in the PEXEL proteins REX3 (S→D), KAHRP (A→D) and PfEMP3 (A→D) with a clear retention in the PV as well as cleaved but non-acetylated (mixed with acetylated) N-termini determined for REX3 (Tarr et al, 2013).

In addition to the fluorescence-based microscopic determination the localization of some chosen A<sup>51</sup> mutants was assessed by differential lysis of iRBCs with tetanolysin (disrupts RBC membrane) and saponin (permeabilizes PVM) followed by western blot analysis (Bhattacharjee et al, 2008). It could be shown that wild-type STEVOR<sup>1-80</sup> as well as A<sup>51</sup>S entered the tetanolysin supernatant representative of the RBC cytosolic fraction, whereas

## DISCUSSION

---

A<sup>51</sup>D and R both accumulated in the supernatant of saponin-treated parasite pellets thereby confirming their restriction to the parasitophorous vacuole (Figure 16).

Since the folding of GFP can interfere with the proper localization of tagged proteins it is recommendable to confirm some of the most important mutant phenotypes with smaller tags (HA, c-myc, FLAG) and immunofluorescence detection (Deponte, 2012; Knuepfer et al, 2005a).

In order to proof that the results were not restricted to STEVOR<sup>1-80</sup> some mutations at position P1' were repeated in a second PEXEL protein. A short soluble GFP-tagged version of KAHRP (KAHRP<sup>1-69</sup>, PEXEL motif: <sup>54</sup>RTLAQ<sup>58</sup>), a major component of parasite-derived knobs on the RBC surface, was chosen for this part (Knuepfer et al, 2005b). Similar to STEVOR<sup>1-80</sup>, A<sup>57</sup>S and T were properly translocated into the RBC cytoplasm, whereas A<sup>57</sup>D and R localized to a bright ring around the parasite indicative of the PV. In contrast to the partially exported A<sup>51</sup>V of STEVOR<sup>1-80</sup>, the corresponding mutant protein was not exported in the sequence context of KAHRP. Unfortunately, technical difficulties prevented mass spectrometric analysis of these mutants.

Remarkably, position P2' (Q<sup>52</sup>) of the PEXEL motif, despite being quite conserved (E/Q/D), was rather permissive towards variable amino acids while maintaining the wild-type export phenotype. Only replacements with positively charged amino acids (Q<sup>52</sup>K, R) abolished translocation capability with an accumulation of the GFP-tagged proteins in the PV. Apparently, in this sequence context drastic charge changes from polar uncharged (Q; E/D: negative) to positive seem to interfere with either processing of the PEXEL motif or consecutive export steps such as protein interactions (e.g. with chaperones) or membrane targeting (Boddey & Cowman, 2013). Mass spectrometric analysis determined normal processing of Q<sup>52</sup>A and N, which was in accordance with the localization of these constructs. In this context, it needs to be mentioned that previous studies are contradictory concerning alanine exchanges of P2' (E/Q/D→A) with some authors claiming a clear retention in the PV (Boddey et al, 2009; Przyborski et al, 2005) while others report normal export (Bhattacharjee et al, 2012a; Gruring et al, 2012). Possible explanations for this discrepancy include the use of diverse vector systems harbouring different promoters that might affect the timing and levels of expression, processing and subsequent export of mutant chimaeras. Additionally, a sufficient distance between the PEXEL motif and the GFP linker is crucial for proper targeting

---

(Chang et al, 2008; Knuepfer et al, 2005a). The effect of alanine mutations could also be influenced by the downstream sequence context of different model proteins. This hypothesis was supported by a decreased export efficiency of the REX3 P2' →A mutant only when combined with multiple downstream mutations in the linker region between the PEXEL motif and GFP (Tarr et al, 2013). Taken together the microscopic and mass spectrometry data acquired in the course of this study as well as the above-mentioned publication (ibid.), there is accumulating evidence in favour of the wild-type export phenotype of P2' →A.

Interestingly, Q<sup>52</sup>R was also cleaved and N-acetylated despite its lacking ability to guide proper export. Guruprasad et al (2011) implicated that D<sup>189</sup> in the S2' subsite of Plasmepsin V might specifically interact with the polar to negative side chains of E/Q/D in position P2', which would exclude tolerance of positively charged amino acids (R, K). Since this assumption would predict a disturbed cleavage of Q<sup>52</sup>R, which was not the case, it is more likely that additional factors apart from cleavage and acetylation might be involved in facilitating translocation of PEXEL proteins beyond the PVM. The same conclusion was drawn by Tarr et al (2013) based on an export-deficient REX3 mutant that accumulated in the PV despite normal processing.

The ability of the newly formed N-terminus to act as an independent signal sufficient for proper trafficking of the protein is controversial. A previous study generated a PEXEL protein whose N-terminus (xE/Q/D) was cleaved by signal peptidase instead of Plasmepsin V. The resulting fragment was identically processed but not exported beyond the PVM (Boddey et al, 2010). From this observation the authors deduced that the information required for PEXEL-mediated protein sorting resides predominantly in the N-terminal RxL sequence and is coupled to events occurring prior or directly during cleavage such as binding to PI(3)P in the ER or interaction of Plasmepsin V with chaperones for transfer of cleaved proteins (Bhattacharjee et al, 2012b; Boddey et al, 2010; Russo et al, 2010). However, a more recent study bypassed PI(3)P binding and cleavage by Plasmepsin V using a viral capsid protease domain fused to mature PEXEL N-termini (xE/Q/D) that releases them upon self-cleavage in the ER (Tarr et al, 2013). In contrast to the former study, these constructs were efficiently exported (normal processing including acetylation was identified in both studies). The authors attributed this discrepancy to differences in cleavage efficiency and accuracy between the signal

## DISCUSSION

---

peptidase and the capsid protease. It was further shown that a free processed N-terminus with an adequate distance to folded domains such as GFP is necessary for proper export and that the composition of the linker region in combination with the mature N-terminus can influence the final localization of the protein (Knuepfer et al, 2005a; Tarr et al, 2013). However, the new N-terminus (Ac-xE/Q/D) is very short and the sequences downstream share little conservation among all putatively exported proteins. It is still unclear if there is a specific interaction of the acetylated N-terminus with the translocation machinery or if general characteristics such as charge or tertiary structure of this region determine subsequent trafficking steps (Spielmann & Gilberger, 2010). In this context it is of great importance to resolve how PEXEL proteins progress beyond the ER. Different models have been proposed including chaperone- or receptor-mediated interactions as well as vesicular trafficking via default or specialized secretory pathways to the PV or confined subcompartments harbouring translocons (PTEX) (Boddey & Cowman, 2013; Elsworth et al, 2014). Furthermore, the increasing number of identified PEXEL-negative exported proteins (PNEPS) with no single identifiable motif implicates a more complex export system than originally assumed (Heiber et al, 2013).

The dissection of the PEXEL motif and its role in protein export can greatly enhance our understanding of this process that is essential to parasite viability and pathogenesis. The mutagenesis screen conducted in this study on the PEXEL motif of STEVOR and KAHRP expands the present data set to hitherto unknown details especially by including positions P2 and P1'. In accordance with previous studies the mutagenesis of P3 (R<sup>48</sup>) and P1 (L<sup>50</sup>) revealed a strict limitation to these amino acids in the context of proper processing by Plasmepsin V (Boddey et al, 2010; Boddey et al, 2009; Hiller et al, 2004; Marti et al, 2004; Russo et al, 2010). Position P2 (L<sup>49</sup>) was permissive towards all introduced amino acid exchanges and maintained normal export and processing thereby challenging any functional role. The relevance of acetylation was indicated for the first time by mutations in P1' (A<sup>51</sup>) resulting in non-acetylated chimeric proteins that were incapable to cross the PVM. In contrast acetylation-prone replacements into serine or threonine recovered the wild-type phenotype. These important results could be confirmed on a microscopic basis with KAHRP as a second model protein.

Surprisingly, mutations at P2' (Q<sup>52</sup>) did not interfere with export apart from positively charged amino acids, which confined the mutant proteins to the PV. This was

unexpected given the sequence conservation of all putative PEXEL proteins at this position. The mass spectrometry analysis of the Q<sup>52</sup>R mutant revealed normal processing despite export deficiency. This observation points to additional aspects to be considered in this process such as the influence of downstream sequence context or the nature of interaction with the export machinery (e.g. protein interactions, membrane targeting).

## 4.2 Characterization of a putative N-acetyltransferase (PfNAT)

Virtually all PEXEL proteins are N-acetylated after Plasmepsin V-mediated cleavage of their motif (Chang et al, 2008). Although the exact role of this N-acetylation is still unclear the addition of an acetyl-group to the primary P1' amine might engage in relevant interactions during PEXEL-mediated protein export such as chaperone recruitment, receptor interaction, membrane targeting or direct recognition by the translocon. A functional relevance of co-translational N-terminal acetylation with respect to protein stability, interaction and localization has been shown in several studies including different organisms (Arnesen, 2011; Dikiy & Eliezer, 2014; Scott et al, 2011; Starheim et al, 2012). In addition, accumulating data elucidate the less frequent process of post-translational N-acetylation (Helbig et al, 2010; Helsens et al, 2011; Polevoda & Sherman, 2000; Van Damme et al, 2011b). Interesting examples in the context of PEXEL proteins are plant chloroplast proteins that become acetylated after cleavage of their chloroplast transit peptide (Bienvenut et al, 2012; Zybaïlov et al, 2008).

The results of the study presented here as well as recently published data (Tarr et al, 2013) indicate this post-translational modification as a necessary prerequisite for proper translocation of the proteins into the RBC cytosol. This conclusion is based on the identification of non-acetylated P1' mutants of STEVOR and REX3 that were retained in the PV. Interestingly, the only mutations that were able to functionally replace the endogenous alanine at P1' (A<sup>51</sup>S, T, partially V) in guiding proper export represent specific acetylation sites of NatA acetyltransferases (Helbig et al, 2010). The next part of this study aimed at identifying the N-acetyltransferase in *P. falciparum* (PfNAT) responsible for this modification. Like Plasmepsin V this enzyme might represent an essential bottleneck and is of great relevance to understand and possibly intervene with the export process of *Plasmodium* effector proteins.

## DISCUSSION

---

Commonly, co-translational N-acetylation occurs in the cytosol and some theories exist on Plasmepsin V and the putative NAT acting on PEXEL motifs on the cytoplasmic side of the ER (Römisch, 2012). However, different independent studies using brefeldin A, an inhibitor of anterograde ER transport, as well as PEXEL mutants with artificial ER-retention signals demonstrate that cleavage by Plasmepsin V most likely happens within the ER compartment (Chang et al, 2008; Osborne et al, 2010; Przyborski et al, 2005). Consequently, the identification of PfNAT was based on a selection of proteins with a putative transferase domain as well as entry signals into the secretory pathway (signal peptide or transmembrane domain). Only one out of ten candidate genes in *P. falciparum* (PfNAT, gene ID: PF3D7\_1437000, PlasmoDB) fulfilled these requirements and was therefore chosen for further studies. The putative acetyltransferase domain shows considerable sequence similarity in the orthologous proteins across other *Plasmodium* species and even other apicomplexan genera (Figure 19, Figure 22). The full-length protein was episomally expressed in *P. falciparum* and localized to the intraparasitic perinuclear compartment characteristic of the ER. In addition, the search for a protein that would shuttle the negatively charged acetyl-CoA across the ER membrane retrieved a putative acetyl-CoA transporter (PfAcT, gene ID: PF3D7\_1036800) based on sequence similarity to the mammalian AT-1 transporter (Jonas et al, 2010). Interestingly, an independent review recently proposed both genes as suitable candidates for the process of N-acetylation in PEXEL proteins (Boddey & Cowman, 2013). Co-expression of PfNAT, Plasmepsin V and PfAcT tagged to mCherry and GFP localized all proteins to the same compartment indicating a spatial accumulation of potentially connected functional components. The correct molecular weights of these fusion proteins were confirmed by Western blot analysis and no processing of the proteins was observed. To further characterize PfNAT, the expression under the endogenous promoter as well as the final localization was investigated by successful single crossover recombination of a GFP-tagged version into the respective locus. This clonal line expressing PfNAT<sup>GFP</sup> exhibited fluorescence in the ER throughout the complete intraerythrocytic development until the release of daughter merozoites. Although PCR analysis revealed recombination within the homology region, Southern blot detection of this clonal line should be conducted to confirm the nature and copy number of plasmid integration.

As previously mentioned, the use of small tags (e.g. FLAG, c-myc, HA) in combination with immunofluorescence analysis can circumvent the problem of GFP tags that potentially interfere with targeting of a protein to its natural destination (Deponete, 2012). Therefore, recombinant parasites expressing PfNAT<sup>FLAG</sup> under the endogenous promoter were created (data not shown). However, this parasite line was abandoned since Western blot analysis with different anti-FLAG antibodies repeatedly showed multiple unspecific bands. Furthermore, the generation of antibodies specific to PfNAT was initiated by cloning and affinity-purification of two His-tagged peptides from *E. coli* lysates but could not be finalized (data not shown).

In the next step, the biological function of PfNAT as a putative transferase was investigated by active-site mutagenesis. The effect of mutations that render enzymes catalytically dead and produce dominant-negative phenotypes has been repeatedly exploited (Campillo et al, 2005; Wagner & Benkovic, 1990). The total enzymatic activity of Plasmepsin V was elegantly shown in *P. falciparum* to be decreased by episomal co-expression of an inactive version that competed for substrate binding resulting in a mixed population of cleaved and uncleaved PEXEL protein (Russo et al, 2010). The identification of the active site within the transferase as well as amino acids that might be essential to catalysis was a prerequisite for this part of the study. In collaboration with Dr. M. Deponete he developed a stable protein model of the C-terminal acetyltransferase domain of PfNAT, which was based on suitable crystal structure-derived sequence alignments with two bacterial acetyltransferases (PDB IDs: 3D8P, 3PP9). Since 3PP9 was resolved in complex with acetyl-CoA, the active site of this enzyme could be determined as well as amino acids that are in close proximity to be likely involved in the catalytic reaction or binding of the thioester (R<sup>104</sup>, 3.45 Å; T<sup>132</sup>, 3.76 Å; N<sup>136</sup>, 2.95 Å; Y<sup>143</sup>, 3.41 Å). The comparison with PfNAT indicated a similar binding pocket and corresponding amino acids could be identified for mutagenesis (R<sup>456</sup>; T<sup>484</sup>; N<sup>488</sup>). Although the active site tyrosine that is frequent among NATs (Y<sup>130</sup> in 3D8P, Y<sup>143</sup> in 3PP9) was replaced by valine in this model the closest tyrosine two amino acids upstream (Y<sup>493</sup>) was chosen for mutagenesis (Toleman et al, 2004; Vetting et al, 2005). Furthermore, two highly conserved glycines were included (G<sup>461</sup>, G<sup>499</sup>) that might be of structural relevance within the transferase domain. All amino acid replacements of the site-directed mutagenesis were carried out under the consideration of maintaining

## DISCUSSION

---

structural integrity while abolishing functional characteristics (e.g. similar size, different functional groups). It was assumed that some of these mutations would impair the catalytic potential of PfNAT thereby reducing the acetylation state of PEXEL proteins to reveal an intermediate export phenotype. To test this hypothesis the mCherry-tagged transferase bearing single, double or triple mutations of the previously mentioned residues was co-expressed with STEVOR<sup>1-80</sup> in *P. falciparum* parasites and analysed by fluorescence microscopy.

In summary, all mutant parasites showed a wild-type export phenotype of this PEXEL protein into the RBC cytoplasm and no dominant-negative effect could be observed. One possible explanation for this result could be that the function of PfNAT is not impaired despite mutations in the putative active site or that the prediction was incorrect. Furthermore, the effects of the mutations, if relevant at all, might be diminished in the background of endogenously expressed wild-type enzyme. It would be interesting to approach the function of the transferase by allelic replacement of the endogenous gene with a mutant gene harbouring non-synonymous as well as synonymous mutations in the codons of all previously mentioned amino acids. The nature of recombination events would also provide valuable information on a possible essentiality of the gene as previously shown for Plasmepsin V (Russo et al, 2010). Finally, the outcome of this part of the study might indicate that PfNAT has different biological targets than exported proteins.

Interestingly, parallel studies by my colleague Dr. C. Sanchez using wild-type and mutated PfNAT expressed in yeast strains lacking the catalytic NatA subunit ( $\Delta$ Ard1p) clearly indicated a functional relevance of this enzyme (unpublished, data not shown). It could be shown that a fragment of PfNAT including the putative transferase domain (excluding transmembrane and terminal regions) could compensate the growth defect and heat stress susceptibility of yeast  $\Delta$ ard1 mutants (Lee et al, 1989; Mullen et al, 1989). Since PfNAT and Ard1p both harbour the GCN5-related N-acetyltransferase domain (Gautschi et al, 2003), this result is likely due to functional complementation as postulated in previous studies on histone acetyltransferases and deacetylases (Gaglio et al, 2013; Wang et al, 1997). Remarkably, the above-mentioned active-site mutations decreased the ability of PfNAT to rescue temperature sensitivity of the yeast  $\Delta$ ard1 strain.

To further advance our understanding of its biological function the deletion of the *PfNAT* gene was attempted in the next part of this study. In *P. falciparum* the replacement of the endogenous gene by double crossover recombination is enhanced by negative selection against the vector backbone. Negative selection marker cassettes on the plasmids encode enzymes that convert exogenously-added innocuous compounds into toxic ones, thereby selecting for parasites that remove these cassettes by double crossover recombination events. For this purpose, vector systems with two different negative selection markers were employed encoding either thymidine kinase (TK, pHTK vector) of the *H. simplex* virus or the bifunctional cytosine deaminase/uracil phosphoribosyl transferase (CDUP, pCC vector) from *S. cerevisiae* (Duraisingh et al, 2002; Maier et al, 2006; Mullen et al, 1992). Both enzymes convert normally harmless ganciclovir and 5-FC, respectively, into toxic metabolites that inhibit the *de novo* pyrimidine biosynthesis pathway and nucleic acid synthesis directly. For disruption of the *PfNAT* gene two sets of homology regions were cloned into the pCC and pHTK vectors to flank the positive selection cassettes for the allelic exchange: ~1 kb each of 5' and 3' untranslated regions (UTR) adjacent to the open reading frame of the gene as well as ~0.5 kb of gene terminal regions (*PfNAT* has a length of 2.2 kb including 2 introns). Previous studies proved the length of 0.5 kb to be sufficient for gene targeting in the parasite (Witola et al, 2008). After transfection and positive selection of *P. falciparum* parasites the transfectants were either directly subjected to negative selection pressure or prior to this cycled repeatedly off the positive selection drug to accumulate single crossover integrants for improved gene targeting. Unfortunately, no parasites harbouring constructs with the (more promising) UTRs as homology regions emerged despite repeated transfections. This might be due to regulatory effects of these sequences exerted on the intermediate positive selection markers or plasmid instability in the parasites. Different drug concentrations of 5-FC and ganciclovir were tested (based on IC<sub>50/90</sub> values and literature data, parasite survival rates and personal communication with experienced collaborators) as well as various parasite cycling rounds and periods followed by careful PCR analysis of extracted genomic DNA.

In summary, it was not possible to generate knockout parasites with a disrupted *PfNAT* locus although both vector systems have been successfully applied in *P. falciparum* (Duraisingh et al, 2002; Maier et al, 2008). There are several potential reasons for this

## DISCUSSION

---

failure including methodological aspects such as suboptimal homology regions (too short, spacing problematic), toxic ‘bystander’ effects on integrants caused by high drug dosage (Maier et al, 2006), low initial transfection efficiency, insufficient cycling periods or plasmid instability under selective pressure. However, this result could also implicate an essential role of PfNAT as shown for Plasmepsin V and calpain (Russo et al, 2010; Russo et al, 2009). A genetic knockout screen by Maier et al (2008) on 83 *P. falciparum* genes revealed that 36% seemed inaccessible to gene disruption and the authors commented, ”While the inability to select for double crossover homologous recombination for some genes is not definitive proof that they are essential under laboratory conditions it is consistent with the proposition that they serve an important function in growth of the parasite in the host erythrocyte.” Interestingly, they identified 11 essential PEXEL proteins out of 46 tested (24%) implicating a biological role of these proteins during intraerythrocytic parasite development. In case of a putative role of PfNAT in propagating correct export of PEXEL proteins the disruption of this gene could exert drastic consequences on parasite viability. It would be useful to investigate whether the knockout attempts are more successful in the presence of an episomal version of PfNAT, a general method to determine essentiality of a gene (Slavic et al, 2010). This idea was approached by co-transfecting a construct encoding the FLAG-tagged transferase together with the pCC knockout plasmid followed by dual positive selection with WR99210 and blasticidin S. Unfortunately, no parasites recovered from the transfection.

As an alternative approach, the conditional excision of the gene sequence encoding the PfNAT transferase domain was attempted using the loxP/DiCre recombinase system, which has recently been adapted to *P. falciparum* (Andenmatten et al, 2013; Collins et al, 2013; Yap et al, 2014). This method is based on the expression of the DiCre recombinase in two inactive subunits, which dimerize upon addition of rapamycin. The active enzyme then recognizes short loxP motifs that flank a DNA region of interest in clonally pre-selected parasites and mediates effective excision or inversion of the intervening sequence within one intraerythrocytic growth cycle (Collins et al, 2013). For this study, the gene sequence encoding the C-terminal part of PfNAT including the transferase domain was flanked by loxP sites and recodoned to ensure recombination to occur upstream within a preceding homology region (~ 1kb). After transfection into the

---

constitutively DiCre expressing *P. falciparum* 1G5 strain (kindly provided by M. Blackman) the parasites were subjected to consecutive cycles of the positive selection marker in order to select for single crossover integration events. Genomic DNA of these parasites was analysed by PCR but no recombination event could be observed in any of the cultures despite various cycling conditions. One possible explanation could be the unavoidable placement of the 5' loxP site into an exonic region of the gene. Although this part of the protein is supposedly unstructured the effect of the additional motif (11 amino acids) might disturb its integrity (Costantini et al, 2007). To circumvent this problem, a second set of vectors was constructed, which comprised longer synthetic parts of *PfNAT* with the initial loxP site placed in an intron or the preceding UTR. Furthermore, a third pre-existing redundant loxP site in the original vector (also provided by M. Blackman) was removed to optimize the construct. Despite these attempts none of the plasmids have integrated so far (ongoing experiment). The efficient expression of the recodoned sequence of *PfNAT* as a necessary prerequisite for successful recombination was controlled by transfection of parasites with a construct encoding a GFP-tagged full-length version (*PfNAT*<sup>synth</sup>). The synthetic protein was indeed expressed and localized to the parasite ER as expected. However, transfection efficiency was extremely low and fluorescent parasites were rapidly lost upon continuous culture. This observation might indicate a reduced preference for replacement of the endogenous gene with the synthetic one and explain the inability to recover single crossover integrants.

As a consequence of the occurring failure to knock out the *PfNAT* gene, the next part of this study used the FKBP degradation domain system to conditionally knock down this putative transferase on protein level. This method is based on the fusion of a protein of interest to a destabilizing domain (DD) derived from the human FKBP protein. This tag targets the chimeric protein to proteasomal degradation unless stabilized by the small ligand Shield1 (commercial name D/D solubilizer, Clontech) (Banaszynski et al, 2006; Chu et al, 2008). It has been successfully applied in other organisms (Herm-Gotz et al, 2007; Madeira da Silva et al, 2009) and to some extent in *P. falciparum* as exemplified by downregulation of parasite calpain, falcipain-2, RESA and CDPK-1 (Armstrong & Goldberg, 2007; Azevedo et al, 2013; de Azevedo et al, 2012; Russo et al, 2009).

## DISCUSSION

---

Provided with the opportunity of this modulation system (kindly supplied by M. Ganter and M.F. Azevedo) the endogenous PfNAT was tagged with a variant destabilization domain (DD24) and subsequently analysed by microscopy as well as flow cytometric analysis. For this purpose, an integration construct encoding GFPDD24 was introduced into the *PfNAT* locus of the *P. falciparum* 3D7 strain by single crossover recombination along a 3'-terminal homology region (~1 kb). A clonal population was retrieved by limiting dilution, which exhibited the same expression and localization of PfNAT<sup>GFPDD24</sup> as the previously generated PfNAT<sup>GFP</sup>. The parasites were continuously grown in the presence of 200nM ligand (D/D solubilizer) to ensure sufficient stabilization with minimal toxic side effects. Microscopic as well as Western blot analysis 24 hours after removal of the ligand revealed an obvious decrease in PfNAT<sup>GFPDD24</sup> fluorescence. Using single-cell microscopic quantification the reduction of protein levels was around 50% compared to ligand-treated parasites and an unspecific effect of the ligand alone on fluorescence levels could be excluded. However, in comparison to clonal PfNAT<sup>GFP</sup> expressing parasites the addition of the DD tag itself diminished fluorescence intensity by around 30%. This observation has previously been reported (though to a lesser extent) and has been attributed to possible instability or mistargeting of DD-tagged fusion proteins even in the presence of the ligand (de Azevedo et al, 2012). The sensitivity of single cell quantification was complemented by the advantage of flow cytometric analysis to acquire data for a large number of cells. The downregulation of PfNAT<sup>GFPDD24</sup> upon ligand removal for 24 hours was determined for purified parasite samples (>90% parasitaemia, 50 000 cells counted) to be in the above-mentioned range of 50% compared to the ligand-treated control while developmental stages and parasitaemias were similar in both samples.

From these data it can be concluded that the DD system was successfully applied to reduce protein levels of endogenously tagged PfNAT by 50%. The downregulation of soluble reporter fusion proteins was around 95% in initial studies on mouse embryonic fibroblasts (Chu et al, 2008). However, it was reported to be considerably less in the *Plasmodium* parasite system with ~70% on average at 0.5  $\mu$ M of ligand (de Azevedo et al, 2012). The effectiveness is assumed to be even more diminished for membrane proteins due to their likely inaccessibility to proteasomal degradation, but some

successful applications have been reported (Banaszynski et al, 2006; Schoeber et al, 2009).

Although 50% reduction of protein levels is not enough to knock down the transferase this approach showed successful modulation of a *Plasmodium* transmembrane protein, which might allow to infer important functional information from further investigations. In this context, it was examined if PfNAT<sup>GFPDD24</sup> parasites displayed an abnormal growth if cultured in absence of the ligand as a consequence of reduced transferase levels. Neither a flow cytometric determination over the period of 48 hours nor careful evaluation of parasitaemias in Giemsa-stained slides over 4 days (by S. Prior) revealed any obvious difference in parasite development. Furthermore, the effect of diminished PfNAT on export of a PEXEL protein was assessed by episomal expression of mCherry-tagged STEVOR<sup>1-80</sup> in the clonal parasite line. It was assumed that STEVOR<sup>mCherry</sup> might accumulate in the PV as a consequence of reduced acetylation. While microscopic analysis clearly showed an expected decrease in fluorescence levels of PfNAT<sup>GFPDD24</sup> in ligand-free parasite samples, the localization of STEVOR<sup>mCherry</sup> was comparable in both treated and untreated cultures. It would be interesting to quantify the protein distribution in order to determine any subtle changes in trafficking of STEVOR<sup>mCherry</sup> but the episomal expression will likely falsify the result due to uneven protein levels caused by plasmid concatomers. The use of a conditional export system would as well be worthwhile to detect any temporal delays in export of the PEXEL protein caused by disturbed acetylation. Unfortunately, the well-established Conditional Aggregation Domain (CAD) System is based on the same FKBP domain and utilizes the same ligand, which renders it incompatible with the DD system (Rivera et al, 2000; Saridaki et al, 2008).

To further characterize PfNAT future investigations should analyse a broader range of possible targets that might be affected by downregulation of the transferase. For this purpose, a pulse-chase experiment on the PFNAT<sup>GFPDD24</sup> expressing parasites was conducted to determine if the total amount of [<sup>35</sup>S]-methionine radiolabelled ('pulsed') proteins exported to the erythrocyte cytoplasm changes dependent on different transferase levels (Wiser & Lanners, 1992). The results indeed indicated a reduction in export of proteins in samples that were pulsed after the ligand was removed for 24 hours (data acquired by Dr. C. Sanchez). This difference was not observed in the parental

## DISCUSSION

---

control parasite line excluding any unspecific effect of the stabilizing ligand on protein export. Despite this promising outcome the exact function of PfNAT in protein export still needs to be verified. First of all, it is of major importance to provide evidence that this protein is indeed an N-acetyltransferase. The establishment of an *in vitro* acetylation assay to detect enzyme-specific transfer of radiolabeled acetyl-CoA onto suitable substrates is a necessary step in further investigations and has proven useful in other studies (Costantini et al, 2007; Herrera et al, 1997; Pradeepa et al, 2009). Suitable fragments of PfNAT (no transmembrane domains, removal of terminal signal sequences) were cloned in the course of this study for heterologous expression in *E. coli* and purified. Unfortunately, the majority of recombinant transferase accumulated in bacterial inclusion bodies despite various modifications in culture conditions, which prevented the finalization of this project (data not shown). Since extraction from inclusion bodies and refolding of the denatured protein into a functionally intact enzyme is challenging further optimizations might be worthwhile to pursue in order to increase solubility (Costa et al, 2014; Gopal & Kumar, 2013).

Although several attempts to knock out the gene encoding PfNAT failed, it was possible to delete the orthologous gene (gene ID: PBANKA\_061180, PlasmoDB) in the rodent malaria parasite *P. berghei* suggesting that it is dispensable for the development in the murine host (in collaboration with M. Singer). The knockout parasites exhibited a slightly reduced blood-stage growth rate per day in mice (~80% of wild type). It would be interesting to investigate possible effects of this gene deletion in mosquito stages or after bite-back transmission to the rodent hosts. The replacement of the *PbNAT* gene with a selection marker cassette encoding mCherry enabled the expression of this fluorescent marker under the endogenous promoter. Similar to GFP-tagged PfNAT, continuous intraparasitic expression throughout the entire intraerythrocytic development was observed with increased fluorescence in schizonts and male gametocytes. This finding was interesting, since previous studies reported an enrichment of putatively exported proteins in early gametocytes of *P. falciparum*, some of them with PEXEL motifs (Silvestrini et al, 2010). If the observed increase in expression of *PbNAT* in gametocytes is pure coincidence or indicates a functional relevance of the protein in gametocytogenesis remains to be elucidated. The ability to knock out the orthologous gene in *P. berghei* implicates that methodological limitations might hamper the same

---

progress in *P. falciparum*. An alternative explanation could be a redundancy in the rodent parasite with another enzyme potentially replacing the function of PbNAT in a knockout background. In support of this hypothesis the genome of *P. berghei* harbours a second putative NAT with an entry signal for the secretory pathway in contrast to the human parasite (gene ID: PBANKA\_112760, PlasmoDB). In addition, the essentiality of the transferase (in case of its proposed function in export) might be determined by the relevance and extent of PEXEL-mediated protein export in both species. *P. falciparum* shows a highly expanded PEXEL-positive exportome, which is in part attributed to the expansion of species-specific protein families (DnaJ, PHIST, STEVOR, RIFIN etc.) as well as the unique devotion to present PfEMP1 on the surface of iRBCs (Boddey & Cowman, 2013). In comparison to more than 400 putative PEXEL proteins in *P. falciparum* only 75 were identified in *P. berghei* and it is assumed that PEXEL-negative proteins represent a larger proportion in this species (Pasini et al, 2013). As a consequence, deletion of PbNAT might be less detrimental in the rodent parasite compared to PfNAT in *P. falciparum*. Finally, a completely different biological target of this protein should be taken into consideration. Given the observed sequence similarities to transferase domains of homologous proteins in other apicomplexan species (Figure 22) that have a reduced or absent PEXEL repertoire it is tempting to assign an alternative or more general function to this enzyme (Gohil et al, 2013; Hsiao et al, 2013; Marti et al, 2004). An interesting example of ER-based protein acetylation includes the transient lysine acetylation of BACE1, a key enzyme in generation of Alzheimer's disease amyloid  $\beta$ -peptide, by ATase1 and ATase2 (Ko & Puglielli, 2009). This modification also occurs in other proteins and seems essential for proper trafficking of BACE1 to the Golgi apparatus, since non-acetylated intermediates are retained and degraded in an ER-Golgi intermediate compartment. Consequently a general role of these membranous transferases as protective chaperones mediating correct maturation of secretory proteins via acetylation has been implicated (Jonas et al, 2010).

In conclusion this part of the study identified a putative N-acetyltransferase in *P. falciparum* (PfNAT) that might be responsible for the prevalent acetylation of PEXEL proteins after cleavage by Plasmeprin V. The localization of this transmembrane protein was exclusively limited to the parasite ER and addition of a GFP tag to the endogenous

## DISCUSSION

---

protein via genetic single crossover recombination proved expression throughout the entire intraerythrocytic development. A model of the putative acetyltransferase domain was established in collaboration with Dr. M. Deponce to determine amino acids suitable for active-site mutagenesis. Despite several different mutations in this domain no dominant-negative effect on export of the PEXEL protein STEVOR<sup>1-80</sup> could be observed. For further characterization several attempts were made to delete the gene encoding PfNAT by double-crossover recombination as well as conditional excision using the loxP/DiCre recombinase system. However, these approaches were unsuccessful although the knockout was possible in the rodent malaria parasite *P. berghei* (in collaboration with M. Singer). Alternatively, the downregulation of the transferase on protein level was achieved using the Destabilizing Domain (DD) system. The reduction of endogenously DD-tagged PfNAT was in the range of 50% in ligand-free compared to ligand-stabilized parasites as determined by quantitative microscopy as well as flow cytometric analysis. No defect in parasite growth or export of STEVOR<sup>1-80</sup> was detected in parasites with destabilized protein levels. The applicability of the DD system to membrane proteins of *P. falciparum* could be confirmed in this study. Furthermore, the clonal parasite line expressing regulable levels of PfNAT form the basis for future investigations on the function of this interesting protein.

## 5 Outlook

In conclusion, this study could show that single amino acid replacements at crucial positions of the PEXEL motif can disturb the processing and final localization of an exported model protein. In addition, the acetylation state of the mature N-terminus after cleavage of the export sequence seems to be a necessary prerequisite for correct protein trafficking. Apart from this modification, recent studies added more complexity by pointing out the importance of sequence stretches downstream of the mature N-terminus (Tarr et al, 2013). A potential convergence of export pathways of PEXEL-positive and -negative exported proteins (PPEPs and PNEPs, respectively) was even suggested based on the findings that their N-termini are functionally exchangeable under certain circumstances (Gruring et al, 2012). In order to gain a better understanding it seems crucial to dissect the nature of the export machinery involved in the transfer of exported proteins from the ER to the PV and beyond. The identification of interaction partners such as chaperones, special cargo receptors or the translocon complex could be attempted by co-immunoprecipitation of conditionally exported PEXEL proteins (Saridaki, 2008). Specifically, the combination of the STEVOR<sup>1-80</sup> mutants generated in this study tagged to the conditional aggregation domain (CAD) of the Reverse Protein Dimerization<sup>TM</sup> system (Rivera et al, 2000) would result in the retention of these mutant chimaeras in the ER. Subsequently, upon ligand-dependent release, the proteins should resume their trafficking route all at once, which allows for controlled timing of fixation and subsequent pull-down of putative accessory factors. It is tempting to speculate that mutant chimaeras of STEVOR<sup>1-80</sup> might engage in different interactions depending on their processing state (cleaved vs. uncleaved, acetylated vs. unacetylated) or export phenotype (Q<sup>52</sup>R normally processed, but not exported). However, the transient nature of these interactions and possible contamination with unspecific proteins during co-immunoprecipitation might be challenging.

In addition to the data obtained in this study, the biological function of the putative transferase (PfNAT) and moreover the proposed link to PEXEL-mediated protein export should be characterized in more detail. Since deletion of the gene was unsuccessful and downregulation on protein levels was only partially achieved (~50%), further suitable molecular tools should be investigated that might be based on transcript stability or translational control. Unfortunately, RNA interference (RNAi) is unavailable in *P.*

## OUTLOOK

---

*falciparum* due to the absence of the enzymology required for RNAi-based ablation of gene expression (Baum et al, 2009). Alternatively, two interesting approaches include the use of the inducible bacterial *glmS* ribozyme (Prommana et al, 2013) for conditional cleavage of target mRNA and a newly described regulable tetracycline repressor (TetR)-based protein-RNA interaction using TetR-binding RNA aptamers for inhibition of target mRNA translation (Goldfless et al, 2012).

Furthermore, the above-mentioned downregulation of PfNAT on protein level using the destabilization domain (DD) tag should be exploited in more detail to reveal possible effects on protein export in general and to support the results obtained from the pulse-chase experiment (chapter 3.2.6). Antibody-based detection of known exported proteins (e.g. KAHRP, PfEMP1, and STEVOR) in the iRBC cytosol might reveal a signal reduction in parasites with reduced levels of PfNAT. This comparative approach could be extended to FACS analysis of iRBC surface epitope recognition using pooled human sera of malaria-exposed patients. Although several components of the cytoadherence complex (including PfEMP1) are PNEPs, indirect effects of reduced transferase levels might occur based on the identification of various parasite chaperones (DnaJ, Hsp40, Hsp70-x) among the PEXEL protein repertoire that assist in correct trafficking of these PNEPs (Kulzer et al, 2012; Kulzer et al, 2010). In addition, surface electron microscopy could be employed to investigate if reduced levels of PfNAT lead to a disturbed assembly of the cytoadherence complex including morphological alterations of the knobs (size, density, elevation) on the surface of iRBCs (Rug et al, 2006).

The establishment of an *in vitro* acetylation assay as a fundamental proof of PfNAT functionality was already suggested (chapter 4.2). An important point to consider in this respect is the composition of eukaryotic NATs as complexes consisting of catalytic and auxiliary subunits (Starheim et al, 2012). The focus of this study was limited to one protein (PfNAT) assuming that it would fulfil all necessary requirements for full transferase activity. This hypothesis of one protein combining several functions is exemplified by the bifunctional *P. falciparum* thymidylate synthase-dihydrofolate reductase (TS-DHFR), an essential enzyme in folate biosynthesis that usually consists of two separate proteins in other organisms (Dasgupta & Anderson, 2008). However, the activity of PfNAT might indeed depend on the formation of a functional complex and the identification of additional accessory protein(s) using crystal structural analysis or

co-immunoprecipitation followed by mass spectrometry might be a necessary step prior to subsequent biochemical experiments.

Finally, another interesting aspect is the characterization of the putative transporter (PfAcT) identified in this study that might supply the lumen of the ER with the membrane-impermeable acetyl-CoA necessary for the N-terminal acetylation process. Loss-of-function studies using gene deletion or knockdown approaches in *P. falciparum* parasites as well as transport studies in artificial liposomes or heterologous expression systems such as *Xenopus laevis* oocytes might prove to be useful for this purpose (Jonas et al, 2010; Summers et al, 2014).

Future investigations on the role of the PEXEL motif, the relevance of N-terminal acetylation and the secretory machinery involved in the process of protein export and host cell remodelling will hopefully contribute to the identification of novel attractive targets for therapeutic interventions against this deadly parasite.



## 6 References

- Aikawa M, Miller LH, Johnson J, Rabbege J (1978) Erythrocyte entry by malarial parasites. A moving junction between erythrocyte and parasite. *J Cell Biol* 77: 72-82
- Alberts B (2008) *Molecular biology of the cell*, 5th edn. New York: Garland Science.
- Alberts B (2010) *Essential cell biology*, 3rd edn. New York: Garland Science.
- Alonso PL, Tanner M (2013) Public health challenges and prospects for malaria control and elimination. *Nat Med* 19: 150-155
- Amino R, Giovannini D, Thiberge S, Gueirard P, Boisson B, Dubremetz JF, Prevost MC, Ishino T, Yuda M, Menard R (2008) Host cell traversal is important for progression of the malaria parasite through the dermis to the liver. *Cell Host Microbe* 3: 88-96
- Andenmatten N, Egarter S, Jackson AJ, Jullien N, Herman JP, Meissner M (2013) Conditional genome engineering in *Toxoplasma gondii* uncovers alternative invasion mechanisms. *Nat Methods* 10: 125-127
- Ansorge I, Benting J, Bhakdi S, Lingelbach K (1996) Protein sorting in *Plasmodium falciparum*-infected red blood cells permeabilized with the pore-forming protein streptolysin O. *Biochem J* 315 ( Pt 1): 307-314
- Ansorge I, Paprotka K, Bhakdi S, Lingelbach K (1997) Permeabilization of the erythrocyte membrane with streptolysin O allows access to the vacuolar membrane of *Plasmodium falciparum* and a molecular analysis of membrane topology. *Mol Biochem Parasitol* 84: 259-261
- Armstrong CM, Goldberg DE (2007) An FKBP destabilization domain modulates protein levels in *Plasmodium falciparum*. *Nat Methods* 4: 1007-1009
- Arnesen T (2011) Towards a functional understanding of protein N-terminal acetylation. *PLoS Biol* 9: e1001074
- Arnesen T, Van Damme P, Polevoda B, Helsen K, Evjenth R, Colaert N, Varhaug JE, Vandekerckhove J, Lillehaug JR, Sherman F, Gevaert K (2009) Proteomics analyses reveal the evolutionary conservation and divergence of N-terminal acetyltransferases from yeast and humans. *Proc Natl Acad Sci U S A* 106: 8157-8162
- Aurrecochea C, Brestelli J, Brunk BP, Dommer J, Fischer S, Gajria B, Gao X, Gingle A, Grant G, Harb OS, Heiges M, Innamorato F, Iodice J, Kissinger JC, Kraemer E, Li W, Miller JA, Nayak V, Pennington C, Pinney DF, Roos DS, Ross C, Stoeckert CJ, Jr., Treatman C, Wang H (2009) PlasmoDB: a functional genomic database for malaria parasites. *Nucleic Acids Res* 37: D539-543

## REFERENCES

---

- Azevedo MF, Sanders PR, Krejany E, Nie CQ, Fu P, Bach LA, Wunderlich G, Crabb BS, Gilson PR (2013) Inhibition of *Plasmodium falciparum* CDPK1 by conditional expression of its J-domain demonstrates a key role in schizont development. *Biochem J* 452: 433-441
- Baca AM, Hol WG (2000) Overcoming codon bias: a method for high-level overexpression of *Plasmodium* and other AT-rich parasite genes in *Escherichia coli*. *Int J Parasitol* 30: 113-118
- Baird JK (2005) Effectiveness of antimalarial drugs. *N Engl J Med* 352: 1565-1577
- Banaszynski LA, Chen LC, Maynard-Smith LA, Ooi AG, Wandless TJ (2006) A rapid, reversible, and tunable method to regulate protein function in living cells using synthetic small molecules. *Cell* 126: 995-1004
- Bannister LH, Hopkins JM, Fowler RE, Krishna S, Mitchell GH (2000) A brief illustrated guide to the ultrastructure of *Plasmodium falciparum* asexual blood stages. *Parasitol Today* 16: 427-433
- Barat LM, Palmer N, Basu S, Worrall E, Hanson K, Mills A (2004) Do malaria control interventions reach the poor? A view through the equity lens. *Am J Trop Med Hyg* 71: 174-178
- Barik S (1997) Mutagenesis and gene fusion by megaprimer PCR. *Methods Mol Biol* 67: 173-182
- Barik S (2002) Megaprimer PCR. *Methods Mol Biol* 192: 189-196
- Baum J, Papenfuss AT, Mair GR, Janse CJ, Vlachou D, Waters AP, Cowman AF, Crabb BS, de Koning-Ward TF (2009) Molecular genetics and comparative genomics reveal RNAi is not functional in malaria parasites. *Nucleic Acids Res* 37: 3788-3798
- Baumeister S, Winterberg M, Durantou C, Huber SM, Lang F, Kirk K, Lingelbach K (2006) Evidence for the involvement of *Plasmodium falciparum* proteins in the formation of new permeability pathways in the erythrocyte membrane. *Mol Microbiol* 60: 493-504
- Baumeister S, Winterberg M, Przyborski JM, Lingelbach K (2010) The malaria parasite *Plasmodium falciparum*: cell biological peculiarities and nutritional consequences. *Protoplasma* 240: 3-12
- Bender A, van Dooren GG, Ralph SA, McFadden GI, Schneider G (2003) Properties and prediction of mitochondrial transit peptides from *Plasmodium falciparum*. *Mol Biochem Parasitol* 132: 59-66

- Berman HM, Westbrook J, Feng Z, Gilliland G, Bhat TN, Weissig H, Shindyalov IN, Bourne PE (2000) The Protein Data Bank. *Nucleic Acids Research* 28: 235-242
- Bernhard-Nocht-Institute (2009) Group Dr. Tim Gilberger: Modifications of the erythrocyte.  
<http://www.bnitm.de/forschung/forschungsgruppen/parasitologie/arbeitsgruppe-gilberger/>
- Bhattacharjee S, Hiller NL, Liolios K, Win J, Kanneganti TD, Young C, Kamoun S, Haldar K (2006) The malarial host-targeting signal is conserved in the Irish potato famine pathogen. *PLoS Pathog* 2: e50
- Bhattacharjee S, Speicher KD, Stahelin RV, Speicher DW, Haldar K (2012a) PI(3)P-independent and -dependent pathways function together in a vacuolar translocation sequence to target malarial proteins to the host erythrocyte. *Mol Biochem Parasitol* 185: 106-113
- Bhattacharjee S, Stahelin RV, Speicher KD, Speicher DW, Haldar K (2012b) Endoplasmic reticulum PI(3)P lipid binding targets malaria proteins to the host cell. *Cell* 148: 201-212
- Bhattacharjee S, van Ooij C, Balu B, Adams JH, Haldar K (2008) Maurer's clefts of *Plasmodium falciparum* are secretory organelles that concentrate virulence protein reporters for delivery to the host erythrocyte. *Blood* 111: 2418-2426
- Biasini M, Bienert S, Waterhouse A, Arnold K, Studer G, Schmidt T, Kiefer F, Cassarino TG, Bertoni M, Bordoli L, Schwede T (2014) SWISS-MODEL: modelling protein tertiary and quaternary structure using evolutionary information. *Nucleic Acids Res*
- Bienvenut WV, Sumpton D, Martinez A, Lilla S, Espagne C, Meinnel T, Giglione C (2012) Comparative large scale characterization of plant versus mammal proteins reveals similar and idiosyncratic N-alpha-acetylation features. *Mol Cell Proteomics* 11: M111 015131
- Bland C, Hartmann EM, Christie-Oleza JA, Fernandez B, Armengaud J (2014) N-terminal-oriented proteogenomics of the marine bacterium *Roseobacter denitrificans* OCh114 using TMPP labeling and diagonal chromatography. *Mol Cell Proteomics*
- Blisnick T, Vincensini L, Fall G, Braun-Breton C (2006) Protein phosphatase 1, a *Plasmodium falciparum* essential enzyme, is exported to the host cell and implicated in the release of infectious merozoites. *Cell Microbiol* 8: 591-601
- Blumenthal R, Habig WH (1984) Mechanism of tetanolysin-induced membrane damage: studies with black lipid membranes. *J Bacteriol* 157: 321-323

## REFERENCES

---

- Blythe JE, Suretheran T, Preiser PR (2004) STEVOR--a multifunctional protein? *Mol Biochem Parasitol* 134: 11-15
- Boddey JA, Carvalho TG, Hodder AN, Sargeant TJ, Sleebs BE, Marapana D, Lopaticki S, Nebl T, Cowman AF (2013) Role of plasmepsin V in export of diverse protein families from the Plasmodium falciparum exportome. *Traffic* 14: 532-550
- Boddey JA, Cowman AF (2013) Plasmodium Nesting: Remaking the Erythrocyte from the Inside Out. *Annu Rev Microbiol* 26: 26
- Boddey JA, Hodder AN, Gunther S, Gilson PR, Patsiouras H, Kapp EA, Pearce JA, de Koning-Ward TF, Simpson RJ, Crabb BS, Cowman AF (2010) An aspartyl protease directs malaria effector proteins to the host cell. *Nature* 463: 627-631
- Boddey JA, Moritz RL, Simpson RJ, Cowman AF (2009) Role of the Plasmodium export element in trafficking parasite proteins to the infected erythrocyte. *Traffic* 10: 285-299
- Bray PG, Martin RE, Tilley L, Ward SA, Kirk K, Fidock DA (2005) Defining the role of PfCRT in Plasmodium falciparum chloroquine resistance. *Mol Microbiol* 56: 323-333
- Breman JG (2009) Eradicating malaria. *Sci Prog* 92: 1-38
- Buchan DW, Minneci F, Nugent TC, Bryson K, Jones DT (2013) Scalable web services for the PSIPRED Protein Analysis Workbench. *Nucleic Acids Res* 41: W349-357
- Bullen HE, Charnaud SC, Kalanon M, Riglar DT, Dekiwadia C, Kangwanrangsan N, Torii M, Tsuboi T, Baum J, Ralph SA, Cowman AF, de Koning-Ward TF, Crabb BS, Gilson PR (2012) Biosynthesis, localization, and macromolecular arrangement of the Plasmodium falciparum translocon of exported proteins (PTEX). *J Biol Chem* 287: 7871-7884
- Bunn H (2011) Approach to the anemias. In *Cecil Medicine*, Goldman L, Schafer A (eds), 24th edn, 161. Philadelphia: Saunders Elsevier
- Burnette WN (1981) "Western blotting": electrophoretic transfer of proteins from sodium dodecyl sulfate--polyacrylamide gels to unmodified nitrocellulose and radiographic detection with antibody and radioiodinated protein A. *Anal Biochem* 112: 195-203
- Butterworth AS, Robertson AJ, Ho MF, Gatton ML, McCarthy JS, Trenholme KR (2011) An improved method for undertaking limiting dilution assays for in vitro cloning of Plasmodium falciparum parasites. *Malar J* 10: 95
- Campillo NE, Paez JA, Lagartera L, Gonzalez A (2005) Homology modelling and active-site-mutagenesis study of the catalytic domain of the pneumococcal phosphorylcholine esterase. *Bioorg Med Chem* 13: 6404-6413

- Carter R, Mendis KN (2002) Evolutionary and historical aspects of the burden of malaria. *Clin Microbiol Rev* 15: 564-594
- Chahaun V, C. E. Chitnis, B. S. Crabb, M. Duraisingh, A. G. Maier, P. Malhotra & J. K. Thompson (2002) *P. falciparum* transfection manual *ICGEB New Dehli*
- Chan WT, Verma CS, Lane DP, Gan SK (2013) A comparison and optimization of methods and factors affecting the transformation of *Escherichia coli*. *Biosci Rep* 33
- Chang HH, Falick AM, Carlton PM, Sedat JW, DeRisi JL, Marletta MA (2008) N-terminal processing of proteins exported by malaria parasites. *Mol Biochem Parasitol* 160: 107-115
- Cheng Q, Cloonan N, Fischer K, Thompson J, Waine G, Lanzer M, Saul A (1998) *stevor* and *rif* are *Plasmodium falciparum* multicopy gene families which potentially encode variant antigens. *Mol Biochem Parasitol* 97: 161-176
- Chima RI, Goodman CA, Mills A (2003) The economic impact of malaria in Africa: a critical review of the evidence. *Health Policy* 63: 17-36
- Chitnis CE (2001) Molecular insights into receptors used by malaria parasites for erythrocyte invasion. *Curr Opin Hematol* 8: 85-91
- Chu BW, Banaszynski LA, Chen LC, Wandless TJ (2008) Recent progress with FKBP-derived destabilizing domains. *Bioorg Med Chem Lett* 18: 5941-5944
- Chua CL, Brown G, Hamilton JA, Rogerson S, Boeuf P (2013) Monocytes and macrophages in malaria: protection or pathology? *Trends Parasitol* 29: 26-34
- Chung DW, Ponts N, Cervantes S, Le Roch KG (2009) Post-translational modifications in *Plasmodium*: more than you think! *Mol Biochem Parasitol* 168: 123-134
- Cogswell FB (1992) The hypnozoite and relapse in primate malaria. *Clin Microbiol Rev* 5: 26-35
- Collins CR, Das S, Wong EH, Andenmatten N, Stallmach R, Hackett F, Herman JP, Muller S, Meissner M, Blackman MJ (2013) Robust inducible Cre recombinase activity in the human malaria parasite *Plasmodium falciparum* enables efficient gene deletion within a single asexual erythrocytic growth cycle. *Mol Microbiol* 88: 687-701
- Cooke BM, Lingelbach K, Bannister LH, Tilley L (2004) Protein trafficking in *Plasmodium falciparum*-infected red blood cells. *Trends Parasitol* 20: 581-589

## REFERENCES

---

- Costa S, Almeida A, Castro A, Domingues L (2014) Fusion tags for protein solubility, purification and immunogenicity in : the novel Fh8 system. *Frontiers in microbiology* 5: 63
- Costantini C, Ko MH, Jonas MC, Puglielli L (2007) A reversible form of lysine acetylation in the ER and Golgi lumen controls the molecular stabilization of BACE1. *Biochem J* 407: 383-395
- Cox FE (2002) History of human parasitology. *Clin Microbiol Rev* 15: 595-612
- Cox FE (2010) History of the discovery of the malaria parasites and their vectors. *Parasit Vectors* 3: 5
- Crabb BS, Cooke BM, Reeder JC, Waller RF, Caruana SR, Davern KM, Wickham ME, Brown GV, Coppel RL, Cowman AF (1997) Targeted gene disruption shows that knobs enable malaria-infected red cells to cytoadhere under physiological shear stress. *Cell* 89: 287-296
- Crabb BS, de Koning-Ward TF, Gilson PR (2010) Protein export in Plasmodium parasites: from the endoplasmic reticulum to the vacuolar export machine. *Int J Parasitol* 40: 509-513
- Cyrklaff M, Sanchez CP, Kilian N, Bisseye C, Simpore J, Frischknecht F, Lanzer M (2011) Hemoglobins S and C interfere with actin remodeling in Plasmodium falciparum-infected erythrocytes. *Science* 334: 1283-1286
- Dasgupta T, Anderson KS (2008) Probing the role of parasite-specific, distant structural regions on communication and catalysis in the bifunctional thymidylate synthase-dihydrofolate reductase from Plasmodium falciparum. *Biochemistry* 47: 1336-1345
- de Azevedo MF, Gilson PR, Gabriel HB, Simoes RF, Angrisano F, Baum J, Crabb BS, Wunderlich G (2012) Systematic analysis of FKBP inducible degradation domain tagging strategies for the human malaria parasite Plasmodium falciparum. *PLoS ONE* 7: e40981
- de Koning-Ward TF, Gilson PR, Boddey JA, Rug M, Smith BJ, Papenfuss AT, Sanders PR, Lundie RJ, Maier AG, Cowman AF, Crabb BS (2009) A newly discovered protein export machine in malaria parasites. *Nature* 459: 945-949
- Deponte M (2012) GFP tagging sheds light on protein translocation: implications for key methods in cell biology. *Cell Mol Life Sci* 69: 1025-1033
- Deponte M, Hoppe HC, Lee MCS, Maier AG, Richard D, Rug M, Spielmann T, Przyborski JM (2012) Wherever I may roam: Protein and membrane trafficking in P. falciparum-infected red blood cells. *Molecular and Biochemical Parasitology* 186: 95-116

- Dhingra V, Vishweshwar Rao K, Lakshmi Narasu M (2000) Current status of artemisinin and its derivatives as antimalarial drugs. *Life Sci* 66: 279-300
- Dikiy I, Eliezer D (2014) N-terminal acetylation stabilizes N-terminal helicity in lipid- and micelle-bound alpha-synuclein and increases its affinity for physiological membranes. *J Biol Chem* 289: 3652-3665
- Dixon MW, Hawthorne PL, Spielmann T, Anderson KL, Trenholme KR, Gardiner DL (2008) Targeting of the ring exported protein 1 to the Maurer's clefts is mediated by a two-phase process. *Traffic* 9: 1316-1326
- Dixon MW, Kenny S, McMillan PJ, Hanssen E, Trenholme KR, Gardiner DL, Tilley L (2011) Genetic ablation of a Maurer's cleft protein prevents assembly of the Plasmodium falciparum virulence complex. *Mol Microbiol* 81: 982-993
- Duraisingh MT, Triglia T, Cowman AF (2002) Negative selection of Plasmodium falciparum reveals targeted gene deletion by double crossover recombination. *Int J Parasitol* 32: 81-89
- Dvorak JA, Miller LH, Whitehouse WC, Shiroishi T (1975) Invasion of erythrocytes by malaria merozoites. *Science* 187: 748-750
- Dyda F, Klein DC, Hickman AB (2000) GCN5-related N-acetyltransferases: a structural overview. *Annu Rev Biophys Biomol Struct* 29: 81-103
- Ellis JG, Dodds PN (2011) Showdown at the RXLR motif: Serious differences of opinion in how effector proteins from filamentous eukaryotic pathogens enter plant cells. *Proc Natl Acad Sci U S A* 108: 14381-14382
- Elmendorf HG, Haldar K (1993) Identification and localization of ERD2 in the malaria parasite Plasmodium falciparum: separation from sites of sphingomyelin synthesis and implications for organization of the Golgi. *EMBO J* 12: 4763-4773
- Elsworth B, Crabb BS, Gilson PR (2014) Protein export in malaria parasites: an update. *Cell Microbiol* 13: 12261
- Engwerda CR, Beattie L, Amante FH (2005) The importance of the spleen in malaria. *Trends Parasitol* 21: 75-80
- Engwerda CR, Good MF (2005) Interactions between malaria parasites and the host immune system. *Curr Opin Immunol* 17: 381-387
- Fleischer B (2004) Editorial: 100 years ago: Giemsa's solution for staining of plasmodia. *Trop Med Int Health* 9: 755-756
- Flick K, Ahuja S, Chene A, Bejarano M, Chen Q (2004) Optimized expression of Plasmodium falciparum erythrocyte membrane protein 1 domains in Escherichia coli. *Malaria Journal* 3: 50

## REFERENCES

---

- Forte GM, Pool MR, Stirling CJ (2011) N-terminal acetylation inhibits protein targeting to the endoplasmic reticulum. *PLoS Biol* 9: e1001073
- Frevert U, Sinnis P, Cerami C, Shreffler W, Takacs B, Nussenzweig V (1993) Malaria circumsporozoite protein binds to heparan sulfate proteoglycans associated with the surface membrane of hepatocytes. *J Exp Med* 177: 1287-1298
- Frischknecht F, Lanzer M (2008) The Plasmodium falciparum Maurer's clefts in 3D. *Mol Microbiol* 67: 687-691
- Gaglio D, D'Alfonso A, Camilloni G (2013) Functional complementation of sir2Delta yeast mutation by the human orthologous gene SIRT1. *PLoS One* 8: e83114
- Gautschi M, Just S, Mun A, Ross S, Rucknagel P, Dubaquié Y, Ehrenhofer-Murray A, Rospert S (2003) The yeast N(alpha)-acetyltransferase NatA is quantitatively anchored to the ribosome and interacts with nascent polypeptides. *Mol Cell Biol* 23: 7403-7414
- Gehde N, Hinrichs C, Montilla I, Charpian S, Lingelbach K, Przyborski JM (2008) Protein unfolding is an essential requirement for transport across the parasitophorous vacuolar membrane of Plasmodium falciparum. *Mol Microbiol*
- Ginsburg H, Stein WD (2004) The new permeability pathways induced by the malaria parasite in the membrane of the infected erythrocyte: comparison of results using different experimental techniques. *J Membr Biol* 197: 113-134
- Gohil S, Kats LM, Seemann T, Fernandez KM, Siddiqui G, Cooke BM (2013) Bioinformatic prediction of the exportome of Babesia bovis and identification of novel proteins in parasite-infected red blood cells. *Int J Parasitol* 43: 409-416
- Goldberg DE, Cowman AF (2010) Moving in and renovating: exporting proteins from Plasmodium into host erythrocytes. *Nat Rev Microbiol* 8: 617-621
- Goldfless SJ, Belmont BJ, de Paz AM, Liu JF, Niles JC (2012) Direct and specific chemical control of eukaryotic translation with a synthetic RNA-protein interaction. *Nucleic Acids Res* 40: e64
- Goldstein ST, Shapiro CN (1997) A recombinant circumsporozoite protein vaccine against malaria. *N Engl J Med* 336: 1760; author reply 1760-1761
- Gopal GJ, Kumar A (2013) Strategies for the production of recombinant protein in Escherichia coli. *The protein journal* 32: 419-425
- Goyal M, Alam A, Iqbal MS, Dey S, Bindu S, Pal C, Banerjee A, Chakrabarti S, Bandyopadhyay U (2012) Identification and molecular characterization of an Alba-family protein from human malaria parasite Plasmodium falciparum. *Nucleic Acids Res* 40: 1174-1190

- Gruring C, Heiber A, Kruse F, Flemming S, Franci G, Colombo SF, Fasana E, Schoeler H, Borgese N, Stunnenberg HG, Przyborski JM, Gilberger TW, Spielmann T (2012) Uncovering common principles in protein export of malaria parasites. *Cell Host Microbe* 12: 717-729
- Günther A (2012) Examination of the function of the PEXEL-motif in protein export in Plasmodium falciparum-infected erythrocytes. Parasitology, Heidelberg,
- Guruprasad L, Tanneeru K, Guruprasad K (2011) Structural Rationale for the Recognition of Arginine at P(3) in PEXEL Motif Containing Proteins of Plasmodium falciparum by Plasmepsin V. *Protein Pept Lett*
- Haase S, de Koning-Ward TF (2010) New insights into protein export in malaria parasites. *Cell Microbiol* 12: 580-587
- Haase S, Herrmann S, Gruring C, Heiber A, Jansen PW, Langer C, Treeck M, Cabrera A, Bruns C, Struck NS, Kono M, Engelberg K, Ruch U, Stunnenberg HG, Gilberger TW, Spielmann T (2009) Sequence requirements for the export of the Plasmodium falciparum Maurer's clefts protein REX2. *Mol Microbiol* 71: 1003-1017
- Haldar KM, N.; Bhattacharjee, S.; Harrison, T.; Hiller, N. L.; Liolios, K.; Murphy, S.; Tamez, P.; Ooij, C. van (2005) Trafficking and the tubulovesicular membrane network. . In *Molecular approaches to malaria*, Sherman IW (ed), pp pp. 253-271 ASM Press
- Hall TA (1999) BioEdit: a user-friendly biological sequence alignment editor and analysis program for Windows 95/98/NT. *Nucleic Acids Symposium Series* 41: 95-98
- Hanssen E, Sougrat R, Frankland S, Deed S, Klonis N, Lippincott-Schwartz J, Tilley L (2008) Electron tomography of the Maurer's cleft organelles of Plasmodium falciparum-infected erythrocytes reveals novel structural features. *Mol Microbiol* 67: 703-718
- Hasenkamp S, Merrick CJ, Horrocks P (2013) A quantitative analysis of Plasmodium falciparum transfection using DNA-loaded erythrocytes. *Mol Biochem Parasitol* 187: 117-120
- Hastings MD, Sibley CH (2002) Pyrimethamine and WR99210 exert opposing selection on dihydrofolate reductase from Plasmodium vivax. *Proc Natl Acad Sci U S A* 99: 13137-13141
- Heiber A, Kruse F, Pick C, Gruring C, Flemming S, Oberli A, Schoeler H, Retzlaff S, Mesen-Ramirez P, Hiss JA, Kadekoppala M, Hecht L, Holder AA, Gilberger TW, Spielmann T (2013) Identification of New PNEPs Indicates a Substantial

## REFERENCES

---

- Non-PEXEL Exportome and Underpins Common Features in *Plasmodium falciparum* Protein Export. *PLoS Pathog* 9: 8
- Helbig AO, Gauci S, Raijmakers R, van Breukelen B, Slijper M, Mohammed S, Heck AJR (2010) Profiling of N-Acetylated Protein Termini Provides In-depth Insights into the N-terminal Nature of the Proteome. *Molecular & Cellular Proteomics* 9: 928-939
- Helsens K, Van Damme P, Degroeve S, Martens L, Arnesen T, Vandekerckhove J, Gevaert K (2011) Bioinformatics analysis of a *Saccharomyces cerevisiae* N-terminal proteome provides evidence of alternative translation initiation and post-translational N-terminal acetylation. *J Proteome Res* 10: 3578-3589
- Henrich P (2008) Charakterisierung der Exportsignale in Proteinen von *Plasmodium falciparum* anhand eines Vertreters der STEVOR-Genfamilie. Parasitology, Heidelberg,
- Herm-Gotz A, Agop-Nersesian C, Munter S, Grimley JS, Wandless TJ, Frischknecht F, Meissner M (2007) Rapid control of protein level in the apicomplexan *Toxoplasma gondii*. *Nat Methods* 4: 1003-1005
- Herrera JE, Bergel M, Yang XJ, Nakatani Y, Bustin M (1997) The histone acetyltransferase activity of human GCN5 and PCAF is stabilized by coenzymes. *J Biol Chem* 272: 27253-27258
- Hiller NL, Bhattacharjee S, van Ooij C, Liolios K, Harrison T, Lopez-Estrano C, Haldar K (2004) A host-targeting signal in virulence proteins reveals a secretome in malarial infection. *Science* 306: 1934-1937
- Ho SN, Hunt HD, Horton RM, Pullen JK, Pease LR (1989) Site-directed mutagenesis by overlap extension using the polymerase chain reaction. *Gene* 77: 51-59
- Hollebeke J, Van Damme P, Gevaert K (2012) N-terminal acetylation and other functions of Nalpha-acetyltransferases. *Biol Chem* 393: 291-298
- Horrocks P, Muhia D (2005) Pexel/VTS: a protein-export motif in erythrocytes infected with malaria parasites. *Trends Parasitol* 21: 396-399
- Horrocks P, Pinches RA, Chakravorty SJ, Papakrivos J, Christodoulou Z, Kyes SA, Urban BC, Ferguson DJ, Newbold CI (2005) PfEMP1 expression is reduced on the surface of knobless *Plasmodium falciparum* infected erythrocytes. *J Cell Sci* 118: 2507-2518
- Hsiao CH, Luisa Hiller N, Haldar K, Knoll LJ (2013) A HT/PEXEL motif in *Toxoplasma dense granule* proteins is a signal for protein cleavage but not export into the host cell. *Traffic* 14: 519-531

- Hwang CS, Shemorry A, Varshavsky A (2010) N-terminal acetylation of cellular proteins creates specific degradation signals. *Science* 327: 973-977
- Ingmundson A, Alano P, Matuschewski K, Silvestrini F (2014) Feeling at home from arrival to departure: protein export and host cell remodelling during Plasmodium liver stage and gametocyte maturation. *Cell Microbiol* 16: 324-333
- Ingmundson A, Nahar C, Brinkmann V, Lehmann MJ, Matuschewski K (2012) The exported Plasmodium berghei protein IBIS1 delineates membranous structures in infected red blood cells. *Mol Microbiol* 83: 1229-1243
- Johnson JD, Denuff RA, Gerena L, Lopez-Sanchez M, Roncal NE, Waters NC (2007) Assessment and continued validation of the malaria SYBR green I-based fluorescence assay for use in malaria drug screening. *Antimicrob Agents Chemother* 51: 1926-1933
- Jonas MC, Pehar M, Puglielli L (2010) AT-1 is the ER membrane acetyl-CoA transporter and is essential for cell viability. *J Cell Sci* 123: 3378-3388
- Jullien N, Sampieri F, Enjalbert A, Herman JP (2003) Regulation of Cre recombinase by ligand-induced complementation of inactive fragments. *Nucleic Acids Res* 31: e131
- Kirk K, Saliba KJ (2007) Targeting nutrient uptake mechanisms in Plasmodium. *Curr Drug Targets* 8: 75-88
- Klemba M, Goldberg DE (2005) Characterization of plasmepsin V, a membrane-bound aspartic protease homolog in the endoplasmic reticulum of Plasmodium falciparum. *Mol Biochem Parasitol* 143: 183-191
- Knuepfer E, Rug M, Cowman AF (2005a) Function of the plasmodium export element can be blocked by green fluorescent protein. *Mol Biochem Parasitol* 142: 258-262
- Knuepfer E, Rug M, Klonis N, Tilley L, Cowman AF (2005b) Trafficking of the major virulence factor to the surface of transfected P. falciparum-infected erythrocytes. *Blood* 105: 4078-4087
- Ko MH, Puglielli L (2009) Two endoplasmic reticulum (ER)/ER Golgi intermediate compartment-based lysine acetyltransferases post-translationally regulate BACE1 levels. *J Biol Chem* 284: 2482-2492
- Kriek N, Tilley L, Horrocks P, Pinches R, Elford BC, Ferguson DJ, Lingelbach K, Newbold CI (2003) Characterization of the pathway for transport of the cytoadherence-mediating protein, PfEMP1, to the host cell surface in malaria parasite-infected erythrocytes. *Mol Microbiol* 50: 1215-1227

## REFERENCES

---

- Kuehn A, Pradel G (2010) The coming-out of malaria gametocytes. *J Biomed Biotechnol* 2010: 976827
- Kulzer S, Charnaud S, Dagan T, Riedel J, Mandal P, Pesce ER, Blatch GL, Crabb BS, Gilson PR, Przyborski JM (2012) Plasmodium falciparum-encoded exported hsp70/hsp40 chaperone/co-chaperone complexes within the host erythrocyte. *Cell Microbiol* 14: 1784-1795
- Kulzer S, Gehde N, Przyborski JM (2009) Return to sender: use of Plasmodium ER retrieval sequences to study protein transport in the infected erythrocyte and predict putative ER protein families. *Parasitol Res* 104: 1535-1541
- Kulzer S, Rug M, Brinkmann K, Cannon P, Cowman A, Lingelbach K, Blatch GL, Maier AG, Przyborski JM (2010) Parasite-encoded Hsp40 proteins define novel mobile structures in the cytosol of the P. falciparum-infected erythrocyte. *Cell Microbiol* 12: 1398-1420
- Kumar N, Zheng H (1992) Nucleotide sequence of a Plasmodium falciparum stress protein with similarity to mammalian 78-kDa glucose-regulated protein. *Molecular and Biochemical Parasitology* 56: 353-356
- Kyes SA, Kraemer SM, Smith JD (2007) Antigenic variation in Plasmodium falciparum: gene organization and regulation of the var multigene family. *Eukaryot Cell* 6: 1511-1520
- Laemmli UK (1970) Cleavage of structural proteins during the assembly of the head of bacteriophage T4. *Nature* 227: 680-685
- Lambros C, Vanderberg JP (1979) Synchronization of Plasmodium falciparum erythrocytic stages in culture. *J Parasitol* 65: 418-420
- Langhi DM, Jr., Bordin JO (2006) Duffy blood group and malaria. *Hematology* 11: 389-398
- Lanzer M, Wickert H, Krohne G, Vincensini L, Braun Breton C (2006) Maurer's clefts: a novel multi-functional organelle in the cytoplasm of Plasmodium falciparum-infected erythrocytes. *Int J Parasitol* 36: 23-36
- Larkin MA, Blackshields G, Brown NP, Chenna R, McGettigan PA, McWilliam H, Valentin F, Wallace IM, Wilm A, Lopez R, Thompson JD, Gibson TJ, Higgins DG (2007) Clustal W and Clustal X version 2.0. *Bioinformatics* 23: 2947-2948
- Lavazec C, Sanyal S, Templeton TJ (2007) Expression switching in the stevor and Pfmc-2TM superfamilies in Plasmodium falciparum. *Mol Microbiol* 64: 1621-1634
- Lee FJ, Lin LW, Smith JA (1989) N alpha acetylation is required for normal growth and mating of Saccharomyces cerevisiae. *Journal of Bacteriology* 171: 5795-5802

- 
- Lee MC, Moura PA, Miller EA, Fidock DA (2008) Plasmodium falciparum Sec24 marks transitional ER that exports a model cargo via a diacidic motif. *Mol Microbiol* 68: 1535-1546
- Limenitakis J, Soldati-Favre D (2011) Functional genetics in Apicomplexa: potentials and limits. *FEBS Lett* 585: 1579-1588
- Ling MM, Robinson BH (1997) Approaches to DNA mutagenesis: an overview. *Anal Biochem* 254: 157-178
- Mackinnon MJ, Read AF (2004) Virulence in malaria: an evolutionary viewpoint. *Philos Trans R Soc Lond B Biol Sci* 359: 965-986
- Macrauld CA, Anders RF, Foley M, Norton RS (2011) Apical membrane antigen 1 as an anti-malarial drug target. *Current topics in medicinal chemistry* 11: 2039-2047
- Madeira da Silva L, Owens KL, Murta SM, Beverley SM (2009) Regulated expression of the Leishmania major surface virulence factor lipophosphoglycan using conditionally destabilized fusion proteins. *Proc Natl Acad Sci U S A* 106: 7583-7588
- Maier AG, Braks JA, Waters AP, Cowman AF (2006) Negative selection using yeast cytosine deaminase/uracil phosphoribosyl transferase in Plasmodium falciparum for targeted gene deletion by double crossover recombination. *Mol Biochem Parasitol* 150: 118-121
- Maier AG, Cooke BM, Cowman AF, Tilley L (2009) Malaria parasite proteins that remodel the host erythrocyte. *Nat Rev Microbiol* 7: 341-354
- Maier AG, Rug M, O'Neill MT, Brown M, Chakravorty S, Szeszak T, Chesson J, Wu Y, Hughes K, Coppel RL, Newbold C, Beeson JG, Craig A, Crabb BS, Cowman AF (2008) Exported proteins required for virulence and rigidity of Plasmodium falciparum-infected human erythrocytes. *Cell* 134: 48-61
- Malaguarnera L, Musumeci S (2002) The immune response to Plasmodium falciparum malaria. *The Lancet infectious diseases* 2: 472-478
- Mamoun CB, Gluzman IY, Goyard S, Beverley SM, Goldberg DE (1999) A set of independent selectable markers for transfection of the human malaria parasite Plasmodium falciparum. *Proc Natl Acad Sci U S A* 96: 8716-8720
- Marti M, Good RT, Rug M, Knuepfer E, Cowman AF (2004) Targeting malaria virulence and remodeling proteins to the host erythrocyte. *Science* 306: 1930-1933
- Mattei D, Ward GE, Langsley G, Lingelbach K (1999) Novel secretory pathways in Plasmodium? *Parasitol Today* 15: 235-237

## REFERENCES

---

- Matthews K, Kalanon M, Chisholm SA, Sturm A, Goodman CD, Dixon MW, Sanders PR, Nebl T, Fraser F, Haase S, McFadden GI, Gilson PR, Crabb BS, de Koning-Ward TF (2013) The Plasmodium translocon of exported proteins (PTEX) component thioredoxin-2 is important for maintaining normal blood-stage growth. *Mol Microbiol* 89: 1167-1186
- Matz JM, Matuschewski K, Kooij TW (2013) Two putative protein export regulators promote Plasmodium blood stage development in vivo. *Mol Biochem Parasitol* 191: 44-52
- Maurer G (1902) Die malaria perniciosa. *Centralbl f Bakt Abt I Orig* 32: 695-719
- Mbengue A, Yam XY, Braun-Breton C (2012) Human erythrocyte remodelling during Plasmodium falciparum malaria parasite growth and egress. *Br J Haematol* 157: 171-179
- McMillan PJ, Millet C, Batinovic S, Maiorca M, Hanssen E, Kenny S, Muhle RA, Melcher M, Fidock DA, Smith JD, Dixon MW, Tilley L (2013) Spatial and temporal mapping of the PfEMP1 export pathway in Plasmodium falciparum. *Cell Microbiol* 15: 1401-1418
- Mehlhorn H (2012) *Die Parasiten des Menschen: Erkrankungen erkennen, bekämpfen und vorbeugen*, 7. Aufl. edn. Berlin: Springer.
- Mehlhorn H, Piekarski G (2002) *Grundriss der Parasitenkunde: Parasiten des Menschen und der Nutztiere*, 6th edition edn.: Spektrum Akademischer Verlag.
- Ménard R (2013) *Malaria methods and protocols*, 2nd edn. New York, NY: Humana.
- Mendis K, Rietveld A, Warsame M, Bosman A, Greenwood B, Wernsdorfer WH (2009) From malaria control to eradication: The WHO perspective. *Trop Med Int Health* 14: 802-809
- Miao J, Lawrence M, Jeffers V, Zhao F, Parker D, Ge Y, Sullivan WJ, Jr., Cui L (2013) Extensive lysine acetylation occurs in evolutionarily conserved metabolic pathways and parasite-specific functions during Plasmodium falciparum intraerythrocytic development. *Mol Microbiol* 89: 660-675
- Miller LH, Baruch DI, Marsh K, Doumbo OK (2002) The pathogenic basis of malaria. *Nature* 415: 673-679
- Mok BW, Ribacke U, Sherwood E, Wahlgren M (2008) A highly conserved segmental duplication in the subtelomeres of Plasmodium falciparum chromosomes varies in copy number. *Malar J* 7: 46
- Mota MM, Pradel G, Vanderberg JP, Hafalla JC, Frevert U, Nussenzweig RS, Nussenzweig V, Rodriguez A (2001b) Migration of Plasmodium sporozoites through cells before infection. *Science* 291: 141-144

- Mota MM, Rodriguez A (2001a) Migration through host cells by apicomplexan parasites. *Microbes Infect* 3: 1123-1128
- Mullen CA, Kilstrup M, Blaese RM (1992) Transfer of the bacterial gene for cytosine deaminase to mammalian cells confers lethal sensitivity to 5-fluorocytosine: a negative selection system. *Proc Natl Acad Sci U S A* 89: 33-37
- Mullen JR, Kayne PS, Moerschell RP, Tsunasawa S, Gribskov M, Colavito-Shepanski M, Grunstein M, Sherman F, Sternglanz R (1989) Identification and characterization of genes and mutants for an N-terminal acetyltransferase from yeast. *EMBO J* 8: 2067-2075
- Mullis K, Faloona F, Scharf S, Saiki R, Horn G, Erlich H (1986) Specific enzymatic amplification of DNA in vitro: the polymerase chain reaction. *Cold Spring Harb Symp Quant Biol* 51 Pt 1: 263-273
- Mundwiler-Pachlatko E, Beck HP (2013) Maurer's clefts, the enigma of Plasmodium falciparum. *Proc Natl Acad Sci U S A* 110: 19987-19994
- Neelam S, Kakhniashvili DG, Wilkens S, Levene SD, Goodman SR (2011) Functional 20S proteasomes in mature human red blood cells. *Experimental biology and medicine (Maywood, NJ)* 236: 580-591
- Nguitragool W, Bokhari AA, Pillai AD, Rayavara K, Sharma P, Turpin B, Aravind L, Desai SA (2011) Malaria parasite clag3 genes determine channel-mediated nutrient uptake by infected red blood cells. *Cell* 145: 665-677
- Osborne AR, Speicher KD, Tamez PA, Bhattacharjee S, Speicher DW, Haldar K (2010) The host targeting motif in exported Plasmodium proteins is cleaved in the parasite endoplasmic reticulum. *Mol Biochem Parasitol* 171: 25-31
- Pachlatko E, Rusch S, Muller A, Hemphill A, Tilley L, Hanssen E, Beck HP (2010) MAHRP2, an exported protein of Plasmodium falciparum, is an essential component of Maurer's cleft tethers. *Mol Microbiol* 77: 1136-1152
- Parsons M, Karnataki A, Derocher AE (2009) Evolving insights into protein trafficking to the multiple compartments of the apicomplexan plastid. *J Eukaryot Microbiol* 56: 214-220
- Pasini EM, Braks JA, Fonager J, Klop O, Aime E, Spaccapelo R, Otto TD, Berriman M, Hiss JA, Thomas AW, Mann M, Janse CJ, Kocken CH, Franke-Fayard B (2013) Proteomic and genetic analyses demonstrate that Plasmodium berghei blood stages export a large and diverse repertoire of proteins. *Mol Cell Proteomics* 12: 426-448

## REFERENCES

---

- Pasternak ND, Dzikowski R (2009) PfEMP1: an antigen that plays a key role in the pathogenicity and immune evasion of the malaria parasite *Plasmodium falciparum*. *Int J Biochem Cell Biol* 41: 1463-1466
- Polevoda B, Sherman F (2000) Nalpha -terminal acetylation of eukaryotic proteins. *J Biol Chem* 275: 36479-36482
- Ponnudurai T, Leeuwenberg AD, Meuwissen JH (1981) Chloroquine sensitivity of isolates of *Plasmodium falciparum* adapted to in vitro culture. *Trop Geogr Med* 33: 50-54
- Pradeepa MM, Nikhil G, Hari Kishore A, Bharath GN, Kundu TK, Rao MR (2009) Acetylation of transition protein 2 (TP2) by KAT3B (p300) alters its DNA condensation property and interaction with putative histone chaperone NPM3. *J Biol Chem* 284: 29956-29967
- Prommana P, Uthaipibull C, Wongsombat C, Kamchonwongpaisan S, Yuthavong Y, Knuepfer E, Holder AA, Shaw PJ (2013) Inducible knockdown of *Plasmodium* gene expression using the glmS ribozyme. *PLoS One* 8: e73783
- Przyborski JM, Miller SK, Pfahler JM, Henrich PP, Rohrbach P, Crabb BS, Lanzer M (2005) Trafficking of STEVOR to the Maurer's clefts in *Plasmodium falciparum*-infected erythrocytes. *EMBO J* 24: 2306-2317
- Quevillon E, Silventoinen V, Pillai S, Harte N, Mulder N, Apweiler R, Lopez R (2005) InterProScan: protein domains identifier. *Nucleic Acids Res* 33: W116-120
- Ramasamy R (1998) Molecular basis for evasion of host immunity and pathogenesis in malaria. *Biochim Biophys Acta* 1406: 10-27
- Ramasamy R, Surendran SN (2012) Global climate change and its potential impact on disease transmission by salinity-tolerant mosquito vectors in coastal zones. *Frontiers in physiology* 3: 198
- Rath A, Glibowicka M, Nadeau VG, Chen G, Deber CM (2009) Detergent binding explains anomalous SDS-PAGE migration of membrane proteins. *Proc Natl Acad Sci U S A* 106: 1760-1765
- Ravindran S, Boothroyd JC (2008) Secretion of proteins into host cells by Apicomplexan parasites. *Traffic* 9: 647-656
- Retief F, Cilliers L (2006) Periodic pyrexia and malaria in antiquity. *S Afr Med J* 96: 684, 686-688
- Ribaut C, Berry A, Chevalley S, Reybier K, Morlais I, Parzy D, Nepveu F, Benoit-Vical F, Valentin A (2008) Concentration and purification by magnetic separation of the erythrocytic stages of all human *Plasmodium* species. *Malaria Journal* 7: 45

- Riglar DT, Rogers KL, Hanssen E, Turnbull L, Bullen HE, Charnaud SC, Przyborski J, Gilson PR, Whitchurch CB, Crabb BS, Baum J, Cowman AF (2013) Spatial association with PTEX complexes defines regions for effector export into *Plasmodium falciparum*-infected erythrocytes. *Nat Commun* 4: 1415
- Risch S (2009) Protein export in *Plasmodium falciparum*: Analysis of two important exported proteins by site-directed mutagenesis and conditional aggregation. Diploma Thesis, Parasitology, University of Heidelberg,
- Rivera VM, Wang X, Wardwell S, Courage NL, Volchuk A, Keenan T, Holt DA, Gilman M, Orci L, Cerasoli F, Jr., Rothman JE, Clackson T (2000) Regulation of protein secretion through controlled aggregation in the endoplasmic reticulum. *Science* 287: 826-830
- Römisch K (2012) Diversion at the ER: How *Plasmodium falciparum* exports proteins into host erythrocytes [v2; ref status: indexed, <http://f1000r.es/VOUzka>]. *F1000 Research* 1
- Rosario V (1981) Cloning of naturally occurring mixed infections of malaria parasites. *Science* 212: 1037-1038
- Rug M, Prescott SW, Fernandez KM, Cooke BM, Cowman AF (2006) The role of KAHRP domains in knob formation and cytoadherence of *P falciparum*-infected human erythrocytes. *Blood* 108: 370-378
- Russo I, Babbitt S, Muralidharan V, Butler T, Oksman A, Goldberg DE (2010) Plasmepsin V licenses *Plasmodium* proteins for export into the host erythrocyte. *Nature* 463: 632-636
- Russo I, Oksman A, Vaupel B, Goldberg DE (2009) A calpain unique to alveolates is essential in *Plasmodium falciparum* and its knockdown reveals an involvement in pre-S-phase development. *Proc Natl Acad Sci U S A* 106: 1554-1559
- Sachs J, Malaney P (2002) The economic and social burden of malaria. *Nature* 415: 680-685
- Saiki RK, Scharf S, Faloona F, Mullis KB, Horn GT, Erlich HA, Arnheim N (1985) Enzymatic amplification of beta-globin genomic sequences and restriction site analysis for diagnosis of sickle cell anemia. *Science* 230: 1350-1354
- Saliba KJ, Kirk K (2001) Nutrient acquisition by intracellular apicomplexan parasites: staying in for dinner. *Int J Parasitol* 31: 1321-1330
- Salvador A, Hernandez RM, Pedraz JL, Igartua M (2012) *Plasmodium falciparum* malaria vaccines: current status, pitfalls and future directions. *Expert Rev Vaccines* 11: 1071-1086

## REFERENCES

---

- Sam-Yellowe TY (2009) The role of the Maurer's clefts in protein transport in *Plasmodium falciparum*. *Trends Parasitol* 25: 277-284
- Sambrook J, Fritsch, E.F., Maniatis, T. (ed) (2001) *Molecular cloning: a laboratory manual*: Cold Spring Harbour Laboratory Press, Cold Spring Harbour, New York
- Sanchez CP, McLean JE, Rohrbach P, Fidock DA, Stein WD, Lanzer M (2005) Evidence for a pfCRT-associated chloroquine efflux system in the human malarial parasite *Plasmodium falciparum*. *Biochemistry* 44: 9862-9870
- Sanyal S, Egee S, Bouyer G, Perrot S, Safeukui I, Bischoff E, Buffet P, Deitsch KW, Mercereau-Puijalon O, David PH, Templeton TJ, Lavazec C (2012) *Plasmodium falciparum* STEVOR proteins impact erythrocyte mechanical properties. *Blood* 119: e1-8
- Sargeant TJ, Marti M, Caler E, Carlton JM, Simpson K, Speed TP, Cowman AF (2006) Lineage-specific expansion of proteins exported to erythrocytes in malaria parasites. *Genome Biol* 7: R12
- Saridaki T. (2008) Protein export in *P. falciparum*-infected erythrocytes: Sorting signals and a conditional protein export system. Heidelberg, p. 126.
- Saridaki T, Frohlich KS, Breton CB, Lanzer M (2009) Export of PfSBP1 to the *Plasmodium falciparum* Maurer's clefts. *Traffic*
- Saridaki T, Sanchez CP, Pfahler J, Lanzer M (2008) A conditional export system provides new insights into protein export in *Plasmodium falciparum*-infected erythrocytes. *Cell Microbiol* 10: 2483-2495
- Schechter I, Berger A (1967) On the size of the active site in proteases. I. Papain. *Biochem Biophys Res Commun* 27: 157-162
- Scherf A, Hernandez-Rivas R, Buffet P, Bottius E, Benatar C, Pouvelle B, Gysin J, Lanzer M (1998) Antigenic variation in malaria: in situ switching, relaxed and mutually exclusive transcription of var genes during intra-erythrocytic development in *Plasmodium falciparum*. *EMBO J* 17: 5418-5426
- Schindelin J, Arganda-Carreras I, Frise E, Kaynig V, Longair M, Pietzsch T, Preibisch S, Rueden C, Saalfeld S, Schmid B, Tinevez JY, White DJ, Hartenstein V, Eliceiri K, Tomancak P, Cardona A (2012) Fiji: an open-source platform for biological-image analysis. *Nat Methods* 9: 676-682
- Schmitz S, Grainger M, Howell S, Calder LJ, Gaeb M, Pinder JC, Holder AA, Veigel C (2005) Malaria parasite actin filaments are very short. *J Mol Biol* 349: 113-125
- Schoeber JP, van de Graaf SF, Lee KP, Wittgen HG, Hoenderop JG, Bindels RJ (2009) Conditional fast expression and function of multimeric TRPV5 channels using Shield-1. *Am J Physiol Renal Physiol* 296: F204-211

- Scholzen A, Minigo G, Plebanski M (2010) Heroes or villains? T regulatory cells in malaria infection. *Trends Parasitol* 26: 16-25
- Schultz J, Milpetz F, Bork P, Ponting CP (1998) SMART, a simple modular architecture research tool: identification of signaling domains. *Proc Natl Acad Sci U S A* 95: 5857-5864
- Scott DC, Monda JK, Bennett EJ, Harper JW, Schulman BA (2011) N-terminal acetylation acts as an avidity enhancer within an interconnected multiprotein complex. *Science* 334: 674-678
- Shemorry A, Hwang CS, Varshavsky A (2013) Control of protein quality and stoichiometries by N-terminal acetylation and the N-end rule pathway. *Mol Cell* 50: 540-551
- Sherman IW (2005) *Molecular approaches to malaria*, Washington, D.C.: ASM Press.
- Shi Y, Mowery RA, Ashley J, Hentz M, Ramirez AJ, Bilgicer B, Slunt-Brown H, Borchelt DR, Shaw BF (2012) Abnormal SDS-PAGE migration of cytosolic proteins can identify domains and mechanisms that control surfactant binding. *Protein Sci* 21: 1197-1209
- Shio MT, Kassa FA, Bellemare MJ, Olivier M (2010) Innate inflammatory response to the malarial pigment hemozoin. *Microbes Infect* 12: 889-899
- Shonhai A, Boshoff A, Blatch GL (2007) The structural and functional diversity of Hsp70 proteins from *Plasmodium falciparum*. *Protein Sci* 16: 1803-1818
- Siddiqui WA, Kan SC, Kramer K, Richmond-Crum SM (1979) In vitro production and partial purification of *Plasmodium falciparum* antigen. *Bull World Health Organ* 57 Suppl 1: 75-82
- Sijwali PS, Rosenthal PJ (2010) Functional evaluation of *Plasmodium* export signals in *Plasmodium berghei* suggests multiple modes of protein export. *PLoS ONE* 5: e10227
- Silvestrini F, Lasonder E, Olivieri A, Camarda G, van Schaijk B, Sanchez M, Younis Younis S, Sauerwein R, Alano P (2010) Protein export marks the early phase of gametocytogenesis of the human malaria parasite *Plasmodium falciparum*. *Mol Cell Proteomics* 9: 1437-1448
- Singh AP, Buscaglia CA, Wang Q, Levay A, Nussenzweig DR, Walker JR, Winzeler EA, Fujii H, Fontoura BM, Nussenzweig V (2007) *Plasmodium* circumsporozoite protein promotes the development of the liver stages of the parasite. *Cell* 131: 492-504

## REFERENCES

---

- Slavic K, Straschil U, Reininger L, Doerig C, Morin C, Tewari R, Krishna S (2010) Life cycle studies of the hexose transporter of Plasmodium species and genetic validation of their essentiality. *Mol Microbiol* 75: 1402-1413
- Smilkstein M, Sriwilaijaroen N, Kelly JX, Wilairat P, Riscoe M (2004) Simple and inexpensive fluorescence-based technique for high-throughput antimalarial drug screening. *Antimicrob Agents Chemother* 48: 1803-1806
- Spielmann T, Gilberger TW (2010) Protein export in malaria parasites: do multiple export motifs add up to multiple export pathways? *Trends Parasitol* 26: 6-10
- Spielmann T, Hawthorne PL, Dixon MW, Hannemann M, Klotz K, Kemp DJ, Klonis N, Tilley L, Trenholme KR, Gardiner DL (2006) A cluster of ring stage-specific genes linked to a locus implicated in cytoadherence in Plasmodium falciparum codes for PEXEL-negative and PEXEL-positive proteins exported into the host cell. *Mol Biol Cell* 17: 3613-3624
- Staalsoe T, Giha HA, Dodoo D, Theander TG, Hviid L (1999) Detection of antibodies to variant antigens on Plasmodium falciparum-infected erythrocytes by flow cytometry. *Cytometry* 35: 329-336
- Starheim KK, Gevaert K, Arnesen T (2012) Protein N-terminal acetyltransferases: when the start matters. *Trends Biochem Sci* 37: 152-161
- Stich A, Fischer K, Lanzer M (2000) Eine Seuche auf dem Vormarsch Die Überlebensstrategie des Malariaerregers. *Biologie in unserer Zeit* 30: 194-201
- Struck NS, de Souza Dias S, Langer C, Marti M, Pearce JA, Cowman AF, Gilberger TW (2005) Re-defining the Golgi complex in Plasmodium falciparum using the novel Golgi marker PfGRASP. *J Cell Sci* 118: 5603-5613
- Struck NS, Herrmann S, Schmuck-Barkmann I, de Souza Dias S, Haase S, Cabrera AL, Treeck M, Bruns C, Langer C, Cowman AF, Marti M, Spielmann T, Gilberger TW (2008) Spatial dissection of the cis- and trans-Golgi compartments in the malaria parasite Plasmodium falciparum. *Mol Microbiol* 67: 1320-1330
- Sturm A, Amino R, van de Sand C, Regen T, Retzlaff S, Rennenberg A, Krueger A, Pollok JM, Menard R, Heussler VT (2006) Manipulation of host hepatocytes by the malaria parasite for delivery into liver sinusoids. *Science* 313: 1287-1290
- Summers RL, Dave A, Dolstra TJ, Bellanca S, Marchetti RV, Nash MN, Richards SN, Goh V, Schenk RL, Stein WD, Kirk K, Sanchez CP, Lanzer M, Martin RE (2014) Diverse mutational pathways converge on saturable chloroquine transport via the malaria parasite's chloroquine resistance transporter. *Proc Natl Acad Sci U S A*
- Sutherland C (2007) A challenge for the development of malaria vaccines: polymorphic target antigens. *PLoS Med* 4: e116

- Tamez PA, Bhattacharjee S, van Ooij C, Hiller NL, Llinas M, Balu B, Adams JH, Haldar K (2008) An erythrocyte vesicle protein exported by the malaria parasite promotes tubovesicular lipid import from the host cell surface. *PLoS Pathog* 4: e1000118
- Tarr SJ, Cryar A, Thalassinos K, Haldar K, Osborne AR (2013) The C-terminal portion of the cleaved HT motif is necessary and sufficient to mediate export of proteins from the malaria parasite into its host cell. *Mol Microbiol* 87: 835-850
- Thorpe GH, Kricka LJ (1986) Enhanced chemiluminescent reactions catalyzed by horseradish peroxidase. *Methods Enzymol* 133: 331-353
- Tilley L, Sougrat R, Lithgow T, Hanssen E (2008) The twists and turns of Maurer's cleft trafficking in *P. falciparum*-infected erythrocytes. *Traffic* 9: 187-197
- Toleman C, Paterson AJ, Whisenhunt TR, Kudlow JE (2004) Characterization of the histone acetyltransferase (HAT) domain of a bifunctional protein with activable O-GlcNAcase and HAT activities. *J Biol Chem* 279: 53665-53673
- Tonkin CJ, Kalanon M, McFadden GI (2008) Protein targeting to the malaria parasite plastid. *Traffic* 9: 166-175
- Tonkin CJ, Pearce JA, McFadden GI, Cowman AF (2006a) Protein targeting to destinations of the secretory pathway in the malaria parasite *Plasmodium falciparum*. *Curr Opin Microbiol* 9: 381-387
- Tonkin CJ, Struck NS, Mullin KA, Stimmler LM, McFadden GI (2006b) Evidence for Golgi-independent transport from the early secretory pathway to the plastid in malaria parasites. *Mol Microbiol* 61: 614-630
- Trager W, Jensen JB (1976) Human malaria parasites in continuous culture. *Science* 193: 673-675
- Trager W, Jensen JB (2005) Human malaria parasites in continuous culture. 1976. *J Parasitol* 91: 484-486
- Turschner S, Efferth T (2009) Drug resistance in *Plasmodium*: natural products in the fight against malaria. *Mini Rev Med Chem* 9: 206-2124
- Tuteja R (2007) Malaria - an overview. *FEBS J* 274: 4670-4679
- Uhlemann ACS, T.; Klinkert, M.; Hviid, L. (2000) Analysis of *Plasmodium falciparum*-infected red blood cells. *MACS and more* 4: 7-8
- van Agtmael MA, Eggelte TA, van Boxtel CJ (1999) Artemisinin drugs in the treatment of malaria: from medicinal herb to registered medication. *Trends Pharmacol Sci* 20: 199-205

## REFERENCES

---

- Van Damme P, Arnesen T, Gevaert K (2011a) Protein alpha-N-acetylation studied by N-terminomics. *FEBS J* 278: 3822-3834
- Van Damme P, Evjenth R, Foyen H, Demeyer K, De Bock PJ, Lillehaug JR, Vandekerckhove J, Arnesen T, Gevaert K (2011b) Proteome-derived peptide libraries allow detailed analysis of the substrate specificities of N(alpha)-acetyltransferases and point to hNaa10p as the post-translational actin N(alpha)-acetyltransferase. *Mol Cell Proteomics* 10: M110 004580
- van Dooren GG, Marti M, Tonkin CJ, Stimmler LM, Cowman AF, McFadden GI (2005) Development of the endoplasmic reticulum, mitochondrion and apicoplast during the asexual life cycle of *Plasmodium falciparum*. *Molecular Microbiology* 57: 405-419
- van Ooij C, Tamez P, Bhattacharjee S, Hiller NL, Harrison T, Liolios K, Kooij T, Ramesar J, Balu B, Adams J, Waters A, Janse C, Haldar K (2008) The malaria secretome: from algorithms to essential function in blood stage infection. *PLoS Pathog* 4: e1000084
- Vaughan AM, Mikolajczak SA, Wilson EM, Grompe M, Kaushansky A, Camargo N, Bial J, Ploss A, Kappe SH (2012) Complete *Plasmodium falciparum* liver-stage development in liver-chimeric mice. *J Clin Invest* 122: 3618-3628
- Vetting MW, LP SdC, Yu M, Hegde SS, Magnet S, Roderick SL, Blanchard JS (2005) Structure and functions of the GNAT superfamily of acetyltransferases. *Arch Biochem Biophys* 433: 212-226
- Wagner CR, Benkovic SJ (1990) Site directed mutagenesis: a tool for enzyme mechanism dissection. *Trends Biotechnol* 8: 263-270
- Walliker D, Quakyi IA, Wellems TE, McCutchan TF, Szarfman A, London WT, Corcoran LM, Burkot TR, Carter R (1987) Genetic analysis of the human malaria parasite *Plasmodium falciparum*. *Science* 236: 1661-1666
- Wang L, Mizzen C, Ying C, Candau R, Barlev N, Brownell J, Allis CD, Berger SL (1997) Histone acetyltransferase activity is conserved between yeast and human GCN5 and is required for complementation of growth and transcriptional activation. *Mol Cell Biol* 17: 519-527
- Wang Z, Obidike JE, Schey KL (2010) Posttranslational modifications of the bovine lens beaded filament proteins filensin and CP49. *Investigative ophthalmology & visual science* 51: 1565-1574
- Whisson SC, Boevink PC, Moleleki L, Avrova AO, Morales JG, Gilroy EM, Armstrong MR, Grouffaud S, van West P, Chapman S, Hein I, Toth IK, Pritchard L, Birch PR (2007) A translocation signal for delivery of oomycete effector proteins into host plant cells. *Nature* 450: 115-118

- White NJ, Pukrittayakamee S, Hien TT, Faiz MA, Mokuolu OA, Dondorp AM (2014) Malaria. *Lancet* 383: 723-735
- WHO (1999) World Health Report. <http://www.who.int/whr/1999/en/index.html>
- WHO (2009) World Health Statistics.  
<http://www.who.int/whosis/whostat/2009/en/index.html>
- WHO (2011) The 10 leading causes of death by income group.  
<http://www.who.int/mediacentre/factsheets/fs310/en/index1.html>
- WHO (2012) World Malaria Report.  
[http://www.who.int/malaria/publications/world\\_malaria\\_report\\_2012/report/en/](http://www.who.int/malaria/publications/world_malaria_report_2012/report/en/)
- WHO (2013) World Malaria Report 2013.  
[http://www.who.int/malaria/publications/world\\_malaria\\_report\\_2013/en/](http://www.who.int/malaria/publications/world_malaria_report_2013/en/)
- Wickert H, Krohne G (2007) The complex morphology of Maurer's clefts: from discovery to three-dimensional reconstructions. *Trends Parasitol* 23: 502-509
- Wickert H, Wissing F, Andrews KT, Stich A, Krohne G, Lanzer M (2003) Evidence for trafficking of PfEMP1 to the surface of *P. falciparum*-infected erythrocytes via a complex membrane network. *Eur J Cell Biol* 82: 271-284
- Wiser MF, Lanners HN (1992) Rapid transport of the acidic phosphoproteins of *Plasmodium berghei* and *P. chabaudi* from the intraerythrocytic parasite to the host membrane using a miniaturized fractionation procedure. *Parasitol Res* 78: 193-200
- Witola WH, El Bissati K, Pessi G, Xie C, Roepe PD, Mamoun CB (2008) Disruption of the *Plasmodium falciparum* PfPMT gene results in a complete loss of phosphatidylcholine biosynthesis via the serine-decarboxylase-phosphoethanolamine-methyltransferase pathway and severe growth and survival defects. *J Biol Chem* 283: 27636-27643
- Wrenger C, Muller S (2004) The human malaria parasite *Plasmodium falciparum* has distinct organelle-specific lipoylation pathways. *Mol Microbiol* 53: 103-113
- Wu Y, Sifri CD, Lei HH, Su XZ, Wellem TE (1995) Transfection of *Plasmodium falciparum* within human red blood cells. *Proc Natl Acad Sci U S A* 92: 973-977
- Yamauchi LM, Coppi A, Snounou G, Sinnis P (2007) *Plasmodium* sporozoites trickle out of the injection site. *Cell Microbiol* 9: 1215-1222
- Yap A, Azevedo MF, Gilson PR, Weiss GE, O'Neill MT, Wilson DW, Crabb BS, Cowman AF (2014) Conditional expression of apical membrane antigen 1 in

## REFERENCES

---

*Plasmodium falciparum* shows it is required for erythrocyte invasion by merozoites. *Cell Microbiol*

Yazdani SS, Mukherjee P, Chauhan VS, Chitnis CE (2006) Immune responses to asexual blood-stages of malaria parasites. *Current molecular medicine* 6: 187-203

Zybailov B, Rutschow H, Friso G, Rudella A, Emanuelsson O, Sun Q, van Wijk KJ (2008) Sorting signals, N-terminal modifications and abundance of the chloroplast proteome. *PLoS One* 3: e1994

## 7 Appendix

### Vector maps

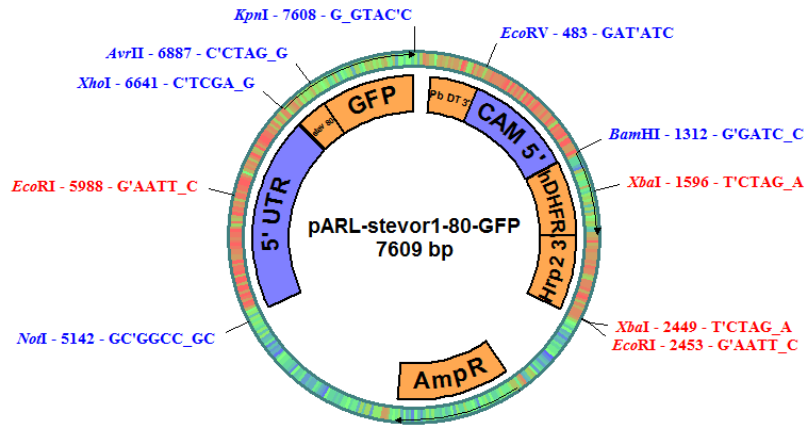


Figure 33. pARL-STEVROR<sup>1-80</sup>-GFP (original vector by T. Gilberger)

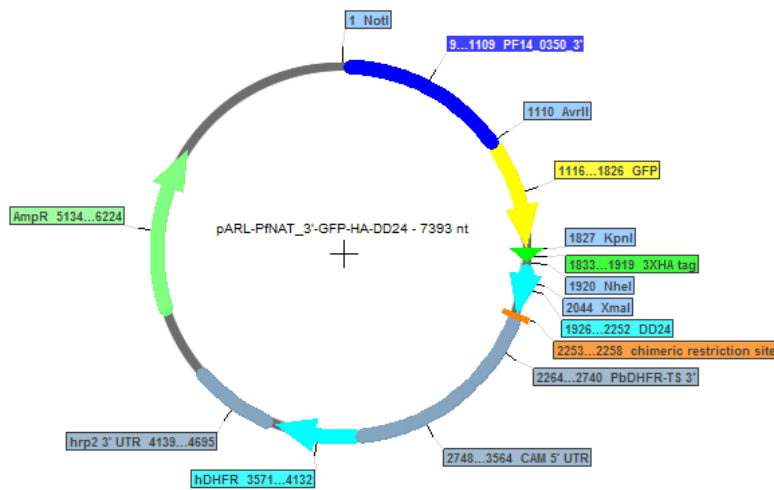


Figure 34. pARL-PfNAT-3'-GFPHADD24 (HADD24 tag provided by M. Azevedo)

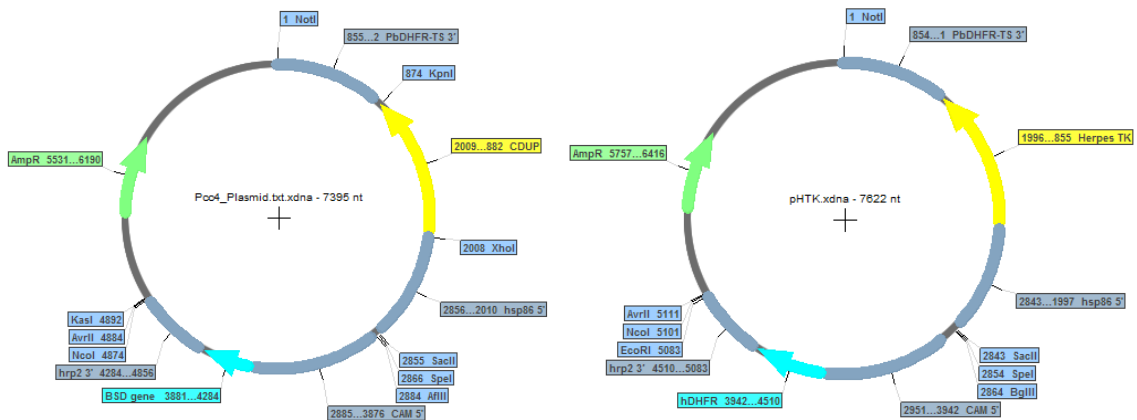


Figure 35. pCC and pHTK vector systems (provided by A. Maier & N. Hertrich),

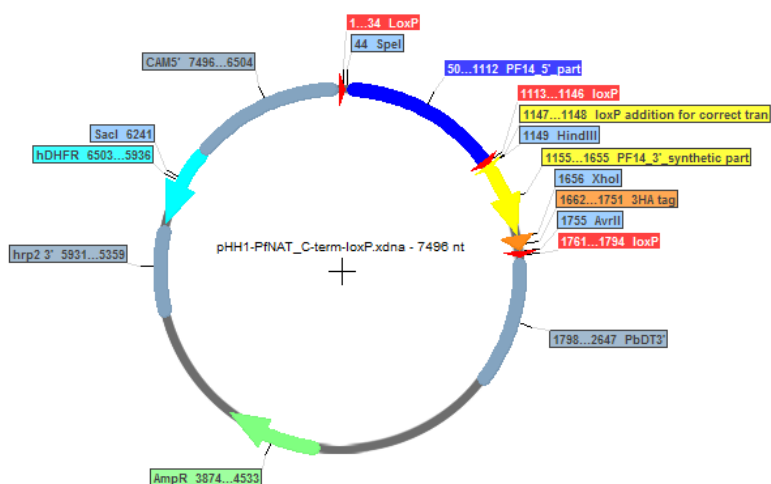


Figure 36. pHH1-PfNAT\_C-term-loxP (provided by M. Blackman)

### Sequences

Lower cases represent introns in genomic DNA, brackets contain new and old gene IDs.

#### STEVOR (PF3D7\_0631900, PFF1550w)

ATGAAGATGTATTACCTTAAATGTTATGTTTAACTTTTAAATAAATGTTTATGATTACCACATTATgtatgtaaaaa  
 aaaaaatacataattattagaataatataaatatacataataaaagaattattatattttgagtacgcatttattaata  
 atcgttttttttttctagGAAAATTATCAAATAACCATTATAACATAAAGGCTCATAACAAATAACACATACAGAATA  
 ACGATAAAATCAAGACTCTTAGCACAAACCCAAATCCATAATCCACATTATCATAATGATCCAGAACTCAAAGAAATAAT  
 TGATAAATGAACGAAGACGCAATAAAGAAATACCAACAACTCATGATCCATATGAACAATTACAAGAAGTAGTAGAAA  
 AAAATGGAACAAAATATAAAGGTGGTAATGATGCAGAACCTATGTCAACGCTAGAAAAAGAATTATTGCAACATATGAA  
 GAAGTGTGGTAACGAAAGTGATATGTTGAAGTCGGGAATGAATACAAATGTTGATGAAAAATCTTCAACATGTGGATG  
 TACTGATATTAATGGTGTGAAATTAGCAAAAACAAAGGAAGAGATAAGTATTTAAAACACTTAAAACATAGATGTACCC  
 GTGGTATATGTTTTGCTCAGTTGGTAGTGCATTGTTAACTATGTTCCGGTTTGGCAGTTGCAAAAAAAGCTGCCGTTGAT  
 GCCATCCTCCTGTATATGTAGCAGCGATTAAAAAGTGTGTATCCTCCAGTTCATTATTTTATATATTTTATGTTGGTTC  
 ATTAACACAGCTCTTAAAGCAACCGAAGCGTGTGCAAGTGTGCAAGTCCAGATATAGTCATACCTGCTACAGGTGCTG  
 CTATAGGTGCATTTCCCCTTATGGTATTGCAGCTTTAGTACTACTTATATAGCTGTTCTACTTATAATATATACATA  
 TGTTATATAGAAGAAGAAAAATTCATGAAACATGAATGCAAGAAACATTTATGTAAGTAA

1023 bp

#### KAHRP (PF3D7\_0202000, PF02\_0020)

ATGAAAAGTTTTAAGAACAAAATACTTTGAGGAGAAAGAAGGCTTTCCTGTTTTTACTAAAATTCTTTTAGTCTCTTT  
 TTTAGTATGGGTTTTGAAGTGCTCTAATAACgtaagttcataaataatataatataatataatataatataatataat  
 atgtgtattttataactttgacatatgtgtatattccttatttttttaccataatattttatataatatttatataatta  
 gtttatttgaacaatatttactccatataatttttcatataatataatataatataatataatataatataatataatataat  
 tatgaaatataatattatataatatttttcttatttttatttttatttttatttttatttttatttttatttttatttttatt  
 ttttttatttttatttttatttttatttttatttttatttttatttttatttttatttttatttttatttttatttttatttttatt  
 ttatttttatttttatttttatttttatttttatttttatttttatttttatttttatttttatttttatttttatttttatttttatt  
 CAATAATGGAACGGATCCGGTGACTCCTTCGATTTAGAAAATAAGAGAACTTTAGCACAAAAGCAACATGAACACCATC  
 ACCACCATCACCATCAACATCAACACCAACACCAAGCTCCACACCAAGCACACCACCATCATCATGAGGAGAAGTAAAT  
 CACCAAGCACACAGGTTACCAACAAGTACATGGTCAAGACCAAGCACACCATCACCATCATCACCACCATCATCAATT  
 ACAACCTCAACAACCCAGGGAACAGTTGCTAATCCTCCTAGTAATGAACAGTTGTA AAAACCCAAGTATTCAGGGAAG  
 CAAGACCAGGTGGAGGTTTCAAAGCATATGAAGAAAAATACGAATCAAAACACTATAAAATTAAGGAAAAATGTTGTCGAT  
 GGTAAAAAAGATTGTGATGAAAAATACGAAGCTGCCAATTATGCTTTCTCCGAAGAGTGCCCATACACCGTAAACGATTA  
 TAGCCAAGAAAATGGTCCAAATATATTTGCCCTAAGAAAAAGATTCCCTCTTGGAAATGAATGATGAAGATGAAGAAGGTA  
 AAGAAGCATTAGCAATAAAAGATAAAATTACCAGGTGGTTTAGATGAATACCAAAACCAATTATATGGAATATGTAATGAG



## APPENDIX

tatttttcagCATAAAATTATTATGGGCACCTATAGTTGATTTCGGTATATAATAAAAGAATTGGAAGGAGGAAAAGTTGG  
ATAATACCACTACAGgttgatttataatctaatcatttgcattatgaaatagatgtctcaaatggcgtatacatat  
aattattactatttggatatacgaattatttatactatattaatttttttatttatttggtaattttttttttttttttt  
tttatttttagCTATTTTGCAGTTTTACGATGATATATTTTAGTAATCATGTCAGTATTTGGTTAGGAGAAAAAGACAATA  
TTCCGAACCTATTTTTCTAACACTTTTTTCTTCTCTTTTTTCTAATGGCTACACAAGATATTGCCGTGGACGGG  
TGGGCTTTAACCATGCTTCTGAAGAAAAATAAAAgtaaaaatggactaacaccacattgaaatataaatatacacaattt  
ggatataaccattatataatataatgcttattatataattatataatataatataatataatataatataatataatata  
cgttatcataatttattgatttatttataattttttttagAGCGGCTTCTACGTGCAATATACTGGGACAAAACATAGGATA  
TTGCTTATCGCAATTATCCTTTTTAACATTAATAACAAAAACATATGCTTCTATATATTCAAAAAATATATTAAGTTTA  
TGTATTTAATATTCAATAAAATCAACATATTATAGAAATGTCTATGAAAAGTTGGATCTTTTGTACCCATCATTTCAACCA  
TTTGTGATATGAAAAAGTTTTTAAAAATCTGGGGGACATTTATACTAATGCTTACTATATTTACCTGTTTTAAGAAAGA  
GATGTCAGATCAAAATGAAGAAAAATAAAATTAATAAAATAGTAATGAAATGGATAATTATAATATTTCAGAAGCACAAA  
AGTGTGACGATAAAATGAATAACGCAAAAATGAATTATCCTAAAAATAAAATAACCAAAATAAGAACAAATGAACATATA  
AAAATAAATGATATAAAAACAAACCAATATTCAAAAACAATCTAGTGAATAAAACGAATTTGCAAATGCAAAAAGATACCTA  
TAAAACATTTGTACGAATTATTATTTCTACCCCAATGAAAATATTTATTTATTTTATTCTTAATTAACCGTTTGCCATTTG  
CTTCTGTAGAGGTAGGAACAAAATTTTAAAAATGTTAAAAAGAGGGATAACTAAAGAGGAATTTGCTATATTTAATCCACTG  
TATATACCTGTATCAATTATATCCCCAGCTATTATTGGGAAAAATTATACAAAAATTGAAGCCACTGGATGTTTATTATTT  
TGGATATGTATTAAGATATTTTCTAATATATTTTATCTACCTTACTACCTATAACCAATATATGTATTCAAAATAAAA  
CACAAAGTACAAATATGAAATTTTATTTTATTATATGTATATATATATGGCACAAGTGTTAATCATTTCATTCGAT  
TTAATGACTGTCTCATCGtaaatcatataaaaatacaaaaataaaagaaataaatattataatgtgtaaatataattcacatc  
tataattttaaaatagtttgtacaacatggtaaaatattctgatataataattatataatataatataatataatataatgat  
gcatttctttttatggttagATGAGTTTTCAAAATATAATATCAGACCCTAAAATAGGAGGGACATATATGACCTTTTTTA  
AATACTGTGAATAATTTGGGCTCACACGtaatttgataataacgtacatatataatataatataatataatataatataatata  
aaatataaaatataatagtatataattattattttgatataataactaacttatttggttatatctttcgacaatatttc  
tttttctcttttcttcttagTGGTCTACTATATTTTTATGTTTACTTGTATTACACTGATAAGGAATTTTGTATAAAGgt  
atataatgatttttctatttttagttatataatataatataatataatctttattttaaataacaattatttggttctacagGAA  
AATGTGTTCTTGTGATGGATTTTATATTCAGATGATATGTCTTTTATAGTTGGAATAATAATTAACAAATATATTCTA  
AGTTTTACGAGAAAGCTACAgtaaaaatgaatctataattattattatagattatataatataatataatataatataatata  
tatataatataatataatataatgtgtatataacctgaaaaattatagttcgccgtatttcatatattctcttttttttt  
tttttttttttttttttttttatagGCTTTTCTTTTAGAAGATTGGAGAACGAAATATATTGGAAAAGAATTTTAA  
2955 bp

### PfPMV (PF3D7\_1323500, PF13\_0133)

ATGAATAATTATTTTTTAAGGAAAGAAAATTTTTTATATGTTTTGTTTTGTTTTGTGAGTATCTTTTTGTATCAAA  
TGTAACAATAATAAAATGTAATAATGTGAAAATAAAATGACAATGTTGAAAAAAAATGAAAATGTGGAAAAAAA  
TTGGCGATATGAAAATAAAATGACAATGTGAAAATAAAATGACAATGTGGGAAATAAAATGACAATGTAATAAAAT  
GCTTCTCAGATTTGTATAAATAAATAATATATGGTGATATAGATGAATATGCTTATTATTTCTAGATATAGATATAGG  
GAAACCATCGCAAAGAATTTCTTTAATCTAGATACAGTTTCATCTTCGTAAAGTTTCCCGTGAATGGTTGTAAAGATT  
GTGGTATTCATATGAAAAACCATATAACTTGAATTATCAAAAACATCATCTATTTTATATTGTAATAAATCCAATTGT  
CCTTATGTTTTAAATGTGTAGGAAATAAATGTGAATATCTTCAATCGTATTGTGAAGGGTCTCAAATATATGGTTTTTA  
TTTTTCAGATATTGTTACTTTACCATCTTATAAATAAAAAATAAAATATCTTTTGAAAAATTAATGGGCTGTCATATGC  
ATGAAGAAAGTTTATTTCTACATCAACAGCCACAGGAGTTCTAGGGTTTAGTTTTGACCAACCGAATGGGGTTCCAACA  
TTTGTGATTTACTTTTTAAACATACTCCTTCTTTAAACCCATATATTCAATATGTGTGTCTGAGCATGGAGGTGAATT  
AATCATAGGTGGTTATGAACCGGATTACTTCTTAAGTAATCAAAAAGAGAAAACAAAAATGGACAAGTCAGATAATAATA  
GTAGTAACAAAGGAAACGTTTCTATAAAAATAAAAAATAATGATAAAAATGATGATGAGGAAAAATAATTCAAAAGATGTA  
ATTGTATCTAATAATGTTGAAGATATTGTGTGGCAAGCTATTACAAGAAAAATTTACTATTACATAAAAAATATATGGTTT  
AGATTTATATGGTACAAACATTATGGATAAAAAAGAATTAGATATGTTAGTAGATTACAGGTAGTACATTTACACATATTC  
CAGAAAATATTTATAACCAAAATAAATTTATTTAGATATTTTATGTATACATGATATGACTAATATATATGAAAATAAAT  
AAAAGATTTAAATTAACAAACGAGTCATTAATAAACCATTAGTATATTTTGAAGATTTTAAACAGCATTAAAAAATAT  
TATTCAAAACGAAAATTTATGTATTAAAAATAGTTGATGGAGTACAATGTTGGAAAAGTTTAGAAAACCTACCAAAATTTAT  
ATATTACCTTGTGCAATAATTATAAAAATGATATGGAACCTAGTTCCATCTATATAAAAAAGGAAAGCTTCTGGTGTAAA  
GGTTTAGAAAACAAGTTAATAATAAACCTATTTTAGGGTTAACCTTTTTTAAAAATAACAAGTTATTTTTGATTTACA  
ACAAAATCAAAATGCATTTATAGAATCTAAATGCCATCTAATTTAACATCATCAAGACCAAGAACCTTTAATGAATATA  
GAGAAAAGAAAATATCTTCTTAAAAGTTCTTATATTAATTTATATTGTTTATGGCTATTATTGGCCTTAACCATACTC  
TTATCTCTTATTCTTTATGTCAGAAAAATGTTTTACATGGATTATTTTCTTTGAGTGATCAAAAATAAATCTCCCATACA  
GGAATCAACATAG 1773 bp

DD24 tag

ATGGGAGTGCAGGTGGAAACCATCTCCCCAGGAGACGGGGCGCACCTTCCCCAAGCGCGGCCAGACCTGCGTGGTGCACTA  
 CACCGGGATGCTTGGAGATGGAAAAGAAAGTTGACTCCTCCCGGGACAGAAACAAGCCCTTTAAGTTTATGCTAGGCAAGC  
 AGGAGGTGATCCGAGGCTGGGAAGAAGGGTTGCCAGATGAGTGTGGGTGAGGAGCCAAACTGACTATATCTCCAGAT  
 TATGCCTATGGTGCCACTGGGCACCCAGGCATCATCCACCACATGCCACTCTCGTCTTCGATGTGGAGCTTCTAGAACT  
 GGAATAA

327 bp

loxP

ATAACTTCGTATAGCATAACATTATACGAAGTTAT

34 bp

GFP tag

ATGAGTAAAGGAGAAGAAGTCTTCACTGGAGTTGTCCCAATTCTTGTGAATTAGATGGTGATGTTAATGGGCACAAATT  
 TTCTGTGTCAGTGGAGAGGGTGAAGGTGATGCAACATACGGAAACTTACCCTTAAATTTATTTGCACTACTGGAAAACCTAC  
 CTGTTCCATGGCCAACACTTGTCACTACTTTCGCGTATGGTCTTCAATGCTTTGCGAGATACCCAGATCATATGAAAACAG  
 CATGACTTTTTCAAGAGTGCATGCCATGCCCCGAAGGTTATGTACAGGAAAGAACTATAATTTTTCAAAGATGACGGGAACATA  
 GACACGTGCTGAAGTCAAGTTTGAAGGTGATACCCTTGTAAATAGAATCGAGTTAAAAGGTATTGATTTTAAAGAAGATG  
 GAAACATTTCTGGACACAAATTTGAATACAACATAAATCACAATGTATACATCATGGCAGACAAAACAAAAGAATGGA  
 ATCAAAGTTAACTTCAAATTTAGACACAACATTTGAAGATGGAAGCGTTCAACTAGCAGACCATTATCAACAAAATACTCC  
 AATTGGCGATGGCCCTGTCTTTTACCAGACAACCATTTACCTGTCCACACAATCTGCCCTTTCGAAAGATCCCAACGAAA  
 AGAGAGACCACATGGTCTTCTTGAGTTTGTAAACAGCTGCTGGGATTACACATGGCATGGATGAACTATAACAAA

717 bp

mCherry

ATGGTGAGCAAGGGCGAGGAGGATAACATGGCCATCATCAAGGAGTTCATGCGCTTCAAGGTGCACATGGAGGGCTCCGT  
 GAACGGCCACGAGTTCGAGATCGAGGGCGAGGGCGAGGGCCGCCCTACGAGGGCACCCAGACCGCCAAGCTGAAGGTGA  
 CCAAGGGTGGCCCCCTGCCCTTCGCGCTGGGACATCCTGTCCCTCAGTTTCATGTACGGCTCCAAGGCCTACGTGAAGCAC  
 CCCGCCGACATCCCCGACTACTTGAAGCTGTCTTCCCCGAGGGCTTCAAGTGGGAGCGCGTGTGAACCTTCGAGGACGG  
 CGGCGTGGTGACCGTGACCCAGGACTCCTCCCTGCAGGACGGCGAGTTCATCTACAAGGTGAAGCTGCGCGGCACCAACT  
 TCCCCTCCGACGGCCCCGTAATGCAGAAGAAGACCATGGGCTGGGAGGCCTCCTCCGAGCGGATGTACCCGAGGACGGC  
 GCCCTGAAGGGCGAGATCAAGCAGAGGCTGAAGCTGAAGGACGGCGGCCACTACGACGCTGAGGTCAAGACCACCTACAA  
 GGCCAAGAAGCCCGTGCAGCTGCCCGGCCCTACAACGTCAACATCAAGTTGGACATCACCTCCCAACGAGGACTACA  
 CCATCGTGGAACAGTACGAACGCGCCGAGGGCCGCACTCCACCGCGGCATGGACGAGCTGTACAAGTAA

711 bp

**List of homologous genes of *PfNAT* in *Plasmodium spec.* (PlasmoDB, access: 5/5/14)**

<u>Organism + strain</u>	<u>Gene ID</u>
<i>Plasmodium falciparum</i> 3D7	PF3D7_1437000
<i>Plasmodium falciparum</i> IT	PFIT_1438200
<i>Plasmodium berghei</i> ANKA	PBANKA_061180
<i>Plasmodium chabaudi chabaudi</i>	PCHAS_061350
<i>Plasmodium knowlesi</i> H	PKH_131240
<i>Plasmodium vivax</i> Sal-1	PVX_084690
<i>Plasmodium yoelii yoelii</i> 17X	PY17X_0614300
<i>Plasmodium yoelii yoelii</i> YM	PYYM_0613400
<i>Plasmodium cynomolgi</i> strain B	PCYB_132200

## APPENDIX

### List of homologous genes of *PfNAT* in other *Apicomplexa*

1. By Marcel Deponte, input sequence PBANKA\_061180 (EuPathDB, access: 25/3/14)

<i>Babesia bovis</i> T2Bo	BBOV_III007850
<i>Cryptosporidium muris</i> RN66	CMU_001670
<i>Neospora caninum</i> Liverpool	NCLIV_043940
<i>Theileria parva</i> Muguga	TP04_0689
<i>Eimeria tenella</i> Houghton	ETH_00010875
<i>Toxoplasma gondii</i> ME49	TGME49_105450

2. Additional information, input sequence PF3D7\_1437000 (EuPathDB, access: 5/5/14)

<i>Babesia microti</i> RI	BBM_III06015
<i>Theileria equi</i> WA	BEWA_009490
<i>Theileria orientalis</i> Shintoku	TOT_040000231
<i>Theileria annulata</i> Ankara	TA10470
<i>Cryptosporidium hominis</i> TU502	Chro.30224
<i>Cryptosporidium parvum</i> Iowa II	cgd3_1900
<i>Toxoplasma gondii</i> GT1	TGGT1_305450

### Markers

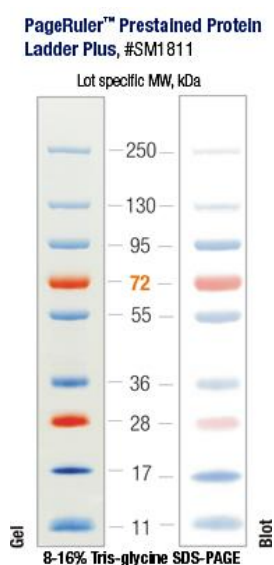


Figure 37. Prestained Protein ladder (Fermentas)

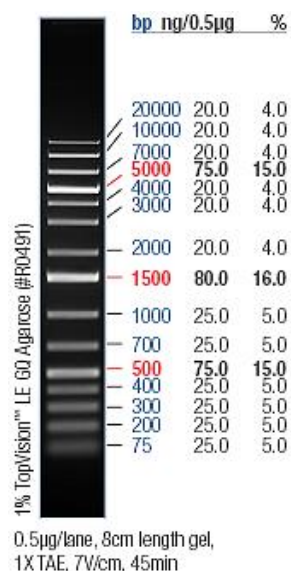


Figure 38. GeneRuler, 1kb+ DNA ladder (Fermentas)